Imperial College London

The Role of JAK2, STAT3 and ERBB2 in Ovarian Cancer

A thesis submitted to fulfil the requirements for the degree of Doctor of Philosophy.

by

James Studd

Imperial College London – Department of Surgery and Cancer

Declaration of Originality:

I declare that all material contained within this thesis is original and of my creation unless otherwise referenced.

Copyright Statement:

Abstract

Background

Ovarian cancer is the most lethal gynaecological malignancy, accounting for an estimated 140,000 deaths per year worldwide. Five year survival rates have not increased significantly in the last 10 years and the acquisition of resistance to chemotherapy remains a significant barrier to improving patient survival. Isogenic cell line models of *in vivo* acquired resistance to chemotherapy were examined to identify differences between sensitive and resistant pairs that might be exploited to sensitise cells to treatment.

Results

Microarray analysis of the isogenic paired sensitive/resistant high grade serous ovarian cell lines PEO1 and PEO4 revealed *IL6* expression is induced by cisplatin exposure. This result was replicated by QRT-PCR and validated in the additional isogenic pair PEA1/PEA2. Western blotting demonstrated the lack of a correlation between IL6 expression and phosphorylation of either Y1007/1008 JAK2 or Y705 STAT3 levels, suggesting IL6 is not driving the constitutive activation of these proteins. Cells did however display dose dependant changes in STAT3, JAK2 and ERBB2 activation in response to cisplatin that differed between sensitive and resistant cells. Resistant clones, PEO4 and PEA2 reduced the activation of these proteins with greater sensitivity to cisplatin dose. Common to all cell lines was a high degree of correlation in the levels of activated JAK2 and ERBB2.

Interfering with cisplatin dependent STAT3 deactivation using IL6 treatment sensitised cells reducing cisplatin IC_{50}, suggesting a functional role for STAT3 in both response, and acquired resistance, to cisplatin. Overexpression and knockdown of STAT3 demonstrated it promotes proliferation and the expression of cyclin D1 and BCL xL/S. STAT3 knockdown increased cisplatin resistance as quantified by IC_{50} whereas STAT3 overexpression potentiated cisplatin induced apoptosis and decreased cisplatin IC_{50}.

Similarly overexpression and knockdown of JAK2 demonstrated it promotes proliferation, in part by regulating STAT3 activation. JAK2 inhibition also increased cellular resistance to cisplatin by attenuating cisplatin induced apoptosis. JAK2 siRNA knockdown also increased cisplatin IC_{50}. Surprisingly knockdown, overexpression and inhibition of JAK2 were all associated with changes in the activation of ERBB2. JAK2 ablation were associated

with decreases in Y1248 phosphorylated ERBB2 whereas overexpression was associated with an increase, changes in activation appear to be driven by changes in protein levels.

GP130 was investigated for due to its role in IL6 signalling and STAT3 activation. mRNA overexpression was detected in resistant cells (2/3 isogenic cell lines) and was associated with growth promotion and cisplatin resistance.

Central Conclusion

Transcriptional regulation of JAK2 in response to cisplatin exposure drives differential behaviour of paired isogenic cell lines. Greater sensitivity of cisplatin resistant cells lines, in their deactivation of STAT3 and ERBB2 is regulated by cisplatin dependent JAK2 downregulation. Downregulation of JAK2 and commensurate reductions in pSTAT3 were associated with reduced proliferation and increased cisplatin resistance. This may be due to reducing the accumulation of DNA double stranded breaks. STAT3 has been suggested as a target for adjuvant chemotherapy, data presented here suggests that in combination with cisplatin STAT3 abrogation would in fact reduce cisplatin effectiveness.

Contents

Abstract 2

Contents 4

Acknowledgements 14

Abbreviations 15

Introduction 17

1. Ovarian Cancer 17

1.1 A general introduction 17

1.2 Staging, Grading and Prognosis 19

1.3 Epidemiology and Risk Factors of Ovarian Cancer 23

1.4 The Genetics of Ovarian Cancer Predisposition 29

1.5 Treatment, Improvements in Survival, Relapse and Recent Novel Therapeutics. 33

1.6 Monitoring and Screening 36

1.7 Different Types of Epithelial Ovarian Cancer 37

1.8 Theories of Pathogenesis 47

1.10 A New Model of Ovarian Carcinogenesis 51

2 IL6, JAK2, STAT3 and ERBB2 with Reference to Ovarian Cancer 55

2.1 The Discovery of JAKs and STATs 55

2.2 Structure of The JAKs and STATs 56

2.3 Activation of JAKs, STATs and Nuclear Import 58

2.4 Functions of STAT3 61

2.5 STAT3 and Cancer 63

2.6 JAK2 and Cancer 70

2.7 ERBB2 and Cancer 71

3. Platinum 76

3.1 Mechanisms of Toxicity 76

3.2 Repair of DNA Platinum Adducts 77

3.3 Mechanisms of Platinum Resistance 81

Aims 84

Methods and Materials 86

1. Cell Lines and Culture 86
2. siRNA 86
3. Cell Viability/Caspase Assay. 87
4. Inhibitors and Treatments 88
5. rIL6 Treatment 89
6. Western Blotting 89
7. Densitometry 90
8. Immunoprecipitation 91
9. RNA Extraction and cDNA Synthesis 91
10. Quantitative Real Time - PCR 91
11. Cloning 93
12. Site-Directed Mutagenesis 94
13. Sequencing 95
14. Plasmid Purification and Transfection 95

15. Flow Cytometry 96

16. Expression Array Profiling 96

16.1 Cisplatin Treatment Microarray (for Figure 12) 96

16.2 Paired Cell Line Expression Profiling Microarray (for Figure 47B) 97

17. Data Collection, Statistics, IC_{50} and Doubling Time Estimations 97

Results 99

Results Chapter 1:- 100

1. Effects of Cisplatin on the IL6/JAK2/STAT3 Axis 101

1.1 Cisplatin Induces IL6 Expression 101

1.2 Cisplatin Modulates Signalling Through JAK2 and STAT3 104

1.3 Cisplatin Resistant Cells Exhibit a Differential Response to Cisplatin in Their Levels of JAK2, STAT3 and ERBB2 Activation. 106

1.4 Cisplatin Causes Both an Increase and Reduction in JAK2 at the Transcriptional Level in a Dose Dependant Manner 115

Discussion :- Results Chapter 1 118

1.1 Cisplatin Induces IL6 Expression 118

1.2 Cisplatin Modulates Signalling Through JAK2 and STAT3 121

1.3 Cisplatin Resistant Cells Exhibit a Differential Response to Cisplatin Treatment in Levels of Activation of JAK2 STAT3 and ERBB2. 122

1.4 Cisplatin Causes Both an Increase and Reduction in JAK2 at the Transcriptional Level in a Dose Dependant Manner 124

Results Chapter 2 :- 125

2. IL6 Responsiveness and the Effects of rIL6 Treatment on Cisplatin Sensitivity..... 126

2.1 Determination of IL6 responsiveness in a Panel of Ovarian cell lines. rIL6 Activates STAT3 but not JAK2 126

2.2 Addition of soluble rIL6RA Restores IL6 Responsiveness in PEA1 and PEA2 127

2.3 rIL6(RA) Treatment Sensitises Cells to Cisplatin..... 128

2.4 Expression of IL6 and IL6RA in a Panel of Ovarian Cell Lines 136

Discussion :- Results Chapter 2 139

2.1 Determination of IL6 responsiveness in a Panel of Ovarian cell lines. IL6 Activates STAT3 but not JAK2 139

2.2 Addition of Soluble rIL6RA Restores IL6 Responsiveness in PEA1 and PEA2 140

2.3 rIL6(RA) Treatment Sensitises Cells to Cisplatin..... 140

2.4 Expression of IL6 and IL6RA in a Panel of Ovarian Cell Lines 141

Results Chapter 3:-. 143

3. JAK2 Contributes to Phosphorylation of STAT3 and ERBB2 and Promotes Growth..... 144

3.1 JAK2 Inhibition Reduces Cisplatin Induced Apoptosis, Reduces Growth Rates and Levels of STAT3 and ERBB2 Phosphorylation 144

3.2 siRNA Mediated Knockdown of JAK2 Inhibits Cell Growth, Increases Cisplatin IC_{50} and Reduces Levels of STAT3 and ERBB2 Phosphorylation. 150

3.3 JAK2 Overexpression Increases Proliferation, pSTAT3 and pERBB2 156

3.4 No Evidence of a Physical Interaction Between JAK2 and ERBB2..... 160

Discussion :- Results Chapter 3 161

3.1 JAK2 Inhibition Reduces Cisplatin Induced Apoptosis, Reduces Growth Rates and Levels of STAT3 and ERBB2 Phosphorylation 161

3.2 siRNA Mediated Knockdown of JAK2 Inhibits Cell Growth, Increases Cisplatin IC_{50} and Reduces Levels of STAT3 and ERBB2 Phosphorylation. 163

3.3 Over Expression of JAK2 Increases Proliferation and Modulates the Activity of ERBB2 164

3.4 No Evidence of a Physical Interaction Between JAK2 and ERBB2 165

Results Chapter 4 :- 166

4. STAT3 Promotes Cell Growth and the Expression of Cyclin D1 and BCL2L1. 167

4.1 An Assessment of the Levels of pSTAT3 Y705 in the Paired Cell Lines PEO1/PEO4 and PEA1/PEA2 167

4.2 siRNA Mediated Knockdown of STAT3 Inhibits Cell Growth, Increases Cisplatin IC_{50} and reduces expression of Cyclin D1 168

4.3 STAT3 Overexpression Increases Cell Proliferation, Cisplatin Induced Apoptosis and Decreases IC_{50}. 177

Discussion :- 187

4.1 An Assessment of the Levels of pSTAT3 Y705 in the Paired Cell Lines PEO1/PEO4 and PEA1/PEA2 187

4.2 siRNA Mediated Knockdown of STAT3 Inhibits Cell Growth, Increases Cisplatin IC_{50} and reduces expression of Cyclin D1 188

4.3 Overexpression of STAT3 Increases, Cell Proliferation. In PEO1 and PEO4 but not SKOV3 STAT3 Overexpression, Increases Cisplatin Induced Apoptosis and Decreases IC_{50}. 191

Results Chapter 5:- 193

5. ERBB2 is Phosphorylated in a Range of Ovarian Cell Lines, where it Promotes Growth, Contributes to Cisplatin Resistance and Activation of JAK2 and STAT3 194

5.1 ERBB2 is Phosphorylated in a Range of Ovarian Cell Lines Without Being Overexpressed. 194

5.2 Sensitivity to the ERBB2 Inhibitor CP-724714 Correlates with Levels of Protein Activation..... 197

5.3 ERBB2 Inhibition Sensitises Cells to Cisplatin 198

5.4 ERBB2 Inhibition Reduces Activation of ERBB1, AKT and ERK1/2 in Cells Lines Possessing Phosphorylated ERBB2 but Not in Those Without 203

Discussion :- Results Chapter 5 206

5.1 ERBB2 is Phosphorylated in a Range of Ovarian Cell Lines Without Being Overexpressed. 206

5.2 Sensitivity to the ERBB2 Inhibitor CP-724714 Correlates with Levels of Protein Activation..... 208

5.3 ERBB2 Inhibition Sensitises Cells To Cisplatin..... 209

5.4 ERBB2 Inhibition Reduces Activation of ERBB1, AKT and ERK1/2 in Cells Lines Possessing Phosphorylated ERBB2 but Not in Those Without 210

Results Chapter 6:- 211

6. GP130 is Overexpressed in Cisplatin Resistant Cells where it

6.1 GP130 is Overexpressed in Cisplatin Resistant Cell Lines PEA2 and PEO23 Relative to Their Sensitive Isogenic Counter Parts 212

6.2 siRNA Mediated Knock Down of GP130 Sensitises PEA2 and SKOV3 but not PEA1 to Cisplatin 214

6.3 siRNA Mediated Knockdown of GP130 Reduces Proliferation in Cisplatin Resistant PEA2 and SKOV3 but not in Sensitive PEA1. 217

6.4 siRNA Mediated knockdown of GP130 Decreases pSTAT3 in SKOV3 but not PEA2 and has no Effect on pERBB2. 219

Discussion :- Results Chapter 6 221

6.1 GP130 is Overexpressed in Cisplatin Resistant Cell Lines PEA2 and PEO23 Relative to Their Sensitive Isogenic Counter Parts 221

6.2 – 6.3 siRNA Mediated Knock Down of GP130 Sensitises to Cisplatin and Reduces Proliferation in PEA2 and SKOV3 but not PEA1 222

6.4 siRNA Mediated knockdown of GP130 decreases pSTAT3 in SKOV3 but not PEA2 and has no effect on pERBB2. 225

Results Chapter 7:- 227

7. ERK1/2 are Phosphorylated in Response to JAK2 Knockdown, JAK2 Inhibition, Cisplatin and IL6 Treatment. Inhibition of ERK1/2 phosphorylation Sensitises SKOV3 to Cisplatin and Reveals a Feedback Mechanism Involving ERBB2, JAK2 and STAT3 228

7.1 ERK1/2 are Phosphorylated in Response to JAK2 Knockdown, JAK2 Inhibition, Cisplatin and IL6 Treatment 228

7.2 Signalling through ERBB2, JAK2, STAT3 and ERK1/2 are also affected by Other Cytotoxic Compounds. 231

7.3 Inhibition of ERK1/2 Phosphorylation Sensitises SKOV3 to Cisplatin and Doxorubicin. While Revealing Feedback Mechanism Involving ERBB2, JAK2 and STAT3 and that ERK1/2 Drives Cyclin D1 Expression 234

Discussion :- Results Chapter 7 238

7.1 ERK1/2 are Phosphorylated in Response to JAK2 Knockdown, JAK2 Inhibition, Cisplatin and IL6 Treatment 238

7.2 Signalling through ERBB2, JAK2, STAT3 and ERK1/2 are also affected by Other Cytotoxic Compounds. 239

7.3 Inhibition of ERK1/2 Phosphorylation Sensitises SKOV3 to Cisplatin and Doxorubicin. While Revealing Both That, ERK1/2 Drives Cyclin D1 Expression, and a Feedback Mechanism Involving ERBB2, JAK2 and STAT3 240

Summary and Conclusions 244

1. The Identification of JAK2 as a Regulator of Response and Resistance to Cisplatin 244

A Summary of the Data 244

In Conclusion 247

2. Effects of JAK2 perturbation are in Part Mediated via STAT3 248

A summary of the Data 248

In Conclusion 249

3. JAK2 Regulates ERBB2 251

A Summary of the Data 251

In Conclusion 252

4. EBRR2 is Frequently Activated in HGS Cell Lines where it Promotes Cisplatin Resistance 253

A Summary of the Data 253

In Conclusion 254

5. GP130 Promotes Growth, Platinum and Resistance, Revealing Different Pathways to STAT3 Activation 255

A Summary of the Data 255

Conclusion 255

6. Mutual feedback between Inhibition of the GP130/JAK2 and ERK1/2 Pathways 257

A Summary of the Data 257

Conclusion 257

Supplementary Methods/Results 261

Brief Description of Contents 261

S1 Preparation of STAT3 pcDNA 3.1 + ... 262

S2.1 PCR amplification of full length STAT3α from OSE-C2 262

S2.2 Cloning of STAT3 into pcDNA 263

S2.3 Site directed mutagenesis of STAT3 264

S2 Preparation of JAK2 pcDNA 3.1 + ... 266

S2.1 PCR amplification of JAK2 from OSE-C2 and pDONNR223 266

S2.2 Cloning of JAK2 into pcDNA3.1+ 267

S2.3 Site Directed Mutagenesis of JAK2 268

S3 Cell Line Mutational Information 270

S4 GP130 Expression Predicts Poor Prognosis in Patients, However Multi-Variable Cox Proportional Hazard Analysis Suggest it is Not an Independent Prognostic Factor. 271

S5 Western blot of JAK2 Inhibitor Treated PEO1 PEO4 274

S6 Knockdown of GP130 in PEO4 275

References 277

Acknowledgements

For their material assistance and advice I would like to thank, in no particular order;

Rakhee Chauhan - for providing THP1 and FDCP1 cells. As well as GM-CSF

Jane Borley and **Paula Cunnea -** for providing RNA and cDNA from PEO14 and PEO23.

Louay Louis - for providing a phospho ERK 1/2 antibody.

Elisa Zanini - for providing IPTG, other cloning materials and advice.

Nona Rama - for providing normal fallopian tube tissue and generally looking after me when I was a young tyke.

Charlotte Whilhelm-Benartzi - for assistance (doing the whole thing) with Cox proportional hazards modelling.

Elaina Maginn – for help with PRISM software.

Michelle Chen – for teaching me western blotting.

Azi 'Asbo' Bashi – for being Azi.

Camila Henrique de Sousa - for not being Azi.

Ed Curry – for processing of the match isogenic cell line copy number data.

Hani Gabra – for the opportunity to work in his lab.

And **Euan Stronach** – for patience, advice, coffee, tolerance, the use of data, and generally being a great supervisor.

Abbreviations

5-YSR – five year survival rate

AJCC – American Joint Committee on Cancer

ASR – age standardised rate (always shown per 100,000)

BRCA – breast cancer associated

BSO - bilateral salpingo-oophorectomy

CI – confidence interval

CTLs - $CD8^+$ cytotoxic T cells

DSB – double strand breaks

DCs - dendritic cells

E2 – estradiol

E – Glutamic Acid

EGF – epidermal growth factor

EMT - epithelial to mesenchymal transition

EOC – epithelial ovarian cancer

ERBB - human epidermal growth factor receptor

F- phenylalanine

FIGO - International Federation of Gynecology and Obstetrics

FSH - follicle stimulating hormone

FSHR - follicle stimulating hormone receptor

GM-CSF - granulocyte and macrophage colony stimulating factor

HGS – high grade serous

HNPCC- hereditary non-polyposis colorectal cancer

HR – hazard ratio

HRT - hormone replacement therapy

IFNα – interferon α

IFNγ – interferon γ

IHC - immunohistochemistry

IP – intraperitoneal

ISGF-3 - IFN signalling gene factor complex 3

IV – intravenous

JAK – Janus Kinase

kDa – kilodlatons

LB - lysogeny broth

LGS – low grade serous

LH - luteinising hormone

LHR - luteinising hormone receptor

LPS – lipopolysaccharide

MMR- mismatch repair

mRNA – messenger ribonucleic acid

NSCLC - non-small cell lung carcinoma

O/N – overnight

OS – overall survival

PARP1 - poly-ADP ribose polymerase 1

PBS(/T) – phosphate buffered saline (with tween 20)

PFS – progression free survival

PPIA - peptidylprolyl isomerase A

PPV - positive predictive value

RNAi – RNA interference

RR – relative risk

SDS – sodium dodecyl sulphate

SEM – standard error of the means

SH2 - SCR homology domain 2

SNP – single nucleotide polymorphism

STAT – signal transducer and activator of transcription

TBS(/T) – TRIS buffered saline (with tween 20)

TBP – TATA binding protein

TCFs - ternary complex factors

UTR – Untranslated region

WT – wild type

Y – tyrosine

Introduction

1. Ovarian Cancer

1.1 A general introduction

Ovarian cancer is the name given to a variety of malignant neoplasms, affecting women, where some or the entire tumour mass is found on either of the ovaries. They are a heterogeneous group of tumours in their histology, prognosis and as is increasingly become clear their molecular aetiology. The classification of ovarian carcinomas is based largely on tumour cell morphology (histology) and to a lesser extent tumour grade, a measure of malignancy. The largest subgroup of ovarian cancers is the adenocarcinoma or epithelial group consisting of around 90% of all malignant tumours.

1.11 Incidence and Prevalence

Ovarian cancer is both the seventh most common cancer and seventh most common cause of death from cancer in women, accounting for 3.7% of cases and 4.2% of cancer deaths worldwide. In 2008 there were an estimated 225,000 new cases and 140,000 deaths due to ovarian cancer worldwide [1]. The overall lifetime risk of developing epithelial ovarian cancer is approximately 1 in 72 and an estimated 1% of women born in 2012 will die from the disease, based on statistics from the US [2]. It is more common is industrialised developed nations than developing ones. The age standardised incidence rate (ASR) in developed nations is 9.3 per 100,000 compared to 4.9 for developing nations, with a worldwide average of 6.3 [3]. Regional variations in parity, number of births a women experiences in her life, are likely to account for a large proportion of this difference. This topic is discussed in greater detail in section 1.1.11.34 on Parity.

1.12 Different Types of Ovarian Cancer

Ovarian tumours are divided into three major histological subgroups, epithelial, stromal/sex chord and germ cell, each associated with their own aetiology and prognosis. Germ cell and stromal/sex chord tumours are more common in younger women being around 4 and 2 times more common in the under 30s than those over 30 respectively [4] they are also more likely to be benign. They each account for around 5% of ovarian cancers but a higher proportion of all neoplasms.

Germ Cell Tumours

Germ cell tumours are thought to arise from primary or secondary oocytes arrested in meiosis I within the ovarian stroma. Germ cells have a mixed histology but the majority are benign. Around 20% – 25% of all ovarian neoplasms are germ cell in origin, but they account for fewer than 5% of malignant cancers. In Asia this figure is around 15%, due to the lower overall incidence of epithelial ovarian cancer in this region. For women under 20 years of age 70% of all tumours are germ cell in origin, and in this age group they account for one-third of ovarian malignancies [5].

Sex Chord Stromal Tumours

Stromal/sex chord tumours also account for around 5% of ovarian cancers. They arise from cells derived from the sex chord, an embryonic precursor of cell in the ovarian stroma that form the lining of the follicles. They can occur at any age but are more common after menopause [6]. The prognosis in sex chord/stromal tumours is generally good. However they are characterised by excessive secretion of either estrogens or androgens which can result in virilisation, the development of male secondary sexual characteristics, such as facial hair.

Epithelial Ovarian Cancers

The vast majority of malignant ovarian neoplasms, around 90%, are epithelial in origin and recent data has strongly suggested that they can arise from any epithelial tissue derived from the coelomic mesothelium, including the peritoneal lining, the ovarian surface,

fallopian tubes and possibly the endometrium. In fact the name ovarian cancer is slightly disingenuous as it implies a shared site of genesis of all tumours that is no longer supported by the evidence.

In comparison to germ cell and stromal tumours epithelial ovarian tumours are very rare in prepubescent girls and much more likely to be malignant. They are most common in post-menopausal women and can be further divided into four predominant histological subtypes; serous, endometroid, mucinous and clear cell accounting for 52%, 13%, 10% and 5% of cases respectively [7]. Although the prognosis varies between each on average they are aggressive cancers from which more than half of women will have died 5 years from diagnosis. A period characterised by successive cycles of treatment, disease remission and disease relapse, in which each successive cycle is characterised by diminishing periods of remission, until chemotherapy that was initially effective, no longer has any effect. In the majority of cases tumours develop chemoresistance, when they stop responding to conventional treatment, ultimately ending in the death of the patient.

Due to the high proportion of all malignant ovarian tumours that the epithelial group accounts for the majority of research has been focused here, accordingly the focus of this document will be on the epithelial ovarian cancer (EOC) and germ cell and stromal tumour will not be further considered.

1.2 Staging, Grading and Prognosis

1.21 Stage

In the UK and Europe epithelial ovarian cancers (EOC) are staged according to the extent of disease progression based on the guide lines established by the International Federation of Gynecology and Obstetrics (FIGO). While in the US the American Joint Committee on Cancer staging convention is used. Both divide the disease into 5 stages based on the following criteria.

Stage I – tumour limited to one or both ovaries
Stage II – tumour has spread to pelvic region.
Stage III – tumour has spread to lower abdomen or lymph nodes.

Stage IV – tumour has spread to distant organ.

Tumour staging is a very important prognostic factor in ovarian cancer. Figure 1 shows the stage specific 5 year survival rates demonstrating the importance of early stage diagnosis.

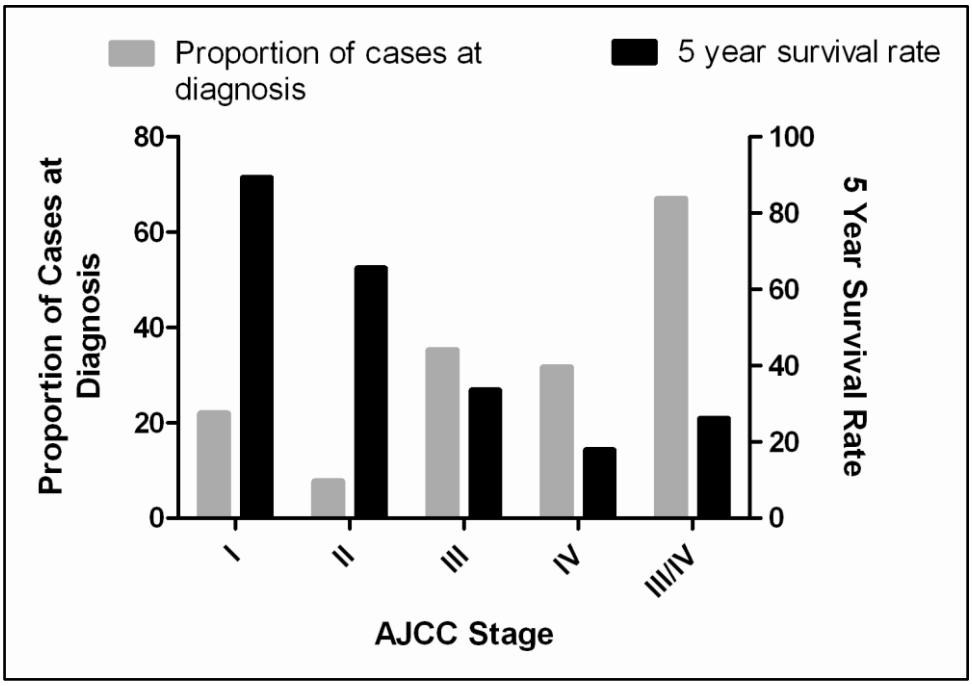

Figure 1. The proportion of cases in each stage of disease at diagnosis and the associated 5 year survival rate based on data from [7]. Stage as defined by the American Joint Committee on Cancer.

Based on patients treated in the US between 1988 and 2001, despite a relatively high 5-YSR for stage 1 of 89% the majority of cases, nearly 70%, present with advanced disease, either stage III or IV, when the prognosis is much less favourable, associated with 5-YSRs of 33.5% and 18% [7] respectively. The 5-YSRs for all stages is 43%. The situation was similar in the UK where although diagnosis of stage 1 disease was associated with a 5-YSR of 92% only 30% of cases presented in this stage compared to 60% presenting in stages III and IV which were associated with 5-YSR of 22% and 5.5% resulting in an average for all stages of 42% [8]. Early stage disease is relatively asymptomatic, this combined with a lack of national screening is responsible for the low rates of early stage detection despite the additional associated mortality.

1.22 Grade

While the criteria for EOC staging are well defined and standardised the same is not true of grading. Grading in ovarian cancer is based less on the extent of disease progression and more on the gross anatomical structure, cytologic appearance and the fine histology of a tumour in order to express its malignant potential. It is a reflection of the recognition that tumours with similar gross histologies and of the same stage can a have very different prognoses. For example based on statistics for serous EOC from the US someone diagnosed with a stage II invasive high grade tumour has a 5-YSR of 66% compared to a 5-YSR of 77% for a stage IV low grade tumour [2]. Figure 2 shows the survival curves for patients divided into those diagnosed with low grade compared to high grade tumours, with an average of both also shown, in a cohort of over 200 patients of EOC, demonstrating a significant difference in survival.

Despite the fact that it has been recognised as an important prognostic factor for at least 15 years and is frequently referred to in research papers, methods used for ascribing grade are variable, frequently subjective and often not even described [9]. For example data used to compile figure 2 tumour grading was carried out using a non-standardised method without quantifying any of the variables involved.

The two main formalised grading criteria are set out by the World Health Organisation (WHO) and FIGO. FIGO criteria uses a three stage method based on the quantity of papillary or glandular structures compared to less differentiated homogenous solid mass.

Grade I <5% solid mass

Grade II >5% <50% solid mass

Grade III > 50% solid mass

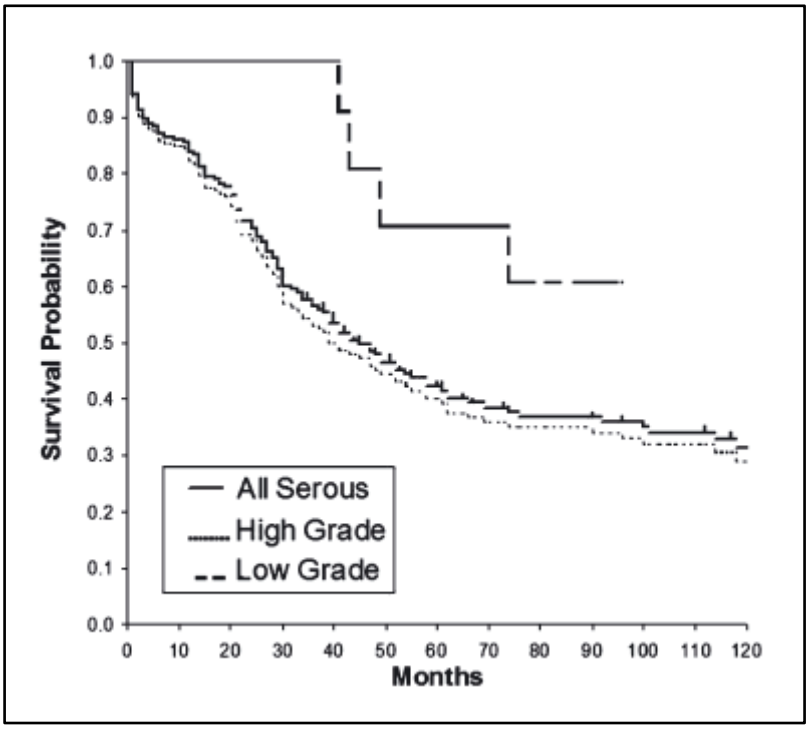

Figure 2. Showing survival curves for high and low grade, ovarian cancer with average for combined cases. Demonstrating survival differences and the lower proportion of low grade case relative to high grade. Figure taken from [10].

The WHO criteria are not quantifiable and assignment to a grade is more subjective, than FIGO criteria. Differences and inconstancy between criteria have contributed to a situation in which the prognostic significance of grade has been variably reported depending on the particular method used, reviewed in [9].

The disparity of prognosis between high and low grade tumours highlights both the purpose of grading and the importance of ensuring effective treatment tailored to the individual's disease specific needs. Especially as tumours of low grade tend to show a poorer response to chemotherapy [11].

Recent advances in our understanding of EOC carcinogenesis and molecular aetiology have led to the recognition that low and high grade disease are fundamentally different and not a contiguous disease, that is high grade disease does not originate from low grade but is high grade in nature at its genesis. This appreciation has given rise to the suggestion that a two tier grading system be adopted with a new set of diagnostic criteria [12]. This is discussed in greater detail in section 1.78 - A New Method for Grading Serous EOC.

1.3 Epidemiology and Risk Factors of Ovarian Cancer

1.31 Age

Perhaps the risk factor that has the clearest association with ovarian cancer risk is age, Figure 3 shows the ASR (age standardised incidence rate per 100,000 of the population) according to age illustrating this relationship. Incidence increases with age year on year, peaking at 80-84, however due to demographics the mode age of diagnosis is between 60-65 years of age. Around 70% of those diagnosed with EOC are over 50 year of age, while the proportion of those under 30 is only 2.7% [13]. Ovarian carcinoma is prepubescent girls is extremely rare however here is some variation in age distribution according to histological subtype. Specifically sex chord/stromal and germ cell are more common in younger women.

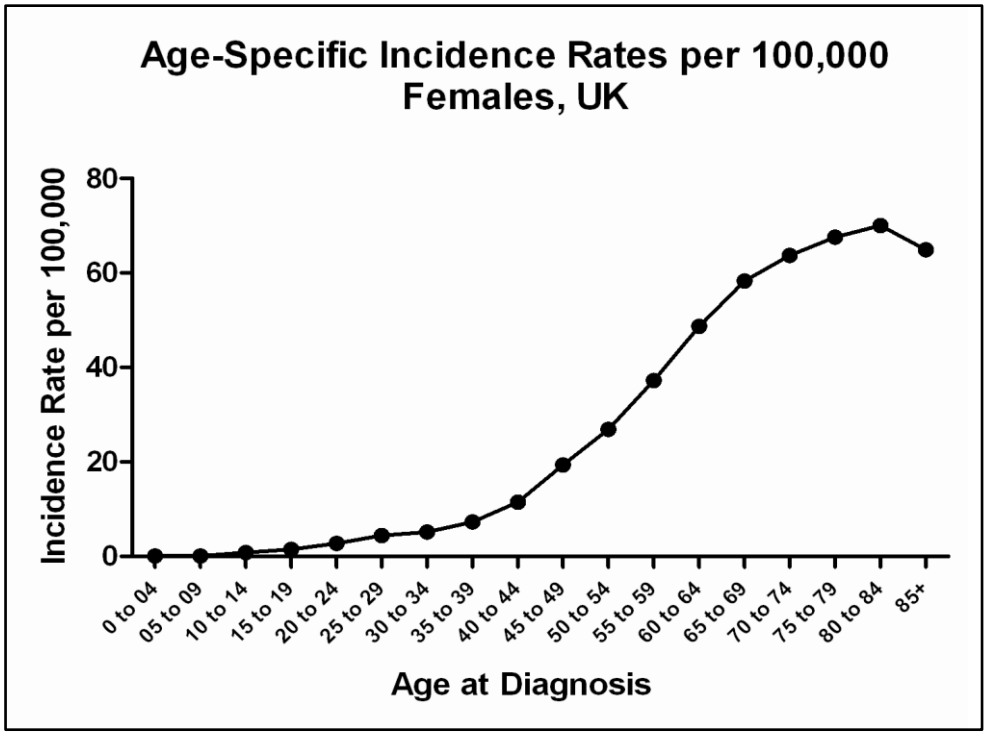

Figure 3. Age standardised incidence rates per 100,000 of the population, data taken from [14], showing the relationship between age and probability of diagnosis.

1.32 Geography and Ethnicity

Incidence rates of EOC are highest amongst white Western women, particularly in Northern Europe where the ASR is 11.8. Rates in East Asian and African populations tend to be far lower, at 4.3 and 4.2 respectively [3].

While geographical variation in ASRs is complicated by exposure to known risk factors, for example the protective effects of pregnancy tend to be more common in less developed regions (see section on parity below), some observed differences might point towards currently unknown environmental or genetic risk factors. These include the observation that women in developed Eastern Asia nations with similar parity to Western counterparts exhibit reduced risk. Women in South Korea and Japan have an ASR of 5.8 and 7.6 respectively compared to 12.8 and 10.8 in the UK and Denmark respectively [3]. Interestingly this protective effect is experienced by emigrants from these nations to the US suggesting a genetic component in people of Eastern Asian descent is responsible. Rates for white US women were 12.8 and 8.8 for Asian US immigrants based on 2009 figures [2,15].

Some of the highest rates of EOC are seen in women of Ashkenazi Jewish decent, who have an estimated incidence of 17.8 , this additional risk is probably accounted for by the higher frequency of mutations in *BRCA1* and *BRCA2* in this population [16,17].

1.33 Family History

It had been appreciated since around the late 70s that a family history of ovarian cancer was associated with an increased risk of developing the disease. A large number of studies have investigated this relationship. In 1998 a meta-analysis was published including a combined 4330 cases, 11905 controls with an additional two cohort studies of 1747 participants which estimated the increased relative risk (RR) of developing the disease at 3.1 (95% CI 2.6-3.7) for those with one first degree relative and 6.0 (95% CI 3.0-11.9) for those with a mother who had ovarian cancer [18]. Families with a high incidence of ovarian cancer are also at greater risk of developing breast cancer, suggesting presence of germline mutations segregating through these families conferring an increased risk to both diseases. Using such families in 1994 breast cancer associated 1 (*BRCA1*) was cloned, and subsequently patented [19]. In one such family 5 of 8 women affected by either breast or ovarian cancer were found to contain mutations in the open reading frame now known as *BRCA1,* that were not observed in controls. The following year the same positional cloning approach led to the identification of *BRCA2*, again putative loss of function mutations were

observed in individuals with disease and not in unaffected controls [20]. The importance of BRCA1 and BRCA2 in predisposition to ovarian cancer is discussed in greater detail in section 1.41 – Hereditary breast and ovarian cancer syndrome (HBOC), on genetics of ovarian cancer.

1.34 Parity

The link between parity, the number of children a women has had, and the risk from ovarian cancer is well established. There is an inverse relationship between parity and risk of invasive ovarian cancer. A meta-analysis of 12 US case-control studies including around 2000 cases and 9000 controls found a combined odds ratio 0.76 ($p<0.01$) for parous women, of one or more full term pregnancies, compared to nulliparous women. Furthermore a strong inverse correlation was observed between the number of full term pregnancies and disease incidence ($r^2= 0.93$) [21]. Similar results were observed in a European meta-analysis, including around 1100 cases and 2700 controls, where an overall relative risk of developing epithelial ovarian cancer of any grade was 0.7 (95% CI 0.6-0.8) for parous vs nulliparous women [22]. Both meta-analyses showed a continuous relationship between number of births and risk, in which each subsequent birth was an associated with an additional decrease in disease incidence. For example the US study showed an OR of 0.6 ($p<0.01$) for a single full term pregnancy compared to an OR of 0.29 ($p<0.01$) women of 6 or more full terms. The mechanism via which pregnancy reduces the likelihood of neoplasia is unknown, but it is theorised to act through the suppression of ovulation and/or exposure to the hormones associated with preventing ovulation during gestation. This view is supported by the coincident observations of the effects of contraceptive pill use, fertility treatment, hormone replacement therapy and oophorectomy. These issues are discussed in greater detail in this section.

1.35 Oral Contraceptive Use

Use of the contraceptive pill has been demonstrated to reduce EOC incidence in a number of studies. The European meta-analysis described above also investigated the effects of oral contraceptive (OC) use. They observed a strong protective effect of OC use in regard

to incidence of epithelial ovarian cancer of any grade. The strongest protective effect was found between 'never users' and 'ever users' (RR = 0.6 95% CI 0.4-0.8) and again there was a correlation between number of years of use and extent of protection [23]. These findings were duplicated in the previous described US meta-analysis. Again degree of protection correlated with length of OC use the greatest effect seen in users of 6 or more years (OR = 0.55 95% CI 0.35-0.86) [21].

1.36 Hysterectomy, Tubal Ligation and Oophorectomy

Tubal ligation is the process of having the fallopian tubes block or severed as a method of sterilisation. For some time it has been observed that women who have undergone the procedure are at a reduced risk from ovarian cancer. A large number of studies have addressed this issue. A meta-analysis of 13 studies of invasive disease found a RR of 0.72 (95% CI 0.66-0.72) [24]. This study also investigated the connection between tubal ligation and the risk posed by each histological subtype. There was a protective effect for all subtypes however the effect was largest for endometrioid cancer (RR= 0.45 95% CI 0.33-0.61) surprisingly there was no significant additional protection to confirmed BRCA mutation carriers (RR = 0.64 95% CI 0.43-0.96).

Hysterectomies are performed for a number of reasons including but not limited to, cancer of the reproductive system (uterus, cervix, ovaries or endometrium), severe cases of uterine fibroids (benign growths) and severe endometriosis. Hysterectomies can involve the removal of the uterus alone or include the ovaries and fallopian tubes, in which case it is known as a bilateral salpingo-oophorectomy (BSO). BSOs are offered to high risk women, mostly known BRCA carriers, or those with a strong family history. Similarly to tubal ligation women who had undergone hysterectomies are at reduced risk of developing ovarian cancer. The RR of combined borderline and invasive disease was 0.74 (95% CI 0.65-0.84) compared to a RR of 0.81 (95% CI 0.68-0.97) for invasive only [24]. Unlike tubal ligation women who have undergone a BSO due to BRCA status receive an additional protective effect relative to the general population and were half as likely to develop ovarian cancer as BRCA carriers who did not undergo the procedure (HR = 0.49, 95% CI 0.37- 0.65) (Rebbeck, Kauff, & Domchek, 2009).

1.37 Infertility and Fertility Treatment

The potential link between infertility, fertility treatment and ovarian cancer is contentious. Results of individual studies has been heterogeneous and attempts to synthesise the available data are both uncommon and inconclusive [25,26]. This is likely, in part, due to the complexity of infertility and the problem of compounding factors. Infertility has a number of causes and potential treatments, further compounded as those women who subsequently become pregnant will experience its protective effects. Despite this some conclusions have been consistent. Those women who were infertile due to endometriosis were at higher risk of ovarian cancer (OR = 1.73 95% CI 1.10-2.71) [25]. Also nulliparous women who had used fertility drugs were at a higher change of developing borderline tumours than nulliparous women who didn't use any drugs (OR = 2.43 95% CI 1.01-5.88) [25].

1.38 Hormone Replacement Therapy

Hormonal changes experienced as a consequence of menopause or oophorectomy are associated with a number of morbidities including osteoporosis, dementia and cardiovascular disease, additionally there are those with no effect on morbidity but nonetheless have a significant impact on quality of life [27]. Federal drug authority (FDA) approval for diethylstilbestrol was originally given in 1941 for the treatment of the direct symptoms of menopause including hot flashes and night sweats and vaginal dryness [28]. Its use increased significantly over the decades since but some studies showed a potential link with increased breast and endometrial cancer. More recently two large studies have addressed whether, overall, HRT confers health benefits, the Woman's Health Initiative in the US [29] a case control study of combined estrogen plus progestin and the Million Women Study [30] a large UK cohort study. The findings of these two studies plus a number of others were subjected to a meta-analysis. Its findings were that long term HRT use was associated with a small increase in incidence of invasive ovarian cancer. Summary relative risks were 1.24 (95% CI 1.15-1.34) for cohort studies and 1.19 (95% CI 1.01-1.40) for cases controls studies. Most at risk were long term (>5 years), current users and uses of estrogen only HRT [31].

1.39 Breast Feeding

Postpartum suckling of the breast provides a physical stimulus capable of delaying the resumption of normal oestrous cycling for up to 9 months. The mechanism responsible for this is not fully understood however it seems to operate via the sensitisation of the hypothalamus to estrogen signalling [32]. The effect of this increased negative feedback reduces the secretion of gonadotrophin releasing hormone which in turn causes lower levels of LH and FSH reducing the probability of ovulation. Based on the known relationships between parity, oral contraceptive use and ovarian cancer, it is perhaps unsurprising that breast feeding is also protective. A number of studies have examined this relationship. The vast majority found breast feeding was indeed protective, in a dose dependant fashion, after accounting for parity and other known variables. Relative risks of ovarian cancer for the greatest duration of breast feeding, at least 16 months, compared to never breast feeders were between 0.6 (95% CI 0.4- 0.7) [33] and 0.73 (95% CI 0.49- 1.10) [34]. Interestingly a more detailed examination of histotype specific effects suggests that greater protection is experienced from endometrioid while no protection is conferred from invasive mucinous types [35]. The lack of protection from mucinous ovarian cancer providing supporting evidence to the emerging view that this type of cancer is not ovarian in origin but usually colon cancer metastasis, see section 1.74 on mucinous cancer.

1.310 Diet and Obesity

A number of studies have shown a link between dietary factors and ovarian cancer risk. The regular consumption of vegetables was found to confer a protective effect in both a prospective cohort and case control study, ORs ranged from 0.44-0.65 [36,37]. Obesity and excess weight have been repeatedly linked to ovarian cancer risk. Weight and risk of ovarian cancer were correlated in a large meta-analysis that suggested a moderate risk associated with being over-weight (OR = 1.2 95% CI 1.0–1.3) and a further increase in risk for obese individuals (OR =1.3 95% CI 1.1–1.5) [38]. It has been suggested that this may be due, in part, to the increased serum estrogen levels associated with increased body mass index [39].

1.4 The Genetics of Ovarian Cancer Predisposition

1.41 Familial Predisposition: Somatic High Penetrance Alleles

Hereditary breast and ovarian cancer syndrome (HBOC)

Of those families with recurrent breast and ovarian cancer, with a suspected high susceptibility allele segregating though it, it is estimated that between 34% and 63% contain a mutation in either *BRCA1* or *BRCA2* [40]. Carriers of BRCA mutations suffer from hereditary breast and ovarian cancer syndrome (HBOC) a dominantly inherited condition with a life time risk (up to 70 years) of 69% and 74% from developing breast cancer for *BRCA1* and *BRCA2* respectively. As well as breast and ovarian cancer, carriers are also at an increased risk of developing additional cancers, although the risk profile differs for carriers of either BRCA1 or BRCA2 mutations. For example, carriers of BRCA1 mutation carriers are at increase risk of colon (RR = 4.1) and prostate (RR = 3.3) cancer, whereas carriers of BRCA2 mutations are at greater risk from prostate (RR = 4.6) and pancreatic (RR = 3.5) cancer. Both types of carriers also exhibit increased predisposition to a range of additional cancers [41,42].

Mutations in *BRCA1* account for the largest proportion of cases of hereditary ovarian cancer, between 24% - 76%, while *BRCA2* mutations were observed in only 1% - 17% depending on the particular study, reviewed in Ramus and Gayther [40]. The overall lifetime risk (up to 70 years of age) of developing ovarian cancer for carriers of *BRCA1* mutations is estimated at 39% - 40% and between 11% - 18% for *BRCA2* [43–45] resulting in roughly a RR of 28 and 8-13 respectively relative to the general population, for white Western women.

BRCA1 is located on chromosome 11q21 and *BRCA2* on 13q12-13. Both genes encode proteins involved in the repair of double stand breaks in DNA by homologous recombination (HR). *BRCA1* encodes a 207kDa ring finger protein with E3 ubiquitin-protein ligase activity while *BRCA2* encodes a 380 kDa protein which plays a role in recruiting RAD51 to sites of DNA damage. Cells deficient in BRCA1 or BRCA2 tend to exhibit chromosomal instability, experiencing both increased frequencies of translocations and microscopic aberrations [46,47], as well as increased sensitivity to DNA damaging agents [48] and PARP1 inhibitors [49].

Despite their high penetrance germline *BRCA* mutations are present in only around 12% - 20% of unselected sporadic cases of invasive disease [50–52]. Notwithstanding that

mutations found only in the tumour in both genes may be important in a proportion of sporadic cases. Both of these studies screened both high and low grade cases revealing the frequency of mutation in borderline or low grade disease was 0%. A histological variation in the distribution of BRCA mutations was also observed. BRCA mutations were found in serous and endometrioid but not mucinous carcinomas (χ^2 p=0.005) (after exclusion of borderline cases).

A link between BRCA status and average age at diagnosis has also been noted. Carriers of *BRCA1* mutations were, on average, diagnosed 4 years earlier than cases of sporadic disease, for whom mean age of diagnosis was 56, while *BRCA2* carriers were on average diagnosed two years later at 58.

Hereditary Non Polyposis Colorectal Cancer (HNPCC), Lynch Syndrome

Lynch syndrome or hereditary non-polyposis colorectal cancer (HNPCC) is a dominantly inherited cancer syndrome caused by mutations in the DNA mismatch repair (MMR) pathway such as *MLH1*, *MSH2*. Members of HNPCC families are at greater risk of developing a number of cancers including colon, endometrioid, stomach, brain and ovarian. The life time risk of ovarian cancer for carriers of MMR group gene mutation is around 6% - 12% compare to about 1.4% for the general population [53]. Mutations in *MLH1* and *MSH2* occur at a similar frequency in Lynch families and confer a similar additional risk [54].

A multicentre retrospective cohort study of families with either a confirmed or probable mutation in either *MLH1* or *MSH2* found a lifetime associated risk of developing ovarian cancer was 6.7% [54]. The total proportion of EOC attributable to mutations in MMR genes is not well investigated however it has been suggested that this is around 2% for invasive disease [55].

Is There Anything Else and Should We Look For It?

Despite the contribution of BRCA it has been estimated they can only explain around 50% of the cases of familial disease [56]. Estimating the proportion of hereditary ovarian cancer due to BRCA mutations is difficult not least due to distinguishing genuine clustering due to high risk allele inheritance verses random clustering by chance. But by examining families with a high frequency of ovarian while ignoring breast cancer combined BRCA mutational

frequencies have ranged from 52% - 81% [57,58]. These figures fall to 36% - 63% when removing families with cases of breast cancer. Suggesting the presence of other high penetrance alleles segregating through these families conferring the excess heritable risk, such estimates come with the caveat that mutational screens frequently rely on hotspot methods and therefore undetected mutations in known susceptibility genes are likely to explain a proportion of the these cases. The contribution of any such hypothetical undetected high penetrance susceptibility gene is likely low, or in other words any such allele is likely rare, as linkage studies of the type that discovered *BRCA1* and *BRCA2* would likely have led to its discovery. Accordingly a number of separate research groups were refining the linkage regions around *BRCA1* and *BRCA2* from multiple families, suggesting that the vast majority of heritable cases are accounted for by these genes. In fact a meta-analysis of multiple breast and ovarian cancer families suggested that in around 85% of ovarian cancer cases either *BRCA1* or *BRCA2* were the likely causal agents, due to linkage to the relevant chromosomal regions [59]. This question was addressed in more detail in a screen of 112 families with at least two first degree relatives with ovarian cancer in which the full coding sequence of both genes was sequenced. In addition other known aberrations were assayed for, including hemizygous deletions, that wouldn't be detected using conventional sequencing of genomic DNA. By focusing on families with multiple cases, which the authors claim will enrich for genuine pathogenic mutations, by excluding families with random clusterings breast and ovarian cancers cases, that might be mistaken for HBOC, *BRCA1* and *BRCA2* mutations were found in 71% and 22% of cases respectively [60]. Although this method may have resulted in the exclusion of families with mutations in genes with a significant but lower penetrance than either BRCA gene, the authors suggest 93% of HBOC can be explained by mutations in these two genes.

Rare High Penetrance Alleles

Recently mutations in three DNA repair genes have been identified conferring an increased risk of ovarian cancer. Interestingly two of these are members of the RAD51 family which play an important role in HR and interact with both BRCA1 and BRCA2. Both studies targeted families with hereditary breast and ovarian cancer without confirmed BRCA mutations. Cases underwent full gene sequencing for either *RAD51D* or *RAD51C* revealing mutations in both. Mutations in RAD51D were associated with a RR of ovarian cancer of 6.3

(CI 95% 2.9-13.8 P= 4.8×10^{-6}) [61] whereas a non-synonymous variant of RAD51C (G264S) was associated with combined breast and ovarian cancer (OR=3.4 95%CI 1.51–7.80 P=5.3×10^{-3}) [62]. An interesting approach was used by deCODE genetics, next generation whole genome sequencing of 457 Icelanders identified novel polymorphisms that were subsequently imputed from a population of nearly 42,000 genotyped using SNP chips. The data set revealed a rare (0.41% allelic frequency) frameshift mutation in BRIP1 (FANCJ) associated with an increased risk of ovarian cancer (OR= 8.13 P=2.8×10^{-14}). Tumours from sufferers with this variant also had LOH at the loci implying a classic tumour suppressor function for this gene [63].

Allele frequencies of these genes in the wider population are likely to be very rare. While the BRIP1 mutation might explain a significant proportion of hereditary HBOC in Iceland it seems likely that this is a founder mutation and will not be found elsewhere at the same level. Given that estimates of all *BRCA1* and *BRCA2* mutation frequencies are between p=0.003-0.0015 [64] and the relative risk of the mutant allele was greater than for *BRCA2* mutations it seems unlikely this discovery will have any relevance outside this population.

1.42 Somatic Low Penetrance Alleles

Less research has been carried out into the genetics of predisposition to sporadic ovarian cancer. In order to identify low penetrance EOC susceptibility loci, in 2009 a large genome wide association study was published that carried out a three stage genotyping exercise using in phase I, 620,000 SNPs discovery, 1890 case 2350 controls, phase II 24,000 SNP validation 5000 case 5400 controls and phase III, single SNP population validation, 3000 case and 5400 controls. The most significant association with ovarian cancer was found for a 12 SNP linkage disequilibrium block on chromosome 9 (9p22.2). The strongest association, for the SNP rs3814113 (P-trend =5.1×10^{-19}) based on data from all three stages, was associated with a decreased risk of developing disease for carriers of the minor allele (OR =0.82, 95% CI 0.79–0.86). rs3814113 is found in a non-coding region between two genes with no obvious role in cancer. The authors estimate the SNP accounts for 0.7% of the hereditary risk of ovarian cancer [65]. The same data set also found significant SNPs located within *MYC* for which the minor allele was also protective (OR=0.76 95% CI 0.70-0.81 P=8×10^{-15}) and *HOXD3* for which the minor allele was associated with increased risk (OR=1.2 95% CI 1.14-1.25 P=3.8×10^{-14}) [66]. The discovery of variants in *MYC* modulating

risk is not surprising as amplification at this loci is a very common feature of ovarian cancer, see section 1.77 - Molecular Characteristics of High Grade Serous Tumours.

1.5 Treatment, Improvements in Survival, Relapse and Recent Novel Therapeutics

1.51 Standard Treatment

Improvements in both 5 year survival, up from 42% to 46% since 1998 [67] and median progression free survival, have been achieved over the past three decades. This has been achieved by, improvements in surgical techniques, the introduction of first cisplatin, in the 1980s and then paclitaxel in the 1990s. Currently the standard first line treatment is surgical debulking followed by combinational chemotherapy of a platinum agent, usually carboplatin, plus a taxol, usually paclitaxel. Carboplatin has largely replaced cisplatin due to its reduced toxicity. Platinum plus taxol is given regardless of stage at diagnosis. Two large studies have demonstrated the superiority of firstly platinum alone compared to no treatment after cytoreductive surgery for stage I/II (5-YRS HR=0.67 95% CI 0.50-0.90 P =.008) [68], and both platinum alone and in combination with taxol in stages III/IV [69].

Despite these advances, improvements in overall survival have been less marked. One estimate suggests that 10 year survival before and after 1988 has increased from 32.2% to 34.4% [70]. More significant gains in 10 year survival for those diagnosed with early stage tumours are overshadowed by the low proportion these cases constitute.

1.52 Surgery

Women presenting with invasive EOC cancer will generally undergo a complete hysterectomy, bilateral salpingo-oophorectomy with omentectomy, debulking of as much of the tumour mass as is reasonable. The success of cytoreductive surgery is strongly correlated with patient survival.

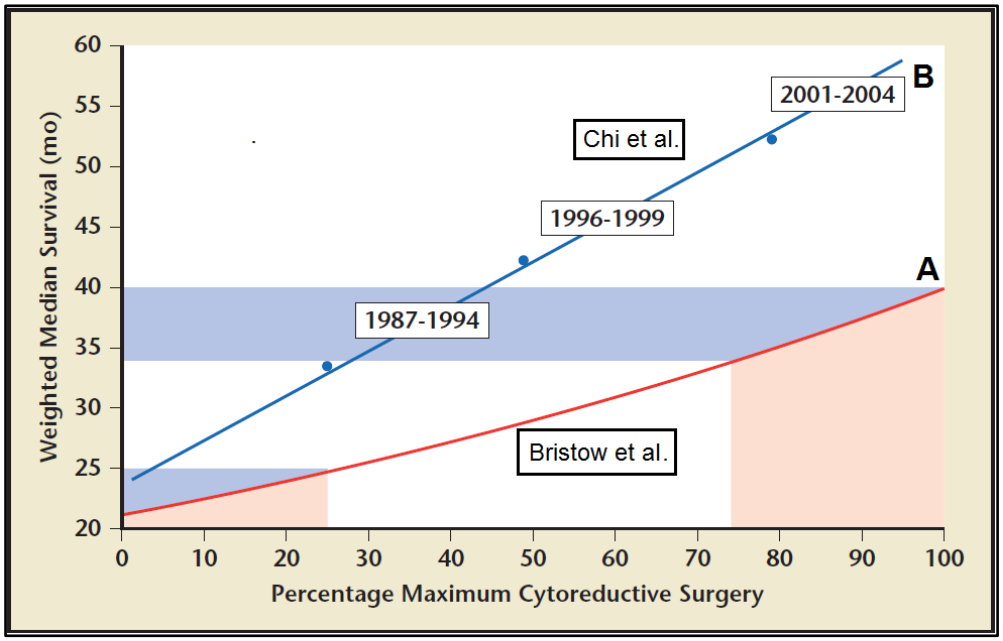

Figure 4. Correlation between percentage of maximum of cytoreduction in debulking surgery, showing the importance of surgical quality and survival. Adapted from [71].

A large meta-analysis of over 6,000 patients who underwent debulking followed by chemotherapy found a linear correlation between the extent of residual disease and survival (P=0.001) [72]. Changes in the recommendations regarding, extent and thoroughness of cytoreductive surgery contributed significantly to improved survival.

Figure 4 shows the relationship observed in the meta-analysis by Bristow et al in line A. Line B shows the trend towards lower remaining residual disease, after debulking since 1987 and the associated increase in survival. In line B, each point relates to the average percentage of disease mass removed for the period shown.

1.53 Relapse and Resistance

Low overall survival in ovarian cancer is primarily due to relapse with platinum resistant disease after initial treatment. Initially response to combination chemotherapy after surgery is high. 80% of patients exhibit a significant reduction in tumour mass and in 40–60% of cases the presence of tumour mass is undetectable after their first course of treatment [73]. However the majority of patients will relapse. Median progression free survival of combination therapy is around 18 months [74]. And subsequent periods of remission are almost

exclusively shorter. The duration of remission can also be used as a prognostic indicator of the probability of response to a second line of therapy.

Response rates of around 50% are seen with single-agent carboplatin treatment in tumours that relapse after more than 12 months following initial treatment. This figure falls to around 15% when the duration of remission is less than 6 months, at which point tumours are considered to be platinum resistant [75]. Tumours that are unresponsive to platinum treatment or advance in stage during treatment are classified as platinum-refractory and in such cases patient care is essentially palliative.

1.54 Recent Novel Therapeutics

Various trials have examined the survival advantage associated with different cytotoxic drug combinations, doses, methods of administration and second bouts of cytoreductive surgery. Improvements in survival have generally been either not observed or marginal especially in relation to overall survival.

A consistent beneficial effect has been demonstrated for intraperitoneal (IP) compared to intravenous (IV) administration of chemotherapy. In one such study combining cisplatin and paclitaxel, PFS for IV administration was 18.3 months compared to 23.8 months for the IP group (log-rank test P=0.05) and median OS also increased from 49.7 and 65.6 months, (log rank test P=0.03) [76].

Two new targeted therapeutics have shown promise in recent trials. Bevacizumab is a humanised monoclonal antibody to vascular endothelial growth factor A (VEGFA). VEGFA is an important angiogenic factor released by hypoxic cells which simulates the growth of vascular endothelial cells providing blood flow to a tumour and facilitating its growth. Three trials have examined the benefit of combining bevacizumab with traditional chemotherapy in upfront treatment. Consistent increases in PFS have been observed, for example 10.3 compared to 14.1 months [77] and 8.4 versus 12.4 months [78] for control versus bevacizumab arms. However neither study was able to demonstrate a change in overall survival and increased toxicity in the combination treatment seems to make the introduction of bevacizumab as a standard treatment unlikely.

Olaparib is a small molecule inhibitor of poly-ADP ribose polymerase (PARP1), an important DNA repair enzyme that has been shown to exhibit synthetic lethality in combination with BRCA inhibition. Synthetic lethality describes the situation in which

inhibition of the function of either one of a pair of proteins has no effect in isolation but when both are inhibited together a cell cannot survive. Logic for the use of this drug is based on the high frequency of BRCA mutations seen in EOC, these concepts are described in more detail at the genetic level in section 1.77 - Molecular Characteristics of High Grade Serous Tumours. The most comprehensive trial examining the effectiveness of olaparib was carried out in relapsed patients and compared to a placebo only arm. An increase in PFS in the treatment arm from 4.8 months to 8.4 months (HR 0.35 CI 0.25 – 0.49 P=0.001) was observed, although there was no interim OS benefit [79]. There is a clear rational behind using olaparib and these promising results warrant further study.

1.6 Monitoring and Screening

1.61 CA125

The most frequently used marker of EOC is the glycoprotein CA125 (also known as MUC16). CA125 was discovered via a screen of antibodies produced from hybridomas, created via the inoculation of mice with ovarian cancer cell lines [80]. Originally termed OC125, as this was the 125th ovarian cancer hybridoma screened, latterly named CA125, for cancer antigen 125, antibodies produced from this hybridoma are now known to target mucin 16, MUC16 [81]. MUC16 is one of a family of cell surface or secreted glycoproteins expressed by epithelial cells that play a role in the lubrication of the epidermal membranes including the lungs, digestive system and uterus. Expression of the antigen was subsequently shown to be present in the serum of over 80% of patients with EOC and levels that correlated with disease progression and response to treatment [82]. Since its discovery CA125 monitoring has become standard practice in the management of EOC and has been evaluated as the basis of a population screen to detect early stage asymptomatic disease. Unfortunately these studies were unable to demonstrate sufficient specificity and as a consequence too many false positives were detected [83]. This can partially be explained by the increased serum levels of CA125 in normal or benign conditions including endometriosis and menstruation [84].

1.62 Screening, beyond Just CA125

Attempts to improve specificity and sensitivity of potential population screens have been made. A recent randomised trial of combination CA125/MUC16 monitoring and transvaginal ultrasound in nearly 80,000 women in the US hoped to demonstrate sufficient positive predictive value (PPV) by combining these two screening methods. A small but non-significant decrease in mortality was observed in the test group but the authors suggested was not justified by the unnecessary surgical intervention and associated complications due to false positives [85]. Screening based on multiple serum markers may provide greater accuracy in the future however such tests are still in the early phase of development. For example Yurkovetsky et al. claim they were able to achieve a high enough specificity to use as a population screen by assaying serum levels of CA125, HE4, CEA and VCAM-1 [86].

The low overall incidence of EOC makes the introduction of national screening programs unlikely until the PPV (the proportion of true positives to all positive results) of potential diagnostic techniques can be improved. The relatively low incidence of EOC increases the requirement of screening methods with very high specificity (the proportion of true negatives identified) in order to prevent an excess number of false positives. As such improving the efficacy of existing treatments may be the most viable method of increasing overall survival and progression free survival in cases of platinum resistant disease.

1.7 Different Types of Epithelial Ovarian Cancer

1.71 General Differences

Epithelial ovarian tumours can be further subdivided, generally into 5 histological subgroups, shown in Table 1 and Figure 5. Until recently all tumours were thought to arise from epithelial tissues descended from the developmental coelomic mesothelium, which lines the peritoneum, ovaries, fallopian tube and uterus, although this may not be true for a large proportion of mucinous tumours that may have been misclassified as ovarian, see below.

Histological Type	Proportion of all ovarian carcinomas (%)	5 year survival (%)
Serous	52.2	38.0
Endometrioid	13.1	70.9
Mucinous	10.2	64.9
Clear cell	5.3	61.5
Undifferentiated	16.8	18.3
Mixed/Mullerian	2.3	29.8

Table 1.Tumour types listed in order of frequency with the corresponding frequency of the epithelial group that each consists. * Mullerian type sometimes not listed in the epithelial group. Data adapted from [7].

The subtypes are based on their differing histological appearance and their names reflect their similarity to other non-cancerous tissues found in the peritoneum. The prognosis for different subtypes of EOC differs substantially, hinting at a divergence in their molecular aetiology.

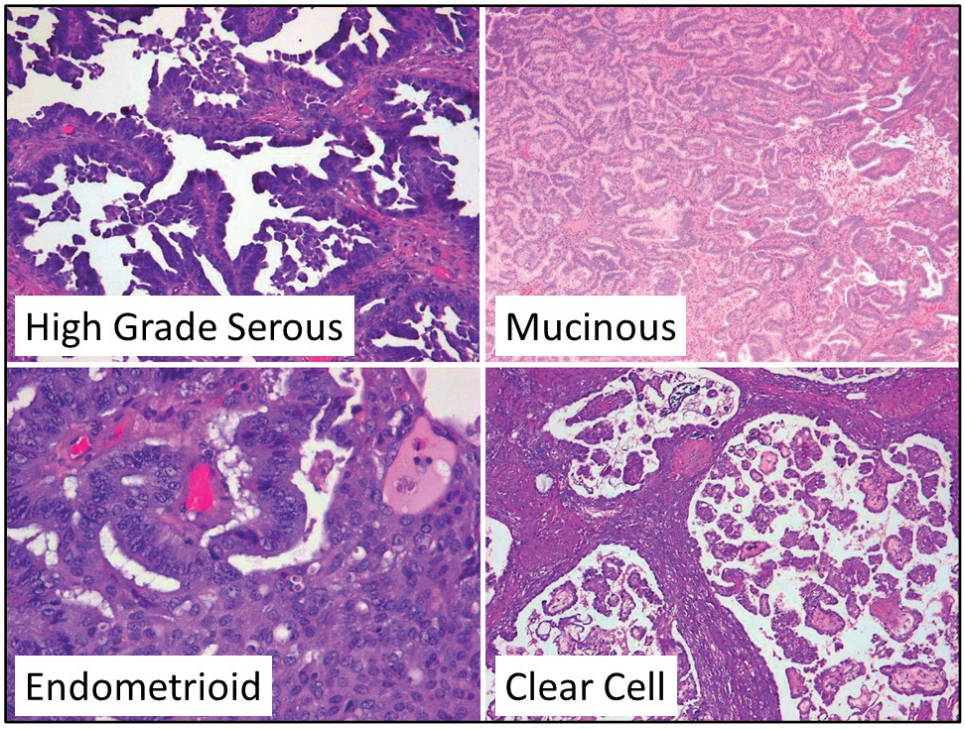

Figure 5. Histotypes of epithelial ovarian cancer showing difference in appearance between the each type. Figure adapted from [87]

1.72 Structure and Development of the Ovary; Some Ovarian Cancer Dogma

Surrounding the ovary, and continuous with the lining of the peritoneal cavity, is a single layer of phenotypically undifferentiated mesothelial cells known as the ovarian surface epithelium (OSE). The OSE and the mesothelial lining of the peritoneal cavity are derived from the same mesodermal coelomic epithelium [88]. During embryonic development the coelomic epithelium overlays the gonadal ridge, the parent structure of the mature ovaries. Differentiation of the coelomic epithelium not only gives rise to the OSE but also the Mullerian ducts, a developmental structure that subsequently forms the fallopian tube epithelium the endometrium and endocervical epithelium [89]. It is generally considered that the tissue of the OSE represents a less well differentiated phenotype than other tissues of the reproductive tract including the endometrium and the endocervix [90,89]. This position is supported by the observation that unlike the remainder of the extant lineages of the coelomic epithelium, OSE does not express the cell surface marker MUC16 (CA125) except in inclusion cysts [91]. This suggests MUC16/CA125 represents a marker of differentiation present in all other coelomic cell lineages not present in the more 'primitive' less differentiated OSE. Further, once neoplasia begins in an inclusion cyst, an invagination of OSE in the ovarian stroma, neoplastic cells become committed to one of the other coelomic cell lineages and begin to express MUC16/CA125.

Partly due to the observation of inclusion cysts the established dogma in ovarian cancer has been that tumours arise from the OSE. The trauma associated with ovulation resulting in OSE tissue becoming trapped within the stroma and exposed to high levels of hormones within these lesions were widely theorised to be crucial events in carcinogenesis. According to this theory tumour progression was associated with differentiation resulting in tumours that more closely resemble mullerian tissues lineages of the fallopian tube, in the case of serous tumours, or the endometrium, in the case of endometrioid tumours, than the undifferentiated OSE. Whilst this model of pathogenesis is not without some evidence it runs contrary to the paradigm as observed in almost all other cancers, that tumour progression is associated with the development of a progressively less well differentiated phenotype.

1.73 Endometrioid Ovarian Cancer

Endometrioid ovarian cancers, so called due to their histological similarity to the endometrium, are associated with a relatively good prognosis, 5 YSR rates are around 71% - 78%. They are generally diagnosed at an early stage (I/II), in over 85% of patients [92]. Suffers of endometriosis are at around two fold risk of developing this type of cancer [93] and around 20% of cases have a history of the condition. Our knowledge of the molecular characteristics of endometrioid ovarian cancer is based largely on studies that have expanded on observations from serous tumours regarding the distribution of KRAS and BRAF mutations. Around a third of endometrioid ovarian tumours are mutant for either KRAS or BRAF in a mutually exclusive fashion with a frequency of around 7%-10% [94] and 24% respectively [95]. P53 mutation is observed in around 60% of cases where mutation status has been correlated negatively with survival [96] and is more frequent in high grade than low grade being found in >80% and <25% respectively [97].

Unlike serous tumours a significant minority, around 30%, of endometrioid tumours possess putative inactivating mutations in the chromatin remodelling gene ARID1A [98] which have been associated with a loss of protein expression in around 50% of cases [99]. Expression profiling of EOC suggested low grade endometrioid tumours cluster with low grade serous whereas high grade endometrioid grouped with high grade serous tumours in hierarchal clustering [100] and that there is a significant difference between those cases associated with endometriosis and those that are not [101].

1.74 Mucinous Ovarian Cancer

Mucinous cancers derive their name from their phenotypic similarity to cell of the endocervix and colon. They account for around 10% of ovarian cancer cases and have a relatively good prognosis. 5-YSR rates are about 65% and around 80% are diagnosed in either stages I or II [92]. Similarly to endometrioid cancer they have been reported by frequently be mutated for *KRAS* in between 38% - 50% [94,102] however conversely this appears to be mutually exclusive with *ERBB2* amplification which is seen in around 20% of cases [102]. *P53* mutations have been observed in around 50% of cases and mutation status was also associated with poor prognosis [103]. Interestingly the legitimacy of the ovarian categorisation of mucinous cancers has been questioned with the observation that around 70% of unselected

cases are metastatic, and originate from the gastrointestinal tract. This suggests primary ovarian mucinous cancers actually represent a far lower proportion of all ovarian carcinomas [104,105].

1.75 Clear Cell Carcinoma

The proportion of tumours with a clear cell histology is significantly higher in Asians versus other ethnicities (P< 0.001). It is more likely to be diagnosed at early-stage (67.3% stage I/II) compared to 19.2% in serous. The majority of cases, around 80%, are diagnosed in stage I or II [92]. Despite the high relative 5-YSR, adjusted for stage, patients with clear cell carcinoma do slightly worse than serous patients for all stages [106]. Clear cell tumours respond particularly poorly to platinum based chemotherapy, with response rate of between 11% to 15% [107]. Endometriosis is a risk factor conferring a 3 fold increase in the likelihood of developing the disease. Cases of Lynch syndrome are more likely to have a clear cell morphology [108]. Unlike either high or low grade serous tumours clear cell carcinoma does not appear to be driven by mutations in either *p53* or *BRAF* mutations found in only 5.3% (n=75) and 1.8% (n=55) of cases respectively, *KRAS* mutations were more frequent seen in 14% (n=92) data compiled from [94–96,109,110]. Instead they are characterised by activating mutations in PIK3CA, observed in around 40% of cases [111] and putative inactivating mutations in ARID1A observed in between 46% and 57% of cases [98,111] which have been associated with loss of protein expression in around 40% of cases [99].

1.76 Undifferentiated

Very little is known about this group and they represent a ‘catch all’ for tumours that are not easily categorised to any of the other histotypes. However their lack of differentiation and very poor 5-YSR may suggest they are aggressive, high grade variants of either serous or a combination of other histotypes.

1.77 Serous Ovarian Cancer

More common than all other types of malignant ovarian tumours combined, serous tumours tend to be aggressive, invasive and associated with a poor 5 year survival ranging from 38% to 42% data adapted from [7] and [10] respectively. Serous tumours are so called because they exhibit phenotypic similarities to cells of the fallopian tube epithelium. Well differentiated serous tumours have a predominantly papillary phenotype, however exhibit a large degree of heterogeneity in appearance. For example they may be solid or cystic or a mixture of both [89].

Serous lesions may be either high or low grade. It was generally considered that both forms were a contiguous disease, in which low grade disease progressed to high grade over time as the tumour became more malignant and invasive. Recent evidence have cast doubt on this assumption suggesting they are in fact distinct diseases [112] with distinct molecular profiles [113], aetiology [95] prognosis, [114] sharing a similar histology, but that do not progress for low to high grade. Due to the subjectivity of grading, estimates of proportions of individual grades vary, however according to the Modified American Joint Committee on Cancer staging system grade 1 tumours represent 6.3% [112] of serous tumours. Using a two tier grading system based largely on the presence of atypical nuclei Seidman et al suggest that low grade tumours represent 9% of unselected serous cancers [12]. Low grade tumours tend to be better differentiated, that is histologically they more closely resemble the fallopian tube epithelium than high grade tumours, and have a greater five year survival 70.7% compared to 40% for high grade [10] and present at a lower mean age of 45-57 years compared to 55-65 for high grade serous [12,114,115]. Similarly to HGS, low grade tumours also present at an advanced stage with 74-96% of patients diagnosed with stage III/IV disease [92,115].

Molecular Characteristics of Low Grade Serous Tumours

Low grade tumours are characterised by activating mutations in either *KRAS* (25-35%) or *BRAF* (33-36%), with a mutation present in one or the other, generally in a mutually exclusive fashion, in 66-68% of cases [95,116]. The true proportion of *KRAS* and *BRAF* mutations may be higher as each of these studies used a mutation hotspot sequencing approach. Both KRAS and BRAF play important roles in activating the MAPK pathway, transducing signals from extracellular growth factors to the nucleus. Both are frequently mutated in a range of cancers including colon [117,118] and lung [119]. In colon cancer activating mutations in either occur early in neoplasia before malignant transformation in around 65%

of cases suggesting they are a key aberration in carcinogenesis for the majority of tumours [120]. Mutational activation of either gene is sufficient to result in constitutive activation of the *MAPK* pathway. Corresponding Anglesio et al discovered mutations in *ERBB2* in 6% of low grade tumours, these were also found to be mutually exclusive with *KRAS*/*BRAF* mutations [121]. Amplification of *ERBB2* has also been shown to cause constitutive signalling via the *MAPK* pathway. Taken together this suggests that selection of mutations leading to increased signalling through the *MAPK* pathway is the most common feature describing low grade serous tumours occurring around 75% of cases.

It remains to be seen what additional proportion of LGS cases will be accounted for by mutations to other MAPK pathway members other candidates would likely include ERBB1, PTEN and PI3K.

Molecular Characteristics of High Grade Serous Tumours

High grade serous (HGS) tumours are characterised by *p53* mutations in almost all cases (96%) [122]. This is in contrast to low grade serous tumours where p53 mutations found in only around 8% of cases [123]. Contributing to the hypothesis that HGS and LGS disease are derived from separate precursor lesions and do not form a disease continuum, *BRAF* and *KRAS* mutations were only observed in 0% and 12% of HGS cases [95,116].

Mutations in *BRCA1* or *BRCA2* were found in 20% of cases; of these 17% were germline the remaining 3% being unique to the tumour [122]. In addition *BRCA1* hypermethylation associated with reduced expression was observed in a further 11%. In total 33% of all HGS lesions were predicted to be deficient in the expression of functional BRCA1 or BRCA2 through either mutation, methylation or deletion. Around a half of all HGS tumours are predicted to be defective in homologous recombination repair due to the loss of functional expression of other pathway members.

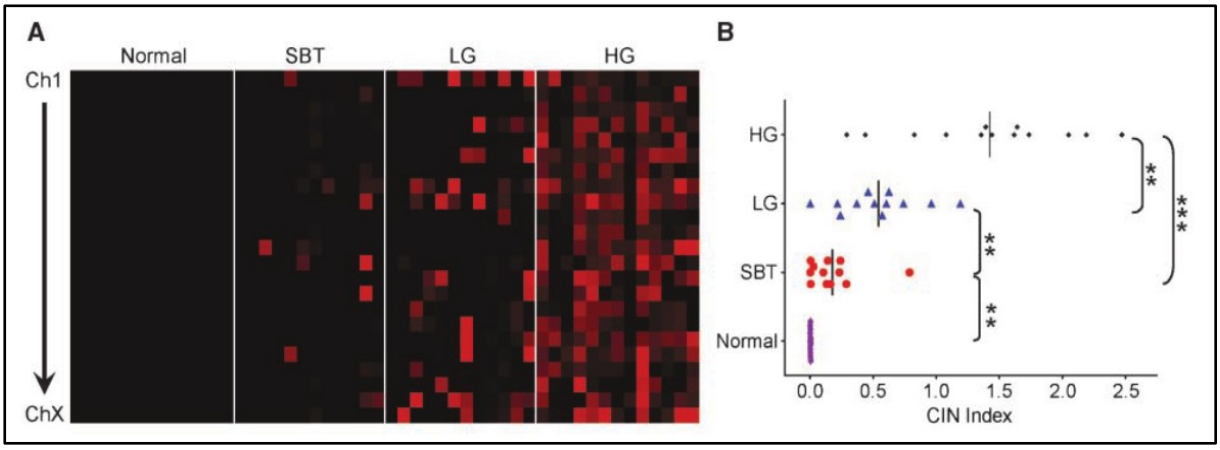

Figure 6. **A.** Showing the chromosomal instability number (CIN) for each chromosome listed vertically, black is low, red is high, in normal tissue, SBT (serous borderline) LG (low grade serous) and HG (high grade serous). Each horizontal block represents one case. **B.** Shows the average CIN per case showing significant differences between each group. Taken from [124]

On a genomic scale, the use of high resolution array comparative genomic hybridisation (aCGH), has demonstrated that HGS tumours exhibit a greater extent of chromosomal instability than normal tissue and LGS tumours. This difference is highlighted in Figure 6. A, shows the average chromosomal instability for each chromosome shown in horizontal rows and per case in the vertical columns for normal controls, serous borderline tumours (SBT), serous low grade (LG) and high grade (HG) tumours. The total genomic instability estimated by the chromosomal instability number (CIN) is shown in B, demonstrating the difference observed between low and high grade.

This result has been duplicated in numerous studies indicating that large scale and a high number of genomic alterations are common features of HGS EOC. Figure 7 shows the combined copy number changes from 361 cases of malignant serous ovarian cancer showing the high frequency of copy number changes in these tumours, while this data set includes LGS the low number and small scale of copy number changes will not significantly change the overall picture. A number of specific copy number changes have also been associated with survival and are therefore likely to contain important oncogenes or tumour suppressor genes [124–126]. Amplification of 8q24 containing the well know oncogene *MYC* is seen in between 72% and 78% of HGS tumours. MYC is a nuclear transcription factor which has a role in growth and survival that has been shown to be either amplified or overexpressed in numerous cancers including breast, lung and colon [127,128].

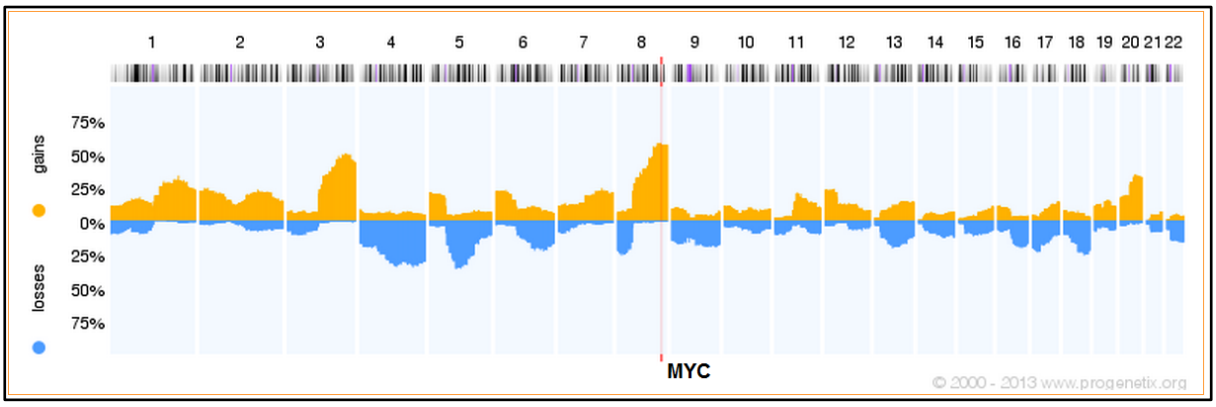

Figure 7. Combined copy number changes from 361 cases of serous ovarian tumours with the MYC locus highlighted on the distal arm of chromosome 8. Proportion of cases with amplifications and deletions over 1Mb windows shown in yellow and blue respectively. Data downloaded from [129].

Deletion of 13q14 containing *RB1* has reproducibly been shown in between 11%-49% of cases. RB1 encodes the well-known cell cycle check point regulator retinoblastoma which plays an important role in inducing G1 cell cycle arrest in response to, amongst others DNA damage.

Amplification of 19q12 containing *CCNE1* is frequently observed, present in between 43% and 45% of cases, and amplification of this loci has been correlated with reduced survival. Perhaps the most common functional alteration observed in HGS EOC is the overexpression of cyclin E1, (*CCNE1*). Previously known for its proto-oncogenic properties in other cancers, CCNE1 has been reproducibly shown to be both genetically amplified, in between 16% and 65% of cases [125,130,131], overexpressed at the mRNA level in around 20% of cases [113,122,125] and correlated with a poor prognosis [122,125]. CCNE1, like all cyclins, has a highly regulated and cell cycle specific expression profile. Expression of CCNE1 peaks in late G1 and is maintained through S phase where it interacts with CDK2 allowing it to promote progression through the G1-S phase cell cycle checkpoint. The CDK2/CCNE1 complex phosphorylates various downstream targets the consequence of which is the expression or inactivation of genes generally required for or inhibitory to DNA replication respectively, for example PCNA and pRB [132].

Two large expression profiling studies of HGS tumours were both able to stratify cases in to four reproducible expression groups with differential survival characteristics, by hierarchical clustering. Both studies identified a mesenchymal cluster characterised by the

expression of specific HOX genes and an immune type group characterised by chemokine and chemokine receptors expression and BRCA1 mutation [100,133,134]. F-score variation analysis between these four groups showed significant correlation suggesting they represent robust different molecular subtypes of disease. The TCGA group was also able to identify a gene signature that was able to significantly distinguish between high and low PFS groups that were validated in three independent data sets, suggesting they are robust and reproducible.

1.78 A New Method for Grading Serous EOC

The realisation that LGS and HGS have unique genetic backgrounds has contributed to the suggestion of a new criterion for grading EOC reflecting this. Not only do LGS tumours not generally appear to progress to HGS but they also respond to chemotherapy differently. Despite the higher 5-year survival and low malignancy of LGS tumours they tend to show a poorer response both clinically and *in vitro*, particularly to platinum agents and taxol [11,135]. A less biased and more standardised approach to tumour grading would likely benefit both patient treatment, by ensuing the appropriate use of chemotherapy, as well as furthering research by improving unambiguous classification based on molecular evidence. As yet the efficacy of any MAPK pathway inhibitor in the treatment of *KRAS*, *BRAF* or *ERBB2* mutant LGS has yet to be formally assessed.

A number of different methods, quantifying various attributes, have been suggested as the basis of a two tier grading system, including those developed by Shimizu/Silverberg [9] Malpica et al [115] and Seidman et al [12].

The criteria established by Malpica et al, using a two tier grading system based on the presence of nuclear atypia and proportion of mitotic cells, has proved to be superior to two newer two tier grading systems, as well as the older FIGO three tier system in two separate studies. Analysis is based on the ability of each criteria to maximally separate the survival curves of cases assigned to either high or low grade categories. The log rank P value of the survival differences were P=0.02, P=0.92 and P=0.25 for the Malpica, FIGO and Shimizu/Silverberg grading criteria and respectively (n=100) [115]. The Malpica criteria also outperformed the Seidman criteria in an independent assessment, log rank P values were P=0.065 and P=0.1 (n=113) [12]. Unfortunately none of the cases were accessed at the

molecular level for the presence of *p53* or *KRAS/BRAF* mutations to assess the correlation of molecular and phenotypic diagnoses.

1.8 Theories of Pathogenesis

1.81 Incessant Ovulation

A number of theories have been proposed to explain the pathogenesis of EOC. One of the earliest and perhaps most prominent of these has been the 'incessant ovulation' hypothesis which was originally published in the early 70s [136]. In this model, repeated ovulation through the OSE causes trauma, both exposing the ovarian stroma to the estrogen rich environment of the lumen and requiring increased proliferation to repair the damage. The later contributing to the accruement of replication errors and driving neoplasia [136]. Incessant ovulation received a boost with the observation of inclusion cysts, cells of the OSE that become trapped in the stroma of the ovary. In these presumptive precursor lesions the OSE appears committed to a more mullerian phenotype, possibly representing an intermediary between normal OSE and one of the more differentiated EOC subtypes [137]. Inclusion cysts have also been shown to express CA125/MUC16 unlike normal OSE [91].

A number of epidemiological observations also support this theory including the protective effects of pregnancy, oral contraceptives use and breast feeding all of which suppress ovulation. In addition ovarian carcinoma in non-human mammals appears very rare. It has been suggested seasonal breeding species or reflex ovulators (species that only ovulate in response to intercourse) are far less likely to reach the sufficient ovulation burden to initiate carcinogenesis [138]. Finally the age standardised incidence rate (ASR) of ovarian cancer of any type, is highest in developed nations and has been steadily increasing corresponding to both regional differences and demographic trends in birth rates.

Despite an apparent logical underpinning the incessant ovulation hypothesis as a model it may be too simplistic. It cannot account for, firstly why progestin only oral contraceptive use, which does not prevent ovulation, also reduces the risk of EOC. Secondly why tubal ligation is at least as good at reducing risk as BSO (except in the case of BRCA carriers) but also does not prevent ovulation. In addition recent molecular evidence has pointed to an alternative tissue, other than the OSE, as the source of precursor lesions of the majority of EOC.

1.82 The Gonadotrophin Hypothesis

The gonadotrophin hypothesis is based on evidence from animals that in certain contexts when exposed to elevated levels of gonadotrophins were at greater risk of ovarian neoplasia. Rats that have had a bilateral oophorectomy where one of the ovaries is retained and transplanted to spleen, prevents estrogen secreted from the ovary from circulating systemically and eliciting its negative feedback on the hypothalamus. Usually estrogens bind to their receptor in the hypothalamus inhibiting the release of gonadotrophin releasing hormone (GnRH) [139]. The consequence of removing oestrous negative feedback is increased secretion of luteinising hormone (LH) and follicle stimulating hormone (FSH) from the pituitary [139]. The ovary transplanted to the spleen of the rats in this experiment exhibited significantly increased levels of neoplasia that was not observed in rats where one ovary was left *in situ*. [140].

More modern evidence has provided support for the hypothesis, levels of serum LH and FSH were found to correlate with malignancy in patients of EOC being lowest in ovarian cysts, then borderline tumours and highest in invasive tumours [141]. The gonadotrophin hypothesis also helps to account for the increase in incidence of EOC with age as LH and FSH levels rise throughout life and are particularly high at and soon after the menopause [142]. In addition it can account for progestin only OC reducing the risk of EOC despite not preventing ovulation.

Despite these improvements on the incessant ovulation hypothesis the theory is unable to account for why gonadotrophin rich infertility treatment is not associated with increased risk of developing invasive cancer. Also studies examining the relationship between gonadotrophins and tumour malignancy found that levels of *FSH* receptor (FSHR) and LHR mRNA were lower in high grade tumours compared to borderline cases [143] and normal OSE [144]. Finally the period a women breast feeds for after childbirth confers additional protection against developing the EOC [21] despite being associated with elevated levels of FSH [145].

1.83 The Hormonal Hypothesis

The hormonal hypothesis represents a more subtle attempt to account for some of the inconsistencies of the incessant ovulation and gonadotrophin hypotheses. It suggests that estrogen and progesterone exposure of the ovaries have differing effects. Specifically that estrogens are neoplastic and progestins are antineoplastic. Evidence on which this is based is more indirect than the two theories described above.

A number of groups have shown that treatment of certain ovarian cancer cell lines with exogenous estradiol (E2) increases proliferation [146–148]. Normal cultured OSE responded in a similar manor to E2 stimulation [146]. Levels of estrogens are far higher in ovarian tissue than serum, around 100 fold, in disease free women [149] exposing the OSE and fallopian tubes to high levels of this mitogenic hormone. Estrogen has also been shown to be carcinogenic in a number of tissues not least breast tissue [150]. It has been suggested that expression levels of estrogen receptor 1 (ESR1) correlate with tumour progression [151]. Due to a potential role for ESR1 a number of trials have accessed the efficacy of the estrogen receptor antagonist, tamoxifen, in the treatment of platinum refractory or relapsed disease. Some potential activity was shown in a meta-analysis of tamoxifen only treatment in a combined 623 cases, response rates of 9.8% were reported with disease stabilisation in 31.9% [152]. Taken together this suggests a scenario in which cells may acquire the ability to respond to estrogen signalling in an aberrant fashion, possibly by up regulating their estrogen receptors, and that this is an important event in tumourigenesis playing a functional role in driving cell growth and survival, if only in a small proportion of cases.

The evidence implicating progesterone is a little more convincing. During pregnancy levels of progesterones, and estrogens, rise consistently however progesterone maintains a higher absolute level throughout and this could account for the risk reduction associated with parity [153]. Twin pregnancies are associated with elevated levels of the progesterone P4 relative to singleton pregnancy [154] and a number of studies have shown an additional protective effect against EOC in women of twin births over single births (RR ranged from 0.81-0.85) [155–157]. This despite the fact that women who experience twin pregnancies tend to have elevated levels of LH and FSH and ovulate more frequently [158,159] which according to the incessant ovulation and gonadotrophin hypothesis would be theorised to put these individuals at greater risk.

Evidence from hormone replacement therapy (HRT) has provided some extra validity to this theory with the discovery that estrogen only HRT confers around double the risk of developing EOC than combination estrogen and progestin HRT, RR - 1.51 (95% CI 1.21-1.88) and 1.24 (95% CI 1.00-1.54) respectively in cohort studies [31]. Similarly the protective

properties of the combined pill appear to be accounted for by the actions of progestin alone and progestin only preparations may confer a small additional benefit [160]. Molecular evidence has also implicated the progesterone receptor (PGR) in carcinogenesis. A number of studies using both quantitative PCR and immunohistochemistry have shown a marked reduction in the expression of the receptor in both EOC cell lines and tumour tissue relative to either normal cultured OSE or borderline tumours [161–163]. Survival analysis also suggests that reduced expression of PGR is associated with a poor prognosis (HR 0.75 95% CI 0.64 - 0.88 P= 0.0004) [164].

1.84 The Inflammation Hypothesis

As is increasingly becoming evident inflammation plays an important role in the development of many cancers. Numerous conditions and infections have been linked to an increased risk of developing cancer including but not limited to, Crohn's and colon cancer, *H. plyori* infection and gastric cancer, and *Hepatitis C* and liver cancer [165]. Each condition is associated with chronic inflammation that is thought to contribute to neoplasia. A number of epidemiological factors have provided evidence for a potential role for inflammation in EOC that cannot easily be accounted for by the other hypotheses. Both talc and asbestos exposure have been to linked to an increased risk, although the lack of any dose response and clear carcinogenic properties in the case of talc, have questioned causality of such a relationship [166]. Both endometriosis [167,168] and pelvic inflammatory disease [169,170] have both been associated with an increased EOC risk of around 30% and 50-90% respectively, although it appears that the increased risk conferred by endometriosis is not shared equally among histotypes having no effect on the incidence of HGS cancer [93]. Tubal ligation is at least as good at reducing EOC risk as BSO posing the question that, if all the tissues of origin of EOC are present what means of carcinogenesis does the procedure prevent? This observation cannot be easily explained by either the incessant ovulation or gonadotrophin hypotheses. It has been suggested tubal ligation may prevent the passage of either environmental contaminants or inflammation from the vagina/uterus to the ovaries.

One interesting interpretation of the effects of tubal ligation, specifically in light of recent findings suggesting the tissue of origin for ovarian cancer is not the ovary but the fallopian tube, is that it the procedure may reduce risk by both reducing the quantity of

precancerous tissue, the fallopian tube itself, and reducing exposure of the remainder to the mitogenic properties of estrogen released from the ovary.

While it has been suggested that ovulation is an inflammatory process [138] there is scant evidence on upregulation of known mediators or associated physiological responses such as increased vascular permeabilisation or leukocyte infiltration.

Finally the widespread and long term use of non-steroidal anti-inflammatories (NSAIDs) particularly aspirin in the treatment of high blood pressure has allowed an assessment of the ability of these drugs to modulate cancer risk. While aspirin use has consistently been shown to reduce the overall incidence of cancer in both observational and randomised controlled trials the subtype specific benefits are less clear [171,172]. Bosetti et al reported a borderline significant reduction in ovarian cancer (RR = 0.91 95% CI .0.81 – 1.01) in their recent meta-analysis. Baandrup et al examined an overlapping dataset, by excluding borderline and low grade cases they found a significant effect was retained only for invasive tumours (RR 0.88 95% CI 0.79- 0.98). Further examination of any histotype specific effects should help to clarify the role inflammation plays in EOC etiology.

1.10 A New Model of Ovarian Carcinogenesis

These hypotheses have been formulated in light of the assumption that the origin of EOC is the OSE. Despite their differences, in specific drivers of carcinogenesis, the above theories fit in with a model of neoplasia in which ovulation results in the formation of inclusion cysts, exposing OSE cells to the mitogen rich stroma and resulting in increased proliferation. Inclusion cysts give rise to, first borderline tumours, that in time undergo malignant transformation giving rise to low grade then aggressive high grade tumours. While this is occurring the phenotypically uncommitted lesions originating from the OSE become more highly differentiated, more closely resembling either the fallopian tube, in the case of serous or endometrium, in the case of endometrioid cancer. This view appears eminently plausible and had until fairly recently been widely held. But despite the existence of a putative precursor lesion, inclusion cysts, on the putative tissue of origin, a delineation of disease progression through a hypothesised low grade to disseminated high grade disease remained difficult. Low grade tumours generally didn't appear to progress to high grade but instead would maintain their low grade appearance through multiple recurrences [173].

Estimates suggest that around 2% of HGS cancers were originally diagnosed as borderline [115], the error caused by misclassification is however unclear. But despite attempts to identify such intermediary lesions the vast majority of disease presents as advanced high grade disease, apparently appearing *de novo*.

A number of strands of evidence have challenged the assumption that the OSE is the tissue of origin for the vast majority of serous and probably each histotype of EOC. The evidence broadly consists of expression profiling and surgical/histopathological evidence.

Expression array profiling of ovarian tumours had demonstrated that each of the histological subtypes generally appears more similar to the tissue it most closely resembles morphologically than the OSE. For example serous tumours were found to be more similar to normal fallopian tube epithelium than OSE whereas clear cell and endometrioid tumours were more similar to the endometrium [174]. In support of this result an examination of the developmentally important and tissue specific *HOX* gene expression signatures of each histotype again highlighted the close similarity between, serous tumours and normal fallopian tube, and endometrioid tumours and normal endometrium [175]. While these observations are not mutually exclusive with the OSE as the tissue of origin of EOC a more parsimonious explanation would be that each tumour arises from its morphologically similar normal tissue. Correspondingly the suggestion that ovarian neoplasms, supposedly derived from the relatively uncommitted OSE become more differentiated as they progress, a process termed metaplasia, is at odds with the vast majority of other cancers that become less well differentiated throughout their development. In fact the level of differentiation is frequently used as a prognostic marker, whereby better defined more differentiated tumours are more likely to be benign and less aggressive.

It has been noted by surgeons and pathologists for some time that tumours morphologically indistinguishable from high grade serous ovarian tumours are found in extra ovarian settings. These are generally classified as primary peritoneal, (in the case of those not involving the ovary, fallopian tube or uterus) or tubal carcinoma (sometimes referred to as high grade tubal carcinoma) for those limited to the fallopian tube. Given the criteria for classification as ovarian simply requires some involvement of the ovarian surface, any invasion of these cells to the OSE would render them ovarian tumours, by definition. This coupled with the diffuse nature of tumour spread in high grade serous cases creates a situation that perpetuates the notion that the OSE is the source of most peritoneal cancers.

The increased incidence of bilateral salpingo oophorectomy (BSO) in high risk women has provided a novel means of monitoring disease progression in a population with a

40% lifetime risk of developing invasive disease, in the case of *BRCA1* mutation carriers [43,44]. In the US the standard clinical recommendation for such women is to undergo a BSO after child birth to minimise risk [176], and indeed this appears to be highly effective, even given a relatively short follow up of 3.5 years (HR 0.20 95% CI 0.07-0.58 P=0.003) for either ovarian fallopian or peritoneal cancer [177].

A number of studies have examined fallopian tubes and ovaries removed during BSOs from high risk individuals for the presence of occult cancer. Reported frequencies of occult cancer are likely subject to variation caused by the accuracy of different screening methods however four of the largest such studies observed and of incidence between 2.2% and 6.2% [177–180]. All cases were verified as positive for either *BRCA1* or *BRCA2* mutation status. In each, occult tumours were found to be isolated to the fallopian tubes at a frequency ranging from 27% [177] to 100% [180] and in all such cases lesions were consistent with a high grade serous classification. A number of groups also made the observation that occult fallopian tumours or tubal carcinomas occurred at higher frequency at the frimbral end closest to the ovary, which might contribute to early invasion of the OSE reducing the detection rate of lesions isolated to the fallopian tubes. As such the proportion of HGS that originate in the fallopian tube seems likely to be higher than reported here.

Finally in relation to BSO based evidence, women who have undergone the procedure are not immune from developing primary peritoneal cancer despite not possessing the putative tissue of origin. Finch et al found that around 0.7% of cases had developed primary peritoneal cancer despite showing no signs of occult cancer in their BSO specimens after an average of 3.5 years follow-up [177].

The relevance of inherited ovarian cancer to sporadic cancer

These observations raise the issue of the similarity or representativeness of inherited *BRCA1/BRCA2* ovarian cancer to sporadic cases. Differences between the histology of inherited and sporadic cases was recently investigated. In an unselected sample of non-mucinous cases unbiased, full gene and proximal regulatory element sequencing of *BRCA1/2* revealed that 20% of cases were carriers of somatic mutations in one or the other gene and that all of these cases were of a high grade serous histology [52].

Despite the fact tumour mutations in *BRCA1* or *BRCA2* are much less common in sporadic HGS cancer the recent large scale TCGA project multiplatform molecular analysis

suggested that around 33% are deficient in functional BRCA1/2 expression due either to mutation, deletion or methylation and around 50% may be homologous recombination deficient due to loss of functional expression of other pathway members [122]. This coupled with the fact that sporadic HGS and hereditary forms of the disease share similar methylation [181,182], expression [183,184] profiles and morphological features, suggests they are essentially the same disease and therefore will have the same precursor lesions.

There are some clinopathological features which are different between sporadic and hereditary forms of EOC, specifically the age of presentation for *BRCA1* carriers and survival, which tends to be higher in inherited cases [185,186]. The increased survival in BRCA mutation carries is discussed in greater detail in section 3.23 - BRCA1, BRCA2 and Homologous Recombination.

2 IL6, JAK2, STAT3 and ERBB2 with Reference to Ovarian Cancer

2.1 The Discovery of JAKs and STATs

Janus kinase 2 (JAK2) belongs to a family of receptor associated tyrosine kinases including JAK1, JAK3 and TYK2, so called due to the conserved presence of both an active tyrosine kinase domain and adjacent pseudo-kinase domain harbouring inactivating mutations in the catalytic region, a feature somewhat like that of the two faced Roman god Janus. JAK2 was identified in 1991 along with JAK1 by cDNA sequencing using degenerate primers based on the sequence of the already known TYK2 [187]. The first evidence of a mechanistic link between the JAK and STAT family came from a functional screen testing the ability of gDNA containing cosmids to restore interferon α (IFNα) signalling in a deficient cell line. The cosmid capable of rescuing IFNα signalling was found to contain full length TKY2 a known gene of previously unknown function [188].

The STATs (signal transducers and activators of transcription) had been known of for slightly longer, since 1990. In mammals the STAT family contains a total of seven transcription factors which share a number of homologous domains, including STAT1, STAT2, STAT3, STAT4, STAT5a, STAT5b and STAT6 and almost all multicellular metazoans contain at least one recognisable STAT [189]. STAT1 was initially identified as a component of the interferon signalling gene factor complex 3 (ISGF-3) which is rapidly formed in the cytoplasm of cells stimulated with IFNα. Once the complex has formed it translocates to the nucleus [190] where it binds ISRE (interferon stimulated response elements) elements, contained with promoter regions of target genes [191]. The binding of ISGF-3 to its consensus sequence is associated with, most frequently, increased expression via the recruitment of transcriptional co-activators such as EP300 [192]. ISGF-3 was subsequently shown to be composed of STAT1, STAT2 and IRF9 (interferon response factor 9) and that stimulation with IFNα was associated with the rapid tyrosine phosphorylation of both STATs, dimerisation and nuclear accumulation [193]. STAT3 was initially known as the acute phase response factor (APRF) and was identified as a factor whose DNA binding and nuclear accumulation was rapidly activated by IL6 [194]. The following year cloning and sequencing revealed the similarity of this gene to STAT1 and it was renamed STAT3 [195].

2.2 Structure of The JAKs and STATs

2.21 STATs

The conserved domains of STAT proteins, shown in Figure 8, include the amino-terminal (N), coiled-coil (CC), DNA-binding (DBD), linker (LK), SRC homology 2 (SH2), tyrosine activation (Y), and transactivation (TAD) domains [196].

The N- terminal domain has been implicated in dimerisation and protein interaction [197]. The coiled-coil domain mediates an array of protein:protein interactions and been shown to be crucial for the binding of many other regulatory factors including IRF-9 [198]. The DNA binding domain consists of a β-barrel immunoglobulin fold structure that directly binds dimer specific DNA response elements [196]. The linker domain has been implicated in transcriptional activation [199]. The SH2 domain is the most conserved domain among STATs and is crucial for receptor recruitment and dimerisation. The transcriptional activation domain is the least conserved, this divergence presumably allows interaction with a unique suite of transactivators. Through its TAD, STAT1 interacts with a range of proteins including CREB binding protein [200]. Mammals express two transcript variants of STAT1, STAT3 and STAT4 known as α and β. For each the β variant lacks the C-term transactivation domain (TAD) and has been linked with a dominant negative effect over the transcriptionally active α variant [201]. Each STAT contains a tyrosine residue in its TAD that is required for activation and DNA binding. This residue is the target of predominantly JAKs but also other kinases, discussed in greater detail in the section below on activation of JAKs and STATs.

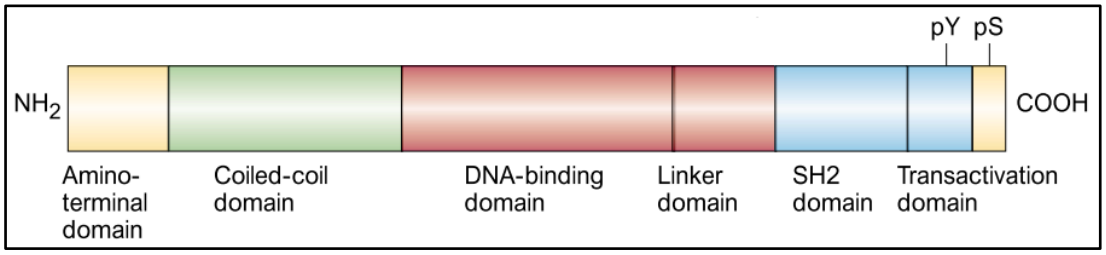

Figure 8. Generalised structure of domains in STAT proteins. From N-terminal domain through to the transactivation domain at the C-terminal. Tyrosine and serine residues subject to phosphorylation are designated with pY and pS respectively, adapted from [202]

STATs 1/3/4/5a and 5b can also be phosphorylated at a conserved serine residue also in TAD contained within the consensus sequence PXSP [203]. The role of serine phosphorylation of STATs is less well understood and appears more STAT specific. Mutational analysis of this residue has shown it is not required for dimerisation or DNA binding but plays a role in modulating the locus specific transcriptional activity of activated STATs possibly by effecting co-activators binding. This effect can be either positive, in the case of IFNγ activated STAT1 at GAS driven genes [204] negative in the case of IRF-1 expression by interleukin 6 (IL6) activated STAT3 [205] or of no effect, for hepatoglobin expression driven by IL6 [206]. Serine phosphorylation can occur in response to a range of kinases including p38 MAPK, MEK1/2 and JNK1 [203].

2.22 JAKs

Mammalian JAKs range in size from 120KDa to 140KDa and contain 7 areas of homology (JH) regions see Figure 9 . These regions fall into a number of recognised protein domains. At the N-terminus and comprising JH regions 5-7 is a FERM (four- point-one, ezrin, radixin andmoesin) domain, which is crucial for cytokine receptor interaction [207]. FERM domains comprise three subdomains; F1 is a ubiquitin-like β-grasp fold, F2 an acyl-CoA-binding-protein-like fold, and F3 which contains a phosphotyrosine binding or PH (pleckstrin homology) domain [208]. The β-grasp subdomain contains a number of residues that in the case of JAK1 are required for interaction and phosphorylation of GP130 [209]. JH regions 3 and 4 exhibit some homology to SH2 domains, however it appears they are not involved in phosphotyrosine binding but rather in receptor binding and membrane localisation [210].

JAKs are perhaps best characterised by their two kinase domains, closest to the C terminal and comprised of JH1 is the active kinase domain, containing a conserved di-tyrosine motif that is auto-phosphorylated after cytokine binding. The second, make up of JH2, is a pseudokinase domain and is devoid of catalytic activity but does play a role in inhibiting the active kinase domain [211]. Clonal mutations in JAK2 at valine 617 (JAK2 V617F) in the pseudo kinase domain are thought to be the causal driver behind the majority of cases of polycythemia vera, essential thrombocythemia, and myeloid metaplasia with myelofibrosis [212,213]. This single amino acid substitution is associated with constitutive activation, elevated levels of auto-phosphorylation and downstream signalling. The valine at this residue appears to function as a inhibitor of JAK2 kinase activity.

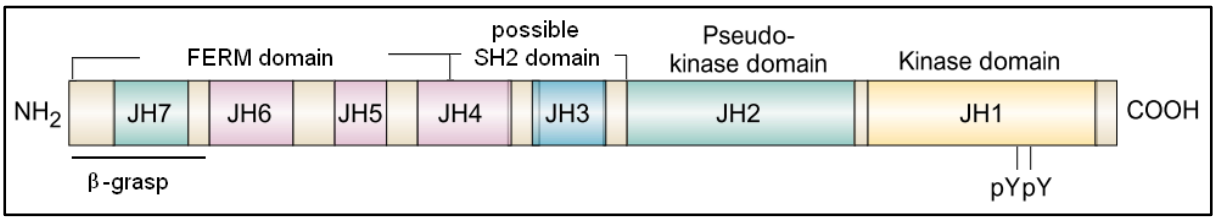

Figure 9. Generalised structure of domains in JAK proteins. From FERM domain at the N-term to kinase domain in the C-terminus. Duel tyrosine residues in the activation loop designated pY adapted from [202].

2.3 Activation of JAKs, STATs and Nuclear Import

2.31 Generalised Activation

Several mechanisms of STAT activation have been described. Classical signalling occurs through the JAK-STAT pathway. This paradigm was established for IFNα signalling and has been broadened by the discovery for the remaining members for the STATs and JAK families.

STATs become phosphorylated in response to a range of cytokines, including interferons, interleukins and other growth and differentiation factors, including but not limited to IFNα, IFNγ, IL6 [214], IL4 [215] and granulocyte and macrophage colony stimulating factor (GM-CSF) [216]. These extracellular messengers have unique but sometimes overlapping effects. For example IFNα induces phosphorylation and dimerisation of both STAT1 and STAT2, whereas IFNγ induces phosphorylation of STAT1 only [193,217]. Consequently IFNα and IFNγ result in the upregulation of unique but overlapping genes. Greater specificity of response can be further specified by tissue specific expression of JAKs, STATs, cytokine receptors and transcriptional co-activators. This specificity confers the ability for different tissues to respond to the same stimulus in apparently contradictory ways. For example STAT3 activation in stems cell is associated with maintenance of pluripotency [218] whereas in B cells it is required for terminal differentiation [219].

STATs are normally present in the cytoplasm in a latent, unphosphorylated, monomeric form, until cytokine binds its cognate receptor at the cell surface. Cytokine receptors are composed of two or more polypeptide subunits and different cytokine receptor subunits are associated with different JAKS. Ligand binding induces receptor subunit oligomerisation

juxtaposing associated JAKS, which auto-phosphorylate and in turn phosphorylate their associated receptor [220]. This creates a docking site for STATs which are recruited to receptors, via their SH2 domains, and also phosphorylated at a specific conserved tyrosine residue, in their TADs, by receptor associated JAKS [221]. Activated STAT then dimerises, forming either homo or hetero dimers, via their SH2 domain and translocate to the nucleus [222]. Specific STAT dimers bind specific DNA response elements inducing the expression of specific genes. For example STAT1 homodimers, induced by IFNγ, bind to gamma activated sequences (GAS) present in the promoters of genes including IRF1, STAT3 and IFNAR2 [223,224]. This type of signalling is also known as type II interferon signalling. In contrast type I interferon signalling as induced by IFNα or IFNβ results in the phosphorylation of both STAT1 and STAT2 and the formation of the ISGF-3 complex which upregulates the expression of genes with an ISRE including OAS, MX1 and MHC class II genes [225].

2.32 Activation of STAT3 with Reference to the IL6-type Cytokine Pathway

The activation of STAT3 occurs broadly in line with the paradigm established for IFNα/γ and STAT1/2. STAT3 is one of the more promiscuous STATs being activated by a wide range of cytokines and growth factors including but not limited to IL6, epidermal growth factor (EGF) [214] leukaemia inhibitory factor (LIF), oncostatin M (OSM), granulocyte and macrophage colony stimulating factor (GM-CSF), [226] and IL10 [227]. As well as being activated via the canonical cytokine/JAK pathway STAT3 can be activated by ERBB1 or ERBB2 [228] and without the need for direct extracellular stimulation by the non-receptor associated SRC family kinase members [229].

Classical STAT3 activation occurs in response to IL6 type cytokines binding to their cell surface receptors. IL6 type cytokines are defined by their common use of the GP130 receptor subunit in conjunction with a ligand specific high affinity receptor subunit reviewed in [208]. IL6 type cytokines are composed of IL6, IL11, LIF, OSM, ciliary neurotrophic factor (CNTF), cardiotrophin factor 1 (CTF1) and, cardiotrophin-like cytokine factor 1 (CLCF1) and each probably activates STAT3 [208]. Each IL6 type cytokine has its own unique high affinity receptor that when bound to ligand forms complex with either one or two molecules of GP130. GP130 expression is ubiquitous, tissue specific responses to IL6 type cytokines are, in part, achieved by a restricted expression profile for ligand specific receptors. For example *IL6RA* expression is largely restricted to certain immune cells, particularly

monocytes and to a lesser extent hepatocytes, whereas OSMR expression is highest in smooth muscle and cardiac mycocytes [230].

GP130, OSMR, and LIFR exhibit significant homology and each receptor contains two highly conserved regions termed box 1 and box 2 in their cytoplasmic domain which play an essential role in JAK binding. Other IL6 type receptors do not contain substantial cytoplasmic domains, cannot recruit JAKs directly, and instead must complex with either GP130 homodimers or a heterodimer of GP130 and LIFR or OSMR to transduce signals. JAKs are constitutively associated with the cytoplasmic domain of each receptor [207] and in the case of JAK1 and GP130 this association is particularly high affinity [231]. Expression of a truncated form of the cytoplasmic domain of GP130 is sufficient for JAK association [232] and mutations in box 1 are capable of abolishing JAK1 and JAK2, binding [233], phosphorylation and signal transduction [232]. Similar results were observed for OSMR, where mutations in box 1 abolished JAK1 binding [234].

GP130 can associate with multiple JAKs; correspondingly treatment with IL6 has been shown to lead to the phosphorylation of JAK1, JAK2 and TYK2, although JAK1 is probably the most important in terms of IL6 signal transduction. Inhibition of JAK1 is capable of significantly reducing the levels of GP130 and STAT3 phosphorylation reducing IL6 dependant downstream gene induction, while the same effect was not observed with the inhibition of either JAK2 or TYK2 [235].

Mutational analysis of the GP130 cytoplasmic domain revealed that STAT3 binding is mediated via 4 phosphorylated tyrosine residues in the motif YXXQ, STAT1 is also capable of binding to two of these sites [236]. Each site binds STAT3 via its SH2 domain however the levels of activated STAT3 produced by each are different, this is likely due to steric factors relating to proximity to receptor associated JAKs [237]. The same motif is found on LIFR and is also capable of binding STAT3 when phosphorylated [238]. The extent that substrate specify is conferred by the interaction between JAKs and STATs appears to be low and largely dictated by the coordinating receptor. SH2 domain swap experiments have shown that receptor binding specificity is determined by this domain. A STAT2 chimera with a substituted STAT1 SH2 domain can be targeted to the IFNγ receptor and phosphorylated with no changes in the motif surrounding the tyrosine residue targeted by JAKs [239].

Once STAT3 has become phosphorylated at tyrosine 705 it forms dimers. In the case of IL6 stimulation these are predominantly STAT3:STAT3 homodimers and to a lesser extent STAT3:STAT1 heterodimers. Dimerisation is again mediated through their SH2 domain [240], while the delinearisation of the specific residues responsible for either receptor recruitment or

dimerisation is complicated by this duel role of the SH2 domain, some residues have been found to abolish dimerisation while having no effect of phosphorylation, in STAT6 [241].

Tyrosine phosphorylated STAT3 (pSTAT3) interacts with importin α5 and α7. Importins are a family of proteins involved in the binding of nuclear localisation signals and transferring substrates from the cytoplasm through the nuclear pore complex. Two adjacent arginine residues have been identified on STAT3 that appear to mediate binding between the two proteins. Mutation of R214/215 was associated with an inhibition of nuclear localisation after stimulation with IL6 [242], or OSM and an abolishment of interaction with either importin [243], while mutation of these residues had no effect on levels of tyrosine phosphorylation post stimulation. Nuclear translocation via the nuclear pore complex is dependent on the interaction with α importins and β importins. α chains provide substrate specificity and directly interact with β chains which couple the complex to the nuclear pore. Importin β1 appears to play a role in nuclear transport of phosphorylated STAT3 as siRNA to this protein was able to prevent it [244].

2.4 Functions of STAT3

The first discovered and classical function of STAT3, although not known to be mediated by the transcription factor until later, is the induction of the acute phase response. Acute phase response is the release of a suite of serum factors produced predominantly by the liver and involved in inflammation. Acute phase proteins were originally defined as the serum proteins released by either primary hepatocytes and hepatoma cells in response to IL6 treatment and includes fibrinogen, heptoglobin and α1 acid glycoprotein [245]. STAT3 was appreciated to be the crucial mediator of IL6 signalling to the cell nucleus required for the up regulation of these genes [246].

Knockout experiments targeting STATs other than STAT3 have generally revealed fairly discrete phenotypes effecting specific pathways and responses. For example STAT1 null mice are viable but characterised by increased susceptibility to viral infection [247], whereas STAT5a null mice are also viable and defects are only apparent post-partum when defects in mammary tissue development prevent milk production [248].

In contrast STAT3 knockout mice are embryonically lethal pre-gastrulation. STAT3 null blastocysts were found to be smaller in size compared to wild type controls and exhibited

other morphological abnormalities [249]. Correspondingly active STAT3 had been detected in developing embryos from 4 to 9 days post fertilisation, although its function at this stage of development is unknown [250]. Interestingly despite the creation of GP130 [251], JAK1 [252], SRC [253] and EGFR [254] knockouts none of these were able to recapitulate the early embryonic lethality of STAT3 ablation. GP130 and JAK1 knockouts were lethal, albeit at a later stage of development, suggesting a non-canonical route to STAT3 activation via an unknown pathway but not involving IL6 type cytokines (including IL6, IL10, LIF, OSM and CNTF).

In order to circumvent the problem of embryonic lethality the CRE LoxP recombination system for the generation of conditional knockouts allowed the assessment of post developmental and tissue specific effects of STAT3 knockout, demonstrating a role in a variety of tissue and processes.

In accordance with early experiments identifying a role for IL6/STAT3 signalling in the induction of acute phase proteins, murine liver cells harbouring a conditional knock out for STAT3 are deficient in this response. This study also revealed that acute phase proteins regulated by a type I IL6 response element (IL6RE), requiring the coactivator CAAT enhancer binding protein (C/EBP) had their upregulation completely reversed by STAT3 ablation whereas those with type II IL6RE were induced however at a reduced level [246].

Conditional knockouts limited to macrophages and neutrophils using CRE recombinase expression driven by the lysozyme M gene promoter were assoicated with chronic inflammation, characterised by increased serum levels of the inflammatory cytokines IFNγ and IL6. Macrophages were also sensitised to lipopolysaccharide induced release of proinflammatory cytokines and mice displayed phenotype of chronic enterocolitis [255]. Mouse keratinocytes deficient in STAT3 due to keratin 5 driven CRE expression exhibited impaired wound healing that was associated with a reduction in *in vitro* cell migration in response to growth factor exposure, including IL6 [256].

Another well documented role for STAT3 is in the maintenance of embryonic stem cell pluripotency. Human stem cell pluripotency was originally maintained by growth with a fibroblast feeder culture, it was subsequently discovered that the factor released by the fibroblasts responsible for this effect was LIF, which functions predominantly through STAT3 via a LIFR GP130 receptor dimer [257]. Inhibition of STAT3 in embryonic stem cells using a decoy DNA sequence was capable of inhibiting pluripotency maintenance and initiating differentiation [218] and STAT3 activation alone, in the absence of LIF, is capable of maintaining pluripotency in murine stem cells [258].

Other Functions for STAT3

Upon activation STAT3 can form both homodimers and heterodimers. For example treatment with IL10 and GM-CSF result in the formation of both STAT3 homodimers and STAT1:STAT3 heterodimers [259] whereas treatment with IL6 is associated with the formation of STAT3 homodimers only. Phosphorylation, dimerisation, nuclear translocation and DNA binding are associated with the upregulation of a range of downstream genes, associated with increased proliferation, for example *CCND1* [260], apoptosis inhibition, for example *BCL2L1* [261] and *BIRC5* [262], angiogenesis including HIF1α and VEGF [263], and general cellular transformation in MYC [264].

More recently a role for STAT3 in immune regulation within the tumour microenvironment has become clear. STAT3 plays an important role in the regulation of cytokines involved in inflammation, upregulating both IL10 and TGFβ [265] while simultaneously downregulating TNFα [266] and IFNγ [259]. IL10 is associated with the inhibition of natural killer cell activity induced during a T_h1 immune response. IFNγ is an important regulator of cytotoxic T cell mediated immunity and via STAT1 upregulates the expression of genes involved in response to viral infection including the RNAse OAS and MHC class I molecules facilitating antigen presentation. TNFα is an important inducer of apoptosis secreted mainly my macrophages but also activated T cells.

2.5 STAT3 and Cancer

One of the first pieces of evidence that STAT3 plays a functional role in cancer was the demonstration it participates in v-SRC mediated cellular transformation. The formation of colonies of v-SRC transformed cells could be either enhanced or inhibited by the over expression of wild type or dominant negative forms of STAT3 respectively [267]. It was subsequently shown that endogenous SRC, as well as other SRC family members, can directly phosphorylate STAT3 on tyrosine residue 705 [229] and that constitutively activating mutations in SRC are present in around 10% of colon cancers [268]. SRC mediated activation of STAT3 has also been shown to play a role in tumour growth and apoptosis inhibition in breast cancer cell lines (Garcia et al., 2001)

Since these early discoveries prominent roles for STAT3 in multiple cancer associated phenotypes including cellular transformation/tumourigenesis [269,270], tumour growth [271],

migration [272], invasion [273], angiogenesis [263], immune evasion/suppression [259,274] and inflammation [270] have been well established. Unlike normal tissue where STAT3 activation is transient and only occurs in response to specific stimuli, constitutively phosphorylated STAT3 has been found in cell lines, primary and tumour tissue from a wide range of cancers including around 90% ovarian cancers [275], breast, 50% of NSCLC [276], prostate, multiple myeloma and non-Hodgkins lymphoma.

Constitutive activation of STAT3 has been observed in response to a range of upstream aberrations including mutations in SRC, seen in around 10% of colon cancers [268] and GP130 that occur in around 60% of inflammatory hepatocellular adenomas [277]. Screening of 93 non-small cell lung carcinomas revealed putative activating mutations in EGFR in 17% of tumours that were associated with elevated pSTAT3 ($p=0.002$). Expression of these variants was capable of increasing levels of pSTAT3 in cell line models [278].

As well as activating mutations in positive regulators, inactivating mutations and reduced expression of negative regulators of STAT3 have also been documented. Inactivation, via either, deletion, methylation or mutation, of the STAT3 negative regulator protein tyrosine phosphatase receptor type D (PTPRD) occurs in around 50% glioblastoma, 20% of breast cancers and 9% of lung cancers. Cells lines deficient in PTPRD were associated with elevated levels of pSTAT3 and downstream genes [279]. Similarly another STAT3 negative regulator the suppressor of cytokine signalling (SOCS) protein 3, is frequently hypermethylated and downregulated in non-small cell lung carcinoma cell lines (NSCLC) [280]. Over expression of SOCS3 is able to reduce levels of pSTAT3 by binding both tyrosine phosphorylated GP130, via its SH2, [281] and JAK2 [282] and either competing with STATs domains for recruitment or inhibiting the activity of JAK2.

The importance of STAT3 in cancer is highlighted not only by its role in multiple phenotypes in multiple cancers, but also that multiple upstream pathways converge on this key regulator to cause its aberrant activation. Mutations or overexpression of multiple upstream factors are important events in a number of different cancers suggesting constitutive activation of STAT3 and upregulation of the suite of tumour promoting genes it regulates confers a strong selective advantage.

2.51 STAT3 in Ovarian Cancer

Screening of ovarian tumour sections by immunohistochemistry has suggested the proportion of cases exhibiting constitutive pSTAT3 in ovarian cancer is very high. Of 303 unselected cases of primary EOCs 86% were positive for pSTAT3 [275]. A smaller sample group of 50 EOCs found 88% to be positive although 30% (n=20) the control group of normal OSE tissue also stained positive [283]. Both studies found significant correlations with nuclear pSTAT3 positivity and overall survival. Intensity of pSTAT3 staining has also been correlated with tumour malignancy being lowest in normal OSE and progressively higher through borderline low grade and high grade tumours respectively [284].

No evidence exists for reoccurring activating mutations in either EGFR, GP130, JAK2 or any other receptor/kinase operating upstream of STAT3 in ovarian cancer. Instead constitutive activation of STAT3 appears to be due to increased IL6 expression in an autocrine and possibly paracrine fashion. Elevated levels of IL6 have been observed in, patient ascites [285,286] serum [286–288], cell lines and in tumour tissue [289,290]. Elevated levels of IL6 have been reproducibly associated with poor prognosis and reduced survival [285,287–289]. Three of the four studies referenced here also found a correlation between IL6 levels and stage. Unfortunately, of the studies listed here only Lane et al carried out a multivariate analysis between progression free survival and ascites IL6 levels, which was found to be significant p=0.033 [285].

The lack of a multivariate analysis in the remaining studies makes the assessment of IL6 as an independent prognostic factor, and not just a co-variable of advanced stage, difficult. A better assessment of the prognostic significance of IL6 expression may be gained from the publicly available TCGA expression data set. Stratifying by stage, III, grade, III, and tumour type, serous, representative of the majority of cases ovarian cancer cases at presentation, and a significantly larger data set than the previously mentioned studies, n=317, the significance of the association was greatly diminished p=0.15 [164]. A continuous multivariate model would likely reduce this association further, suggesting IL6 expression is probably a surrogate of stage and possibly tumour burden.

Scambia et al found a progressive increase in the levels of IL6 in the serum of a cohort of unselected ovarian cancer patients according to tumour stage. On average serum IL6 concentrations were 4.7 times higher in stage IV than stage I. A significant association was seen in relation to both survival and response to chemotherapy p= 0.0009 and p=0.022 respectively [287]. However to what extent this effect was mediated by the association between IL6 with stage was not assessed.

Constitutive IL6 secretion of ovarian cancer cell lines is frequent but not always observed *in vitro* however *in vivo* culture in murine xenograft models or co-culture with noncancerous cells can both induce and increase the expression of IL6 in cells [291,292] and this effect has also been noted for IL6R [290]. This effect hints at one of the emerging roles of STAT3 in communicating between the tumour and cells within the microenvironment. A role that has been highlighted by experiments showing STAT3 inhibition *in vivo* has a greater effect than *in vitro* for the same cell line [293]. These issues are discussed in greater detail in section 2.52 below 'IL6 STAT3 and communication between cells of the tumour microenvironment'.

Inhibition of STAT3 in ovarian models has suggested it plays a similar role as other cancer systems. Knockdown of STAT3 has been reported to reduce tumour cell growth both *in vitro* [294] and *in vivo* [293] reduce migration [284] and invasion as well as induce apoptosis [295].

STAT3 has been proposed to play a role in platinum resistance [296], although it has not been identified as upregulated in array based screens for mediators of platinum resistance [297,298]. The clearest demonstration of a drug resistance role has been in relation to paclitaxel. By culturing SKOV3 and OVCAR3 cells in progressively higher concentrations of paclitaxel Duan et al were able to generate resistant clones with higher secretion of IL6, pSTAT3 and *BLC2L1* expression. Inhibition of STAT3 signalling using siRNA was able to reverse increased drug resistance, almost to the levels of parental lines [299].

Epithelial to mesenchymal transition (EMT) is characterised by reduced cell to cell adhesion and the adoption of a more motile, invasive phenotype that has been implicated in metastasis. Epithelial cells stimulated to undergo EMT demonstrate enhanced invasion and metastatic properties in vivo and gene expression signatures of invasive cell lines replete for genes with known role in EMT [300]. STAT3 has been shown to play a crucial role in the transduction of EGF mediated EMT in multiple cell line models including EOC [301,302].

2.52 IL6 / STAT3 and Communication between Cells of the Tumour Microenvironment

Sensitisation

In addition to induced IL6 secretion of ovarian cancer cells in xenograft models, expression of soluble IL6 receptor (sIL6RA) the expression of which is also elevated in ovarian cancer tissue, can be induced *in vitro* [290,292]. Expression of IL6RA is restricted to specific tissues and an absence of the receptor *in vivo* is associated with unresponsiveness to IL6. However cells may secrete a truncated soluble form of receptor which can be formed by either alternative splicing or proteolytic cleavage [303]. Both truncated forms lack the transmembrane domain but retain agonistic properties. The soluble receptor is able to bind IL6 and the ubiquitously expressed GP130 conferring IL6 responsiveness on unresponsive cells and sensitising others. Consequently tumours are able to induce constitutive pSTAT3 in tumour infiltrating immune cells and this reciprocal cross talk has been shown to promote tumour growth, angiogenesis and immune evasion [259].

Angiogenesis

IL6 acts as an angiogenic factor upregulating both *VEGF* and *HIF1α* enhancing the migration of endothelial cells. Gel foam sponges which allow the infiltration of cells seeded with IL6 are subject to greater vascularisation when implanted *in vivo* than untreated controls [292]. Transfection of murine xenografts of A2780 cells with a shRNA plasmid targeting STAT3 showed reduced levels of tumour vascularisation. Tumour sections from STAT3 knockdown animals stained for CD31, an endothelial marker were found to have significantly lower levels than controls [304]. In addition STAT3 knockdown tumours exhibited reduced expression of VEGF, cyclin D1, BCL2 as well as a significantly lower tumour burden.

Inflammation

The first known function of STAT3 was in the induction of the acute phase response. The acute phase response is now better understood as the liver's systemic response to localised inflammation ensuring appropriate negative feedback. Inflammation has been associated with the carcinogenesis of numerous cancer types and there is a link between both endometriosis and pelvic inflammatory disease and endometrioid ovarian cancer [169,170]. The vast majority of gastric and liver cancers are strongly associated with infections which cause

chronic inflammation, caused by Helicobacter pylori and hepatitis virus B and C respectively [305]. It has also been noted that inflammation caused by infection with such agents, including hepatitis virus B, are associated with STAT3 activation.

Immune evasion

The consequences of tumour IL6 secretion on immune cells are multifaceted and only recently coming to light, however one important target for immune evasion are dendritic cells (DCs). Under normal conditions, without challenge, DCs are in an immature state where they present self-antigen, inhibit T_H activation and promote self-tolerance. Dendritic cells are activated in response to a range of stimuli including lipopolysaccharide (LPS), dsRNA and certain cytokines. Once activated DCs shift from a role promoting self-tolerance to one of antigen presentation and T_H activation. IL6 and STAT3 have been shown to be crucial in the maintenance of dendritic cell immaturity [306]. IL6 treatment is able to suppress LPS induced DC activation and this is dependent on downstream STAT3 activation. Tumour cells can directly influence DC maturity. DCs exposed to media conditioned by tumour cells transfected with the dominant negative STAT3β isoform expressed higher levels of the mature DC markers MHCII and the co-stimulatory protein CD80 than untransfected controls. Xenografts of tumours cells with ablated STAT3 signalling using STAT3β also contained a higher number of infiltrating macrophages, neutrophils and cytotoxic $CD8^+$ T cells [266].

Macrophages are another target for immune evasion mediated by STAT3. Factors secreted by tumour cells have been shown to have a role in influencing the nature of an immune response elicited by macrophages. Using a conditional knockout xenograft model in animals with STAT3 WT monocytes, tumour infiltrating macrophages were found to secrete high levels of IL23, a cytokine with tumourigenic properties. However in animals with STAT3 null monocytes IL23 secretion was significantly reduced. Instead tumour infiltrating DCs now secreted IL12, a cytokine with tumour inhibiting properties, where WT monocytes had expressed none [274]. IL23 and IL12 are both heterodimeric, IL23 being composed of a IL23A (19KDa), IL12B (40KDa), dimer and IL12 composed of a IL12A (35KDa), IL12B dimer [307]. IL23 had been previously shown to play a role in tumour development in knockout mice. IL23 null mice ($IL23A^{-/-}$) exhibited reduced tumour formation in response to carcinogen exposure and tumours exhibited greater degrees of infiltrating $CD8^+$ cytotoxic T cells (CTLs), the converse was true of IL12 null mice (IL12A-/-) who developed significantly

more tumours than WT controls and exhibited a lower number of infiltrating $CD8^+$ cells [308]. IL12 has a well-documented role in promoting the differentiation and expansion of T_H1 cells [307] which in turn are crucial for mounting an efficient immune response to intracellular pathogens, primarily through their release of IFNγ and subsequent activation of CTLs. T_H1 and CTL have reproducibly been shown to confer multiple anti-tumour effects; CTLs can directly induce cell death in tumour cells and T_H1 cytokines can induce senescence and apoptosis in tumour cells via their slew of cytokine production [309]. In addition IL23 p19 expression is significantly elevated in not just ovarian but also lung breast and colon cancers [308].

IL23 may elicit its pro-tumour properties via the promotion and maintenance of a novel population of T_H cells characterised by the constitutive secretion of IL17, termed T_H17 cells. Interestingly this form of T cells is dependent on IL6 exposure for its differentiation [310] and T cells without STAT3 are unable to produce T_H17 cells in response to stimulation whereas STAT3 overexpression resulted in T cells which were sensitised to IL6 and secreted increased levels of IL17 [311]. In addition both subunits of the IL17 are transcriptionally regulated directly by STAT3 [312]. As well as IL17, T_H17 cells secrete large amounts of IL22 both cytokines are pro-inflammatory and can stimulate a wide variety of cells inducing the expression of further mediators of inflammation such as TNFα and prostaglandins [313].

Illustrating the importance of STAT3 in cancer, when considered in relation to the hallmarks of cancer [314], the next generation, a review paper in its second iteration which since its publication in 2011 has been cited 4500 times (at the time of writing) STAT3 plays an important role in 5 of 10 of the hallmarks, including 2 of the 4 newly added ones, underlying the need to understand how this factor contributes to cancer tumourigenesis and progression in each one of these areas.

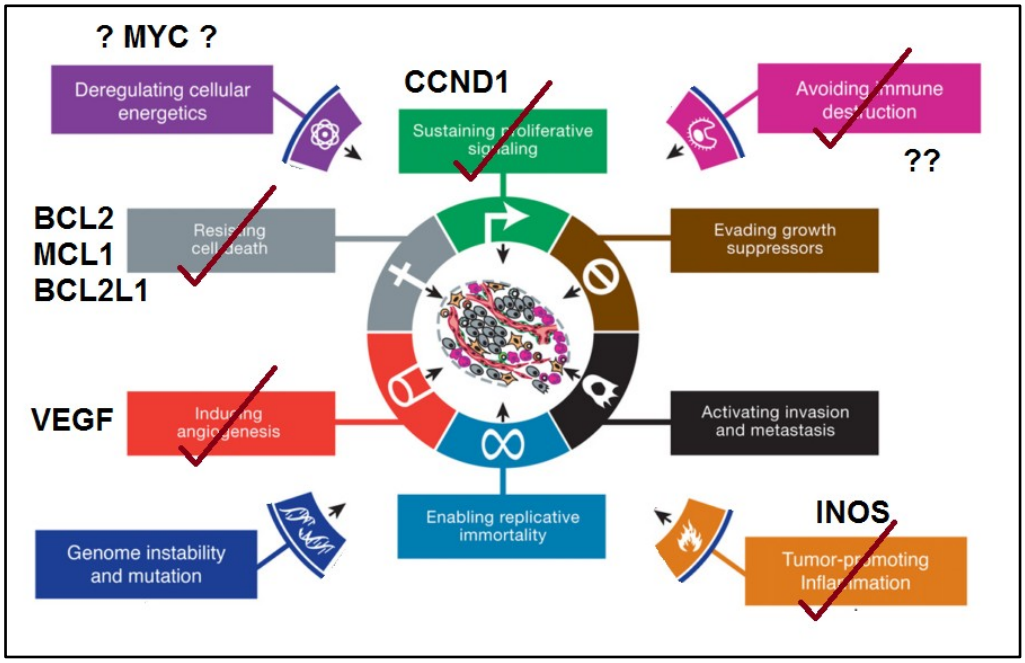

Figure 10. STAT3 and the hallmarks of cancer. Those hallmarks in which STAT3 has been shown to play a role have highlighted with a tick and STAT3 regulated genes known to play a role in those hallmarks have been added. Figure adapted from [314].

2.6 JAK2 and Cancer

The literature on JAK2's role in cancer is smaller and less illustrious than STAT3's despite their close association. A role for JAK2 in oncogenic STAT3 signalling is generally by inference. This is partly due to the redundancy of STAT3 activation by different receptor associated JAKs and potentially the various additional kinases that have been reported to active STAT3. However despite this apparent promiscuity, regardless of the upstream aberration or activator driving constitutive STAT3 phosphorylation, JAKs appear to be an obligate requirement [278,315,316], suggesting regardless of the specific upstream driver ultimately a JAK is responsible for phosphorylating STAT3.

JAK2's best known association with cancer is independent of STAT3, and predominantly affects STAT5. A single base mutation at valine residue 617 leading to an amino acid substitution of phenylalanine (JAK2 V617F) in the pseudo kinase domain of JAK2 was originally found to cause polycythaemia vera, a haematological malignancy of erythrocyte progenitor cells [213]. Since its initial identification the JAK2 V617F mutation has been found to cause almost all cases of polycythaemia vera, essential thrombocythemia, and

myeloid metaplasia with myelofibrosis [212]. Cloning and expression of mutant JAK2 V617F revealed it exhibits significantly higher levels of auto phosphorylation which was not transmitted to the wild type protein [212]. Presence of the JAK2 mutation results in constitutive pSTAT5 which could be reversed with the JAK2 specific inhibitor TG101348, inhibition of pSTAT5 was observed in conjunction with reduced proliferation and increased apoptosis in JAK2 V617 mutant cell lines [317].

Outside of haematological malignancies, JAK2 has been implicated in transducing signals from ERBB2 to STAT3 independently of other JAKs in a number of cell lines [316]. This is of particular relevance to ovarian cancer as amplification of ERBB2 is observed in around 7% of cases of HGS [122] in addition mutations of ERBB2 are seen in around 6% of LGS cases [121]. Coupled with immunohistochemical data from ovarian tumour samples demonstrating a correlation between ERBB2 expression and pSTAT3 ($p=0.002$) [275], implies ERBB2 is an important driver of STAT3 in a minority of ovarian cancers.

It has been suggested that STAT3 activation, which is seen in around 50% of cases of NSCLC, is driven predominantly by JAK2. A screen of 7 NSCLC cell lines, which do not express JAK1, were all sensitive to the dual JAK1 and JAK2 kinase inhibitor sunitinib, which reduced levels of pSTAT3, resulted in lower colony formation in clonogenic assays and reduced tumour size in xenografts [318].

2.7 ERBB2 and Cancer

2.71 Basic Biology

Human epidermal growth factor receptor 2, ERBB2, also known as HER2 is a member of the epidermal growth factor family of receptors (ERBB family) including EGFR (HER1), ERBB3 (HER3) and ERBB4 (HER4). The ERBB proteins are a family of membrane spanning receptors that bind epidermal growth factor (EGF) type extra cellular signalling molecules, including, EGF, transforming growth factor (TGF-α) and neuregulins, transmitting their signal to a number of pathways within the cell.

In order to transduce signals triggered by the binding for extracellular messengers ERBB receptors must first dimerise [319]. In the absence of ligand ERBB receptors exist as inactive monomers. Ligand binding results in a conformational change exposing the

dimerisation domain allowing binding [320]. Unlike JAKs, ERBB receptors do not require phosphorylation for catalytic activity. ERBB receptors can both homodimerise and heterodimerise, the result of which is to juxtapose each receptor's kinase domain with target residues on the adjacent receptor, allowing trans-phosphorylation. Receptor trans-phosphorylation creates docking sites for proteins with SH2 domains and is required for the recruitment various downstream factors including SHC1 [321], which links ERBB receptors to the MAPK (mitogen activated phosphate kinase) pathway, and PIK3R1 (p85) [322] the regulatory subunit of PI3K (phosphoinositide 3-kinase), which activates the AKT/mTOR pathway.

One such MAPK pathway induced by ERBB activation is the RAS/RAF/MEK/ERK cascade. This cascade, initiated by the activation of membrane associated RAS, results in the phosphorylation and activation of the extra cellular related kinases ERK1 and ERK2, also known as mitogen activated protein kinase, MAPK3 and MAPK1. Activated ERK1 and ERK2 in turn phosphorylate the transcription factors FOS and JUN which form a heterodimer and translocate to the nucleus where they bind the AP-1 element found in the promoter region of numerous genes including *CCND1*, *MYC* and *VEGF* (reviewed in [323]). Increased signalling via the RAS/RAF/MEK/ERK pathway results with the activation and upregulation of genes associated with proliferation, differentiation and angiogenesis.

ERBB2 is unique among the ERBB2 family in that no ligand capable of binding the receptor has been identified. Instead the receptor exists in an open conformation in which the dimerisation domain, usually only exposed by ligand binding in EGFR, is permanently accessible and able to interact with other ERBB receptors [324]. While it appears that ERBB2 does not homodimerise [325] and therefore would not be predicted to activate downstream signalling in isolation, it might be predicted to confer greater sensitivity to ligand induced activation of other ERBB receptors. This hypothesis supported by two observations; firstly that maximal activation of ERBB2 requires the presence of other ERBB proteins [326] and secondly ERBB dimers involving ERBB2 have greater signal activation potential then dimers that do not include ERBB2 [327]. ERBB2 possess two predominant trans-phosphorylation sites that are closely linked to the signal transduction capabilities of the protein, tyrosines 1248 and 1221/1222 both of which has been linked to the activity of the RAS/RAF/MEK/ERK pathway [328,329].

2.72 Role in Breast and Ovarian Cancer

These unique features of ERBB2 go some way to explaining why it is perhaps the most oncogenic of all ERBB family members. ERBB2 was discovered originally in mice as the factor driving mutagen induced transformation of rodent cell lines. The transfection of DNA from mutagenized cells was capable of transforming the 'normal' NIH/3T3 mouse fibroblast line, transferring the mutagenized phenotype [330]. Transformed cells were subsequently used to inoculate mice, that were, in turn used to purify an antibody that bound to a 185KDa protein, now known to be ERBB2, found in cell lysates from the original mutagenized rat cells [331]. The importance of ERBB2 as an oncogene in cellular transformation was confirmed when it was demonstrated that overexpression of ERBB2 alone, was sufficient to transform NIH/3T3 cells [332]. Subsequent sequencing of the gene and identification of the human homologue rapidly led to the first identification of ERBB2 amplification in breast cancer [333].

ERBB2 is now known to play a prominent role in breast cancer where gene amplification and protein overexpression has been observed in between 30-42% and 18-20% of invasive ductal carcinoma cases, the most common type of breast cancer [334,335].

The prognostic significance of ERBB2 expression is complex and probably dependant on disease stage, treatment history and chemotherapy regime. Despite this several large studies have shown a clear relationship between copy number and poor survival in breast cancer. Two large studies examining the relationship between copy number, in pre-treatment biopsies, and either disease free survival (n=1056) or risk of disease recurrence (n=580), using multivariate analyses found significant associations with both outcomes [336,337].

While ERBB2 is only amplified in around 5% of HGS ovarian cancers [122,338] a number of studies have reported elevated protein expression in a significantly higher proportion. Due to the nature of immunohistochemistry (IHC), the technique generally used for such estimates, reported frequencies vary. One large study of 1420 cases suggests the frequency of overexpression is closer to 16% of invasive EOC [339].

Although the prognostic significance of ERBB2 overexpression is less well studied in ovarian cancer, and identifying correlations is complicated by the smaller proportion of cases they represent, a number of studies have found significant associations between either copy number or protein overexpression and PFS/OS and response to chemotherapy. For example two such studies examining ERBB2 expression by IHC found a significant association with reduced OS and PFS, in multivariate models [340,341]. Meden et al also found ERBB2 to an

independent prognostic factor, 51 of 275 patients 18%, screened by IHC, were found to be ERBB2 overexpressers and median survival of this group was 20 months compared to 33 months for non overexpressers [342].

Confirming the importance of ERBB2 in driving breast cancers *in vivo,* treatment with the ERBB2 inhibiting antibody, trastuzumab, has been shown to confer survival benefits in patients with confirmed genomic amplification [343].

2.73 ERBB2 Drug Interactions

In spite of the prognostic importance of ERBB2 a number of studies examining different chemotherapy regimens, specifically those including a taxol, doxorubicin and cyclophosphamide, have shown a significantly higher response rates in ERBB2 positive breast cancer cases verses other molecular subtypes [334,344]. In both studies tumour tissue was preoperative and chemotherapy was first line. A randomised trial of cyclophosphamide, doxorubicin and paclitaxel as individual treatments arms has suggested that the specific agent ERBB2 overexpression confers sensitivity to is paclitaxel, this arm only provided a significant survival advantage in ERBB2 amplified cases verses those without [345].

Converse to its apparent role in sensitising to paclitaxel some *in vitro* and early clinical data has suggested ERBB2 overexpression might not only contribute to upfront response to platinum based therapy, but also that as a therapy ERBB2 inhibition might combine synergistically with cisplatin and other DNA damaging agents. For example isobolograms conducted in the ERBB2 amplified breast cancer cell SKBR3 showed that trastuzumab combined synergistically with cisplatin in reducing cell viability (combination index 0.48 P=0.003). Synergy was not confined to cisplatin as other genotoxic drugs were also found to act synergistically with trastuzumab including etoposide and thiotepa [346].

The majority of clinical studies investigating the prognostic importance of ERBB2 expression in ovarian cancer did not examine this specifically in relation to platinum based chemotherapy, however given that carboplatin is the standard frontline treatment, any effect on drug response is likely to have an overall survival effect. Meden at al investigated the relationship between platinum chemotherapy dose and OS in ovarian cancer cases overexpressing ERBB2. They found a dose response relationship in patients without ERBB2 overexpression, that was not present in those overexpressing the protein [347].

In addition Lassus et al found a significant association between *ERBB2* copy number and poor response to therapy, reduced PFS and OS (n=401) [338]. In this study the majority of patients (86%) were treated with single agent platinum and ERBB2 was also found to be an independent prognostic marker.

Taking these studies together suggests ERBB2 confers resistance to platinum based chemotherapy in ovarian cancer.

3. Platinum

3.1 Mechanisms of Toxicity

Cisplatin (Figure 11) and carboplatin belong to a group of platinum containing compounds including transplatin and oxaliplatin. Common to all these compounds is their ability to form DNA adducts and act as alkylating agents. Once cisplatin has entered a cell hydrolysis removes chlorine groups replacing them with positively charged water groups (Figure 11b). The product is an aquated, positively charged, electrophilic species capable of reacting with nucleophilic sites on DNA, RNA and protein [348].

Aquated platinum compounds attack nucleophilic N7 atoms of imidazole rings in purine bases. Cisplatin forms around 65% guanine:guanine 1,2(GpG) intrastrand crosslinks between sequential residues (Figure 11C), followed by 25% adenine:guanine 1,2(ApG) and 5% guanine: nucleotide: guanine 1,3(GpNpG) intrastrand links and a small percentage (<5%) of interstrand links [349]. The formation of DNA platinum crosslinks results in inhibition of DNA synthesis [350], RNA transcription [351] G2 cell cycle arrest and apoptosis [352].

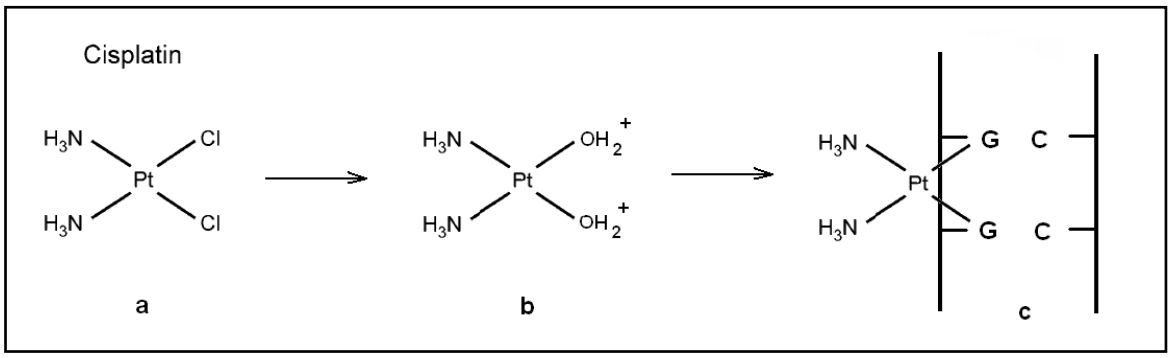

Figure 11. **a)** Structure of cisplatin. **b)** upon entering a cell chloride groups are substituted for positively charged water groups. **c)** Platinum DNA adducts are predominantly formed between adjacent intrastand guanine residues 1,2(GpG) adducts.

1,2(ApG) or 1,2(GpG) crosslinks are considered responsible for the vast majority of cisplatin cytotoxicity. Transplatin, an optical isomer of cisplatin, is sterically incapable of forming these crosslinks that constitute 90% of the adducts formed by cisplatin [353]. It retains

the ability to form other types of interstrand and intrastrand crosslinks but exhibits far reduced cytotoxicity. In addition 1,3(GpNpG) adducts are repaired around 15 times more efficiently than 1,2(A/GpG) lesions [354], suggesting it is the persistence of intrastrand lesions between sequential bases 1,2(A/GpG) that are responsible for the majority of cisplatin's cytotoxicity. Notwithstanding that in tumours with mutations in specific DNA repair genes, for example homologous recombination thought to be responsible for repair of interstrand links, may experience greater toxicity from these lesions.

3.2 Repair of DNA Platinum Adducts

3.21 Nucleotide Excision Repair and Testicular Cancer

Platinum intrastrand DNA adducts appear to be predominantly repaired by the nucleotide excision repair (NER) pathway, the same mechanism responsible for the repair of structurally similar cyclobutane-pyrimidine-dimers formed by UV radiation. Platinum resistant tumours have been shown to overexpress the NER proteins ERCC1 and XPA [355], whereas cell lines cultured from sufferers of xeroderma pigmentosum, deficient in NER, are especially sensitive to platinum drugs [356].

Similarly testicular germ cell tumours (TGCT) which are usually deficient in NER are generally exquisitely sensitive to cisplatin in comparison to most other cancer lines. This sensitivity has allowed cure rates of $\geq 99\%$ for early stage disease in response to combination cisplatin chemotherapy [357]. Even in the case of metastatic disease cure rates of between 80% are observed [358]. The hyper sensitivity of TGCT to cisplatin may be explained by a low efficiency of platinum DNA adduct repair, conferred by reduced expression of NER components. A panel of testicular cell lines was found to have reduced levels of adduct removal relative to bladder lines [359]. A screen of 6 TGCT lines in comparison to a panel of non-testicular cancer lines revealed a significant reduction in expression of the NER proteins XPA , XPF and ERCC1 [360], supporting a functional role for these proteins in platinum sensitivity, supplementation with recombinant XPA XPF/ERCC1 was also able to restore platinum adduct repair in two NER deficient TGCT lines to levels comparable with controls [361].

3.22 High Mobility Group Proteins

Why 1,2(A/GpG) lesions should be repaired less efficiently and result in greater toxicity is not fully understood however there is some evidence pointing to the role of high mobility group (HMG) proteins, specifically their ability to bind regions of DNA containing adducts. The formation of 1,2(A/GpG) adducts causes a conformational change unwinding DNA by 13°. This is in contrast to the unwinding caused by the formation of 1/3(GpNpG) adducts of 23 ° [362]. The unwinding caused by 1,2(A/GpG) adducts may create binding sites for HMG proteins that inhibit the recruitment of DNA repair proteins preventing adduct removal. HMG1 binds cisplatin treated DNA at a far higher stoichiometric ratio than either DNA treated with transplatin or untreated DNA [363]. In addition cell free models of adduct repair, in which HMG proteins are absent, showed greater efficiency of repair of 1,2(A/GpG) lesions than expected relative to *in vivo* models. This was coupled with a significant inhibition of 1,2(A/GpG) adduct repair upon the addition of recombinant HMG1 protein *in vitro*, relative to 1,3(GpNpG) lesions [364].

3.23 BRCA1, BRCA2 and Homologous Recombination

It is well documented that germ line mutations in *BRCA1* and *BRCA2* increase the lifetime risk of developing both ovarian and breast cancer. Around 10% of ovarian cancer patients suffer from an inherited form of the disease, the majority of which are caused by mutations in these genes. Estimates of the frequency of germ line BRCA mutations in cases of inherited ovarian cancer have ranged from 52% - 81% [57,58].

BRCA1 and BRCA2 are important regulators of the repair of double stranded breaks (DSB) by homologous recombination (HR) and non-homologous end joining (NHEJ) [365].

Tumour mutations in *BRCA1* and *BRCA2* are relatively less common in sporadic ovarian cancer being found in around 10% of cases [122,366]. However reduced expression by either loss of heterozygosity or promoter methylation is more common. Down regulation or loss of BRCA1 expression has been found to correlate with tumour grade, occurring in 16% of benign, 38% of borderline, and 72% of ovarian carcinomas [367].

The observation that in stage matched EOC cohorts, patients with inherited mutations in *BRCA1* or *BRCA2* have significantly increased survival versus sporadic cases provided the first clue that BRCA1/2 might play a role in platinum resistance [186,368–371]. Rubin et al found

that median OS for advanced stage disease was 77 months for patients with a BRCA1 germ line mutation, compared to 29 months for sporadic matched controls (P=0.001). Cass et al also found a significant advantage in PFS of 49 months versus 19 (P=0.16) and OS of 91 months versus 54 (P=0.046) as well as increased response to primary chemotherapy (100% vs 50%) (P=0.01) in combined BRCA hereditary cases versus sporadic controls. A similar effect was observed in *BRCA2* mutants in isolation, which were associated with a significantly higher primary chemotherapy response rate of 100% vs 82% (P=0.02), longer OS (HR=0.33 95% CI 0.16-0.69 P=0.003) and PFS (HR=0.40 95% CI 0.22-0.74 P=0.004) compared to BRCA wild-type cases [371]. Given the correlation between response to chemotherapy and survival, these results strongly implicate a role for BRCA1 and BRCA2 or HR in general in the repair of DNA cisplatin adducts.

More direct evidence that BRCA1 plays a role in the repair of platinum adducts originated from a number of studies in breast cancer cell lines in which knockout or over expression of BRCA1 resulted in either sensitisation or resistance to cisplatin respectively [372–374]. In two of these studies restoration of BRCA1 expression in the null HCC1937 breast cancer line was associated with up to a 20 fold increase in cisplatin IC_{50} [373].

Given that BRCA1 downregulation, at both the protein and mRNA levels, has been reported to be a common event in sporadic EOC, occurring in an estimated 72%-90% of cases [366,367], suggests that patients of sporadic disease without BRCA1 mutations but partial downregulation, will also receive a survival advantage in response to platinum treatment. Put another way the high response rates of HGS EOC generally to cisplatin, appear in part due the high frequency of aberations in the HR pathway observed in this group. However as yet an acessment of the relationship between HR functionality and sensitivity to cisplatin has not been conducted.

But a mixed stage cohort of platinum naive patients were screened for tumour expression of BRCA1 on presentation. Patients grouped as BRCA1 low expressers had a significantly increased survival after single agent carboplatin treatment relative to the high BRCA1 group. All patients were screened and verified to be BCRA1 wild-type [375].

Taken together this implies a model of BRCA function in the maintenance of genomic integrity in response platinum treatment, where the loss of BRCA during tumourigenesis inhibits the ability of tumour cells to repair their DNA after cisplatin dependant damage, therefore increasing the probability that a failure of repair and subsequent genomic instability will result in the induction of apoptosis and lower tumour burden. Patients with either inherited mutations or, in the case of sporadic disease, reduced expression, are therefore

likely respond better to platinum treatment and have better survival than their functional BRCA expressing counter parts.

How BRCA1/2 mediate repair of platinum adducts is not fully understood. But cisplatin has been shown to cause the formation of DSB in dividing but not senescent cells [376]. Although cisplatin doesn't cause DSB in cell free models it has been shown that single strand lesions caused by other agents can be converted into DSB during replication, termed replication runoff [377]. This process appears to occur via combination of repair of the adduct, which involves the formation of a single strand break, which becomes double stranded as a consequence of nascent strand stalling during DNA replication.

The HR pathway is most active during S - G2 phases when sister chromatids are available for recombination [378]. Generation of DSB results in the BRCA2 dependant recruitment of RAD51 [379]. BRCA1 is also recruited to DNA DSB foci and this is dependent on ATM phosphorylated H2AX [380]. Once recruited to site of DNA damage, ATM is also able to phosphorylate BRCA1 [381], which is required for the phosphorylation of CHK1, a key regulator of G2-M cell cycle arrest in response to DNA damage [382]. It is unclear whether BRCA1 functions exclusively via canonical HR or through alternative pathways, in the repair of cisplatin adducts as BRCA1 interacts with a large number of proteins including RAP80, the MRN complex, RAD51 and BRCA2 forming distinct complexes with specific roles in the DSB repair response [383]. BRCA1 has also been implicated in enhancing NER [384], influencing which DSB repair pathway is used, HR or non-homologous end joining [385] as well as initiating G2 – M arrest.

3.24 Other Mechanisms

Evidence for the importance of other DNA repair pathways is less clear. Cell lines deficient in mismatch repair (MMR) components are surprisingly 2-3 fold more resistant to cisplatin than their MMR proficient counterparts [386]. In addition, A2780/cp70 an *in vitro* derived cisplatin resistant ovarian cell line was re-sensitised to the levels of the parental strain with the restoration of hMLH1 expression [387]. It is believed that MMR contributes to platinum resistance through a failure to repair adducts and a corresponding MMR dependant induction of apoptosis. This theory is partly based on the observation that human hMSH2/hMSH6 dimers are capable of binding 1,2:GpG adducts *in vitro* [388].

It is perhaps surprising therefore that patients with Lynch syndrome, HNPCC, associated ovarian cancer patients due to mutations in the MMR pathway genes do not receive any differential survival effects relative to matched controls [389].

3.3 Mechanisms of Platinum Resistance

A large number of studies have investigated mechanisms of platinum resistance, the majority of these using *in vitro* derived resistant cell lines. Despite identifying a number of potential targets, drawing clinically relevant parallels has been more difficult. Correspondingly very little progress has been made in the development of drugs to target mediators of resistance in patients with resistant disease. Improvements in survival over the previous two decades have largely been due to improvements in surgical practice.

3.31 Reduced Cellular Accumulation of Platinum

Although it was initially thought that cisplatin entered the cell via passive diffusion alone it seems that active transport into and out of the cell both play a role in regulating intracellular platinum concentration. A number of copper transporters have been implicated in both influx and efflux of cisplatin including CTR1 [390] and ATP7B [391]. Reductions in the accumulation of intracellular platinum in the order of 20-70% has been found in cell lines, including ovarian, displaying varying degrees of resistance [392]. Decreased expression of CTR1 has been correlated with resistance in lung lines and ATP7B was over expressed in a panel of cisplatin resistant lines including the ovarian line SKOV3. A functional role for ATP7B was confirmed with knock-out and transfection experiments that were able to increase sensitivity and restore wild type phenotype. Expression profiling of ovarian tumours also revealed a significant poor prognosis associated with increased ATP7B levels [391].

3.32 Inactivation by Glutathione

Glutathione (GSH) is a tripeptide containing an electrophilic thiol group capable of forming adducts with aquated cisplatin. Glutathione-platinum adduct formation sequesters

nucleophilic groups on aquated cisplatin preventing their crosslinking with DNA. Using *in vivo* cultured platinum resistant derivatives of the ovarian line A2780 a correlation was found between increasing IC_{50} and cellular levels of GSH. Increasing levels of y-glutamylcysteine synthetase (yGCS) and y-glutamyl transpeptidase (yGT) involved in GSH synthesis were also linked to resistance in this study. Interestingly the only model of *in vivo* acquired resistance used in this study, the isogenic cell line pair PEO1 and PEO4, exhibited no such correlation. Similar findings were also reported in another ovarian *in vitro* cultured model of resistance showing over expression of glutathione s transferase pi (GSTpi) in resistant populations relative to parental lines [393]. GSTpi is able to directly catalyse the addition of cisplatin to GSH. Extending these findings to clinical samples has proved more difficult. Immunohistochemical staining of ovarian tumour sections was unable to find any link between GSTpi and either prognosis or resistance [394]. Another study found that increased GSTpi expression in patient matched pre and post relapse biopsies was associated with a poor prognosis [395] .

3.33 Increased DNA Damage Repair

Nucleotide excision repair (NER) is considered to be the most important DNA repair pathway in the removal of platinum adducts, accordingly it might be expected that over expression of NER rate limiting proteins may contribute to resistance. The NER genes *XRCC5*, *XRCC6* and *ERCC5* were found to be over expressed in selected ovarian cell lines by microarray relative to parental strains [393]. Knockdown of the NER protein ERCC1 by shRNA transfection was able to sensitise two cisplatin sensitive ovarian cell lines, A2780 and OVCAR10, reducing their IC_{50} roughly 3 fold to treatment [396].

Some evidence of a potential clinical relevance for increased NER activity in resistance has emerged although involving different NER genes. *ERCC1* and *XPAC* were significantly overexpressed assessed by QRT-PCR in platinum resistant ovarian tumour samples relative to platinum naïve [355].

Mutations and reduced expression of various MMR proteins has been correlated with resistance in *in vitro* models of acquired resistance in ovarian cancer [397,398]. A border line significant loss of expression of hMLH1 was observed in a number of ovarian tumours at relapse vs first surgical intervention (p=0.059) [398]. A similar correlation was not observed in

other MMR members. It appears these initial finding have not been replicated in larger clinical data sets.

Recently a novel role for BRCA1 and 2 resistance acquisition has emerged. There have been a number of examples of reversion mutations in both BRCA1/2 restoring expression of a functional protein associated with the acquisition of resistance.

Tumour tissue from two patients with platinum resistant familial ovarian cancer contained a reversion mutation in BRCA2 correcting the inherited frame shift mutation [399]. In this study the same type of mutation was observed in a pancreatic cell line selected for platinum resistance and resulted in the expression of functional BRCA2 protein assessed by siRNA. A similar report using the same approach produced comparable results. Cisplatin selection of BRCA2 mutant prostate and lung lines induced reversion mutants restoring functional BRCA2 expression. *In vivo* findings have been duplicated in cases of acquired cisplatin resistant in carriers of somatic BRCA mutants [400]. The reported frequency of these reversion mutations in patients was 2/2 [399] and 1/5 [400]. These findings were also extended into the isogenic ovarian cell line pair PEO1 and PEO4. PEO1 a platinum sensitive cell line was found to be BRCA2 mutant and PEO4 its resistant isogenic pair also contained a reversion mutation restoring expression of a functional protein [401].

Reversions were also found in BRCA1 mutant familial ovarian cancer. In a screen of patients with recurrent disease who had relapsed with both resistant and sensitive tumours, 4/6 resistant tumours contained a BRAC1 reversion mutation whereas 0/3 sensitive tumours contained the secondary mutation [402]. Another interesting result implicating BRCA1 in cisplatin resistance is the p53 $^{flox/flox}$ BRCA1 $^{flox/flox}$ K14 mouse model. This strain is homozygous for floxed p53 and BRCA1 such that when Cre recombinase is activated in the developing mouse mammary gland homozygous mutations in both genes are created that cannot be repaired by small insertion/deletion mutations [403]. Such tumours failed to develop resistance and instead repeatedly relapse with platinum sensitive disease.

Aims

1) Investigate the effects of IL6 expression induced by cisplatin:
    a) Identify downstream mediators of IL6 signalling.
    b) Assess the effects of the activation of downstream signalling.
    c) Investigate the role, if any, of IL6 expression in cisplatin resistance.

2) Identify possible drugable targets for adjuvant chemotherapy:
    a) siRNA and small molecule inhibitor assays will be used to examine the plausibility of inhibition of IL6 pathway to modulate cisplatin sensitivity.
    b) Examine possible interactions with known oncogenes, for example STAT3.

3) Investigate the role that differential activation of JAK2, STAT3 and ERBB2, observed between sensitive and resistant cells, might play in acquired resistance to cisplatin using a combination of techniques:
    a) siRNA, overexpression, small molecule inhibitors and recombinant protein treatments will be used to test whether perturbation of the above proteins has any effect on cisplatin sensitivity.
    b) A focus on levels of phosphorylated proteins will address whether pathway effect of cisplatin are mediated by changes in total protein or activation only.
    c) Examine the expression of known transcriptional targets of STAT3 in response to either cisplatin or experimental perturbation.
    d) With a reference to existing literature and public datasets identify other genes/proteins likely to interact with the above that might be relevant to ovarian cancer and drug resistance.

4) Examine the role of GP130 in cisplatin resistance and whether this is connected to previously identified changes in JAK2 STAT3 and ERBB2.

5) Investigate the activation of potentially redundant/compensatory pathways to JAK2/STAT3 which might be effected by either cisplatin exposure or perturbation using for example siRNA.

Methods and Materials

1. Cell Lines and Culture

All cell lines were maintained in RPMI media (Sigma Aldrich) supplemented with 10% foetal calf serum (First Link), 0.2mM L-glutamine (Gibco), 50U/ml penicillin and 50ug/ml streptomycin (Gibco). All cell lines cultured at 37^0C (expect OSE-C2 which is maintained at 33^0C) in a 5% CO_2 humidified incubator. All cell lines were routinely tested for mycoplasma infection.

Cell lines used - PEO1, PEA1,PEO14, OVCAR3, IGROV3, A2780 – platinum sensitive EOC. PEO4, PEA2, PEO23, SKOV3 – platinum resistant EOC. All cancer cells lines are believed to originate from patients with high grade serous ovarian cancer, except OSE-C2 which is a 'normal', SV40 transformed ovarian surface epithelial cell line. PEO1/PEO4, PEA1/PEA2 and PEO14/PEO23 are isogenically derived from three individuals when they were chemosensitive and after they had relapsed with chemoresistant disease. PEO1, PEA1 and PEO14 being cisplatin sensitive PEO4, PEA2 and PEO23 resistant. IC_{50} of each sensitive line is around 2µM and for resistant cells is around 10µM.

For additional information regarding mutation status of the cell line described here please see supplementary methods section S3.

2. siRNA

24 hours after seeding, cells were transfected as follows. 1µl/ml, final concentration, of transfection reagent 1 (Dharmacon) was incubated with 99µl/ml, final concentration, optimem (Invitrogen) for 5 minutes prior to the addition of and equal volume of siRNA diluted to 2µM in siRNA buffer (Dharmacon). This mixture was incubated for 20 minutes then added to 800µl/ml of antibiotic free media to give a final concentration of 50nM siRNA except PEO4 which was transfected at 100nM final concentration. Cells were incubated for 48 hours. After 48 hours transfection cells were trypsinised and reseeded, in normal antibiotic media, into 6 well plates for protein/RNA lysates and 96 well plates for cell viability and apoptosis assays. 24 hours after seeding media was aspirated and cells washed in PBS then

lysed for protein or RNA lysates. For apoptosis assays media was replaced with either normal fresh media or media supplemented with cisplatin at the indicated concentration for 24 hours before apoptosis, or at the indicated time for other cell viability assays. For apoptosis assays cells were reseeded into 96 well white opti-plates (Perkin Elmer) and for cell viability assays into normal clear plates.

siRNA sequences used are as follows;

STAT3 1 – UAUCAGUAAGCCUUUGCCC-tg.
STAT3 3 - UCACUCACGAUGCUUCUCC-gc.
STAT3 4 - UUGCUGGCCGCAUAUGCCC-aa.
STAT3 5 – UAUUUCAACACCAAAGGCC-ag
JAK2 2 – AUUUAUUAAAGUCCUUAGG-ac.
JAK2 3 – UUCUCCACCAAUAUAUUUC-tc.
JAK2 4 – AAGAACUGGAUCUAUUUGC-tt.
JAK2 5 – UUUAUCUCCUCCACUGCAG-at.
GP130 1 – UAUUUCUCAAACUAGAUGC-tc
GP130 2 – UAGCUCACCAUGUUAUCCC-ag.
GP130 3 – UACCUCAGUUCCUCUUUGC-tt.
GP130 4 – UUGCUCUCU GCUAAGUUCC-ct.

All siRNAs were designed using Dharmacon's proprietary algorithm (http://www.thermoscientificbio.com/design-center/) and synthesised by MWG Eurofins, with the exception of LAMIN A/C and Non Targeting (Dharmacon). All MWG synthesised siRNAs contain 3' overhangs of two template specific DNA residues. In each experiment a mock transfected sample was used as a control to which transfection reagent but no siRNA was added.

3. Cell Viability/Caspase Assay.

Cell viability was quantified using the MTT assay. 3-(4,5-Dimethylthiazol-2-yl)-2,5-diphenyltetrazolium bromide (MTT) (Sigma) was added to media to final concentration of 0.5 mg/ml. Cells were then incubated at 37^0C for 2 hours and reactions stopped by the

addition of an equal volume of 10% SDS with 0.01% concentrated (37%) hydrochloric acid. Plates were then incubated for 8-24 hours in the dark and absorbance read at 562nm.

The MTT assay is based on NAD(P)H dependant oxidoreductase activity which is linked to general metabolic activity, as such and like all measures of cellular viability, it is an approximation. However for future purposes all references to viability and proliferation are based on MTT results and therefore suffer from the limitations inherent in the assay.

Levels of apoptosis were estimated using the caspase 3/7 glo assay (Promega), according to manufacturer's guidelines. After the addition of an equal volume to regent to each well, plates were incubated for 1.5 hours and quantified using a Pherastar luminometer (BMG). As the caspase glo assay measures the activity of caspase 3 and caspase 7 it is not a definitive measure of apoptosis and doesn't account for caspase independent apoptosis, despite this future references to the quantitation of apoptosis are based on this assay.

For both assays cell free controls were deduced from all others values.

4. Inhibitors and Treatments

JAK2 inhibitor TG101348 (Active Biochem) was suspended to 50mM in sterile DMSO aliquoted and stored at -20^{o}C. ERBB2 inhibitor CP-724,714 (Selleck Chemicals) was suspended to 50mM in sterile DMSO aliquoted and stored at -20^{o}C.
For JAK2 or ERBB2 inhibitor treated caspase assays cells were exposed O/N for between 14-18 hours with inhibitor at the stated concentration. Cells were then retreated with the same concentration alone or in combination with cisplatin and incubated for 24 hours prior to carrying out caspase/viability assays. For IC_{50} and growth curve assays cell were treated once at the stated concentration and incubated for either the stated length of time, or for IC_{50}s 72 hours. Protein lysates taken after O/N inhibitor treatment.

MEK1/2 inhibitor PD0325901 (Selleck Chemicals) was suspended to 50mM in sterile DMSO aliquoted and stored at -80oC with desiccation. For MEK1/2 inhibitor caspase assays cells were treated for 6 hours with cytotoxic drug either, cisplatin, doxorubicin or paclitaxel at the stated concentration. Cells were then treated with the indicated concentration of inhibitor incubated for an additional 18 hours prior to caspase assay and protein lysates preparation.

5. rIL6 Treatment

rIL6 and rsIL6RA (Peprotech) were suspended to 50µg/ml in sterile PBS with 0.1% m/v BSA, aliquoted and stored at -20^{o}C. For apoptosis assays PEA1 and PEA2 were treated with both rsIL6RA and rIL6 final concentrations 75ng/ml and 50ng/ml respectively. All other cell lines were treated with rIL6 only at final concentration 50ng/ml. For caspase assays cells were stimulated with rIL6(RA) for 30 minutes before the addition of cisplatin, with the same concentration of rIL6(RA), cells were incubated for a further 24 hours before caspase/viability assays. For IC_{50} assay cell were treated simultaneously with rIL6(RA) and cisplatin and incubated for 72 hours before performing the MTT assay.

6. Western Blotting

Prior to collection cells were washed in PBS. Whole cell lysates were collected in 2% SDS lysis buffer supplemented with protease inhibitor cocktail (Roche) and phosphatase inhibitor cocktail II (Calbiochem) at the manufacturers recommended concentration. Protein concentration was estimated using the micro BCA assay (Pierce) according to manufacture's guidelines and quantified by measuring absorbance at 562nm. Lysates were diluted in Laemmli buffer and incubated at 95^{0}C for 5 minutes in the presence of either 0.05M DTT or 1% v/v β-mercaptoethanol. Samples were loaded onto 8% - 12% Tris/glycine PAGE gels and separated at 200V for around 1hr using a Bio-rad Mini-Protean Tetra Cell in 1x SDS Tris/glycine buffer. After electrophoretic separation protein was transferred on to a nitrocellulose membrane (median pore size 0.2um) (Bio-Rad), in chilled (4^{o}C) Tris/glycine buffer with 20% v/v methanol at 100V for 1hr. Membranes were then blocked in either 5% non-fat milk (Sainsburys) in PBS/T or 5% bovine serum albumin (Sigma) in TBS/T in an antibody dependant fashion for around 1hr. Antibody dilutions were made up in blocking buffer and applied to membranes overnight at 4^{o}C. Membranes were then washed in either TBS/T or PBS/T for at least 3 x 5 minutes each with agitation. HRP conjugated secondary antibodies (Dako) were prepared in blocking buffer at a 1/2000 dilution and applied to membranes for at least 1 hour. Membranes were then washed in TBS/T or PBS/T for at least 3 x 5 minutes. Bands were visualised using Immobilon ECL reagent (Millipore, UK) after a 5 minute incubation, photographic films (Kodak, UK) were applied to the membranes and developed using a Konica Monolta SRX101. Membrane striping when used was carried out

using a harsh 2% SDS, 62.5mM Tris pH 6.8, 0.8% β-Me buffer. Buffer was warmed to 50°C prior to addition of β-Me, membranes were incubated with agitation for 30 minutes before at least 4 x 10 minutes washes in PBS/T.

Antibodies used are as follows; STAT3 (BD biosciences - 610189) 1/3000 5% milk PBS/T. STAT3 phospho Y705 (Cell Signalling - 9145) 1/1000 BSA TBS/T. JAK2 (Cell Signalling – 3230) 1/1000 BSA TBS/T. JAK2 phospho Y1007/Y1008 (Cell Signalling – 3776) 1/1000 BSA TBS/T. ERBB2 (Epitomics – 2064-1) 1/1000 – 1/5000 milk PBS/T. ERBB2 phospho Y1248 (Abcam – 47755) 1/1000 milk PBS/T. GP130 (Millipore - 06-291) 1/1000 milk PBS/T. β-tubulin (Sigma - T4026) 1/10,000 milk PBS/T. HSP60 (Cell Signalling -) 1/3000 milk PBS/T. ERK1/2 (Cell Signalling – 4695) 1/2000 milk PBS/T. ERK phospho T185/Y187 + T202/Y204 (Abcam – 50011. Cyclin D1 (Eptiomics – 2261-1) 1,5000 milk PBS/T. BCL-XL * (Cell Signalling – 2764) 1/1000 milk PBS/T. H2AX (Cell Signalling – 2577) phospho S139 1/1000 BSA PBS/T. GFP (Abcam – AB296) 1/1000 milk PBS/T. P27 (BD – 610242) 1/1000 milk PBS/T. PAN AKT (Cell Signalling – 4691) 1/2000 milk PBS/T. AKT phospho S473 (Cell Signalling – 9271) 1/1000 BSA TBS/T. ERBB1 (EGFR) phospho 1068 (Abcam - AB5644)

* Despite being described as a BCL-XL antibody it detects both splice variants originating from the BCL2L1 locus, predicted at the sequence level and evidenced from western blots. The two transcript variants from the BCL2L1 locus are generally referred to as BCL-xL and BCL-xS, where L refers to the large anti-apoptotic variant and S to small pro-apoptotic variant.

7. Densitometry

Western blot films were scanned using a standard office scanner (Brother DCP-130) at max resolution (1200 x 1200 dpi) in grey scale. Band quantification was conducted using Image J (National Institute of Health). After background normalisation manual area under curve estimates were made.

8. Immunoprecipitation

Lysates were taken in non-denaturing lysis buffer, containing Triton X-100 1%, NaCl 150mM, Tris-HCl pH – 7.2 50mM, EDTA 2mM, protease inhibitor cocktail (Roche) and phosphatase inhibitor cocktail II (Calbiochem). 500ul of cold (4^{o}C) lysis buffer was added to a 15cm dish on ice and cells collected using a cell scraper. Lysates were incubated with agitation for 10 minutes at 4^{o}C to aid lysis. Around 500ug of protein was diluted to 1ml in cold lysis buffer and 10µl of JAK2 antibody added and incubated at 4^{o}C overnight in an orbital shaker. 50ul of a protein A sepharose (Sigma) slurry was added to each sample, and incubated at 4°C for 1hour in an orbital shaker. Beads were sedimented by centrifugation at 13,000rpm for 5 minutes and supernatant removed. Beads were gently resuspended in 1ml of cold lysis buffer and washed a further 3 more times. Finally beads were resuspended in Laemmli buffer containing 0.05M DTT and western blotted as normal.

9. RNA Extraction and cDNA Synthesis

Total RNA was extracted using the RNAeasy plus kit (Qiagen) according to manufacturer's guidelines. Purity of extracted RNA was estimated using a NanoDrop ND-1000 (Thermo Scientific). 1-2 µg of RNA was incubated at 65°C for 5 minutes and then 4°C for 5 minutes with 0.5µg/µg of oligo dT_{15} in 12.3ul of RNA diluted in RNAse free H_20 (Gibco). After incubation RNA and oligo dT_{15} were mixed with 7.7ul of MMLV reverse transcriptase reaction mix resulting in the final concentrations of 1x MMLV RT Buffer (Promega, UK), 0.4mM dNTPs and 3U/ul MMLV reverse transcriptase (Promega). Samples were incubated for 1 hour at 37°C, followed by 2 minutes at 95°C. Thermal cycling carried using an MJ PTC200 (MJ Research).

10. Quantitative Real Time - PCR

cDNA was diluted 1/100 in RNAse free H_20. 2ul of diluted cDNA was added to 1x Platinum SYBR Green qPCR SuperMix-UDG (Invitrogen), 0.2 µl ROX Reference Dye (Invitrogen) and a final concentration of 625nM for each primer, in a final volume of 10ul.

Amounts of transcript were estimated using the standard curve method. Five-fold dilutions series of a pooled cDNA sample was used to construct a standard curve for each primer pair, specific primers efficiency estimates were made and used to calculate the relative transcript abundance. Raw gene expression data was normalised to PPIA. Reactions were run using a 7900HT Fast Real-Time PCR System (Applied Biosystems). Thermal cycling conditions were as follows 50 ºC for 2 minutes, 95ºC for 2 minutes, 40 cycles of 95ºC for 30 seconds, 55 ºC for 30 seconds and 72ºC for 30 seconds. Followed by a dissociation step of 95ºC for 15 seconds, 56ºC for 15 seconds and 95ºC for 15 seconds. Data analysed using SDS software (Applied Biosystems) and all primers verified to produce a single product by melt curve and genuine mRNA expression validated by comparison to reverse transcriptase negative controls.

Primers used are as follows;

PPIA F –CTGCACTGCCAAGACTGA
PPIA R – GCCATTCCTGGACCCAAA.
JAK2 F- GCCCTGGGGTTTTCTGGTGCC
JAK2 R- CCGGCACATCTCCACACTCCC.
IL6 F – TCGAGCCCAGGGAACGAA
IL6 R – GCAACTGGACCGAAGGCGCT
ERBB2 F- TGGCCTGTGCCCACTATAAG
ERBB2 R – AGGAGAGGTCAGGTTTCACAC
STAT3 F- AGCATCCTGAAGCTGACCCAGGT
STAT3 R – TCGGCAGGTCAATGGTATTGCTGC.
IL6RA F – CCCCTCAGCAATGTTGTTTGT
IL6RA R – CACAGCCTTTGTCGTCAGG
GP130 F - CGGACAGCTTGAACAGAATGT
GP130 R - GTCTCCAAGTGTGTTTCCCTTC.
TBP F - TGCACAGGAGCCAAGAGTGAA
TBP R - CACATCACAGCTCCCCACCA

All primers were synthesised by Invitrogen at standard, desalted, purity.

11. Cloning

Wild type STAT3α cDNA was amplified from RNA purified from the normal OSE cell line OSE-C2. Primers incorporated restriction sites for NheI and Hind III for the forward and reverse primers respectively. Primers used are as follows STAT3 NheI F – CTGAGCTAGCCCCTGATTTTAGCAGGATGG STAT3 HindIII R – TGAAAGCTTTAGGCGCCTCAGTCGTATCT. Primers synthesised by Invitrogen using standard purity. PCR was carried out using Phusion DNA polymerase kit (New England Biolabs). Final reaction volume was 40µl containing 1 x HF DNA Polymerase buffer (with Mg^{2+}), 0.25mM each dNTP, 0.5uM of each primer, 0.02U/µl of Phusion DNA polymerase and 2ul of a 1/20 dilution of OSE-C2 cDNA (synthesis described above). Thermal cycling conditions were as follows, 95ºC for 1 minutes, 35 cycles of 95ºC for 30 seconds, 58 ºC for 30 seconds and 72ºC for 1 minutes 30 seconds.

PCR products were gel purified using Qiagen spin columns according to manufacturer's guidelines. Briefly bands relating to STAT3 were excised from the gel, weighed and dissolved the appropriate volume of GQ buffer, all subsequent steps performed according to the manufacture's guidelines expect the 70% ethanol wash was carried out twice and on both occasions PCR products were incubated in 70% ethanol buffer for 2mins.

Eluted PCR product and pcDNA 3.1(+), 2µg, (Invitrogen) were then digested in a final reaction volume of 20µl containing 10 units of NheI and HindIII (New England Biolabs), 1 x NEB 1 buffer, 1 x BSA at 37^{o}C for 1.5 hours. Vector and PCR products were purified after digestion using minelute and standard columns (Qiagen) respectively according to manufacturer's guidelines.

PCR products and vector were then mixed and ligated in a final volume of 10µl containing 1 x ligase buffer, 1mM ATP, 0.1U/µl DNA ligase (Bioline), cut vector pcDNA 3.1(+) and digested STAT3 PCR products were mixed at a molar ratio of 1:2 respectively containing a total DNA content of 100ng. Reactions were ligated at 4^{o}C O/N.

2.5µl of ligation reaction products were used transform gold efficiency alpha select chemically competent cells (Bioline) according to the manufacture's guidelines. 200µl of the resultant transformation reaction was plated onto lysogeny broth (LB) agar plates supplemented with 50µg/ml ampicillin. Single colonies were picked and used to inoculate cultures of LB also supplemented with 50µg/ml of ampicillin and incubated at 37^{0}C O/N in an orbital shaking incubator. Plasmid DNA was prepared from O/N cultures using a miniprep

kit (Qiagen) according to manufacturer's guidelines. Presence of STAT3 insert was validated using both restriction digest described above and sequencing see below.

JAK2 was cloned in a similar fashion however it was not possible to amplify full length JAK2 from cDNA. For this reason a human JAK2 was PCR cloned from pDONR223, sourced from Addgene (http://www.addgene.org/23915/) courtesy of William Hahn and David Root [404]. Primers used are as follows and incorporated restriction sites for NheI and ApaI in the forward and reverse primer respectively, JAK2 NheI F – CTGAGCTAGCGCATGGGAATGGCCTG JAK2 ApaI R - TGAGGGCCCTTCTTTCA TCCAGCCATGTT. Primers synthesised by Invitrogen using standard purity. JAK2 PCR product was purified using Qiagen minetlute kit according to manufacturer's guidelines. JAK2 PCR product and 2µg of pcDNA were digested in a final vol of 20µl 1x NEB buffer 4, 1x BSA with 10U of ApaI and NheI (New England Biolabs) at 25°C for 1hr followed by incubation at 37°C for 1hr. PCR and vector digest products were purified using minelute and standard columns (Qiagen) respectively according to manufacturer's guidelines. Ligation, bacterial, transformation and sequence validation were conducted as previously described.

12. Site-Directed Mutagenesis

Site directed mutagenesis was carried out using quick change II kit (Stratagene). Reactions were carried out according to manufacturer's guidelines using 5ng of template plasmid DNA. 2.5 µl of quick change reaction products were used to transform competent *E. Coli* as described above. Presence of mutations verified using sequencing.

Primer used are as follows;

STAT3 Y705E F – CAGGTAGCGCTGCCCCAGAGCTGAAGACCAAGTTTATC.

STAT3 Y705E R – GATAAACTTGGTCTTCAGCTCTGGGGCAGCGCTACCTG

STAT3 Y705F F – GTAGCGCTGCCCCATTCCTGAAGACCAAG.

STAT3 Y705F R – CTTGGTCTTCAGGAATGGGGCAGCGCTAC

JAK2 Y1007/1008 F - ACCAAAGTCTTGCCACAAGACAAAGAAGAAGAAAAAGTAA AAGAACCTGGTGAAAGTCCC

JAK2 Y1007/1008 R – GGGACTTTCACCAGGTTCTTTTACTTTTTCTTCTTCTTTGTCT TGTGGCAAGACTTTGGT.

JAK2 Y1007/1008F F – AAGTCTTGCCACAAGACAAAGAATTCTTTAAAGTAAAAGA ACCTGGTGAAAG

JAK2 Y1007/1008F R – CTTTCACCAGGTTCTTTTACTTTAAAGAATTCTTTGTCTTG TGGCAAGACTT.
JAK2 V617F F – AGCATTTGGTTTTAAATTATGGAGTATGTTTCTGTGGAGACGAGA
JAK2 V617F R – TCTCGTCTCCACAGAAACATACTCCATAATTTAAAACCAAATG CT.

Primers were designed on the Agilent website (https://www.genomics.agilent.com/CollectionSubpage.aspx?PageType=Tool&SubPageType=ToolQCPD&PageID=15) and were synthesised by MWG eurofins at standard purity.

13. Sequencing

Sequencing was carried using BigDye terminator v3.1 cycle sequencing kit (Applied Biosystems) according to manufacturer's recommendations. Sequencing reaction products were separated on an Applied Biosystems 3730 capillary DNA sequencer. Reactions and separation were carried out by Beckman Coulter Genomics.
Primers used were as follows; CMV F –CGGGGTCATTAGTTCATAGCC. BGH-PA R – TAGAAGGCACAGTCGAGG. STAT3 AR –TTCTGCCTGGTCACTGACTG. STAT3 BF – CGTGGTGACGGAGAAGCA. STAT3 BR –CAGTCACAATCAGGGAAGCA. STAT3 CF –TGCATTGACAAAGACTCT GG. STAT3 CR –CCCATGATGATTTCAGCAAA. STAT3 DF -GGCCATCTTGAGCAC TAAGC.
JAK2 AR –AGTGGGGTTTGATCGTTTTC. JAK2 BF –TCCTCGTTGGTATTGCAGTG. JAK2 BR –AAATTGGGCCATGACAGTTG. JAK2 CF –CAAGCAAACCAAGAGGGTTC JAK2 CR –TGCAGTTGACCGTAGTCTCC. JAK2 DF –TGGAAACTGTTCGCTCAGAC. JAK2 DR -GCAGGAAGCTGATGCCTATC. JAK2 EF-GCCAAAGGACATTCTTCAGG. JAK2 ER –GTTGCCAGATCCCTGTGG. JAK2 FF –AGTGCTGGTCGGCGTAATC.
Primers were synthesised by Invitrogen at standard, desalted, purity.

14. Plasmid Purification and Transfection

Once sequences of wild type or mutant constructs were verified a 40% glycerol stock, stored at -80^{0}C, was used to inoculate a culture of around 100ml of LB containing final

concentration of 50µg/ml of ampicillin (Sigma) for pcDNA 3.1 (+) or specinomycin (Sigma) (100µg/ml) for pDONR223 . Cultures were incubated at 37°C in an orbital shaking incubator O/N. Transfection grade DNA was prepared using a maxiprep kit (Qiagen) according to manufacturer's guidelines.

Transfection was carried out using effectene (Qiagen) based on an optimised ratio of DNA to effectene of 1:5. Briefly per well of a 6 well plate 400ng of DNA was added to 2ul of effectene, all other parameters were preformed according to manufacturer's guidelines. Cells were transfected for 24 hours in antibiotic free media, after which cells were reseeded for caspase, MTT assays and protein lysates.

15. Flow Cytometry

After treatment with cisplatin for the indicated time cells were trypsinised with 1x trypsin EDTA (Sigma). For each well of a 6 well plate cells were pelleted and resuspended in 500ml of PBS followed by 4.5ml of -20°C 70% v/v ethanol. Cell were fixed at -20°C for at least O/N. Cells were then pelleted and resuspended in 1ml of 1x propidium iodide (PI) solution (20µg/ml propidium iodide (Sigma), 50µg/ml RNase (Sigma) in PBS). Cells were stained for at least 2 hours at room temperature. Flow cytometry was carried on a FACS Calibur (Becton Dickinson) quantifying fluorescence in channel FL3. Data analysis was carried using FlowJo software (Tree Star Inc.) using the automated cell cycle analysis and Dean/Jett/Fox algorithm for quantitation of cells in each phase.

16. Expression Array Profiling

16.1 Cisplatin Treatment Microarray (for Figure 12)

RNA was prepared using TriReagent (Sigma) and hybridized to U133A gene chip (Affymetrix) at the genomics core, Lawrence Berkeley National Laboratory, CA, USA. All labelling and hybridisation steps conducted according to manufactures recommendations (http://www.affymetrix.com/Auth/support/downloads/library_files/hgu133plus2_libraryfile.zip). Data analysed using the Genespring GX Software Package (Aglient) following Lowess

background normalisation and robust multi-array (RMA) normalisation. Preparation of material carried out by Euan Stronach.

16.2 Paired Cell Line Expression Profiling Microarray (for Figure 48B)

RNA was prepared using TriReagent (Sigma) and hybridised to Sanger Hver1.2.1 10K cDNA microarrays at the Sanger Institute, Cambridge. Briefly total RNA from each cell line was reverse transcribed incorporating either Cy3 or Cy5 dyes (Amersham). cDNAs from sensitive and resistant paired lines were co-hybridised and scanned (ScanArray Express, Perkin Elmer). Each cell line comparison was carried out in quadruplicate, with dye swap labelling. Full details of the microarrays and protocols can be found at http://www.sanger.ac.uk/Projects/Microarrays/arraylab/arrays.shtml. Images files were quantified using Quantarray v3.0 (Packard) followed by analysis using the Genespring GX software package (Aglient). Array data was Lowess normalised and averaged between quadruplicates. T-tests were performed with Benjamini-Hochberg false discovery rate correction. Preparation of material carried out by Euan Stronach.

17. Data Collection, Statistics, IC_{50} and Doubling Time Estimations

Quantitative data presented for QRT-PCR, caspase 3/7 apoptosis assays, or MTT cell viability assays were all comprised from three technical replicates for each independent experimental replicate. Technical replicates from individual experiments were disregarded, if they deviated from their closest numerical replicate by more than twice the difference between the remaining two replicates. Numerical values shown for QRT-PCR, apoptosis and cell viability assays were averaged between individual experimental replicates after the exclusion of such technical replicate outliers.

Expression data, either QRT-PCR or western blotting (where quantified), was subject to an additional batch normalisation, in order to make comparisons between different experimental replicates more consistent. This was conducted as follows, after a raw expression values have been normalised, to a house keeping gene or loading control, it was further normalised to the mean normalised expression for the entire experimental replicate for a given gene. This is as opposed to normalising to an experimental control, usually an untreated or vehicle. For example for a given experiment for 10 samples examining STAT3

expression, raw STAT3 expression for each sample would be normalised to the raw expression of a keeping gene for that sample. The average of this normalised value was calculated for each of the 10 samples in the experiment, giving the average normalised STAT3 expression value for a specific experiment. Each normalised STAT3 expression values was then further 'batch' normalised to this average value.

IC_{50} estimates were made in Prism software package (GraphPad Software, Inc.) unless otherwise specified. When IC_{50} estimations were not made in Prism they were calculated as follows. Replicates of a particular experiment were averaged and plotted. The IC_{50} was then interpolated using a least squares model. 95% CI margins were estimated by making an IC_{50} estimation, in the same manner as previously described, for each individual replicate and calculating the error between these replicate specific IC_{50}. This error was used to calculate 95% CIs. Which were applied to the interpolated IC_{50} from the average of the replicates. T-test p values (paired) were calculated between the replicate specific IC50s for cisplatin alone and cisplatin plus rIL6(RA). Unless otherwise stated all T-test are students T-tests.

Results

Section

Results Chapter 1:-
Effects of Cisplatin on the IL6 / JAK2 / STAT3 Axis

1. Effects of Cisplatin on the IL6/JAK2/STAT3 Axis

1.1 Cisplatin Induces IL6 Expression

Expression microarray analysis of the cisplatin sensitive/resistant isogenic cell line pair PEO1 and PEO4 revealed *IL6* mRNA expression is induced by exposure to cisplatin. Figure 12 shows the fold change in *IL6* expression normalised to untreated time matched controls. Cell lines were treated with 25µM cisplatin for 4, 8 and 24 hours. *IL6* expression increased at each time point reaching a maximum at 24 hours when sensitive PEO1 cells expressed 4 times more *IL6* than untreated time matched control. Resistant PEO4 cells experienced roughly half this at 1.9 times control levels.

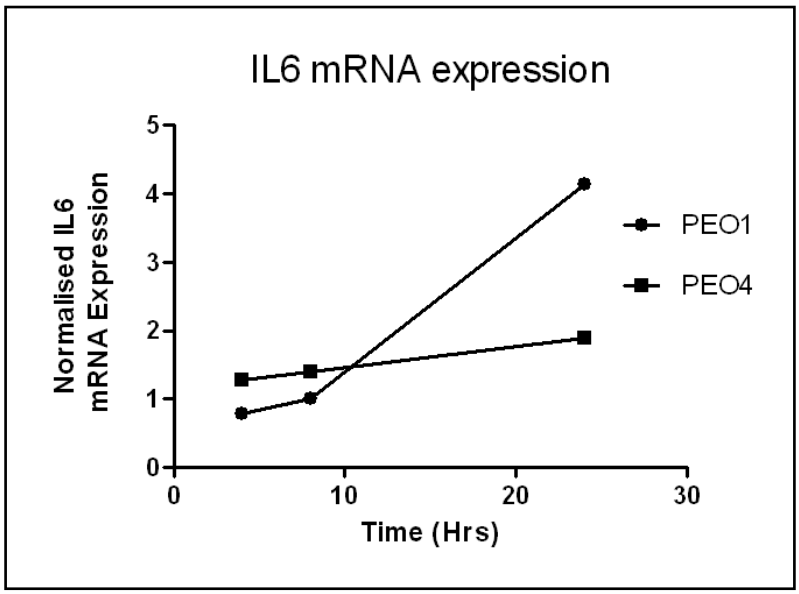

Figure 12. Expression microarray data showing the effect of cisplatin treatment on *IL6* expression. Array data of robust multi-array average (RMA) normalised *IL6* mRNA levels. PEO1 cisplatin sensitive and PEO4 cisplatin resistant cells exposed to 25µM cisplatin for 4,8, and 24 hours. Each data point shows the fold change relative to an untreated time matched control.

Due to a well documented role in tumourigenesis and tumour progression it was decided to validate this result using QRT-PCR in both the original cell line pair, PEO1, PEO4, and the additional isogenic sensitive/resistant pair PEA1, PEA2. Cisplatin dependant upregulation of *IL6* suggested this cytokine may play a pro-survival role after cisplatin

exposure, and the difference in magnitude of induction observed between the sensitive and resistant cells of the isogenic pair suggested a differential role for IL6 in the cisplatin response of each. The two sensitive/resistant isogenic cell lines pairs PEO1, PEO4 and PEA1, PEA2 were treated with two concentrations of cisplatin. Sensitive PEO1 and PEA1 cells were treated with 2.5μM and 5μM whereas the resistant PEO4 and PEA2 were treated with 5μM and 12.5μM. The 2.5μM and 12.5μM concentration represent roughly the IC_{50} of the sensitive and resistant cells respectively of each pair. As the 24 hour time point was both the final time point, in this experiment, and also associated with the highest induction of *IL6*, additional time points of 48 and 72 hours were included to examine whether expression would continue to rise. *IL6* mRNA expression was measured and normalised to the expression of the house keeping gene *PPIA* and further normalised to time matched untreated controls, the results are shown in Figure 13.

In each cell line cisplatin induced *IL6* expression in a time and concentration dependant fashion. In sensitive cells *IL6* expression peaked at 48 hours when it was 4.4 ($p=0.016$) and 4.3 ($p=0.063$) times background for 2.5μM treatment and 8.7 ($p=0.081$) and 7.4 ($p=0.23$) times background for 5μM treatment in PEO1 and PEA1 respectively. In resistant PEO4 cells *IL6* levels remained fairly constant between 48 and 72 hours. At 48 hours 5μM treatment induced 2.3 fold induction compared to 5.5 fold for 12.5μM treatment ($p<0.001$). In resistant PEA2 cells levels of *IL6* rose between 48 and 72 hours for both concentrations of cisplatin used however at 48 hours 5μM treatment induced a 1.8 fold increase ($p=0.086$) compared to 4.1 for 12.5μM treatment. A comparison of the 5μM treatment in each pair showed consistency with the array data, *IL6* induction was greater in magnitude in cisplatin sensitive cells. Fold increase in sensitive cells at 5μM was 8.7 and 7.4 for PEO1 and PEA1 respectively compared to 2.3 and 1.8 for resistant PEO4 and PEA2 respectively.

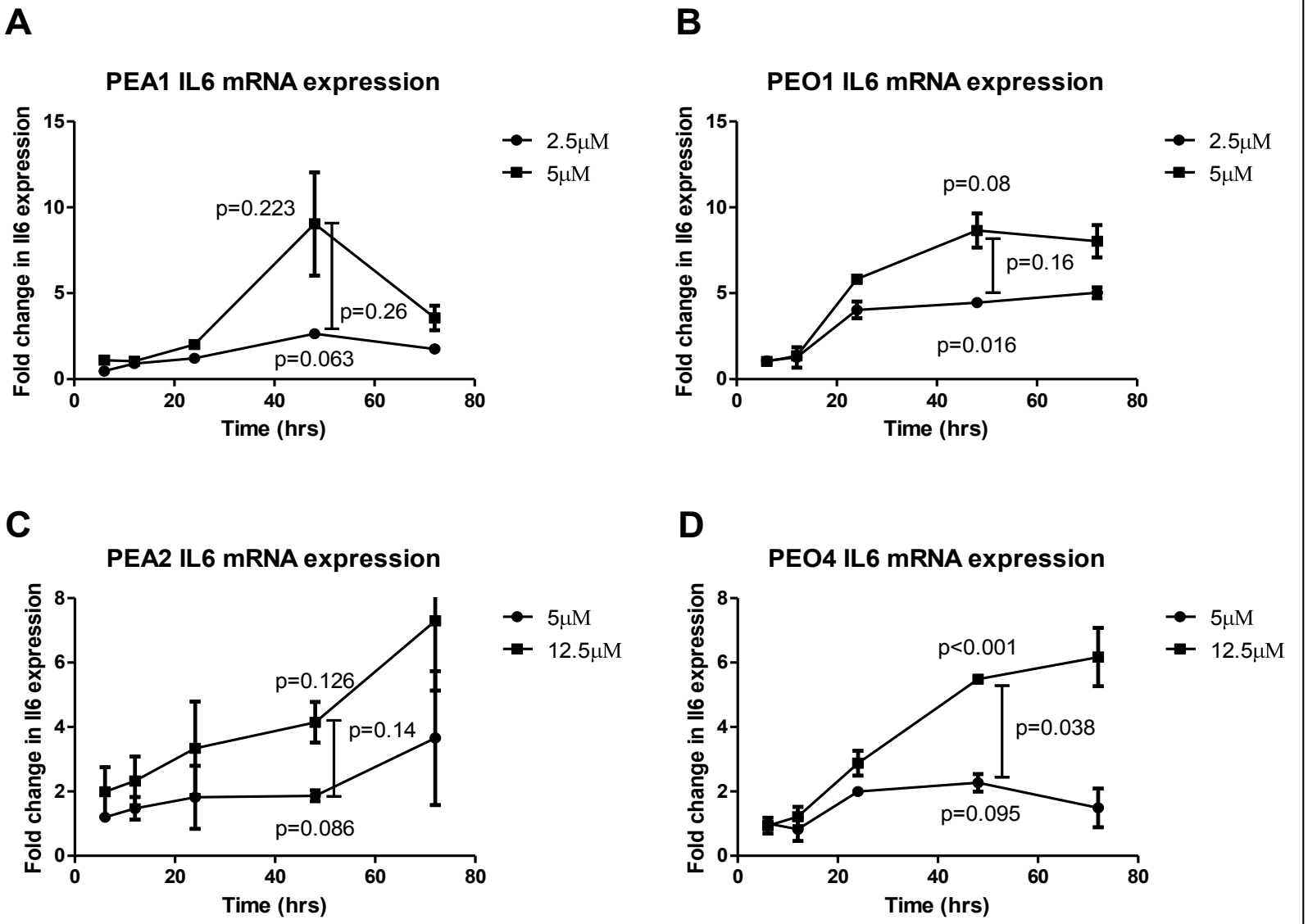

Figure 13. QRT-PCR analysis of *IL6* mRNA expression in response to cisplatin treatment. Cells were treated for 6, 12 ,24, 48 and 72 hours with the indicated concentration of cisplatin. Raw IL6 expression levels were normalised to PPIA and further normalised to an untreated time matched control. Each data point is the mean of 2 separate experiments. P values for individual concentrations are one sample students T-test (average is =1). P values between samples, indicated by horizontal bars, are two sample T test. All test are paired and two tailed. **A**, PEA1, **B**, PEO1, cisplatin sensitive cells. **C**, PEA2, **D**, PEO4 cisplatin resistant cells.

1.2 Cisplatin Modulates Signalling Through JAK2 and STAT3

IL6 signals via STAT3 activation. In order to correlate cisplatin dependent changes in *IL6* expression with downstream signalling protein lysates were prepared. Cells were treated at 12 and 24 hours with 2.5µM cisplatin for sensitive PEO1 and PEA1 and 12.5 µM cisplatin for resistant PEO4 and PEA2 cells, prior to lysis and western blotting. Results are shown in Figure 14A and B.

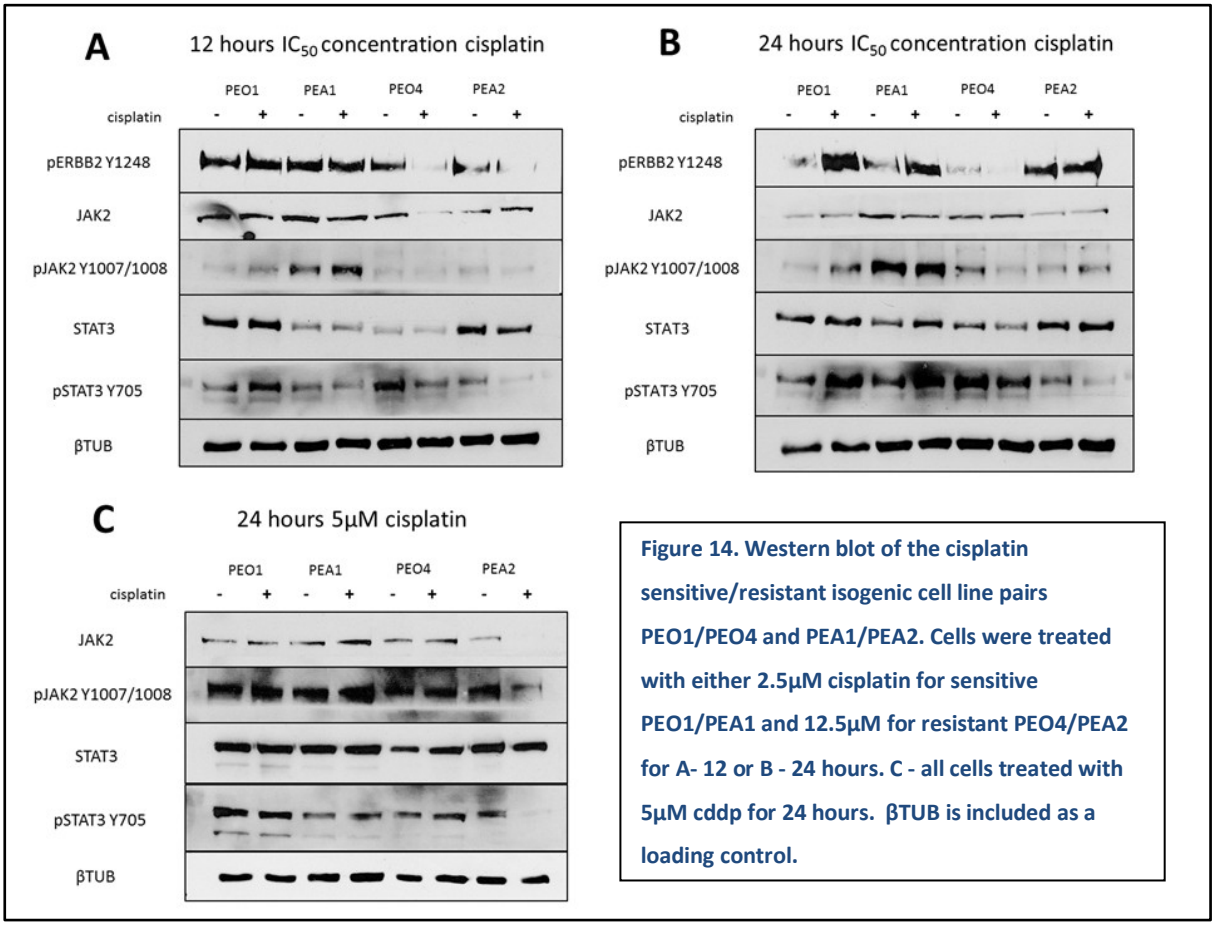

Figure 14. Western blot of the cisplatin sensitive/resistant isogenic cell line pairs PEO1/PEO4 and PEA1/PEA2. Cells were treated with either 2.5µM cisplatin for sensitive PEO1/PEA1 and 12.5µM for resistant PEO4/PEA2 for A- 12 or B - 24 hours. C - all cells treated with 5µM cddp for 24 hours. βTUB is included as a loading control.

Western blotting was conducted to examine the effect on total and phosphorylated levels of STAT3 and JAK2. It has been reported that ERBB2 and JAK2 interact and ERBB2 can activate STAT3 via JAK2 (Ren & Schaefer, 2002), for this reason levels of phosphorylated ERBB2 were also examined. In sensitive PEO1 and PEA1 cells treated with 2.5µM cisplatin an increase in tyrosine 705 phosphorylated STAT3 (pSTAT3) was observed,

this effect was most clear after 24 hours of exposure. Conversely resistant PEO4 and PEA2 cells treated with 12.5µM cisplatin saw a reduction in their levels of pSTAT3, apparent at both time points. Changes in pSTAT3 were mirrored by changes in the levels of tyrosine 1007/1008 phosphorylated JAK2 (pJAK2) and tyrosine 1248 phosphorylated ERBB2 (pERBB2). After 12 hours (Figure 14A) exposure 12.5µM treated resistant cells exhibited a marked downregulation in the levels of pERBB2. Conversely 2.5µM treated sensitive cells saw an increase in their levels of pERBB2 which was most pronounced at 24 hours (Figure 14B). It was not possible to reliably detect of levels of total ERBB2 due to the levels of expression of the protein, which was only readily detectable at the protein level in the ERBB2 amplified cell line SKOV3, however both protein and mRNA expression of ERBB2 has been validated in each of the cell lines examined here (see Figure 33 and Figure 43B).

To examine whether observed differences in behaviour between cisplatin sensitive and resistant cells were due to the concentration of drug used or a feature of acquired resistance, cells were treated with an identical concentration of cisplatin (5µM) for 12 and 24 hours. The results for the 24 hour exposure are shown in Figure 14C and were very similar to the 12 hour exposure (data not shown). Previous changes in levels of pSTAT3 and pJAK2 were reversed, in PEO1 PEO4 and PEA1 no change in the either phospho protein was seen. A reduction in JAK2, pJAK2 and pSTAT3 was still seen in PEA2.

These results suggested that observed differences in behaviour of resistant cells when exposed to an IC_{50} concentration of cisplatin was a function of both dose of cytotoxic drug and, for PEA1 and PEA2, acquired resistance, as they behaved differently at the same concentration. STAT3 regulates the expression of a number of downstream genes that play a role in survival and growth. The upregulation of different STAT3 genes could have different effects in the context of cisplatin exposure. For example STAT3 upregulates cyclin D1 (CCND1) which promotes cell division and proliferation. The upregulation of this gene may not be selective in response to a DNA damaging cytotoxic drug. STAT3 also regulates BCL-xL an inhibitor of apoptosis which would be expected to confer a survival advantage if upregulated in response to an apoptosis inducing chemotherapy agent such as cisplatin.

1.3 Cisplatin Resistant Cells Exhibit a Differential Response to Cisplatin in Their Levels of JAK2, STAT3 and ERBB2 Activation.

Results obtained in Figure 14A and B suggested that resistant clones of isogenic pairs might respond differently to cisplatin in terms of phosphorylation of STAT3 JAK2 and ERBB2. However these results were obtained by treating sensitive and resistant cells with differing cisplatin concentrations, 2.5µM and 12.5µM respectively. In addition Figure 14C, showed no clear change in STAT3 phosphorylation in three of the four cell lines, suggesting that differences in behaviour of sensitive and resistant clones specifically, increases in pSTAT3 in sensitive PEO1 and PEA1, at 2.5µM, and STAT3 deactivation in resistant PEO4 and PEA2, at 12.5µM, were simply concentration dependant. To investigate whether differences in the phosphorylation of STAT3 JAK2 and ERBB2 are determined by cisplatin concentration alone or whether they are a feature of acquired resistance to chemotherapy a titration was conducted.

Cells were treated with increasing concentrations of cisplatin, from 1µM to 25µM, for a period of 24 hours. Western blotting was conducted to examine dose specific effects on the levels of phosphorylation and expression of these proteins, cyclin D1 was included as a measure of STAT3 activation and S139 phosphorylated H2AX (pH2AX) to demonstrate cisplatin dependant DNA damage.

Figure 15 shows the results obtained from the sensitive/resistant isogenic pair PEO1 PEO4. In both PEO1 and PEO4 cisplatin induces a dose dependant decrease in levels of pSTAT3 (shown in A). In PEO1 a small but insignificant (p=0.29), 30% increase in pSTAT3 was observed in response to 1µM cisplatin before a step wise decrease with each successive increase in cisplatin. After exposure to 15µM cisplatin pSTAT3 levels in PEO1 and PEO4 had dropped to below 15% of untreated levels in both cell lines and exposure to 25µM was associated with a drop of more than 99%. Figure 15A shows the pSTAT3 cisplatin IC_{50} (the concentration required to reduce STAT3 phosphorylation by 50%) which was 7.8µM in PEO1 and PEO4, suggesting that any difference observed Figure 14A and B was a factor of the different cisplatin concentrations used in this experiment.

Significant differences in the levels of pJAK2 were found between PEO1 and PEO4, see Figure 15B. In PEO1 levels of pJAK2 rose to 3 fold untreated levels (p=0.003 paired T-test) when exposed to 2µM cisplatin, at the same concentration levels of pJAK2 remained largely unchanged in PEO4. Changes in pJAK2 levels between PEO1 and PEO4 were statistically significant at 1µM (p= 0.042), 4µM (p=0.009), 8µM (p=0.019) and 10µM

(p=0.003) (T-test unequal variance), in all of which PEO1 had increased levels of pJAK2. Above 2μM cisplatin, levels of pJAK2 in PEO1 decreased and by 15μM no significant difference between the two cell lines was seen. At 25μM levels had fallen to around 30% of untreated levels in both, (31% in PEO1 and 33% in PEO4).

Similar changes in pERBB2 were found between PEO1 and PE04, shown in C. In PEO1s treated with 1μM cisplatin pERBB2 increased 24 fold (n=2) above which levels dropped for each successive increase in cisplatin. Fold changes in PEO1 and PEO4 were significantly different at 8μM (p=0.025 T-test unequal variance). A smaller increase in pERBB2 occurred in PEO4 of around 40% untreated levels between 1μM and 8μM. In both cell lines at 15μM cisplatin pERBB2 had fallen to under 1% of untreated levels.

Cisplatin induced changes in the levels of total JAK2 between PEO1 and PEO4 were very similar to those of pJAK2. However the increase in total JAK2 in PEO1 was lower than for the activated phospho-protein. JAK2 expression peaked at 4μM when a 62% increase over untreated was seen (p=0.075 paired T-test). This was roughly half the increase of the phosphorylated protein, suggesting the ratio of phospho and total JAK2 is not constant and is also affected by cisplatin, in a dose dependant manner. In PEO4 no increase in JAK2 was seen at lower concentrations of cisplatin, instead levels sequentially fell reaching a minimum at 25μM where they were 13% of untreated levels (p=0.011 paired T-test). At this concentration, JAK2 expression had also dropped below untreated levels in PEO1 falling to 35%.

In both PEO1 and PEO4 STAT3 expression was reduced by cisplatin exposure, however the magnitude of this decrease was lower than that occurred of pSTAT3, suggesting that changes in the activation of STAT3 and not the overall expression of the protein are the most important changes caused by cisplatin exposure. Reductions in overall STAT3 expression might be caused by reduced positive feedback as STAT3 has been found to bind its own promoter sequence in a similar manner to other STAT proteins [405].

STAT3 regulates the expression of a number of genes, including cyclin D1 which was probed as a measure of STAT3 transcriptional activity in response to cisplatin. Consistent with cisplatin dependant changes in STAT3 activation cyclin D1 expression also decreased upon exposure in both cell lines, shown in Figure 17A and B. Samples were also probed with a S139 phosphorylated H2AX antibody to ensure cisplatin induced DNA double strand breaks were formed, these are associated with H2AX phosphorylation and foci formation. As expected increasing cisplatin concentrations were associated with increased pH2AX,

suggesting changes in other proteins are due to the dose dependant genotoxic effects of cisplatin, see Figure 17A and B.

Figure 16 shows the cisplatin dependant fold changes in pSTAT3, pJAK2, pERBB2 and STAT3 that occurred in the isogenic cell line pair PEA1, PEA2. Changes in the levels of pSTAT3 differed significantly between PEA1 and PEA2, shown in Figure 16A. In cisplatin sensitive PEA1 cells cisplatin concentrations of between 1μM and 8μM were associated with an increase in STAT3 activation, which peaked at 1.9 fold untreated levels when exposed to 1μM cisplatin (p=0.070 paired T-test). After which pSTAT3 levels fell progressively, in response to 25μM cisplatin STAT3 phosphorylation had dropped to 8% of untreated levels (p=0.016 paired T-test). This was in contrast to the resistant cell line PEA2 where no increase in pSTAT3 was observed at lower concentrations of cisplatin. Instead STAT3 activation decreased in a step-wise fashion falling to 18% (p=0.030 paired T-test) and 9% (p=0.009 paired T-test) untreated levels after 15μM and 25μM exposure respectively. The cisplatin pSTAT3 IC_{50} was significantly higher in PEA1 (13.6μM 95% CI: 10.0–19.6μM) compared to PEA2 (2.2μM 95% CI: 1.5-3.2μM).

The cisplatin dose response of pJAK2 and pERBB2 also differed significantly between PEA1 and PEA2. Despite this the profiles of both phospho proteins, were very similar to each other, within a particular cell line. In PEA1 pJAK2 and pERBB2 were elevated relative to untreated controls between 1μM and 15μM cisplatin. Both peaked at 4μM cisplatin where pERBB2 and pJAK2 were 6.3 fold (p=0.09 paired T-test) and 3 (p=0.14 paired T-test) fold untreated levels. In contrast in PEA2 a more modest increase of 1.5 fold, in both pJAK2 and pERBB2 occurred, which was only seen at the lowest, 1μM, concentration of cisplatin. After which there was a progressive decrease in the levels of both, 15μM cisplatin caused pERBB2 to drop to 29% (p=0.039 paired T-test) of controls and 25μM caused pJAK2 to decrease to 47% (p=0.087 paired T-test). A significant difference in the cisplatin induced fold change of pERBB2 between the isogenic pair was seen at 4μM (p=0.042 unequal variance T-test). No significant changes were observed in the expression of STAT3 either between either isogenic pair or in response to cisplatin.

Cisplatin dose dependant effects on cyclin D1 and pH2AX for PEA1 and PEA2 are shown in Figure 17C and D. A small but non-significant increase in cyclin D1 expression was observed in PEA1 when exposed to 1μM cisplatin. In contrast to cisplatin dependent changes in pSTAT3 in PEA1 and PEA2 no significant differences occurred in cyclin D1, instead expression decreased at a similar rate in both, data not shown. In both cell lines a dose

dependant increase in the levels of pH2AX was seen consistent with the changes seen in these proteins being due to the genotoxic nature of cisplatin.

A cisplatin titration was also conducted on the cisplatin resistant, ERBB2 amplified cell line SKOV3. In PEO1, PEO4, PEA1 and PEA2 it was not possible to probe for ERBB2 as expression is not high enough. SKOV3 allowed for an assessment for the cisplatin dependant effects on ERBB2 signalling. Specifically whether cisplatin caused changes in activation of this protein alone or whether changes in phosphorylation were due to changes in overall expression. This experiment was carried out 3 times and a representative western blot is shown in Figure 17E.

Consistent with cell lines previously described dose dependant changes signalling in STAT3 JAK2 and ERBB2 occurred on cisplatin exposure. SKOV3 responded in a manner somewhat intermediate between sensitive and resistant cells. ERBB2 Y1248 phosphorylation increased around 1.5 fold untreated levels when exposed to between 2μM and 4μM but decreased to around 1% at 25μM. Levels of ERBB2 expression were largely unchanged regardless of the concentration of cisplatin used, suggesting changes occurred only at the level of ERBB2 activation (data of western blot densitometry not shown). Levels of pJAK2 and pSTAT3 were also elevated at these concentrations unlike resistant PEO4 and PEA2s, peaking at 3 and 2 fold untreated respectively. Activation of proteins decreased at higher cisplatin concentrations. pSTAT3 fell to under 50% and pJAK2 returned to basal levels in response to 25μM exposure.

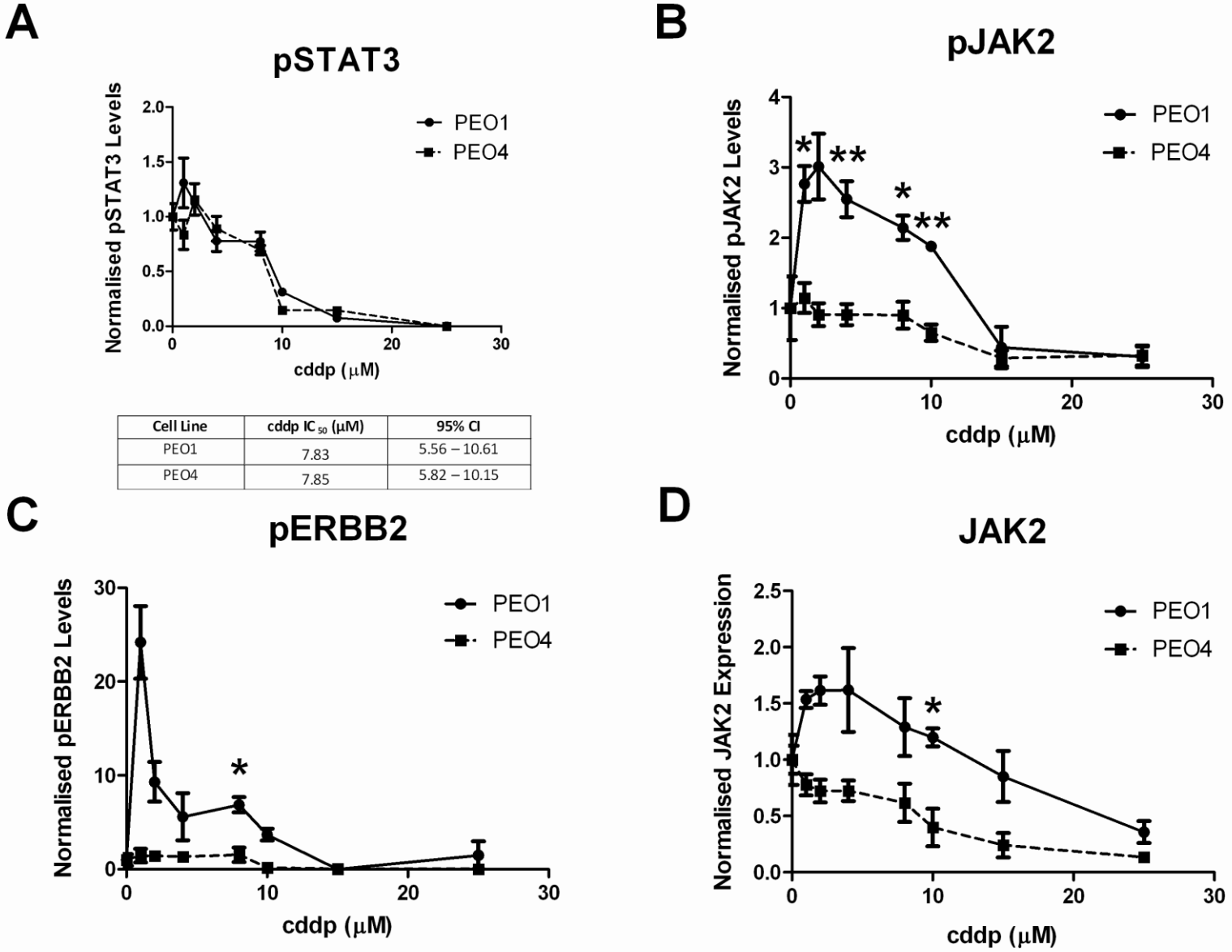

Cell Line	cddp IC_{50} (μM)	95% CI
PEO1	7.83	5.56 – 10.61
PEO4	7.85	5.82 – 10.15

Figure 15. Western blot of cisplatin (cddp) titration in PEO1, PEO4 sensitive/resistant isogenic cell line pair. Cells exposed to the indicated concentration of cddp for 24 hours. Western blotting conducted in triplicate for each target except pERBB2 in PEO1 (n=2). Protein bands quantified using Image J and normalised to the geomean of βTUB and HSP60. Normalised values were further batch normalised before averaging. Error bars show the SEM of these values. All values are shown relative to untreated (0μM cddp) controls, to show fold changes. Antibodies - pSTAT3 – pY705. pJAK2 – pY 1007/1008. pERBB2 pY1248. T-tests performed between PEO1 sensitive and PEO4 resistant cells at each cddp concentration; * $p < 0/05$, ** $p < 0.01$. In **A**, IC_{50} estimations with confidence interval estimates made in Prism software package.

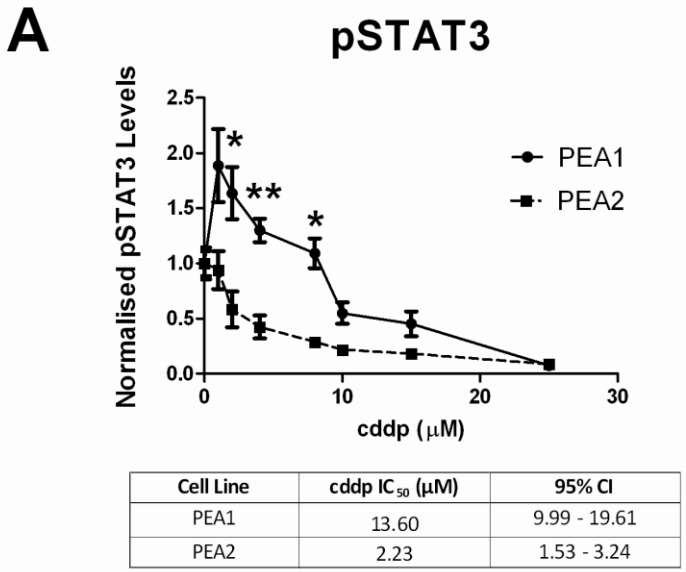

Cell Line	cddp IC_{50} (μM)	95% CI
PEA1	13.60	9.99 - 19.61
PEA2	2.23	1.53 - 3.24

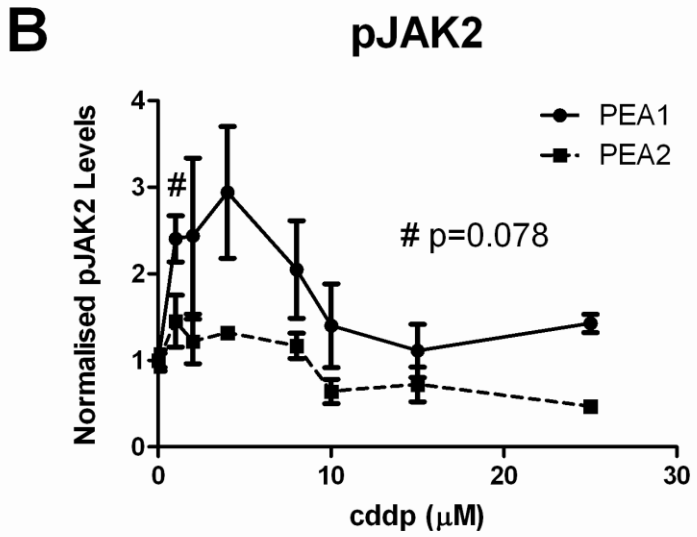

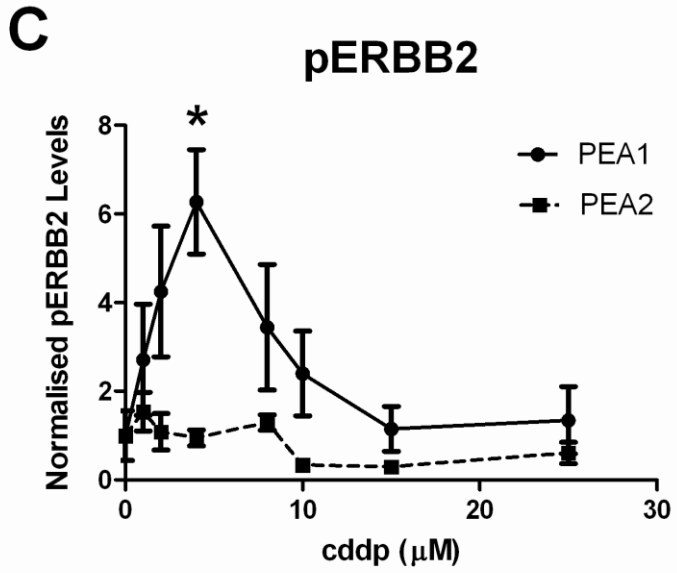

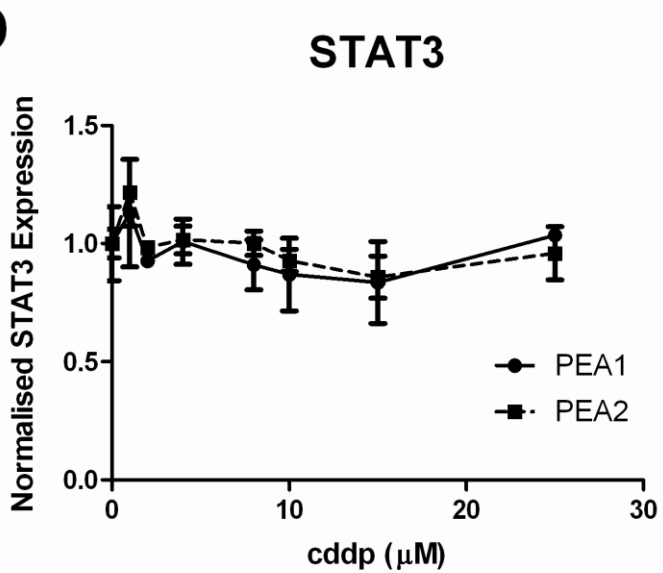

Figure 16. Western blot of cisplatin (cddp) titration in PEA1, PEA2 sensitive/resistant isogenic cell line pair. Cells exposed to the indicated concentration of cddp for 24 hours. Western blotting conducted in triplicate for each target. Protein bands quantified using Image J and normalised to the geomean of βTUB and HSP60. Normalised values were further batch normalised before averaging. Error bars show the SEM of these values. All values are shown relative to untreated (0μM cddp) controls, to show fold changes. Antibodies - pSTAT3 – pY705. pJAK2 – pY 1007/1008. pERBB2 pY1248. T-tests performed between PEA1 sensitive and PEA2 resistant cells at each cddp concentration; * p < 0/05, ** p < 0.01. In **A**, IC_{50} estimations with confidence interval estimates made in Prism software package.

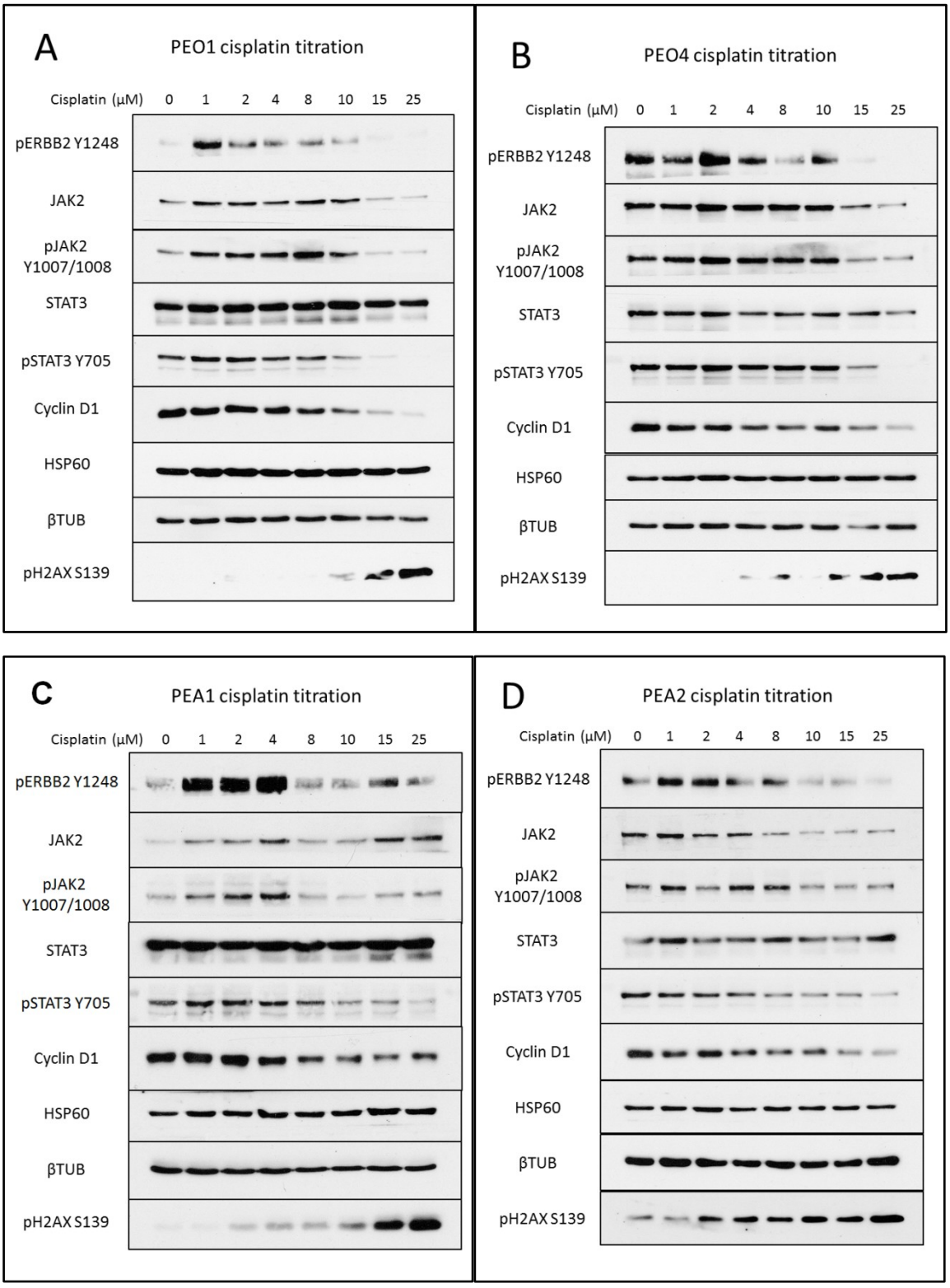

Figure 17. Representative western blots use to generate Figure 15 and Figure 16.

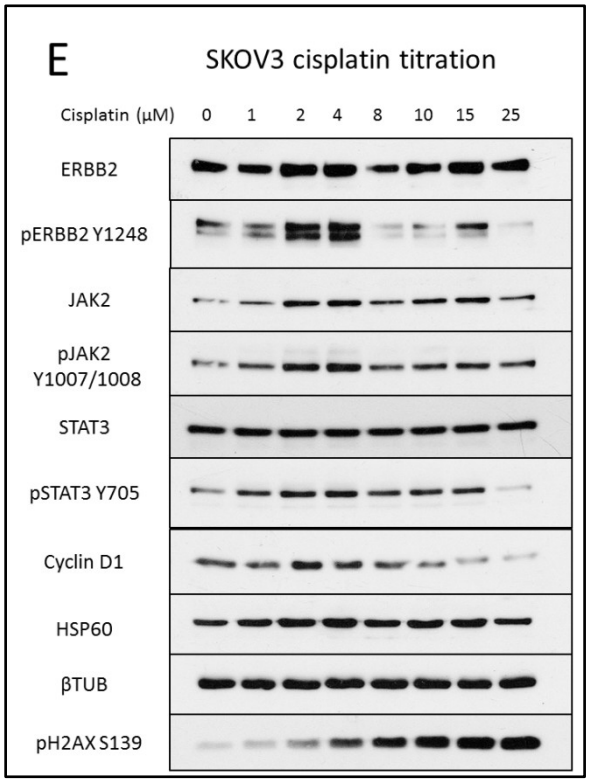

Figure 17. Representative western blots use to generate Figure 15 and Figure 16.

1.31 Levels of pERBB2 Y1248 and pJAK2 Y1007/1008 Correlate Highly

A visual inspection of cisplatin response profiles of pJAK2 and pERBB2 (Figure 15B/C and Figure 16B/C) in each cell line suggested a high degree of correlation exists between the two. To examine and quantify this further the average normalised values for phosphorylated JAK2 and ERBB2 for each individual cell line was plotted and linear regression performed. The results are shown in Figure 18. The linear correlation is displayed on each graph and for comparison the corresponding correlation between pERBB2 and JAK2 expression is shown. In each case the correlation between the levels of each activated protein was above 0.8, and as high as 0.94 in PEO4, demonstrating a high degree of similarity in the way these proteins responded to cisplatin treatment. For each cell line the correlation between both phospho variant was higher than between overall JAK2 expression and pERBB2, showing that cisplatin changes in ERBB2 activation more closely matched levels of JAK2 activation than levels to total JAK2 protein expression which might suggest a degree of co-regulation.

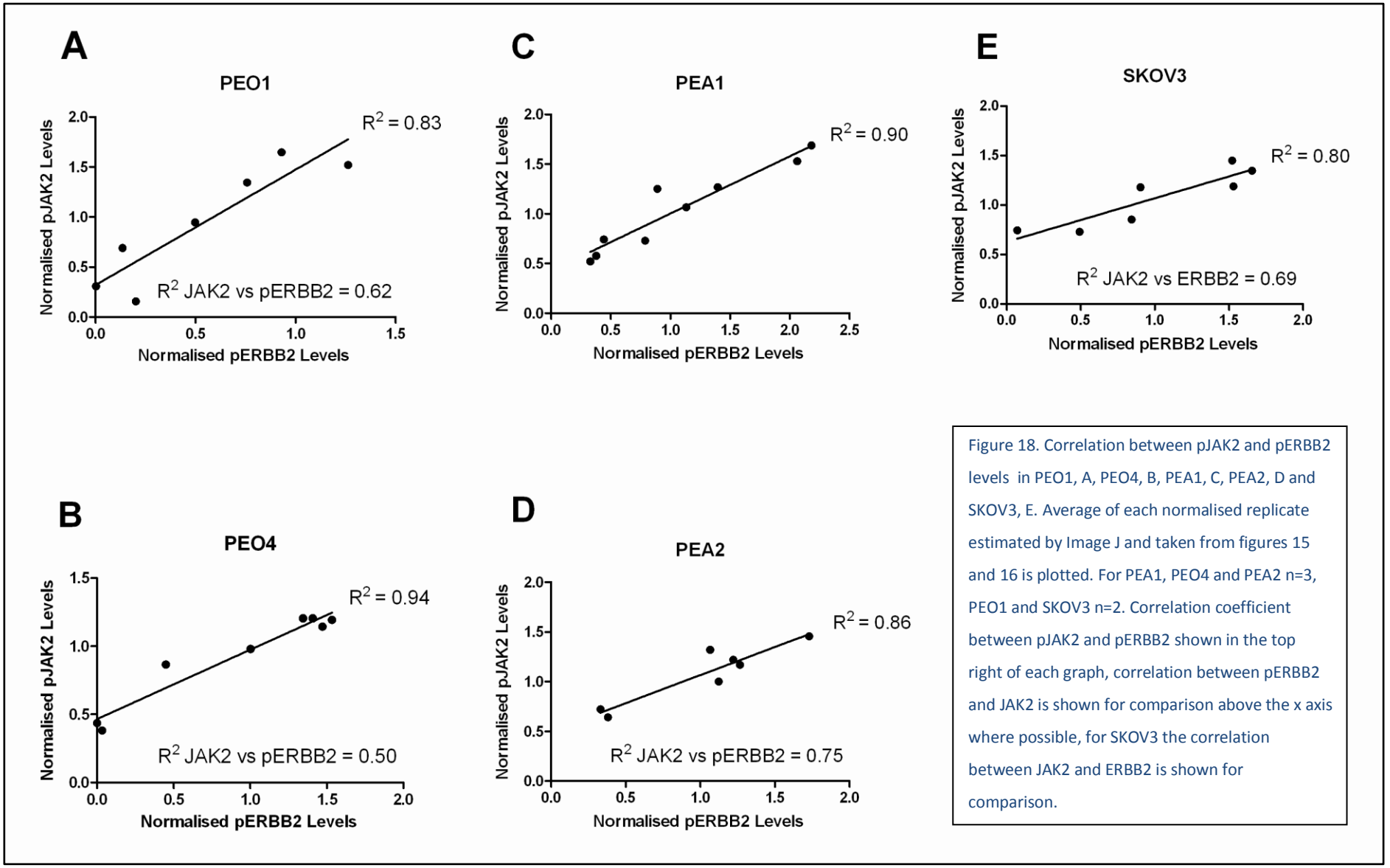

Figure 18. Correlation between pJAK2 and pERBB2 levels in PEO1, A, PEO4, B, PEA1, C, PEA2, D and SKOV3, E. Average of each normalised replicate estimated by Image J and taken from figures 15 and 16 is plotted. For PEA1, PEO4 and PEA2 n=3, PEO1 and SKOV3 n=2. Correlation coefficient between pJAK2 and pERBB2 shown in the top right of each graph, correlation between pERBB2 and JAK2 is shown for comparison above the x axis where possible, for SKOV3 the correlation between JAK2 and ERBB2 is shown for comparison.

1.4 Cisplatin Causes Both an Increase and Reduction in JAK2 at the Transcriptional Level in a Dose Dependant Manner

Figure 15D illustrates the changes in JAK2 protein expression associated with cisplatin exposure in the sensitive/resistant pair PEO1/PEO4. Low concentrations, between 1μM and 8μM, were associated with either increased protein expression, observed in PEO1 and SKOV3, or marginal decreases in resistant PEO4 and PEA2. However in all cell lines, except SKOV3, higher concentrations, above 15μM, caused reduced protein expression. When treated with 25μM cisplatin expression of JAK2 fell to 17% untreated in PEA2, 16% in PEO4 and 45% in PEO1. To investigate whether changes in JAK2 expression were transcription or post transcriptional QRT-PCR was performed. Cisplatin sensitive PEO1 and PEA1 cells were treated with 2.5μM, whereas resistant PEO4 and PEA2 were treated with 12.5μM. If cisplatin dependant changes in JAK2 protein expression were transcriptionally regulated an increase in *JAK2* mRNA should be found in PEO1 and PEA1 and a decrease in PEO4 and PEA2. *ERBB2* mRNA expression was also quantified to examine the possibility that cisplatin dependant changes in pERBB2 might be also be transcriptionally regulated, although results from SKOV3 suggested they are not, as levels of ERBB2 didn't alter significantly upon cisplatin treatment.

Figure 19A shows the cisplatin induced changes in *JAK2* mRNA levels in the two isogenic pairs PEO1, PEO4 and PEA1, PEA2. When exposed to 2μM cisplatin PEO1 and PEA1 experienced an increase in both pJAK2 Y1007/1008 and overall JAK2 protein expression. When exposed to 2.5μM cisplatin PEO1 exhibited no significant differences in JAK2 mRNA relative to untreated time matched controls. An increase in *JAK2* mRNA expression of 1.5 fold ($p=0.018$) was observed in PEA1. When treated with either 10μM or 15μM cisplatin resistant PEO4 and PEA2s experienced a decrease in both pJAK2 and JAK2. Correspondingly when treated with 12.5μM cisplatin both cell lines saw a reduction in *JAK2* mRNA ($p= 0.033$ $p=0.014$ one sample T-test equal variance), which fell to 74% and 72% of untreated controls respectively. With the exception of PEO1 changes in *JAK2* mRNA expression closely mirrored JAK2 protein expression suggesting cisplatin dependant changes in JAK2 are, at least partially, transcriptionally regulated.

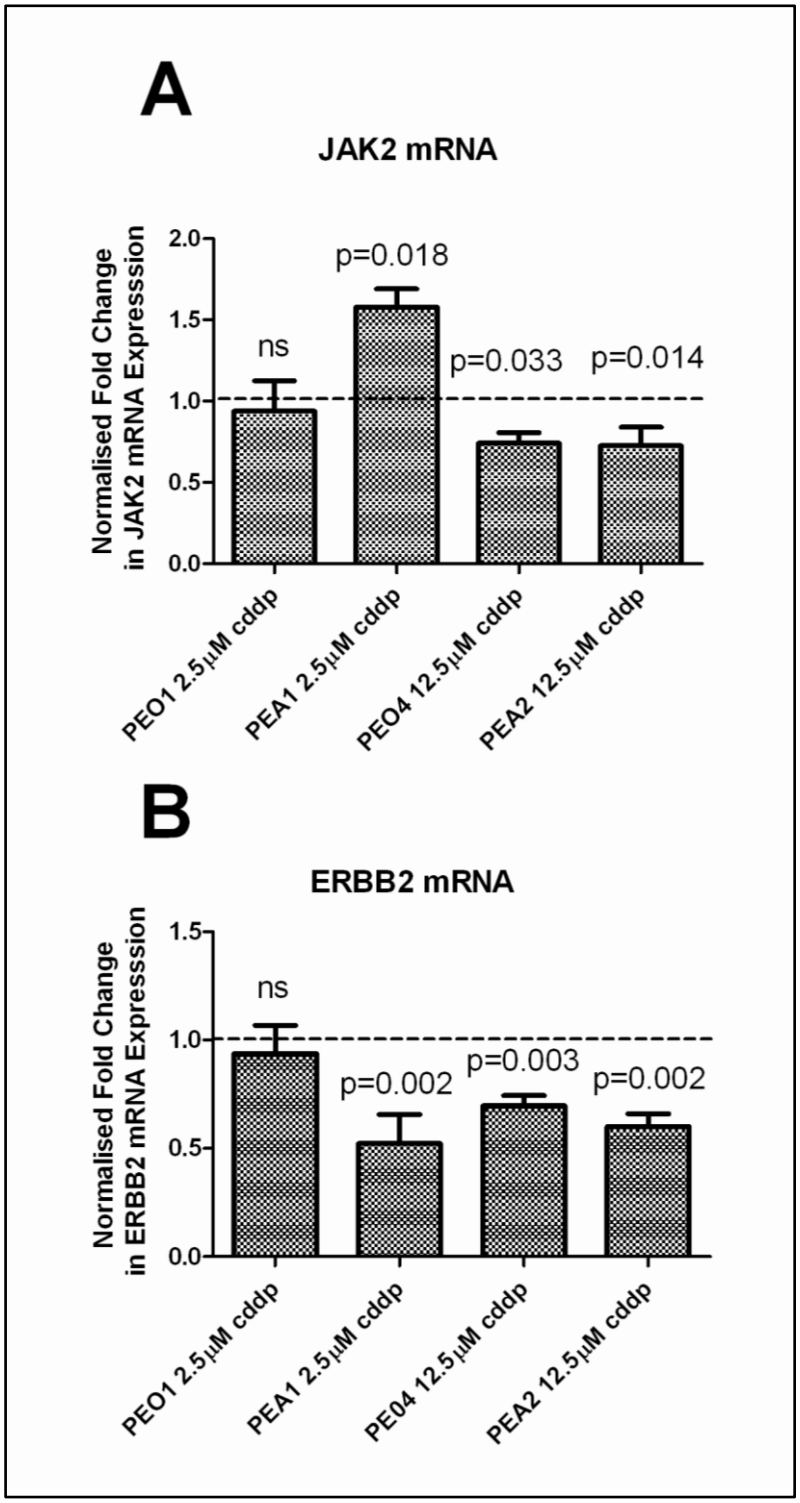

Figure 19. QRT-PCR data of cells treated with cisplatin at the indicated concentration for 24 hours. Each experiment repeated in triplicate, in each replicate JAK2/ERBB2 expression was normalised to PPIA. The average fold change in normalised JAK2/ERBB2 expression relative to time matched untreated controls is shown error bars represent the SEM in this value. P values show results of a one sample equal variance T-test testing the hypothesis that cisplatin treated cells are significantly different from untreated in normalised expression =1.

In contrast to JAK2, cisplatin dependant changes in ERBB2 phosphorylation could not be accounted for at the transcriptional level. This might have been predicted based on the cisplatin titration carried out in SKOV3 showing no significant changes in ERBB2, see figure 17D. Cisplatin dependant changes in *ERBB2* mRNA expression are shown in Figure 19B. In three of four cell lines examined a significant decrease in *ERBB2* mRNA was detected after cisplatin exposure. The extent of this reduction was similar in PEA1 ($p=0.002$), PEO4 ($p=0.003$) and PEA2 ($p=0.002$) where levels fell to 52%, 70%, and 60% of untreated controls respectively. Reductions in ERBB2 didn't correlate with the dose of cisplatin used in PEA1 and PEA2 expression fell by a similar amount (52% and 60% of untreated respectively), despite a 5 fold difference in dose. Regardless less of the concentration used or the cell line exposed cisplatin was associated with a decrease in ERBB2 mRNA expression. With the exception of PEO1 this data suggests that cisplatin causes a reduction in *ERBB2* mRNA and that changes in phosphorylation are more likely due to protein activation.

Discussion :- Results Chapter 1

1.1 Cisplatin Induces IL6 Expression

First suggested by the expression microarray experiment and subsequently replicated by QRT-PCR, sensitive cells experience a greater cisplatin dependent induction of *IL6* mRNA than their resistant isogenic partner. The magnitude of this difference was very similar for both pairs of cell lines. In 48 hour, 5μM exposed cells, sensitive lines experienced a 3.8 fold and 4.1 fold greater increase than their resistant pair, for PEO1/PEO4 and PEA1/PEA2 respectively.

Recently evidence has been growing around the ubiquitous nature of this response in various human cell types, both cancerous and normal, as a consequence of exposure to a variety of DNA damaging agents. Increased IL6 expression has been noted in human colorectal carcinoma cells [406], lung adenocarcinoma cells [406], immortalised human fibroblasts [407], normal and cancerous human epidermal keratinocytes [408] in response to radiation and the anthracycline doxorubicin. The addition of cisplatin to the list of agents capable of inducing IL6 expression adds further weight to the suggestion that the key event stimulating this induction is DNA damage. The mechanism of this induction was further examined by Rodier et al who found radiation induced IL6 secretion was dependant on each of NBS1 (Nijmegen Breakpoint Syndrome 1), ATM (ataxia telangiectasia mutated) and CHK2 (checkpoint kinase 2) expression, firmly linking IL6 induction to DNA damage and more specifically, ATM mediated double strand break repair.

Another interesting piece of evidence that supports the notion of a connection between DNA damage repair or more specifically HR competency is the observation that BRCA1 loss via either promoter methylation or mutation has been significantly correlated with the presence of tumour infiltrating CD8+ T-cells in HGS ovarian tumours [409]. The presence of tumour infiltrating T-cells was also correlated with improved survival this result has been recently been reproduced in a larger data set [134].

If DNA damage induced IL6 secretion was dependant on a functional HR pathway BRCA mutant tumours would not upregulate IL6 when treated with chemotherapy, which in

turn would not exert its immune evasive effects and therefore would be predicted to contribute to increased tumour infiltration and survival.

The dependence of DNA damage induced IL6 secretion on ATM, NBS1 and CHK2 expression offer some interesting possibilities. NBS1 is part of the MRN complex, which also includes MRE11A and RAD50, together they are the initial sensor of DSB, required for recruitment of ATM to DBS foci [410]. ATM not only phosphorylates CHK2 which in turn is responsible for phosphorylating and stabilising p53, but it is also required for activation of BRCA1. Activation of CHK2 and p53 have numerous downstream effects including regulation of the cell cycle and apoptosis, whereas BRCA1 is more exclusively associated with the repair of DSB by HR, a process for which it is required.

As such the dependence of DNA damage induced IL6 induction on ATM has two interesting potential implications. Firstly, it might offer an explanation for the increased expression of *IL6* in sensitive cells. Secondly it might allow the potential use of IL6 as a biomarker of HR competency.

Relating to the first point, cisplatin exposure induces SSB that, if not repaired, transition to DSB through DNA replication. Cisplatin also reduces levels of JAK2 pERBB2 and pSTAT3 more efficiently in platinum resistant cell lines. STAT3 is a driver of cell proliferation via expression of genes such as cyclin D1 and MYC. Therefore it appears that resistant cells are better able to reduce proliferation in response to cisplatin exposure, possibly allowing them more time to repair SSB, preventing them from transitioning to DBS and therefore reducing the activation of ATM and subsequent induction of IL6. As such IL6 might function as a read out of cisplatin resistance, whereby resistant cells, better able to repair SSB before they transition in DSB, potentially do not upregulate IL6 to the same degree.

Second it offers the potential of using induced IL6 expression as a biomarker of resistance and potentially homologous recombination competency. This would be particularly relevant to ovarian and breast cancer if it were shown that IL6 induction was dependant on BRCA1 or BRCA2, or more generally on a functioning HR pathway. As it could result in IL6 being a useful biomarker to predict response to chemotherapy, by constituting a HR competence assay, as well as allowing the monitoring of acquisition of platinum resistance.

Patients with germline BRCA1/2 mutations who develop ovarian cancer tend to respond better to chemotherapy and as a consequence has a significantly better survival than sporadic cases [411]. While HR deficiency is clearly an important mechanistic feature of tumourigenesis in ovarian, and breast cancers, it also renders cells in culture hyper sensitive

to DNA damaging agents such as cisplatin [401]. Furthermore the acquisition of platinum resistance has been linked to the restoration of functional BRCA1/2 protein expression and restored HR competency in germline cases [402]. In addition to the cases of germline mutation integrated genomic analysis of expression, methylation, copy number and DNA sequence has suggested that deregulation of the HR pathway, caused by a multitude of aberrations other than inherited mutation of BRCA1 or BRCA2 is a common event in around 50% cases of sporadic disease [122]. Whether or not these people respond better to platinum based chemotherapy is currently unknown. However there is clear logic for predicting that they would, and if DNA damage induced *IL6* expression was dependant on a functional HR pathway, it could be a potential biomarker for 'BRCAness' in sporadic cases.

The importance of HR competency screening in ovarian tumours is highlighted by recent clinical trials on PARP inhibitors such as olaparib. Clinical data on PARP inhibitors [49,412] has supported *in vitro* findings [413] regarding synthetic lethality of PARP inhibitors in HR deficient backgrounds. Further trials are on going to evaluate the efficacy or PARP inhibitors in this setting but given the common nature of HR pathway aberrations in sporadic cases of ovarian cancer, a simple assay of HR competency and therefore a predictor of PARP sensitivity could be a useful tool for informing and monitoring treatment. Also Fong et al showed decreased response to PARP inhibition with olaparib was associated with increased platinum resistance of patients.

Therefore were it the case that DNA damage induced IL6 expression is BRCA dependant, if tumours did not secret IL6 in response to cisplatin it would imply those individuals are HR deficient and therefore likely to respond well not only to chemotherapy but also PARP inhibitors. A transition from no IL6 response to a response would also indicate a likely reversion to HR competency, and as a consequence potentially not only the onset of the chemotherapy resistance but also the lack of synthetic lethality with PARP inhibition, as has been observed in patients and cell line models selected for HR competency by cisplatin treatment.

The PEO1 cells used in this experiment have been reported to be mutated for BRCA2 and would therefore be expected to provide a means to validate this hypothesis [401]. Unfortunately the particular lineage of PEO1 cells used in this experiment, and throughout this study, contain a reversion mutation that restores the open reading frame of BRCA2 [414]. However an examination of PEO1 cells possessing this mutation or additional BRCA1/2 mutant cells lines would allow for a validation of this hypothesis. Specifically if either BRCA1/2 mutant cell lines were found to be deficient in DNA damage induced IL6

upregulation and this response could be restored with overexpression of wild type BRCA1/2 this would provide compelling evidence for the theory.

1.2 Cisplatin Modulates Signalling Through JAK2 and STAT3

Having identified increased *IL6* expression in response to cisplatin, the next step was to examine the activation of its canonical downstream signalling partners. The phosphorylation and DNA binding activity of STAT3 was discovered in response to IL6 treatment, therefore it was predicted that cisplatin induced IL6 exposure would be associated with an increase in STAT3 activation and expression of STAT3 regulated genes. Given the role of STAT3 in regulating the expression of anti-apoptotic proteins such as BCL-xL and BIRCH5 this suggested a potential mechanism of resistance to cisplatin, in which a cell's increased expression of *IL6*, in response to cisplatin, has pro-survival effects presumably mediated through STAT3. Although this was not supported by the increased magnitude of IL6 induced in the sensitive line of each isogenic pair, it remained possible that resistant cells were for example more sensitive to IL6 or had higher basal expression.

Therefore it was surprising to note the differences between cisplatin dependant changes in STAT3 and JAK2 activation and IL6 expression, see Figure 14. There appears to be an inverse correlation between the magnitude of IL6 induction and activation of JAK2 and STAT3. Data shown in Figure 13 suggests a dose relationship between cisplatin exposure and *IL6* expression. In each cell line examined higher concentrations of cisplatin were associated with increased *IL6* expression. However Figure 14 suggests an inverse dose relationship with cisplatin exists for phosphorylated STAT3 and JAK2. Using the same concentrations and length of exposure low (2.5µM) concentrations of cisplatin caused an increase in STAT3 and JAK2 activation. But moderate (5µM) and high (12.5µM) concentrations were associated with either no overall change or a reduction in the activation of both proteins, when the opposite would be predicted occur, on the basis of IL6 expression. That is with each increase in cisplatin dose the activation of STAT3 and JAK2 would increase in line with *IL6* expression.

Two caveats to the data presented in this section are the twin assumptions implicit in predicting a link between *IL6* mRNA levels and STAT3 activation. Firstly that the cells in question are capable of responding to IL6 stimulation, that is do they express the necessary proteins to propagate the signal? This issue is dealt with in mainly in the following results

chapter 2, however protein expression of GP130, JAK1, JAK2 and STAT3 has been validated in both isogenic pairs.

Secondly that an increase in *IL6* mRNA expression translates to an increase in levels of IL6 circulating in the cell culture media, which was never validated. However in light of other reports of IL6 protein secretion in response to other DNA damaging agents discussed in the section above it seems reasonable to assume this is true. Although it might be reasoned that results in section 1.2, specifically Figure 14, showing a lack of a correlation between STAT3 activation and *IL6* expression imply that one of the two assumptions above are incorrect.

Results in Figure 14 have three additional potential implications. First, that there is a correlation between cisplatin dose and signalling through two important pro-survival and pro-proliferative factors known to be important drivers tumourigenesis and cancer growth, those being ERBB2 and STAT3. And second that there might be a difference in the response of sensitive and resistant cells to cisplatin in terms of activation of these genes. Due to the conditions used in the experiment that formed Figure 14 it was not possible to discern which of these, or indeed whether both, were true. For this reason a cisplatin titration was carried out to more closely examine the relationship between dose and activation of STAT3 and ERBB2 proteins between sensitive and resistant cells and whether this response might play a role in acquired resistance to chemotherapy.

Finally synchronous changes in the levels of pJAK2, pSTAT3 and pERBB2 suggested a potential regulatory link between these proteins. A link between JAK2 and STAT3 is well documented however a potential link between JAK2 and ERBB2 is less well understood. A cisplatin titration would also allow a more detailed inspection of any synchronous dose dependant changes in the activation of these proteins.

1.3 Cisplatin Resistant Cells Exhibit a Differential Response to Cisplatin Treatment in Levels of Activation of JAK2 STAT3 and ERBB2.

The different cisplatin dose response profiles of JAK2, ERBB2 and STAT3 between sensitive and resistant cells revealed by the titration experiment confirms each of the three additional potential implications described in the section above. They were, firstly, that cisplatin causes dose dependant changes in the activation of these proteins. This was also

extended to one downstream gene cyclin D1 whose expression profile was similar to the phospho profile of its transcriptional regulator STAT3.

Secondly that sensitive and resistant cells respond differently to cisplatin in the activation of JAK2 and ERBB2, for both pairs, and STAT3 for PEA1 and PEA2. At first this result might seem counterintuitive. Generally speaking ERBB2 and STAT3 are considered pro-survival, and consequently it might be expected that any differential behaviour between sensitive and resistant cells would be in the form of greater activation of these proteins in resistant cells after cisplatin exposure to overcome other apoptotic signalling. Another interpretation might be that reduced activation of these proteins reduces expression of proliferative, factors such as cyclin D1, reducing doubling times and allowing additional time for the repair cisplatin DNA lesions before S phase, DNA replication and the transition of these lesions into DSB. This theory is given credence in light of the results showing that equivalent doses of cisplatin induce a larger fold upregulation of *IL6* in sensitive cell lines and IL6 induction by radiation has been shown to be dependent on ATM, a protein crucial for DSB repair.

Thirdly, Figure 18, showing the correlation seen between levels of pJAK2 and pERBB2 provided further evidence of a regulatory link between these two proteins. In each cell line the highest correlation occurred between the phospho levels of each protein, in each $R^2 > 0.8$. This was higher than the correlation between pERBB2 and total JAK2. In SKOV3 where data was available for a total verses total correlation, this was lower than either phospho to total or phospho to phospho correlations. This not only strengthens the case for a functional link between the two proteins but also implies that relationship is dictated by levels of active phosphorylated protein. While this data is not evidence of a direct interaction, given that both proteins are kinases it is tempting to speculate that one is substrate for the other. A clue regarding the direction of such a relationship is provided by the effect of cisplatin on total JAK2 expression. At higher concentrations of cisplatin protein expression of JAK2 was decreased, suggesting that the concomitant decrease in levels of pJAK2 was at least in part due to this. This raises the possibility that a decrease in levels of total and consequently phosphorylated JAK2 might be driving cisplatin dependant changes in STAT3 and ERBB2 phosphorylation.

1.4 Cisplatin Causes Both an Increase and Reduction in JAK2 at the Transcriptional Level in a Dose Dependant Manner

Data showing that high dose cisplatin reduces JAK2 expression suggested this decrease might drive concomitant changes in phosphorylation of STAT3 and ERBB2. Further clues regarding the mechanism of this process were provided by an examination of cisplatin induced changes in *JAK2* mRNA levels. PEA1 cells treated with 2.5μM cisplatin experienced an increase in *JAK2* mRNA levels mirroring changes at the protein level. Similarly in PEO4 and PEA2 treated with 12.5μM cisplatin experienced a decrease in *JAK2* mRNA which also mirrored changes seen at the protein level at this dose, suggesting cisplatin dependant changes in transcriptional levels of JAK2 could be the key initial event resulting in the reduction of levels of activated STAT3 and ERBB2.

Results Chapter 2:-
IL6 Responsiveness and the Effects of rIL6 Treatment on Cisplatin Sensitivity

2. IL6 Responsiveness and the Effects of rIL6 Treatment on Cisplatin Sensitivity

2.1 Determination of IL6 responsiveness in a Panel of Ovarian cell lines. rIL6 Activates STAT3 but not JAK2

The potential effects of cisplatin induced IL6 secretion in ovarian cancer cell lines are unknown. The function of such signalling could be either autocrine, paracrine or both. In addition the profile of cisplatin induced IL6 upregulation and STAT3 activation did not correlate. Increasing cisplatin concentrations were associated with increased IL6 expression but decreased STAT3 activation. For example in PEO1 cells exposed to 5μM cisplatin experienced a 6 fold increase in *IL6* mRNA after 24 hours, however levels of pSTAT3 at the same time had fallen to 67% when exposed to a concentration of 4μM.

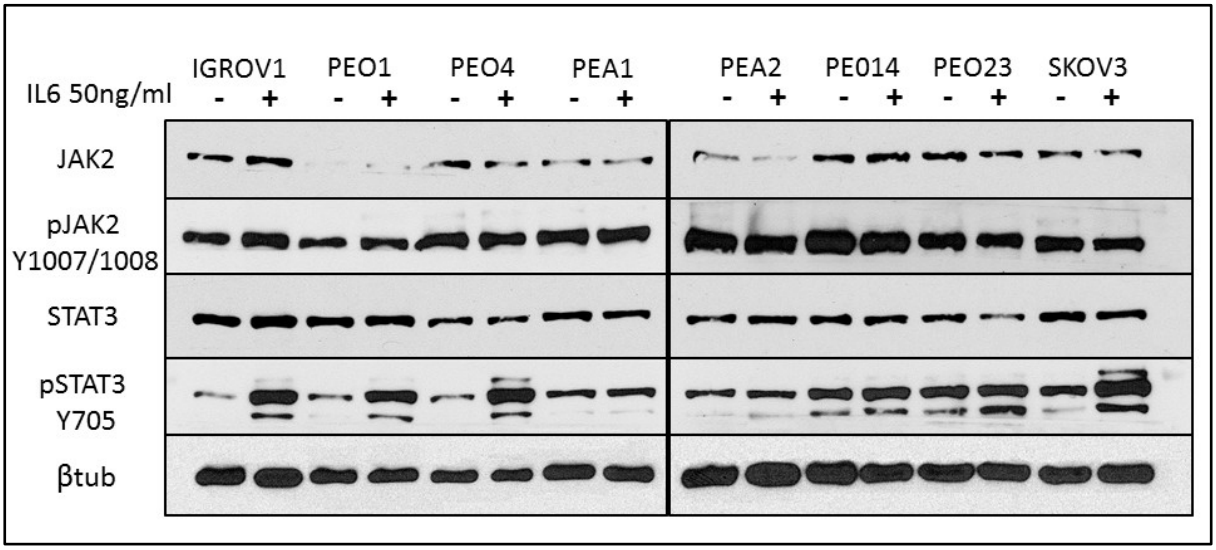

Figure 20 Western blot of rIL6 treatment. Cell were stimulated with rIL6 (diluted in 0.01% BSA m/v), at a final concentration of 50ng/ml or an equivalent volume of diluted BSA for 40 minutes before lysis. Experiment was repeated twice and the same results were obtained each time. Western blot was combined from two membranes processed simultaneously.

To assess whether cisplatin dependent IL6 upregulation is functional *in vitro* cells were exposed to exogenous rIL6 and western blotting used to examine the activation of

downstream proteins. IGROV1, a HGS ovarian cell line, was used as a positive control as they have previously been reported to be IL6 responsive.

Figure 21 shows the effect of exogenous rIL6 exposure in the three isogenic cell line pairs PEO1/PEO4, PEA1/PEA2 and PEO14/PEO23 plus SKOV3 on the activation of STAT3 and JAK2. STAT3 activation is the downstream event most commonly associated with IL6 exposure and many of its effects are dependent on this activation. Therefore an increase in pSTAT3 and IL6 responsiveness are considered synonymous. Response to rIL6 was binary, cells either responded or did not respond unambiguously. As previously reported IGROV1 responded to rIL6, in which a small increase in pJAK2 was also apparent. PEO1 PEO4 and SKOV3 were also responsive to exogenous rIL6. The remainder of the cell lines tested, PEA1 PEA2 PEO14 and PEO23, were not.

PEA1 and PEA2 were not responsive to rIL6 treatment, suggesting the function of cisplatin induced IL6 expression is purely paracrine, in these cells lines. Cisplatin induced changes in pSTAT3 therefore appear unrelated to IL6 expression.

2.2 Addition of soluble rIL6RA Restores IL6 Responsiveness in PEA1 and PEA2

Given that PEA1 and PEA2 have significantly different pSTAT3 responses to cisplatin exposure it was hypothesised that PEA2's ability to more sensitively deactivate STAT3 might play a role in cisplatin resistance, and therefore that increasing STAT3 activation might sensitise cells to treatment. However Figure 20 demonstrates that PEA1 and PEA2 were both unresponsive to IL6. IL6 signals through a receptor dimer of the ubiquitously expressed GP130 and the more tissue specific IL6RA. Via, either expression of a specific truncated transcript variant, or proteolytic cleavage of the full length protein a soluble form of IL6RA (sIL6RA) can be produced. Secreted sIL6RA is capable of acting as an agonist, forming ligand bound dimers with GP130 and conferring IL6 responsiveness on cells that do not express this receptor. For this reason PEA1 and PEA2 were examined for the ability of sIL6RA to restore IL6 responsiveness. Cells were treated with 75ng/ml of rsIL6RA, either alone or in combination with rIL6 to access the effects of STAT3 activation, the results are shown in Figure 21. Consistent with results obtained previously rIL6 alone had no effect on STAT3 activation. In both PEA1 and PEA2 rsIL6RA treatment was associated with an increase in pSTAT3 and for PEA2 this was similar in magnitude to combination IL6 +

IL6RA treatment. In PEA1 maximal pSTAT3 induction was observed in combination treatment. These results suggest firstly, that PEA1 and PEA2 do not respond to rIL6 due to a lack of expression of IL6RA and secondly that both cell lines constitutively express IL6, assuming that cell don't respond to bovine IL6 in culture serum, as rsIL6RA alone activated STAT3. For convenience, subsequently the addition of either rIL6 only, in the case of PEO1 PEO4 and SKOV3, and rIL6 + rsIL6RA, for PEA1 and PEA2, shall be referred to as rIL6(RA).

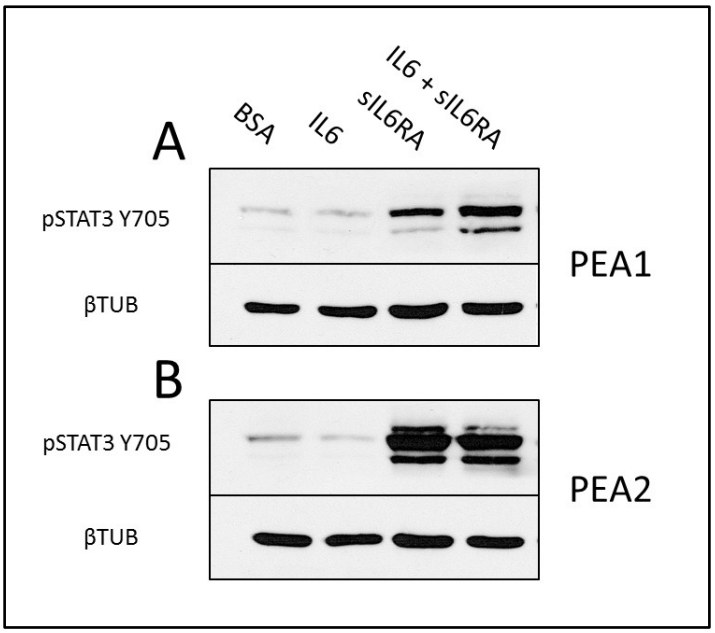

Figure 21. Western Blot of PEA1, A and PEA2 B cells treated with rIL6 (50ng/ml) rsIL6RA (75ng/ml) or combined rIL6 + rsIL6RA (IL6RA) (total 125ng/ml) or an equivalent volume of diluted (0.01% m/v) BSA, for 30 minutes prior to lysis.

2.3 rIL6(RA) Treatment Sensitises Cells to Cisplatin

2.31 rIL6(RA) Treatment Increases Cisplatin Induced Caspase 3/7 Activation

STAT3 drives the expression of a number of genes including the anti-apoptotic *BCL-xL/S* and *BIRC5*, the proliferative *CCND1*, and the angiogenic *HIF1α* and *VEGF* [305]. The

effects of cisplatin induced changes in pSTAT3 levels are therefore difficult to predict. Elevated pSTAT3 in the presence of cisplatin could confer a survival advantage, for example via increased expression of anti-apoptotic genes. Or conversely, elevated pSTAT3 could be deleterious to tumour survival by increasing proliferation and therefore reducing the time in which cells are able repair cisplatin DNA adducts contributing to the generation of DSB and genomic instability.

To access any potential role for STAT3 signalling in mediating either platinum resistance or tumour response to cisplatin exposure cells were activated with rIL6(RA) prior to cisplatin treatment. The cisplatin sensitive/resistant pair PEO1/PEO4 and resistant SKOV3 cells were treated with 50ng/ml of rIL6 alone prior to cisplatin exposure whereas PEA1 and PEA2 were treated with rIL6 (50ng/ml) and rsIL6RA (75ng/ml), to restore IL6 responsiveness. BSA was used as a vehicle control as this used as a carrier for rIL6 and srIL6(RA). Cells were treated with rIL6(RA) for 30 minutes prior to the addition of cisplatin at 10μM for sensitive PEO1 and PEA1 cells and 25μM for resistant PEO4, PEA2 and SKOV3 cells. After 24 hours of cisplatin exposure levels of cleaved and activated caspase 3 and caspase 7 were quantified. Cells were also incubated with a range of cisplatin concentrations for 72 hours to allow the assessment of any IL6 dependant change in cisplatin IC_{50}.

In each cell line tested treatment with rIL6(RA) alone had no effect on caspase 3/7 activation. However combination rIL6(RA), cisplatin treatment was associated with a potentiation of cisplatin induced caspase 3/7 activation. This effect was significant for PEO1 ($p=0.006$), PEO4 ($p=0.040$), PEA2 ($p=0.002$) and SKOV3 ($p=0.003$) but not PEA1 ($p=0.158$) in paired T-tests. Figure 22 shows cell viability normalised caspase 3/7 activation levels in sensitive PEO1 and PEA1 when treated with 10μM cisplatin resistant PEO4 PEA2 and SKOV3 when treated with 25μM cisplatin.

Figure 22F shows the fold increase in activated caspase 3/7 associated with combination rIL6(RA), cisplatin treatment compared to cisplatin alone for each cell line. The degree of sensitisation achieved in resistant PEO4 and PEA2s was higher than their sensitive isogenic pairs. In PEO1 and PEO4 this difference was significant ($p=0.037$). rIL6(RA), cisplatin combination treated PEO1s had an 18% increase in the activation of caspase 3/7 relative to cisplatin alone, whereas PEO4s had a 36% increase. Similarly PEA1 had a 20% increase in cisplatin induced caspase 3/7 activation, compared to 39% in PEA2.

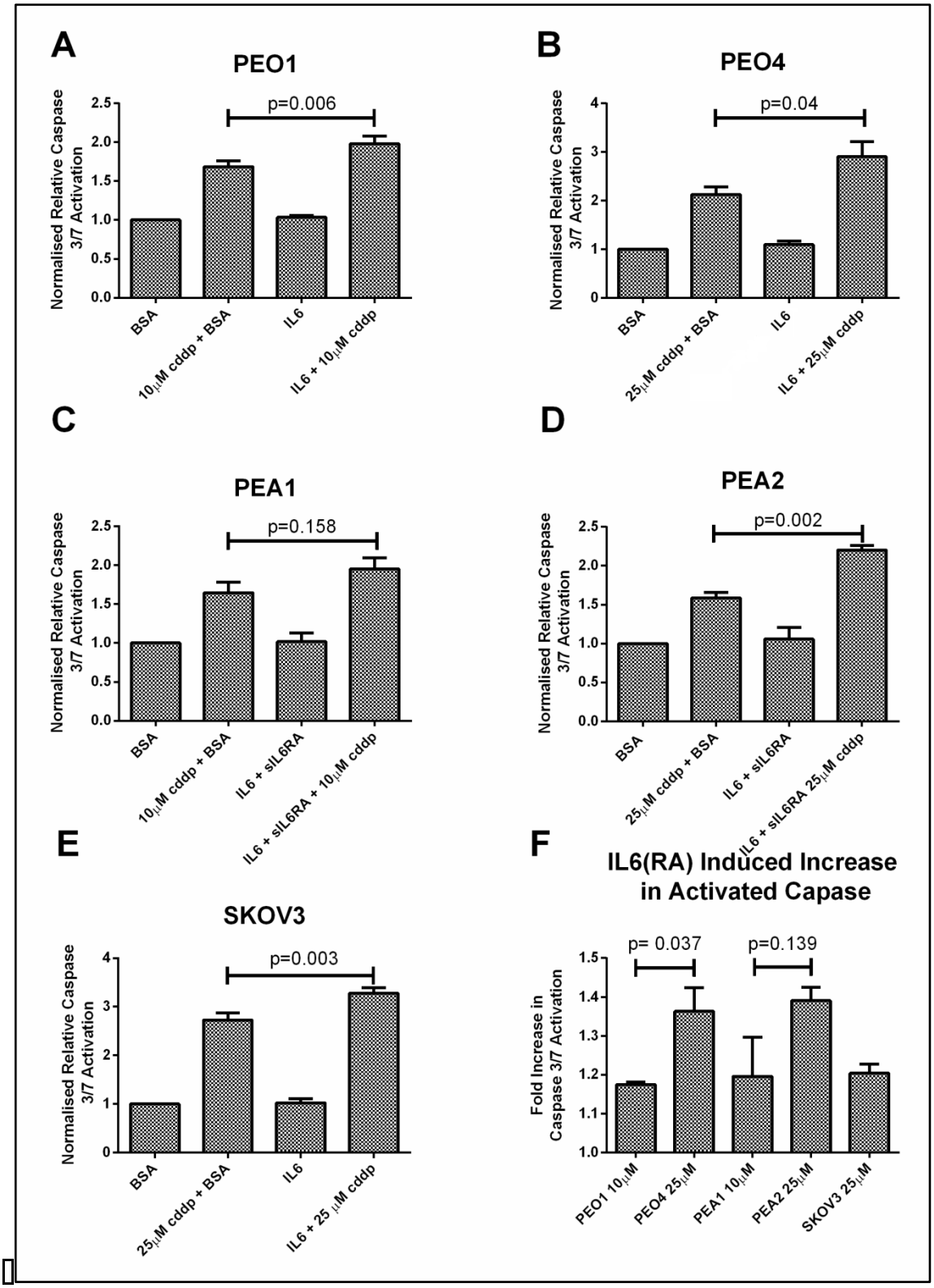

Figure 22. Caspase 3/7 activation plots of rIL6 treatment in combination with cddp. **A- E**, cells treated with 50ng/ml of rIL6 (A,B and E) or rIL6 + rsIL6RA (75ng/ml) (B and C) 30 minutes prior to cisplatin exposure at 10μM (A and C) or 25μM (B, D, and E) for an 24 hours. After which levels of activated caspase 3 and 7 were quantified and normalised to cell viability. F shows the fold increase in caspase 3/7 activation in the cddp and rIL6(RA) combination treatment verses cddp alone. All graphs are the average of 3 independent replicates and error bars

represent the standard error of the means (SEM) for each replicate. For A – E p values are calculated from a paired T-test of the fold normalised caspase activation between cddp treated and cddp + rIL6(RA) treated cells.

Whether the increased sensitisation of resistant lines was due to the increased concentration of cisplatin to which they were exposed or factors relating to acquired resistance is unclear.

2.32 rIL6(RA) Treatment Reduces Cisplatin IC_{50}

Results obtained in Figure 22 demonstrate the ability of rIL6(RA) treatment to potentiate cisplatin induced apoptosis. To examine whether this effect might reduce cisplatin IC_{50}, cells were exposed to a range of cisplatin concentrations either alone or in combination with rIL6(RA). The results are displayed in Figure 23 and summarised Table 1. In each cell line a significant difference in combination rIL6(RA) plus cisplatin verses single agent cisplatin treatment was observed, however significant differences were not always observed at all concentrations.

CELL LINE	TREATMENT	CDDP IC_{50} (µM)	95% CI	T-test P VALUE
PEO1	BSA	3.05	1.26 - 4.84	0.015
	rIL6	2.14	0.37 – 3.90	
PE04	BSA	16.1	14.9 - 17.2	0.005
	rIL6	14.1	13.2 - 15.1	
PEA1	BSA	3.11	2.03 – 4.20	0.017
	rIL6 + rsIL6RA	2.02	0.98 – 3.05	
PEA2	BSA	17.7	12.74 – 22.65	NA
	rIL6 + rsIL6RA	NA	NA	
SKOV3	BSA	8.51	4.14 – 12.9	0.067
	rIL6	5.88	1.94 – 9.81	

Table 1 shows the cisplatin IC_{50} for each cell line for either vechicle control (BSA) or in combination with rIL6(RA). IC_{50} values were interpolated from average viability measurements (average of three independent experiments) using a least squares model. 95% CI margins and t-test (paired) p values for each treatment, cisplatin alone or in combination with rIL6(RA), were calculated using the IC_{50} values determined in each independent experiment.

The addition of rIL6 reduced the cisplatin IC_{50} of PEO1 by 30% from 3µM to 2.1µM, the 95% CI of these two values did overlap however a paired T-test of the interpolated IC_{50}s

from each replicate was significant (p=0.015). A similar pattern arose in the other cell lines tested. rIL6 stimulation of PEO4 was associated with a 12.5% reduction in cisplatin IC_{50} from 16μM to 14μM, again 95% CI overlapped but a paired T-test was significant (p=0.005). rIL6 + rsIL6RA stimulation reduced PEA1s IC_{50} by 35%, from 3.1μM to 2μM (p=0.017). It was not possible to calculate a reliable ICμM for PEA2 due to the gradient of response in combination cisplatin rIL6 + rsIL6RA treatment, see Figure 23D. However when exposed to 5μM cisplatin a significant difference in cell viability was seen between single and combination treatment, which decreased by an additional 86% (p=0.02).

Relative cell viabilities at this concentration were 0.79 for cisplatin alone and 0.62 for combination treatment. At all other concentrations of cisplatin no difference was observed, why PEA2s should only respond to 5μM cisplatin when in combination with rIL6(RA) is unclear. The rIL6 induced cisplatin IC_{50} shift seen in SKOV3 was similar to sensitive PEO1 and PEA1, falling 31% from 8.6μM to 5.8μM. Again the 95% confidence intervals for cisplatin and combination cisplatin and rIL6 overlapped, a T-test for each replicate IC_{50} was borderline significant (p=0.067).

The three platinum naïve cell lines, comprising the two sensitive lines PEO1, PEA1 and SKOV3, showed the greatest effect on their cisplatin IC_{50} on the addition of rIL6(RA), which fell by around 30% for all. This is in contrast to the two resistant lines, PEO4 and PEA2 which saw smaller decreases in IC_{50}, down 12.5% in PEO4 and showing no difference in PEA2. Results obtained from the cisplatin titration (see Figure 15 and Figure 16, results section 1.3) suggested that resistant lines had acquired the ability to reduce signalling through JAK2, and in the case of PEA2 STAT3 also, to a greater extent on cisplatin exposure than their sensitive counterparts. Therefore it might have been expected that artificially maintaining a high level of STAT3 activation, with the addition of rIL6, would have more of an effect in cisplatin resistant, cells particularly PEA2, this was not the case. A possible explanation for PEA2 only responding to 5μM cisplatin differentially might be its increased sensitivity to STAT3 deactivation in response to cisplatin exposure. Potentially, despite elevated STAT3 activation, at concentrations of cisplatin above 5μM levels, pSTAT3 levels are not significantly higher in rIL6(RA) treated cells compared to untreated cells.

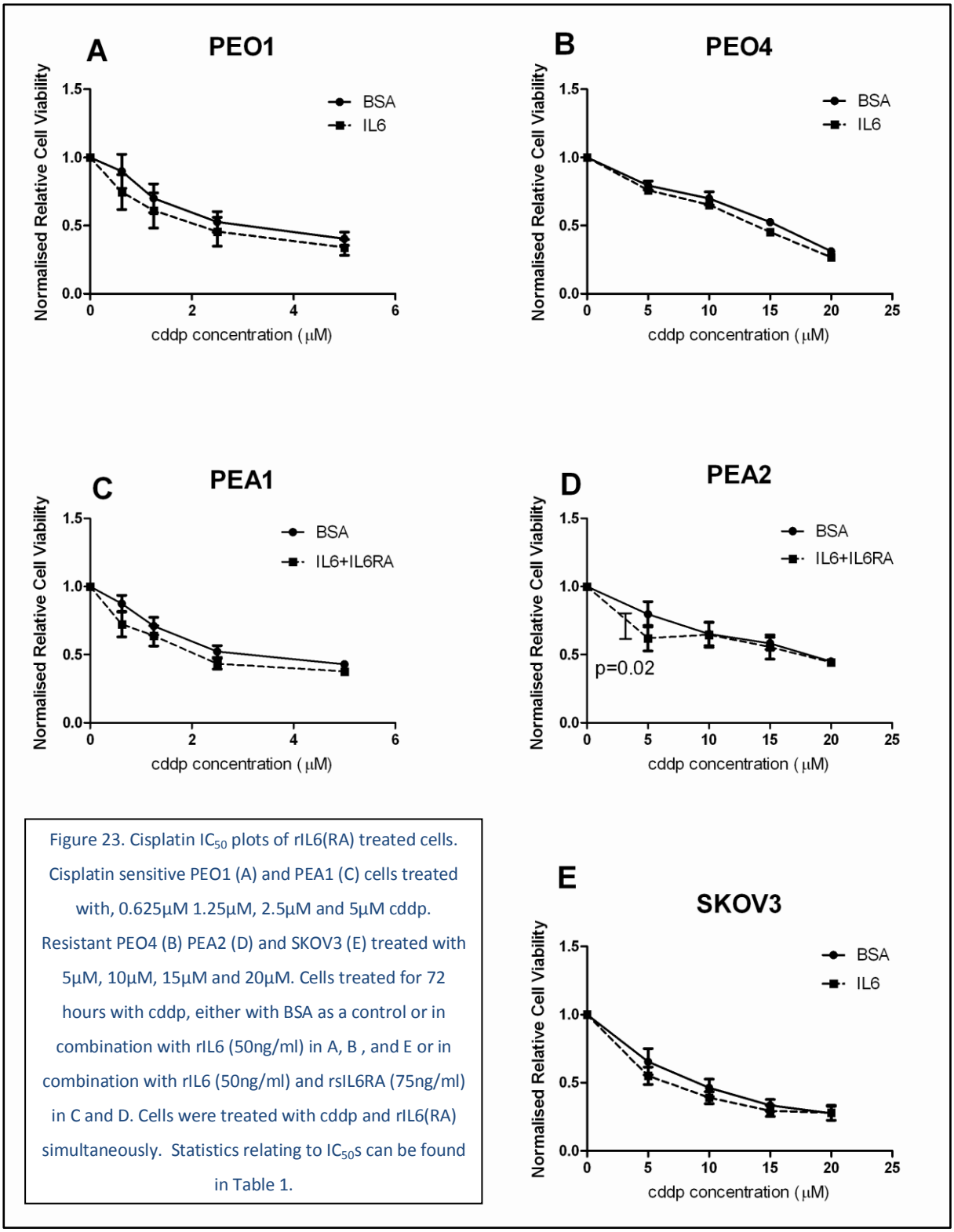

Figure 23. Cisplatin IC_{50} plots of rIL6(RA) treated cells. Cisplatin sensitive PEO1 (A) and PEA1 (C) cells treated with, 0.625μM 1.25μM, 2.5μM and 5μM cddp. Resistant PEO4 (B) PEA2 (D) and SKOV3 (E) treated with 5μM, 10μM, 15μM and 20μM. Cells treated for 72 hours with cddp, either with BSA as a control or in combination with rIL6 (50ng/ml) in A, B , and E or in combination with rIL6 (50ng/ml) and rsIL6RA (75ng/ml) in C and D. Cells were treated with cddp and rIL6(RA) simultaneously. Statistics relating to IC_{50}s can be found in Table 1.

2.33 rIL6(RA) Treatment Resulted in Elevated pSTAT3 24 hours After Stimulation. Different Cell Lines Exhibit Differential Levels of pSTAT3 After Combination Cisplatin, rIL6(RA) treatment.

The effects of cytokine stimulation are generally considered to be rapid and transient. To ensure that rIL6 was capable of increasing STAT3 activation over a period of 24 hours, to maximise the potential of interfering with cisplatin dependant changes in signalling western blotting was conducted. Cell were stimulated with rIL6, in the case of PEO1, PEO4 and SKOV3, or rIL6 and rsIL6RA, for PEA1 and PEA2, and either lysed after 30mins, first two lanes, or treated to cisplatin for an additional 24 hours before lysis. The results are shown in Figure 24.

In each cell line treatment with rIL(RA) was associated with a rapid and significant increase in the levels of pSTAT3, as measured at 30mins. A small increase in pJAK2 was also apparent. Small increases in the STAT3 regulated gene cyclin D1 were also observed in PEA1 PEA2 and SKOV3.

An increase in the levels of pSTAT3 was still apparent after 24 hours of stimulation in each line, however when combined with cisplatin some differences were seen. When exposed to 25μM cisplatin PEO4 PEA2 and SKOV3 (figure 13B, D and E) saw reduced levels of pSTAT3, relative to untreated cells, consistent with previous results. However cisplatin in combination with IL6(RA) caused an additional reduction in pSTAT3 levels in PEO4 and SKOV3, relative to cisplatin alone, whereas in PEA2 pSTAT3 remained above untreated controls, suggesting the reason PEA2 responded differentially to 5μM cisplatin in combination with IL6(RA) only in Figure 23, is not due the cell lines greater sensitivity in reducing STAT3 activation in response to cisplatin.

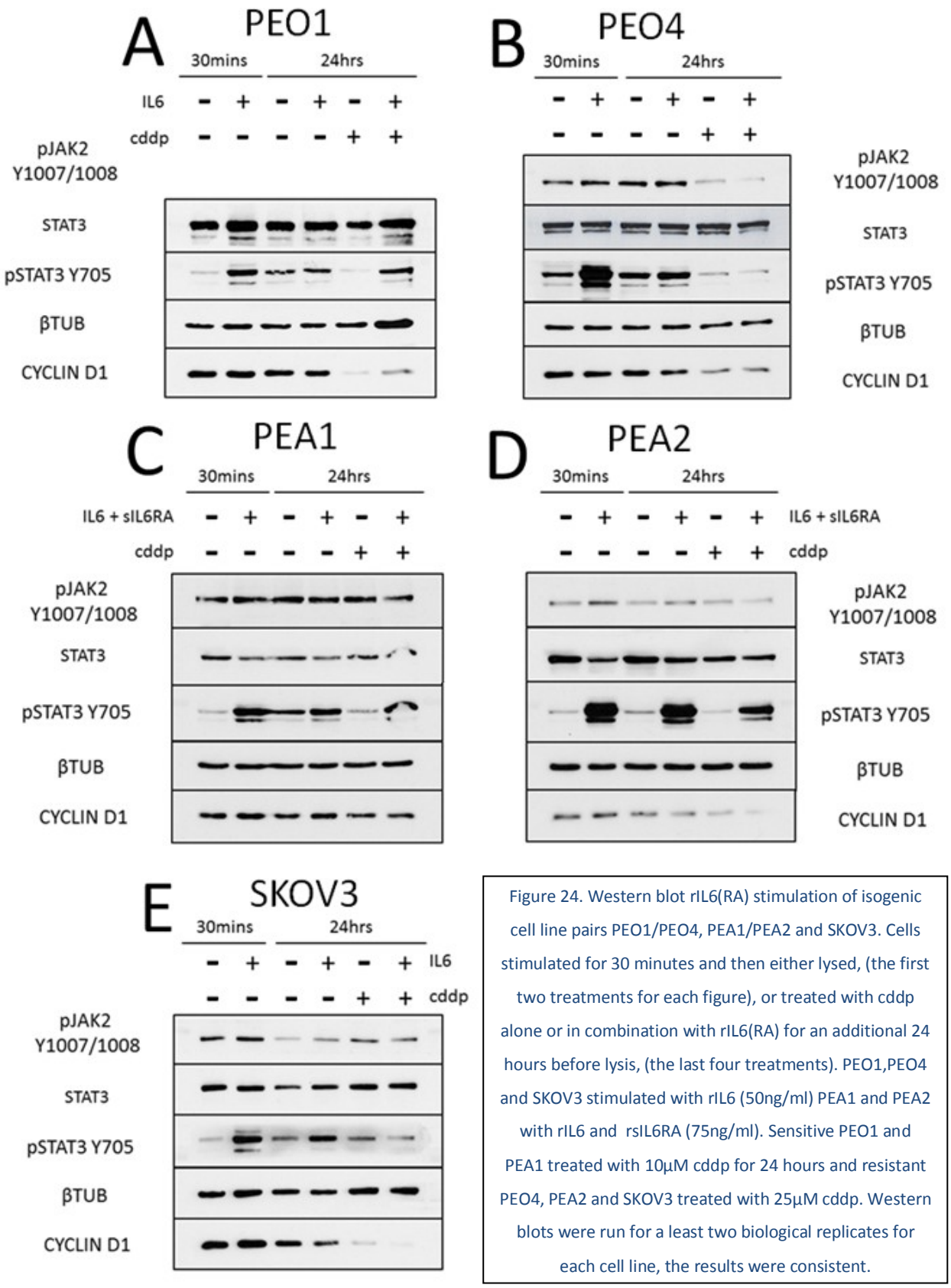

Figure 24. Western blot rIL6(RA) stimulation of isogenic cell line pairs PEO1/PEO4, PEA1/PEA2 and SKOV3. Cells stimulated for 30 minutes and then either lysed, (the first two treatments for each figure), or treated with cddp alone or in combination with rIL6(RA) for an additional 24 hours before lysis, (the last four treatments). PEO1,PEO4 and SKOV3 stimulated with rIL6 (50ng/ml) PEA1 and PEA2 with rIL6 and rsIL6RA (75ng/ml). Sensitive PEO1 and PEA1 treated with 10μM cddp for 24 hours and resistant PEO4, PEA2 and SKOV3 treated with 25μM cddp. Western blots were run for a least two biological replicates for each cell line, the results were consistent.

2.4 Expression of IL6 and IL6RA in a Panel of Ovarian Cell Lines

2.41 IL6 Expression in a Panel of Ovarian Cells Does Not Correlate With Cisplatin Resistance.

Results shown in Figure 21, in which the responsiveness of PEA1 and PEA2 to IL6 could be restored with the addition of sIL6RA alone, suggested that both constitutively express IL6. In both cell lines the addition of sIL6RA alone increased STAT3 activation, and in PEA2s this was not further increased by the addition of IL6. This implies both; that the level of endogenous IL6 expression is physiologically relevant, that it can elicit a response and that PEA2 expresses greater quantities than PEA1.

A number of studies have shown a link between serum [287], ascites [285] and tumour [289] levels of IL6 and survival in ovarian cancer, all of which showed a negative relationship between IL6 levels and one or both of PFS and OS in multivariate models.

To further investigate whether *IL6* mRNA expression differed between PEA1 and PEA2 and other ovarian cell lines QRT-PCR was performed, the results are shown in Figure 25A. *IL6* expression was also examined in the other isogenic pair PEO1 and PEO4, and the other EOC lines SKOV3, OVCAR3, A2780, as well as the immortalised normal ovarian surface epithelium line OSE-C2.

All cell lines unambiguously expressed *IL6* at the mRNA level, with the exception of A2780. Expression was considered unambiguous when cDNA expression for a particular gene was far in excess of an equivalent reverse transcriptase negative control diluted by the same factor. The range of IL6 expression varied widely, excluding A2780, SKOV3 contained the lowest amount of *IL6* mRNA which was over 300 times lower than PEA2 which expressed the highest.

Overexpression of *IL6* in PEA2 was observed relative to its isogenic partner PEA1 ($p=0.002$) which expressed approximately 7.4 times as much mRNA. Conversely PEO4 expressed significantly less *IL6* mRNA, around 23 fold less, than its cisplatin sensitive isogenic partner PEO1 ($p=0.04$).

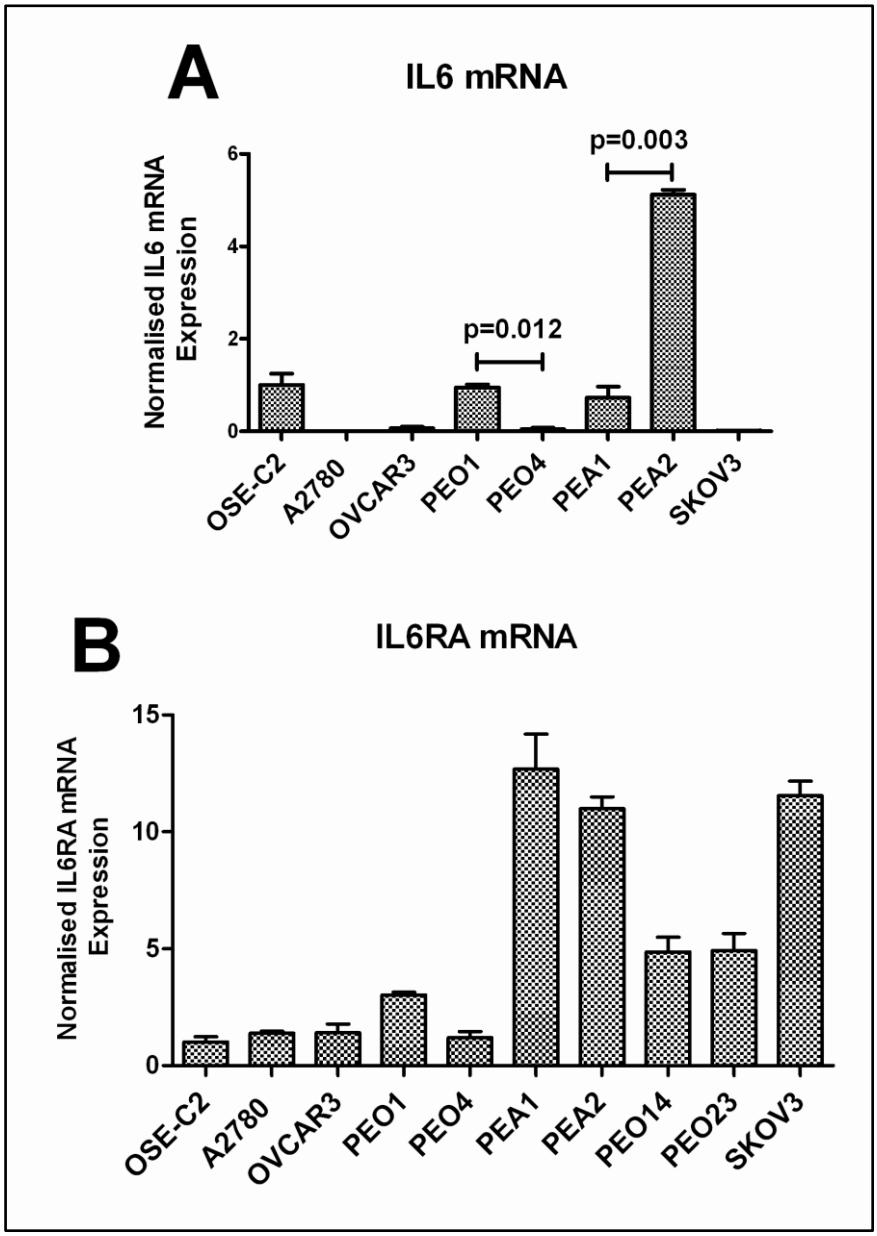

Figure 25. QRT-PCR of a panel of ovarian HGS cell lines including the normal immortalised OSE-C2. IL6 and IL6RA expression was normalised to the geometric mean of PPIA and TBP and averaged over three independent experiments for IL6, **A**, and four for IL6RA, **B**. Expression is shown relative to OSE-C2. Error bars represent the SEM of the normalised replicates. P values calculated using a paired T-test from each replicate normalised gene expression level.

The increased constitutive expression of IL6 in PEA2 may explain why the magnitude of STAT3 activation observed in response to sIL6RA treatment was not significantly different when combined with exogenous IL6 treatment, suggesting the extent of STAT3

activation in PEA2 is limited by the quantity of sIL6RA supplemented. The increased expression of *IL6* in PEA2 might also explain the persistent elevation of pSTAT3 seen in combination with 25μM cisplatin treatment (seen in Figure 24D), when PEO4 and SKOV3 saw significant reductions in pSTAT3. sIL6RA supplementation might confer greater temporal responsiveness to the high levels of IL6 already present in the supernatant and increased by cisplatin exposure.

2.42 IL6RA mRNA expression Does not Correlate With IL6 Responsiveness

All cell lines examined were found to express *IL6RA*. Absolute expression appeared low based on the number of cycles of QRT-PCR required to cross the cycle threshold relative to other mRNA species tested, data not shown. While the cycle threshold is not directly comparable between different primers pairs, it can provide a rough approximation of absolute expression levels. Expression varied less for IL6RA than IL6, a 13 fold difference was observed between the highest, PEA1, and lowest, OSE-C2, expressing cell lines. Unusually, with the exception of SKOV3, the highest expression of *IL6RA* was seen in those cell lines which were unresponsiveness to IL6 stimulation, shown in Figure 20. Paired cisplatin sensitive and resistance isogenic cell lines did not express significantly different amounts of IL6RA. Why cells expressing the highest quantity of IL6RA would be unresponsive to IL6 stimulation is unclear.

Discussion :-

Results Chapter 2

2.1 Determination of IL6 responsiveness in a Panel of Ovarian cell lines. IL6 Activates STAT3 but not JAK2

Cell lines responded in a binary fashion to rIL6 exposure, where response is defined as an increase in STAT3 Y705 phosphorylation. Response was either unambiguously positive or negative. There was no correlation with cisplatin resistance and of the three isogenic pairs examined response within each pair was the same, although it did differ between different pairs. Therefore cisplatin dependant *IL6* upregulation observed in PEO1,PEO4 and PEA1,PEA2 also verified in SKOV3 (data not shown) occurred irrespective of a cells ability to respond in a autocrine fashion. This suggesting the consequence of IL6 secretion is, at least in the case of PEA1 and PEA2 exclusively paracrine function signalling to non-tumour cells in the microenvironment that are no longer present in cell culture. Indeed even in IL6 responsive PEO1, PEO4 and SKOV3 cells *IL6* expression is not predictive of pSTAT3 levels implying; the effects of increased IL6 are not autocrine, and constitutive STAT3 activation in these cell lines is not due to IL6/GP130 signalling.

This however may be an oversimplification as IL6 responsiveness can be conferred on unresponsive cells by the expression of sIL6RA from neighbouring tissues, whether this occurs in humans *in vivo* appears unknown. But in mice sIL6RA has been detected in peritoneal washings from normal control mice the expression of which was increased when human tumour xenograft were introduced, regardless of whether the tumour expresses IL6RA [290]. As such it appears tumour host interactions may be able to confer IL6 responsiveness on cells *in vivo* that would not respond *in vitro*.

2.2 Addition of Soluble rIL6RA Restores IL6 Responsiveness in PEA1 and PEA2

Tissue specific response to IL6 exposure is generally mediated by restriction of IL6RA expression. Expression of GP130 the other obligate receptor for IL6 responsiveness, which also acts as the low affinity co-receptor for LIF and OSM, is more ubiquitous, as are the other proteins required for a functional signalling pathway. Therefore IL6RA was the most obvious factor to investigate IL6 unresponsiveness. The restoration of IL6 responsiveness with rsIL6RA suggests that PEA1 and PEA2 don't express this protein. Also both cell lines experienced an increase in pSTAT3 levels when exposed to the receptor alone, implying both express constitutive levels of IL6. The fold increase of pSTAT3 was far greater in PEA2 than in PEA1 suggesting that PEA2 expresses higher constitutive levels of IL6, and that this expression is likely to be physiologically relevant for any surrounding tissue sensitive to IL6.

2.3 rIL6(RA) Treatment Sensitises Cells to Cisplatin

Figure 15 and Figure 16 showed reduced STAT3 activation in response to high dose cisplatin exposure. Hyper-activation of STAT3 using rIL6(RA) provided a means of interfering with cisplatin dependant reductions in STAT3 phosphorylation to access whether deactivation is functional. The ability of rIL6(RA) treatment to sensitise to cisplatin represents the first data suggesting cisplatin dependant changes in STAT3 activation are functional, and more specifically that reduced activation reduces cisplatin induced apoptosis. The particular downstream mediators of this effect are unknown, however the fact that IL6(RA) increased cisplatin induced caspase activation suggests that this sensitisation effect is probably mediated via proliferative factors as opposed to anti-apoptotic ones. STAT3 is a transcriptional regulator of a number of genes, including *BIRCH5* a direct inhibitor of caspase 3 and 7 and *BCL2L1* (BCL-xL/S) which also inhibits caspases activation but via an inhibition of cytochrome C release. As such, an increase in cisplatin induced apoptosis associated with IL6 exposure is more easily explained via a potential increase in proliferation rates. A STAT3 dependant increase in proliferation could have the effect of increasing the proportion of cisplatin induced DNA SSB that are not repaired and transition to DBS, through DNA replication by reducing the time a cell has to repair adducts. This hypothesis is supported by

both, cisplatin dependant down regulation, and *IL6* upregulation of Cyclin D1 (see Figure 17 and Figure 21 respectively), an important driver of the G1 to S phase transition.

Given that excessive activation of STAT3 was associated with a potentiation of cisplatin induced apoptosis, greater sensitivity to down regulating signalling via STAT3 would be predicted to confer a degree of cisplatin resistance. A downregulation of STAT3 signalling at basal levels would likely have consequences that negatively impact tumour growth, for example via the downregulation of genes promoting vascularisation and cell division. Therefore selection for a greater sensitivity to DNA damage, in terms of deactivating STAT3, may allow a cell to benefit from its proliferative effects in normal conditions, without the presence of high dose cisplatin and to more rapidly respond to the changing selective environment brought about by the administration of chemotherapy. This appears to be the case for PEA1 and PEA2, PEA2 reduces its phosphorylation of STAT3 with significantly greater responsiveness to cisplatin.

A comparison of the fold increase in apoptosis induction observed when treating with combination cisplatin and rIL6(RA) revealed a greater fold increase in resistant PEO4 and PEA2 cells (see Figure 22F). While it might be tempting to speculate that this is due to a feature of acquired resistance however it seems more likely that the different concentrations of cisplatin are responsible for the difference. Were a difference noted in the degree of sensitisation between sensitive and resistant cells using the same concentration of cisplatin this would provide evidence of an acquired mechanism. This remains a relevant experiment to carry out.

2.4 Expression of IL6 and IL6RA in a Panel of Ovarian Cell Lines

For both of the isogenic pairs assayed resistant cells expressed significantly different quantities of *IL6* mRNA compared to their sensitive counterpart (Figure 25A). Both sensitive lines (PEO1 and PEA1) expressed a similar amount of *IL6* however PEO4 (the resistant pair of PEO1) expressed significantly less *IL6* whereas PEA2 (the resistant pair of PEA1) expressed significantly more. Increased expression in PEA2 is not unexpected as rsIL6RA alone was able to increase pSTAT3 levels and to a higher degree in PEA2 (see Figure 21). This apparent selection for opposing expression levels of *IL6* seems contradictory, however when evaluated in terms of both the IL6 responsiveness of the cell lines in question and the

ability of IL6 exposure to potentiate cisplatin induced apoptosis, it may be possible to reconcile these contradictions.

Given that IL6 secretion is a common event, generalisable to normal non-cancerous tissue and DNA damaging agents as a whole, it seems reasonable to predict that the vast majority of cells exposed to cisplatin will increase their secretion of IL6. Based on evidence shown here rIL6(RA) exposure is associated with both a potentiation of cisplatin induced apoptosis and a reduction in cisplatin IC_{50}, implying cells responsive to IL6 would be rendered more sensitive to cisplatin by the secretion of IL6, either from the tumour itself or surround normal tissue. In this manner PEO4 may have been selected for both lower basal, and lower infold cisplatin induced IL6 expression, as the responsive nature of this cell line might confer a survival disadvantage to the tumour by sensitising it to cisplatin exposure.

This is in contrast to PEA1 and PEA2 both of which were unresponsive to IL6 exposure. As such they may benefit from paracrine signalling with local tissue via IL6 secretion, potentially increased vascularisation, local inflammation and reduced immune tumour surveillance, without experiencing the adverse effects of increased pSTAT3 levels when concentrations of cisplatin are high. This assumes that PEA1 and PEA2 remain unresponsive to IL6 *in vivo*.

To illustrate how different basal *IL6* expression corresponds to absolute expression levels induced by cisplatin, by factoring the fold changes observed in Figure 13, in response to 5μM drug PEA2 had the highest expression at, 9.5 followed by PEO1 (8.2), PEA1 (5.3) and finally PEO4 with 0.12, all values are normalised arbitrary IL6 expression levels, showing that, despite the increased fold in cisplatin dependent *IL6* induction of sensitive cell lines, resistant PEA2 maintains a higher absolute level of expression either at background or post drug treatment.

Results Chapter 3:-
JAK2 Contributes to Phosphorylation of STAT3 and ERBB2 and Promotes Growth.

3. JAK2 Contributes to Phosphorylation of STAT3 and ERBB2 and Promotes Growth

3.1 JAK2 Inhibition Reduces Cisplatin Induced Apoptosis, Reduces Growth Rates and Levels of STAT3 and ERBB2 Phosphorylation

In response to cisplatin exposure the ovarian HGS cell lines PEO1, PEO4, PEA1, PEA2 and SKOV3 exhibited changes in JAK2 protein expression. Typically this was a small increase at concentrations of cisplatin of around 2-4μM, while at higher concentrations typically above 15μM JAK2 expression was generally reduced. Cisplatin dependent changes in JAK2 protein expression were mirrored by changes in levels of phosphorylation of STAT3 and ERBB2. In the case of ERBB2 a high correlation existed between the expression of the phosphorylated forms of these two proteins (see Figure 18). The consequences of these dose dependent changes in STAT3 JAK2 and ERBB2 on cisplatin resistance are unknown. To investigate the functional consequences of reduced JAK2 activation and any role this may play in either the activation of pSTAT3 and pERBB2 or cisplatin response, the JAK2 inhibitor TG101348 was used. TG101348 is a potent and specific ATP competitor of JAK2. TG101348 has an IC_{50} for JAK2 of 3nM in *in vitro* kinase assays and a 35, 135 and 334 fold selectivity over JAK1 TYK2 and JAK3 respectively [317].

3.11 JAK2 Inhibition Reduces Cisplatin Induced Apoptosis

The role of JAK2 in cisplatin induced apoptosis is unknown. The mirrored changes observed between JAK2 protein expression and the phosphorylation of ERBB2 and STAT3 suggested a potential link between these proteins, in which modulation of JAK2 expression regulate their activity. In order to evaluate the consequences of cisplatin dependant down regulation of JAK2 and whether its downstream effects are mediated by changes in total protein or phosphorylated JAK2 the inhibitor TG101348 was used. Cells were exposed to either cisplatin plus inhibitor, in combination, or inhibitor alone, at various concentrations. After 24 hours exposure to cisplatin levels of activated caspase 3/7 were quantified and used to estimate the level of apoptosis induced, the results are shown in Figure 26.

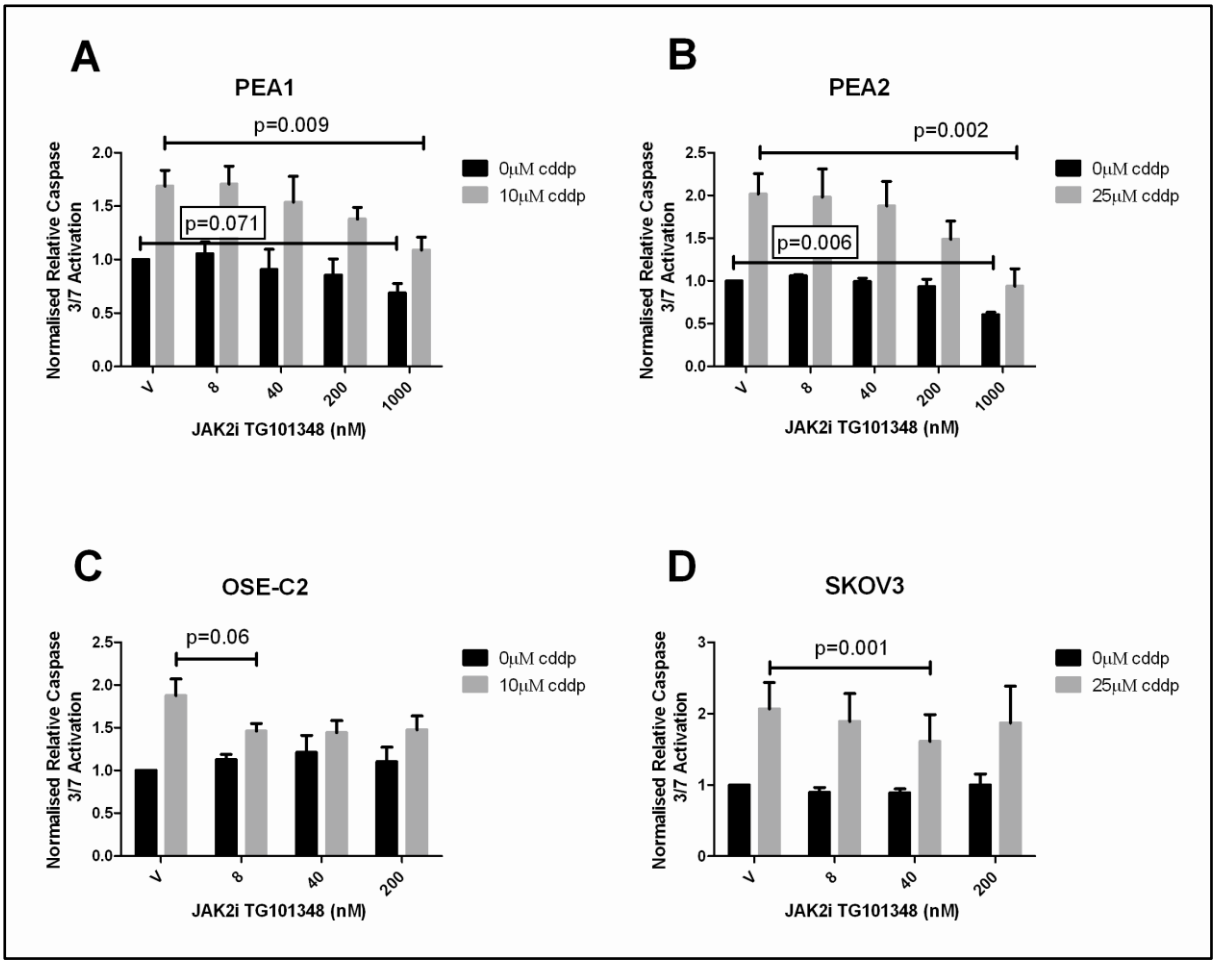

Figure 26. Cisplatin apoptosis assay in combination with the JAK2 inhibitor TG101348. Cells were exposed to TG101348 at the indicated concentration overnight followed by either repeated treatment with TG1010348 at the same concentration alone, black bars, or in combination with cisplatin, grey bars. Cisplatin sensitive PEA1 (**A**) and OSE-C2 (**C**) were treated with 10μM cddp and resistant PEA2 (**B**) and SKOV3 (**D**) were treated with 25μM cddp, all cells exposed to cddp for a further 24 hours. Caspase 3/7 activation was normalised to cell viability for each treatment. The average of three independent experiments is shown, error bars represent the SEM of the normalised caspase activation over the three replicates. P-values are paired T-tests except in the case of inhibitor alone at 0μM (V) and 100nM which were one sample unequal variance.

In each cell line examined JAK2 inhibition (JAK2i) was associated with a significant reduction in cisplatin induced caspase 3/7 activation. In the isogenic pair PEA1 PEA2 there was a dosage dependant relationship between levels of activated caspase in either single agent or combination treatment, the greatest degree of apoptosis inhibition occurring when cells were exposed to the highest concentration of TG101348, 1μM.

For example in PEA1, treatment with 1μM of TG101348 reversed cisplatin induced apoptosis (p=0.009 paired T-test) and the inhibitor alone reduced background apoptosis by

over 30% (p=0.071 one sample unequal variance T-test). This effect was more pronounced in PEA2 in which the apoptotic induction resulting from 25μM cisplatin was reversed by the addition of 1μM JAK2 inhibitor (p=0.002 paired T-test) and this concentration of inhibitor reduced background levels of apoptosis by 40% (p=0.006 one sample unequal variance T-test). The immortalised normal OSE cell line, OSE-C2 was also assayed to test whether targeting JAK2 would have effects unique for cancer cell lines. OSE-C2 cells responded in a similar manner to PEA1 and PEA2 showing a reduction of cisplatin induced apoptosis of approximately 50% at 8nM and 40nM. A dose dependant effect was not observed in OSE-C2, concentrations of inhibitor above 200nM were associated with single agent toxicity (data not shown). SKOV3 exhibited the smallest reversal of cisplatin induced apoptosis, which fell maximally by 40% at 40nM of inhibitor (p=0.001). This concentration of inhibitor also reduced background caspase 3/7 activation by 10% although this result was not statistically significant.

3.12 JAK2 Inhibition Reduces Proliferation

Given the hypothesised role for JAK2 in the regulation of pSTAT3 and pERBB2, the result of JAK2 inhibition reducing cisplatin induced apoptosis appears a counterintuitive one, given that the roles of STAT3 and ERBB2 are generally considered to be pro-survival, although it is consistent with results obtained for rIL6(RA) treatment, which increased pJAK2, pSTAT3 and cisplatin induced apoptosis (see Figure 22). Results shown in Figure 26 might be more easily explained if JAK2 were a driver of proliferation, in which case reduced JAK2 expression, associated with high concentrations of cisplatin, reduced proliferation rates facilitating the repair of cisplatin – DNA adducts, protecting the cell from subsequent apoptosis. This may underlie a mechanism of acquired resistance to cisplatin, as resistant cells were better able to reduce expression of JAK2 after chemotherapy. Therefore the effects of JAK2 inhibition on proliferation were examined.

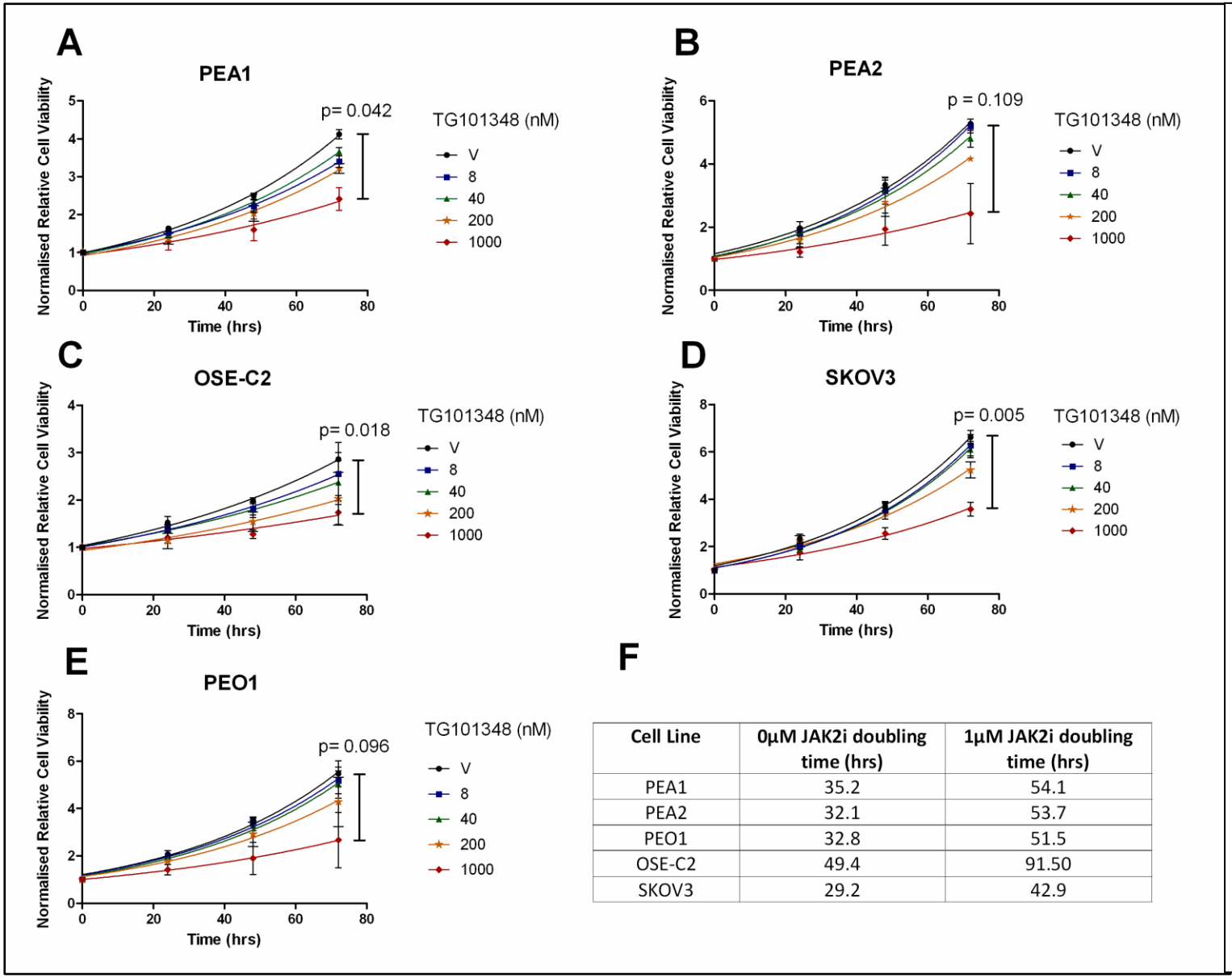

F

Cell Line	0μM JAK2i doubling time (hrs)	1μM JAK2i doubling time (hrs)
PEA1	35.2	54.1
PEA2	32.1	53.7
PEO1	32.8	51.5
OSE-C2	49.4	91.50
SKOV3	29.2	42.9

Figure 27. Proliferation assay showing the effects of JAK2 inhibitor TG101348 on growth. Cells were treated with vehicle control (V) or JAK2 inhibitor at 8nM, 40nM, 200nM and 1000nM for 72 hours. After incubation cell viability quantified using MTT assay. Lines based on exponential regression, which was also used to calculate estimated doubling times shown in F. Each figure shows the average of three independent experiments. Error bar show the SEM between replicates and p values calculated from a paired T-test between V and 1000nM inhibitor treated cells.

The effects of JAK2 inhibition on cell proliferation are shown in Figure 27, both cancer cell lines and 'normal' OSE-C2 were affected. A significant decrease in cell viability was seen in PEA1, (p=0.042), SKOV3 (p=0.005) and OSE-C2 (p=0.018) cells after 72 hours incubation relative to untreated controls, in paired T-tests, see Figure 27A, 16C and 16D respectively. A similar effect occurred in PEA2 and PEO1 however this was not statistically significant, see Figure 27B and E. All cells experienced dosage dependant effect on cell proliferation inhibition, the greatest inhibition occurring when cells were exposed to 1μM TG101348. The lowest concentration used 8nM was either associated with a marginal effect or no effect. The greatest magnitude of growth inhibition was observed in normal OSE-C2 cells where 1μM of TG101348 was associated with an 85% increase in doubling time from 49.4 hours to 91.5 hours. The remaining cells lines experienced smaller changes to their doubling times, the lowest of which was SKOV3 which increased 47% from 29.2 hours to 42.9 hours, PEA1 was marginally more effected experiencing a 54% increase in doubling time. A summary of the changes in estimated doubling time between vehicle treated and 1μM inhibitor treated is shown in Figure 27F.

3.13 JAK2 Inhibition Reduces Levels of pSTAT3 and pERBB2

Previous data showing simultaneous changes in the levels of pJAK2, pSTAT3 and pERBB2 suggested a regulatory link might exist between these proteins (see figures 4, 5 and 7). JAK2 is a known kinase of STAT3 and a functional role for JAK2 in the phosphorylation of STAT3 has been reported elsewhere [415]. A functional role for JAK2 in maintaining the phosphorylation of ERBB2 has not been reported, although they have been found to act co-operatively in the phosphorylation of STAT3 [316]. Simultaneously to the generation of Figure 26 and Figure 27 protein lysates were also prepared. Cells were treated with either vehicle control (DMSO) or TG101348 for between 16-18 hours prior to lysis before being analysed for levels of EBRR2 and STAT3 phosphorylation by western blotting.

The isogenic pair PEA1 and PEA2 have been previously analysed for copy number variants and found to not to be amplified for ERBB2 [416]. As a normal control, SV40 transfected, OSE cell line OSEC-C2 would be predicted to be both not amplified for ERBB2, and also not to have constitutively phosphorylated ERBB2. Alternatively SKOV3 cells are ERBB2 amplified [417] and express high levels of constitutive phospho ERBB2.

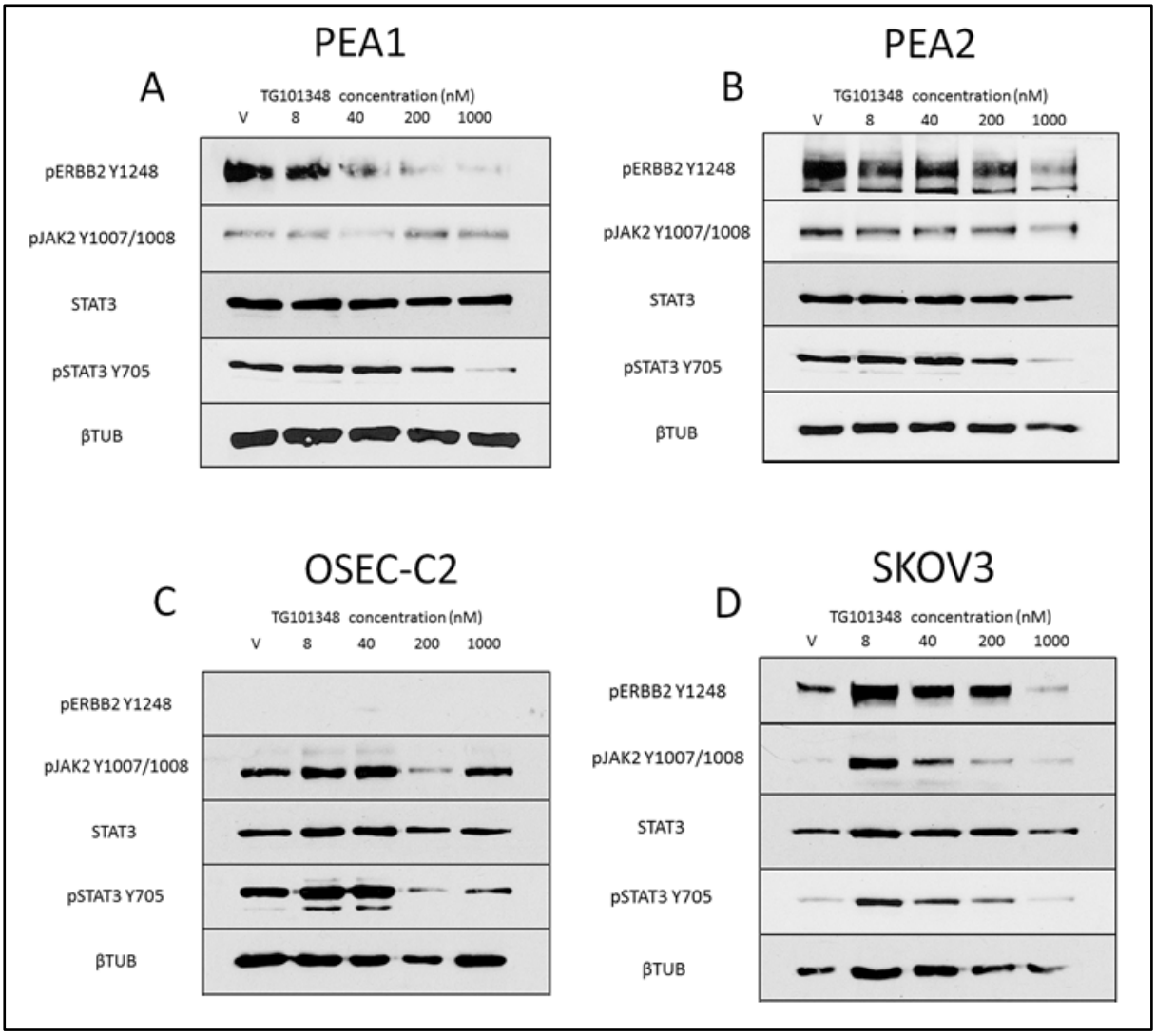

Figure 28. Western Blot analysis of JAK2 inhibitor (TG101348) treated cells. Cells were treated with the indicated concentration of inhibitor dissolved in DMSO or vehicle control (V) for between 16 and 18 hours before lysis. Western blots were run from at least two biological replicates for each cell line. The results obtained were consistent. Probing for Y1248 phosphorylated ERBB2 in OSE-C2 occurred in parallel to other cell line which acted as a positive control. βTUB is included as a loading control.

TG101348 is an ATP competitor that prevents JAK2 from phosphorylating its substrates [418], therefore no direct effect on JAK2 phosphorylation is expected. As predicted no effect on levels on JAK2 phosphorylation was detected. This is in contrast to the levels of pSTAT3 which fell in a dose dependant manner in each cell line. At 1μM of inhibitor a large drop in pSTAT3 was observed in each cell line whereas there was no obvious effect on the levels of total STAT3 implying the inhibitor is acting in a specific on target fashion. As

suggested from the cisplatin titration experiment (see figure 17) PEA1 PEA2 and SKOV3 contained detectable levels of Y1248 phosphorylated ERBB2 whereas the normal cell line OSE-C2 did not, a similar quantity of protein was loaded for each cell line. In each cell line expressing phosphorylated ERBB2 a dose dependant reduction was also observed. The magnitude of this reduction was similar to that seen for STAT3, except that ERBB2 phosphorylation appears more sensitive to JAK2 inhibition that STAT3. For example in PEA1 and PEA2 experienced a reduction in pERBB2 at 8nM of inhibitor, whereas a reduction in pSTAT3 was not apparent at this concentration.

In addition to confirming the presence of a functional link between JAK2 and STAT3 and ERBB2 the use of a kinase inhibitor, that has no effect on the levels of total JAK2 protein (see supplementary section Figure Sa and B), suggests that the reduction observed in the levels of phosphorylation of STAT3 and ERBB2 are due to the kinase activity of JAK2 and not the level of total protein. When exposed to cisplatin this reduction in JAK2 activity is in part achieved by a transcriptional reduction in JAK2 expression, however the same changes in STAT3 and ERBB2 could be recapitulated with a reduction in JAK2 activity alone and without effecting total expression levels.

3.2 siRNA Mediated Knockdown of JAK2 Inhibits Cell Growth, Increases Cisplatin IC_{50} and Reduces Levels of STAT3 and ERBB2 Phosphorylation.

Treatment with the JAK2 inhibitor TG101348 was associated with a reduction in proliferation in a panel of ovarian cell lines including the normal line OSE-C2. Cell free kinase assays have demonstrated TG101348 also has activity towards the receptor tyrosine kinases FLT3, and RET with IC_{50}s of 15nM and 48nM respectively [317]. In order to validate the results obtained using this inhibitor and ensure their specificity, siRNA mediated knock-downs of JAK2 were carried out in the isogenic pair PEA1 PEA2 and SKOV3. To avoid potential confounding results a total of 5 different siRNA species were considered, the first two of which were discarded due to either off target effects or poor activity against JAK2 expression.

Cells were treated with 50nM final concentration of a single siRNA species for 48 hours, before growth assays, apoptosis and cisplatin assays were performed. Protein lysates

were also taken to both validate JAK2 knock-down and examine the effects on down-stream signalling.

3.21 siRNA Mediated Knockdown of JAK2 Inhibits Cell Growth

Proliferation assays conducted on cells depleted for JAK2 by means of siRNA recapitulate results obtained using the JAK2 inhibitor TG101348. siRNA knockdown of JAK2 was associated with significant reductions in cell viability after 72 hours of growth for at least one of three siRNAs in the three cell line tested. In PEA2 each individual siRNA species resulted in a significant reduction in viability after 72 hours. Each siRNA reduced viability and to a similar degree, within each cell line, and data noise contributed to P values not achieving significance, at the p=0.05 cut-off, where this occurred. Each cell line experienced a similar proportional change to their doubling time when JAK2 was depleted (see Figure 29D). In PEA1 this increased on average 25% from 39.5 to 49.4 hours, PEA2 by 30% from 37.2 to 48.6 hours and increased 27% in SKOV3 from 33 to 41.9 hours, in each calculation the average doubling time for each of the three siRNA was used.

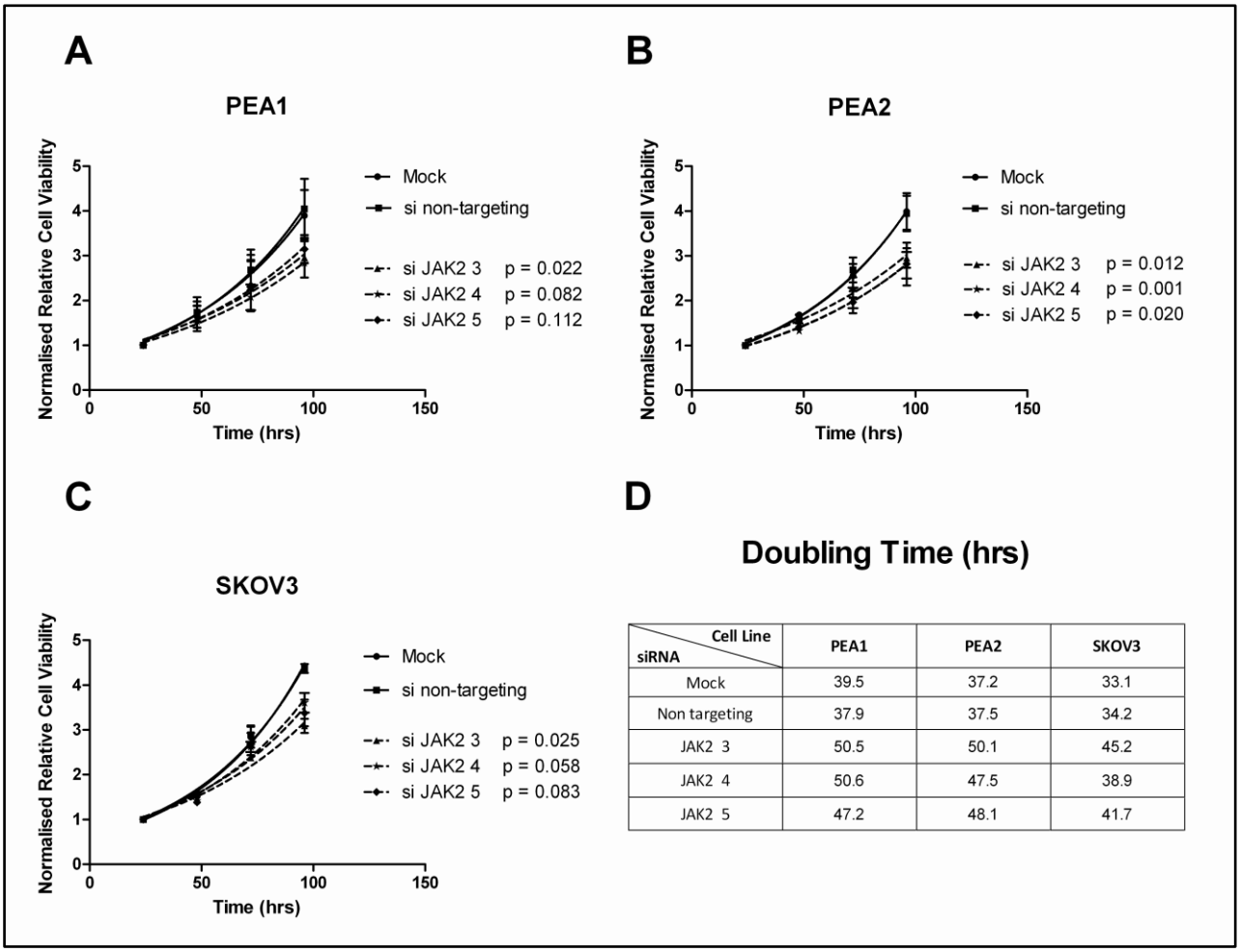

Cell Line / siRNA	PEA1	PEA2	SKOV3
Mock	39.5	37.2	33.1
Non targeting	37.9	37.5	34.2
JAK2 3	50.5	50.1	45.2
JAK2 4	50.6	47.5	38.9
JAK2 5	47.2	48.1	41.7

Figure 29. Proliferation assay showing the effects of JAK2 knockdown in PEA1, A PEA2, B and SKOV3, C. Cells were treated with a final concentration of, 50nM single species siRNA, except for mock transfected controls which contained no siRNA, for 48 hours. Viability for each treatment is normalised to the 24hr time point. Each point is the average of 3 independent biological replicates and error bar show the SEM between these replicates. Lines are plotted using a least squares exponential regression model, which was also used to estimate doubling times analysis carried out in Prism software package. P values are calculated from a paired T-test for each siRNA against mock transfected controls at the 72hour time point. Table **D** shows the estimated doubling times for each treatment in hours.

3.22 siRNA Mediated Knockdown of JAK2 Increases Cisplatin IC_{50}

rIL6(RA) stimulation, resulting in elevated pSTAT3, was associated with a decrease in the cisplatin IC_{50} of PEO1, PEO4, PEA1 and SKOV3, as well as a potentiation of its apoptotic induction. Further, given that JAK2 is downregulated at the transcriptional level in response to high concentrations of cisplatin and when this situation is mimicked by inhibiting JAK2, using TG101348, an attenuation of cisplatin induced apoptosis was observed.

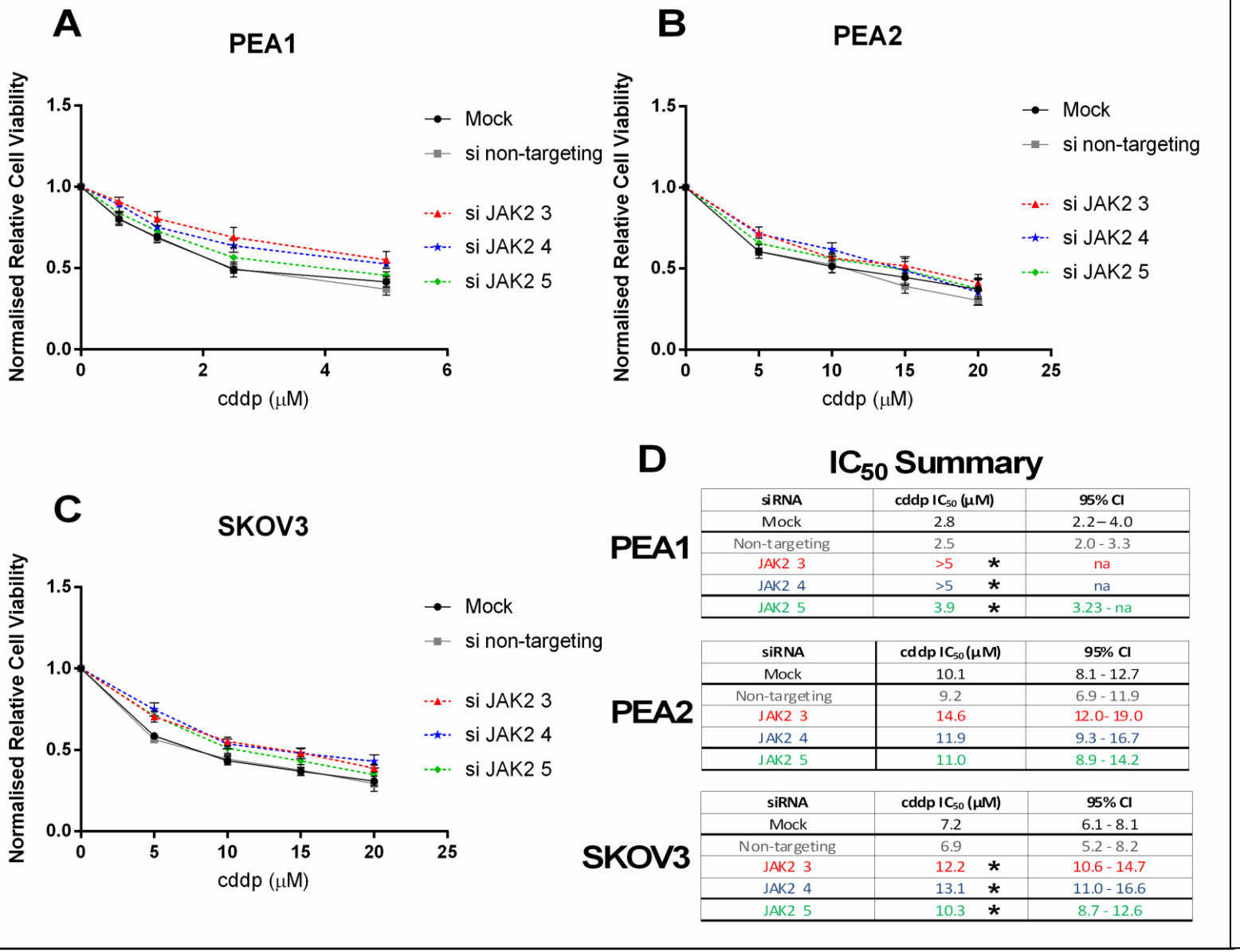

D IC_{50} Summary

PEA1

siRNA	cddp IC_{50} (μM)		95% CI
Mock	2.8		2.2 – 4.0
Non-targeting	2.5		2.0 - 3.3
JAK2 3	>5	*	na
JAK2 4	>5	*	na
JAK2 5	3.9	*	3.23 - na

PEA2

siRNA	cddp IC_{50} (μM)	95% CI
Mock	10.1	8.1 - 12.7
Non-targeting	9.2	6.9 - 11.9
JAK2 3	14.6	12.0- 19.0
JAK2 4	11.9	9.3 - 16.7
JAK2 5	11.0	8.9 - 14.2

SKOV3

siRNA	cddp IC_{50} (μM)		95% CI
Mock	7.2		6.1 - 8.1
Non-targeting	6.9		5.2 - 8.2
JAK2 3	12.2	*	10.6 - 14.7
JAK2 4	13.1	*	11.0 - 16.6
JAK2 5	10.3	*	8.7 - 12.6

Figure 30. Cisplatin IC_{50} of PEA1, A, PEA2, B and SKOV3 C, in response to JAK2 knockdown. Cells were transfected with either, one of three JAK2 siRNAs, a non-coding siRNA or no siRNA (mock transfected) for 48 hours. After which they were treated with the indicated concentrations of cisplatin for 72 hours before MTT viability assay was conducted. Viability shown is relative to 0μM treated cells and averaged over three or four independent biological replicates. IC_{50} estimations were interpolated from this average. 95% CI boundaries were calculated using a least squares model in the software package Prism.

* no overlap at p = 0.05

D shows a summary of interpolated IC_{50} values.

If JAK2 is signalling through STAT3, as suggested by western blot data of inhibitor treated lysates, knockdown of JAK2 should be associated with an increase in cisplatin IC_{50}.

As well as reducing rates of cellular proliferation JAK2 knockdown was associated with a significant increase in cisplatin IC_{50} of PEA1 and SKOV3, results show in Figure 30. In each cell line the three species of JAK2 siRNA were associated with an increase in cisplatin IC_{50}. In PEA1 and SKOV3 each JAK2 siRNA was associated with a significant increase in the cisplatin IC_{50}, based on non-overlapping 95% confidence intervals, these values are summarised in Figure 30D. While in PEA2 each species of siRNA was associated with an increased IC_{50}, none achieved significance. This appears to be largely due to the magnitude of effect observed in this line. The magnitude of IC_{50} increase between PEA1 and SKOV3 was very similar and higher than seen in PEA2. The average increase in IC_{50} for the three siRNA was 66% in PEA1 and 65% in SKOV3. The actual figure in PEA1 may have been higher as two siRNA were associated with an undetermined IC_{50} that was in excess of 5μM cisplatin, representing at least a 79% increase. Percentage increases in SKOV3 ranged from 43%, for siRNA 5 to 82% for siRNA 4.

3.23 siRNA Mediated Knockdown of JAK2 Reduces Levels of Y705 Phosphorylated STAT3

Simultaneous to carrying out the experiments in the preceding two sections protein lysates were collected allowing for the validation of knockdown and an assessment of downstream signalling effects. Cisplatin treatment had demonstrated simultaneous decreases in pERBB2 and pSTAT3 with decreased JAK2 protein expression. JAK2 inhibition had provided the first functional evidence, within these systems, that JAK2 was a functional regulator of both STAT3 and ERBB2. The utilisation of siRNA allowed for a more rigorous assessment of the specificity of these effects. JAK2 knockdown recapitulated the effects of JAK2 inhibition. In each cell line examined JAK2 knockdown was associated with a reduction in pSTAT3, and with the exception of PEA2, a reduction in pERBB2. Generally reductions in pSTAT3 were not as large as observed in response to JAK2 inhibition, which might suggest that the additional reduction associated with inhibitor treatment was due to off target specificity for another STAT3 kinase.

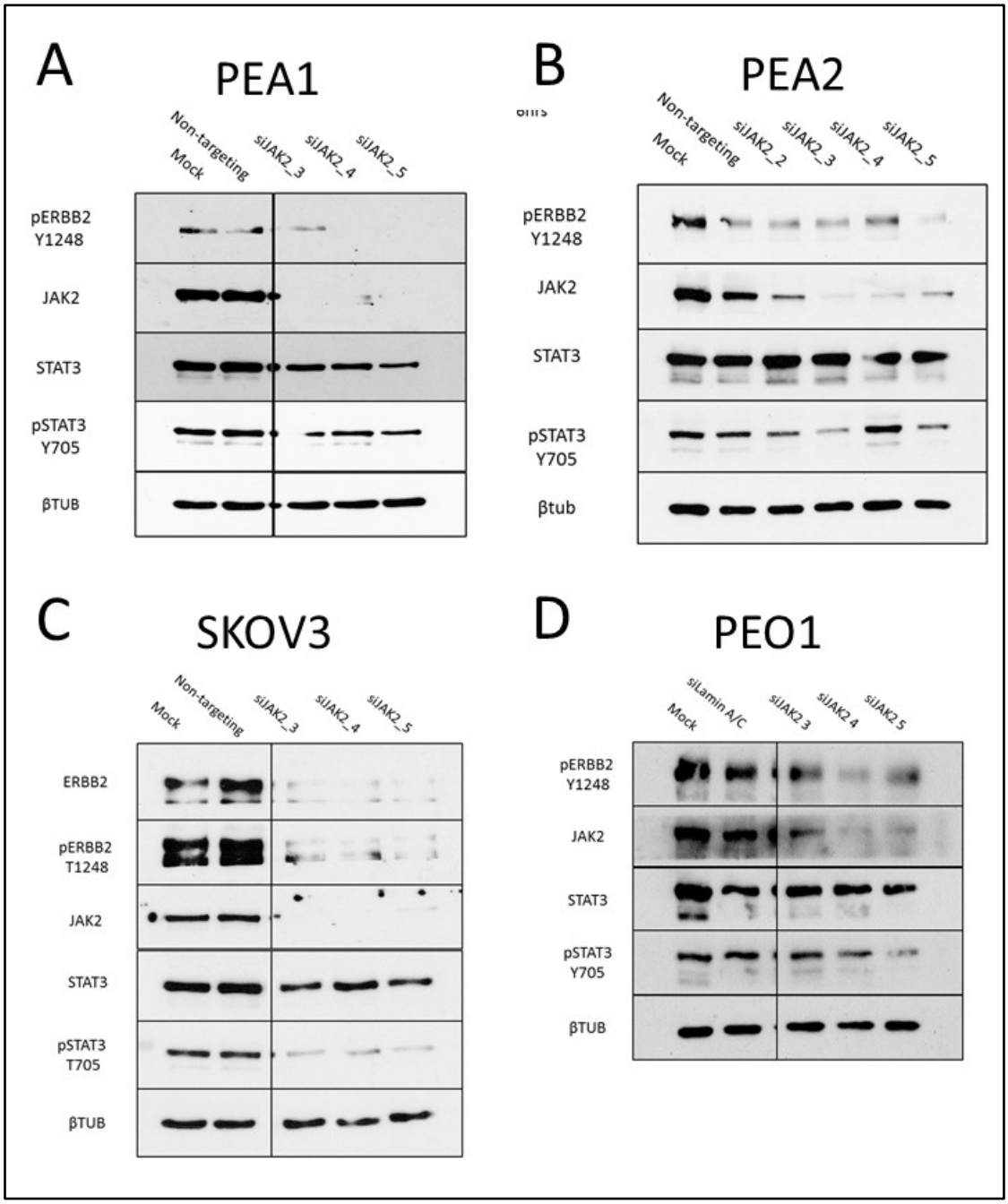

Figure 31. Western blot JAK2 RNAi. Cells were transfected with either no siRNA (mock) or a negative control either, non-targeting or lamin A/C siRNA, or 1 of 3 or 4 JAK2 siRNAs for 48 hours before reseeding for an additional 24 hours before lysis. Samples from at least two replicates were analysed and the results shown are representative.

Each siRNA was capable of reducing levels of pSTAT3 with the exception of siJAK2 4 in PEA2. The siRNA JAK2 2 was excluded from western blots of PEA1, SKOV3 and PEO1, and for all phenotype data shown in the previous two sections because of a low

efficiency of knockdown relative to remaining siRNAs. However in the western blot for siJAK2 transfected PEA2 shown above it was included, as in this particular replicate the siRNA achieved a reasonable degree of knockdown which was coincident with a reduction in pSTAT3. This acts to substantiate the view that the increase in pSTAT3 seen in response to transfection with siJAK2 4 in PEA2 is an off target effect and artifactual. An increase in pSTAT3 in response to transfection with siJAK2 4 was observed in each replicate for PEA2 but none of the other cell lines used. The reason for this is unclear.

Reductions in pSTAT3 were often accompanied by smaller absolute reductions in total protein expression. This was most apparent in PEA1 and SKOV3. This effect is not unexpected as STAT3 is a self-regulating gene capable of binding its own promoter, a property it shares with a number of other STAT proteins [419]. This result is also consistent with small reductions in protein expression in response to cisplatin treatment.

Knockdown of JAK2 was also associated with reductions in pERBB2 consistent with JAK2 inhibitor treatment. It was not generally possible to detect ERBB2 protein levels in cell lines other than SKOV3, as a consequence ERBB2 protein expression was not assessed in JAK2 inhibitor treated cells. Therefore it was unclear whether reductions in Y1248 phosphorylation were simply a consequence of reduced protein expression. Results obtained here suggest that JAK2 knockdown causes reductions in total ERBB2 protein expression based on data from SKOV3. This result is in contrast to those shown in Figure 17 showing only a modest change in total ERBB2 expression in response to cisplatin treatment. However far greater reductions in JAK2 expression were achieved by RNAi than cisplatin treatment, so this comparison may not be entirely valid. Reductions in pERBB2 and ERBB2 in SKOV3 were large in magnitude but transient in nature, although not shown, depressed pERBB2 generally only lasted for 24 hours before levels returned. In fact once reductions had been reversed frequently increases in pERBB2 were observed, despite the continued knockdown of JAK2.

3.3 JAK2 Overexpression Increases Proliferation, pSTAT3 and pERBB2

Both small molecule and siRNA inhibition of JAK2 have shown a role for the protein in regulating the activation of STAT3 and ERBB2. The role of JAK2 in phosphorylating STAT3 is well-documented and data presented here confirms the predicted function.

However a role for JAK2 in regulating ERBB2 is more novel and data presented here have not clearly demonstrated whether the nature of this interaction is at the level of phosphorylation of total protein expression. To further understand this interaction a JAK2 overexpression construct was prepared, the methodological results relating to this are shown in supplementary methods results section S2. A number of mutant variants of the wild type sequence were generated to address the importance of JAK2 phosphorylation in its ability to regulate both STAT3 and ERBB2, including the constitutive phosphorylation mimic Y1007/1008E, the constitutive dephosphorylation mimic Y1007/1008F and the clinically relevant V617F constitutively active form. Results are only shown relating to the wild type and, Y1007/1008F unphosphorylatable form of the construct.

3.31 Over Expression of JAK2 Increases Proliferation and Modulates the Activity of ERBB2

PEA1 and SKOV3 cells were transfected with either empty vector pcDNA, WT JAK2 or Y1007/1008F JAK2 for 24 hours. Cells were then reseeded for proliferation assay and protein assessment allowing 24 hours for recovery. In both PEA1 and SKOV3 transfection with wild type JAK2 was associated with a significant increase in levels of cell viability after 96 hours relative to empty vector transfected cells ($p=0.040$ and $p=0.047$ respectively). Correspondingly doubling time in WT JAK2 transfected cells was reduced marginally from 30 hours to 28 hours in PEA1 and from 34 hours to 30 hours in SKOV3.

In PEA1 transfection with the unphosphorylatable form of JAK2 (Y1007/1008F), in which the duel tyrosine sites required for phosphorylative activation have been mutated to phenylalanine, behaved as predicted, having no effect on proliferation relative to empty vector ($p=0.7$). Whereas in SKOV3 transfection with Y1007/1008F JAK2 was associated with an increase in proliferation, while this failed to achieve significance ($p=0.14$) this was predominantly due to one replicate which preformed differently from the remaining three. Exclusion of this replicate the non-significant p-value above decreases becoming highly significant ($p=0.007$).

Lysates from JAK2 transfected cells were also prepared to validate overexpression and examine any effects on signalling, results are shown in Figure 32C. In both cell lines overexpression resulted in an increase in JAK2 expression, and validating the preparation of the mutant constructs only transfection with the wild type sequence resulted in an increase in

levels of pJAK2 Y1007/1008. Transfection with WT JAK2 was associated with an increase in levels of pSTAT3 in both cells lines which was accompanied by a corresponding increase in the STAT3 regulated genes cyclin D1, in PEA1 and, BCL2L1 in SKOV3. Different genes were used as a read out of STAT3 activation predominantly due to the quality of western blots produced and JAK2 overexpression did also result in an increase in cyclin D1 in SKOV3, data not shown.

This activation of STAT3 by WT JAK2 was reversed by transfection with the Y1007/1008F mutant in PEA1. However in Y1007/1008F transfected SKOV3 cells pSTAT3 remained elevated relative to empty vector transfected cells. Assuming that the mutant Y1007/1008F vector is indeed incapable of phosphorylating STAT3 this would imply that something other than JAK2 is responsible for this increase.

Like phosphorylated STAT3, transfection with WT JAK2 was associated with an increase in Y1248 phosphorylated ERBB2 in both cell lines, this was most clear in PEA1. This increase was also experienced at the level of total protein. Again these effects were reversed in PEA1 upon transfection with the inactive mutant form of JAK2. Whereas in SKOV3 increases in Y1248 ERBB2, experienced with WT over expression, were not reversed with Y1007/1008F overexpression. Also no changes were apparent at the levels of total protein. However saturation of the signal for total ERBB2 may have prevented the detection of differences between the different treatments.

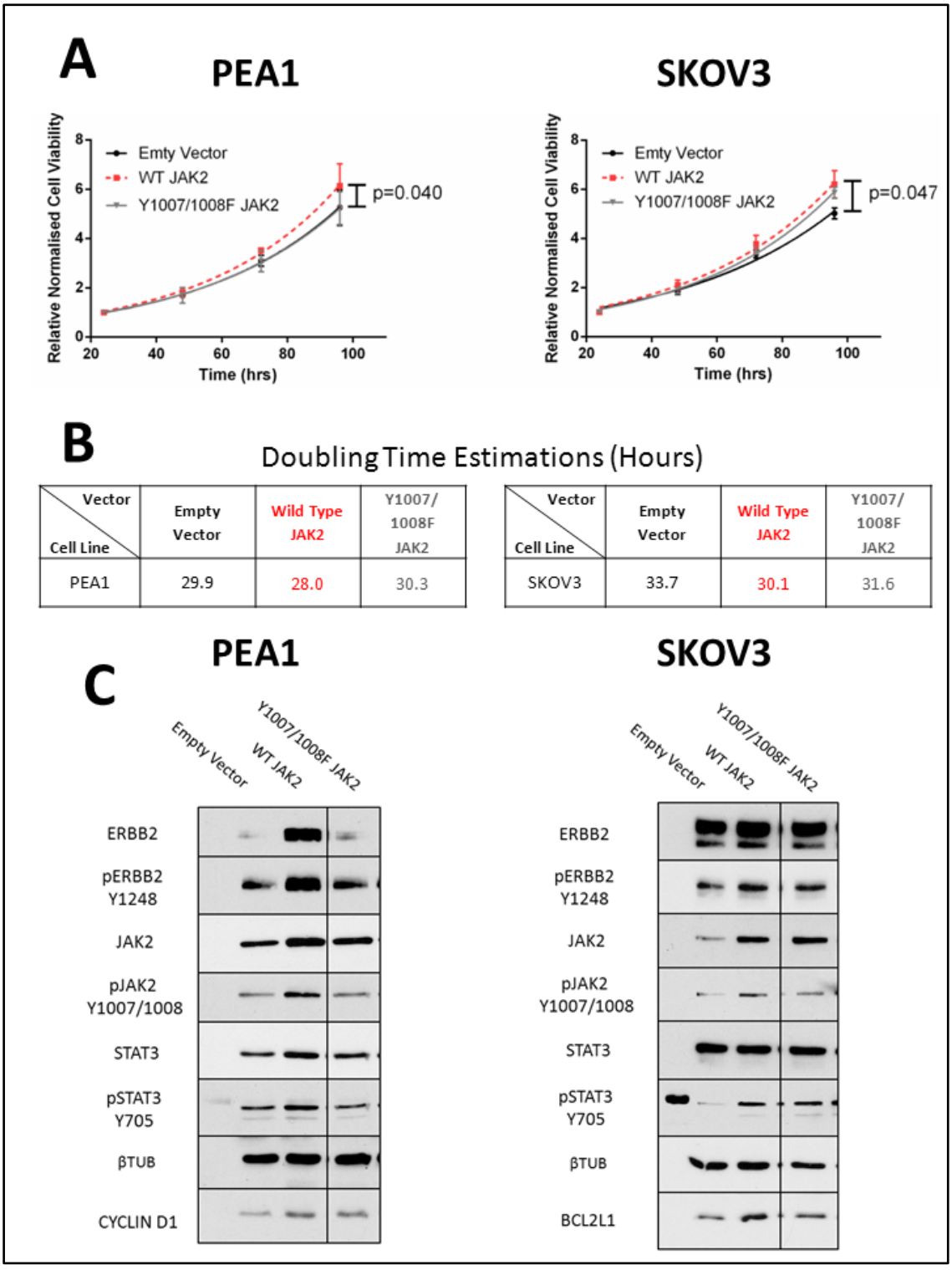

Figure 32. Overexpression of JAK2 in PEA1 and SKOV3. **A,** proliferation assay after overexpression with JAK2 pcDNA3.1. Cells were transfected with either empty vector, WT, or Y1007/1008F JAK2, for 24 hours, prior to carrying out proliferation assay. Cell viability estimates made using MTT assay. Treatments normalised to 0 hours. Values are the average of n=4 separate biological replicates, exponential growth curve drawn in PRISM software. P-values show the significance of paired T-test between WT JAK2 and empty vector transfected. **B**, doubling time estimates made in PRISM software based on exponential regression fit for each treatment shown in A, times in hours. **C,** western blot for cells after JAK2 overexpression. Cell were transfected for 24 hours and allowed a further 24 hours for recovery prior to lysis. Lysates from at least two separate biological replicates were run and the results shown here are representative.

3.4 No Evidence of a Physical Interaction Between JAK2 and ERBB2

The nature of any interaction between JAK2 and ERBB2 presented here is unclear. A physical interaction has been previously described and this was the initial reason for investigating ERBB2 in response to cisplatin treatment [316]. Partially based on this evidence a direct interaction was hypothesised to be the driver of the effects shown above. To further investigate this possibility JAK2 was immunoprecipitated. There was no evidence of an interaction in any cell line examined including ERBB2 overexpressing SKOV3s, see figure 33.

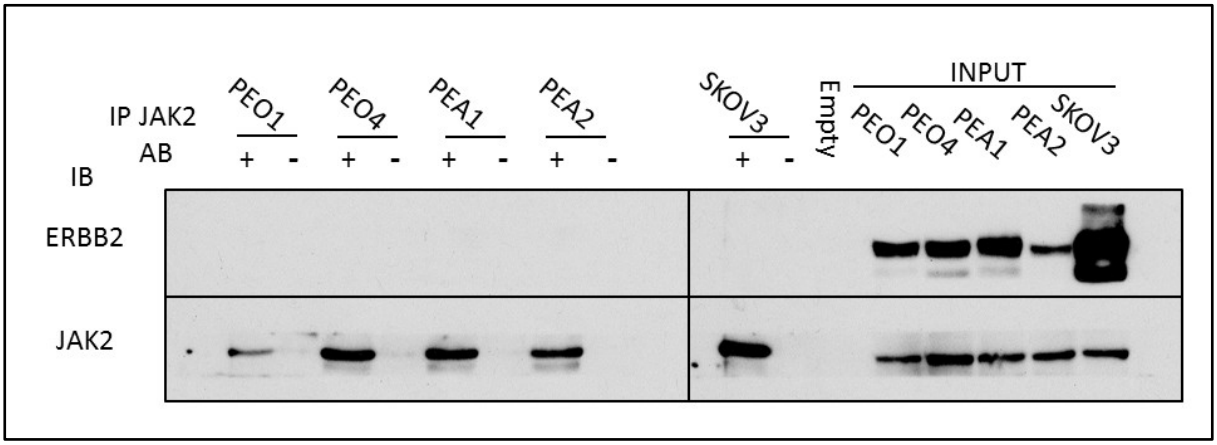

Figure 33. Immunoprecipitation of JAK2. Lanes marked with + included JAK2 antibody those with – contained beads only to control for indirect interaction for JAK2 with beads. Input contains non precipitated lysate to control for presence of protein in sample. This experiment was repeated 3 times under differing conditions, the replicate shown above was carried as described in methods and materials, each replicate gave the same results.

Discussion :-

Results Chapter 3

3.1 JAK2 Inhibition Reduces Cisplatin Induced Apoptosis, Reduces Growth Rates and Levels of STAT3 and ERBB2 Phosphorylation

Use of the JAK2 inhibitor, TG101348, provided the first functional evidence, initially suggested by cisplatin exposure data, that JAK2 both regulates the activity of STAT3, ERBB2 and possibly via these mediators, apoptosis and cell proliferation. JAK2 inhibition protected cells against cisplatin induced apoptosis, reduced proliferation rates and mimicked cisplatin dependant changes in pSTAT3 and pERBB2, suggesting these changes, in JAK2 expression, protect the cell from apoptosis possibly by reducing proliferation rates and allowing for additional DNA repair. It also provides a functional explanation for the apparent selection towards increased sensitivity to the reduction of JAK2 expression after cisplatin exposure, observed in the resistant pairs of PEO1/PEO4 and PEA1/PEA2.

The use a kinase inhibitor also provides evidence these changes are driven not by changes in protein expression but the kinase activity of JAK2. As cisplatin caused a reduction in both pJAK2 and total JAK2 it was not possible to speculate which change was driving these effects. This activity of JAK2 is in keeping its conventional role as a STAT kinase, and is therefore not unexpected.

These results support the emerging role for JAK2 as a regulator of ERBB2, a function that is apparently also dependent on its kinase activity rather than absolute expression. The mechanism of interaction between JAK2 and ERBB2 is unclear, although it appears from evidence in SKOV3 (Figure 31C) that JAK2 regulates ERBB2 at the total level and not phospho level, suggesting against the most parsimonious explanation, that JAK2 simply phosphorylates ERBB2 at Y1248.

The presence of readily detectable levels of pJAK2 apparently driving proliferation and the phosphorylation of two well-known oncogenes might suggest that its inhibition might have useful therapeutic potential. JAK2 is the key driver of Polycythemia vera a haematological malignancy, 90% of case of which contain the constitutive activating

mutation V617F [212]. Largely due to its role in Polycythemia vera and other haematological malignancies a number of small molecule inhibitors targeting JAK2 have been developed for clinical use, including TG101348. When considered alongside the difficultly in targeting STAT proteins with direct inhibition and that STAT3 activation is observed in around 70% of all malignant ovarian tumours [420] JAK2 might represent an attractive target for reducing STAT3 signalling. As STAT3 is activated in a high proportion of cases inhibiting JAK2 could therefore target a large proportion of sufferers, providing JAK2 is the active kinase in the majority. A number of publications have implicated various kinases in the activation of STAT3, these are discussed in introduction section 2.32. Data presented here suggests that JAK2 would play a major role in maintaining evaluated STAT3 phosphorylation in a high proportion of them, as each cell line assessed responded to JAK2 inhibition with reduced STAT3 activation.

Therefore JAK2 inhibitors might offer a means of easily targeting a large proportion of cases. However this must be considered in light of two additional factors, first the likelihood of JAK2 inhibition having tumour specificity and second how this might combine with existing treatment regimes.

Firstly on the issue of specificity, the 'normal' OSE cell line OSE-C2 was examined both for its levels of constitutive pSTAT3/pJAK2 activity and JAK2 inhibitor response. Results from OSE-C2 must be evaluated in respect of two caveats; firstly recent developments regarding the tissue of origin of HGS ovarian have suggested that the majority are not derived from the OSE but fallopian tube epithelium. Second OSE-C2 expresses constitutive levels of pSTAT3 whereas tissue taken directly from the ovary has been reported to express none [421,422].

Despite these shortcomings it is the best normal control available. The JAK2 inhibitor functioned in much the same way in this 'normal' control as the tumour cell lines suggesting that there would be the potential for systemic and potentially undesirable effects if used in patients. This view is contradicted by recent results from a phase 1 trial which have suggested TG101348 is both well tolerated and effective in cases of JAK2 V617F driven myelofibrosis [423].

Secondly and of greatest concern in relation to the use of a JAK2 inhibitor in a clinical setting is the implied antagonism in combination with cisplatin. JAK2 inhibition appears to mimic some of the effects of cisplatin treatment protecting cells from cisplatin induced apoptosis. A cells ability to respond to cisplatin, in terms of JAK2 expression, also appears to have been selected for as both PEO4 and PEA2 are significantly more sensitive to

reducing JAK2 expression when exposed to cisplatin. Therefore inhibiting JAK2 also mimics some aspects of cisplatin resistance, indeed PEO4, PEA2 and PEO23 have lower proliferation rates than their sensitive isogenic partner and equivalent dose of cisplatin induce less apoptosis, much like the effects of inhibiting JAK2. Taken together, the protective effect of JAK2 inhibition on cisplatin induced apoptosis, provides fairly strong evidence that combining these two compounds is likely to result in antagonism. It would be interesting both mechanistically and in light of potential clinical implications to more formally investigate this interaction using isobologram analysis.

3.2 siRNA Mediated Knockdown of JAK2 Inhibits Cell Growth, Increases Cisplatin IC_{50} and Reduces Levels of STAT3 and ERBB2 Phosphorylation.

siRNA knockdown of JAK2 was able to recapitulate the growth inhibitory effects of JAK2 inhibition, as well as reductions in pSTAT3 and ERBB2, providing convincing evidence that these effects are on target.

One interesting difference that emerged from the siRNA data was the extent of reductions in pSTAT3. Reductions in response to TG101348 were very high and generally resulted in almost undetectable levels of phosphorylation at the highest concentration of inhibitor, 1μM. This is in contrast to the extent of reductions achieved with siRNA. Despite the very high efficiency of knockdown achieved in especially PEA1 and SKOV3, reductions in pSTAT3 were not complete. In PEA1 and SKOV3 JAK2 siRNAs were able to able to reduce levels of protein below the threshold of detection, despite this, and most apparent in PEA1, reductions in pSTAT3 were incomplete to modest. This disparity between inhibitor and siRNA suggests additional STAT3 kinases not targeted by siRNA are inhibited by, TG101348, especially at higher concentrations. The most obvious candidates mediating this additional effect would be the other JAKs. Protein expression of JAK1 and TYK2 has been demonstrated in these cells lines (data not shown). Further examination of these proteins would be required to assess the contribution they make to STAT3 activity.

JAK2 siRNA also mirrored JAK2 inhibition in reducing ERBB2 phosphorylation. The inclusion of the ERBB2 overexpressing cell line SKOV3 allowed for an assessment of both phospho and total proteins levels of ERBB2 associated with JAK2 knockdown, it was only possible to detect protein expression in this cell line. Figure 31C shows the effect of

JAK2 knockdown in SKOV3 on total ERBB2 expression, which was decreased by each siRNA. Given the role of these two proteins and their cellular localisation is was tempting to speculate that JAK2 was simply acting as a kinase of ERBB2. This data suggests that the regulation is instead at the level of absolute expression and that reductions in pERBB2 detected in other cell lines are simply a surrogate of reduced protein levels. Given the novelty of this interaction between JAK2 and ERBB2, a link had been previously reported [316] however little subsequent work has been published to establish the mechanistic nature of the link, it would be important to investigate this further. For example an examination of ERBB2 mRNA expression would reveal whether the regulation was transcriptional. Alternatively the use of the proteosomal inhibitor MG132 in conjunction with JAK2 knockdowns could imply whether decreased expression is due to protein degradation, if the compound was able to reverse this effect. However data shown in Figure 19B, showing similar reductions in ERBB2 mRNA levels regardless of the cisplatin concentration to which cells are exposed, suggests that JAK2's regulation of ERBB2 is more likely at to be the protein level. Otherwise increases in ERBB2 mRNA would have been expected in PEO1 and PEA1 when treated with 2.5µM cisplatin.

Data produced using TG101348 had suggested that antagonism would exist between JAK2 abrogation and cisplatin. The presence of potential antagonism was more formally assessed in response to siRNA transfection in the form of IC_{50} shift assays. In each cell line examined JAK2 knockdown was associated with an increase in cisplatin IC_{50}, although this failed to achieve significance in PEA2. This suggests that targeting JAK2 in combination with cisplatin would be unfavourable and would confer protective effects on tumour cells, possibly my mimicking both mechanism of cisplatin response and resistance. Returning to the point raised in the previously section relating to the possible therapeutic use of JAK2 inhibitors, this data implies that while they may have some activity as a single agent combining then with cisplatin is unlikely to produce desirable results.

3.3 Over Expression of JAK2 Increases Proliferation and Modulates the Activity of ERBB2

Consistent with JAK2 inhibition and siRNA data, JAK2 overexpression increased proliferation rates. Overexpression was associated with both an increase in pSTAT3 and cyclin D1 which could account for these effects. The behaviour of ERBB2 in PEA1 and

SKOV3 in response JAK2 over expression differed. In PEA1, data supports a role for JAK2 functioning in a canonical fashion, where elicitation of an effect is dependant on catalytic activity, as upregulation of ERBB2 was reversed on transfection with the Y1007/1008F mutant. This would imply a model in which JAK2 activates a STAT protein, which either directly or via intermediaries, transcriptionally upregulates ERBB2. JAK2 overexpression in conjunction with QRT-PCR for ERBB2 mRNA would help to address this.

Conversely in SKOV3, JAK2 overexpression caused an increase in ERBB2, apparently only at the phospho level, and without the requirement for catalytic activity. Whether this is the reflection of a genuine divergence in the mode of regulation between these two proteins remains unclear. However given that SKOV3 is ERBB2 amplified this could be the basis for a potential difference. However results from western blotting were consistent with proliferation, increased proliferation was reversed on transfection with the kinase dead mutant only in PEA1 whereas in SKOV3 transfection with either JAK2 construct had an effect consistent with changes in ERBB2, suggesting this is a genuine effect and not artifactual. An examination of alternative ERBB2 amplified cells would help to resolve these disparities.

3.4 No Evidence of a Physical Interaction Between JAK2 and ERBB2

In the preceding three sections the link between JAK2 and ERBB2 has been discussed, with a view to inferring the probable nature of this relationship. The initial paper demonstrating a link between the two proteins reported a physical interaction by immunoprecipitation [316]. However here in 5 cell lines and using three different protocols, all of which were capable of precipitating JAK2, no detectable quantities of ERBB2 were co-precipitated, including in the ERBB2 overexpressing cell line SKOV3, suggesting that, in these systems, JAK2 doesn't directly regulate ERBB2 but instead acts through an intermediary. As mentioned previously additional experiments to establish changes in ERBB2 mRNA/protein levels after JAK2 perturbation would help to clarify these issues.

Results Chapter 4 :-
STAT3 Promotes Cell Growth and the Expression of Cyclin D1 and BCL2L1

4. STAT3 Promotes Cell Growth and the Expression of Cyclin D1 and BCL2L1.

4.1 An Assessment of the Levels of pSTAT3 Y705 in the Paired Cell Lines PEO1/PEO4 and PEA1/PEA2

Results shown in Figure 16 demonstrate that resistant PEA2 cells are significantly more responsive to cisplatin, in terms of reducing STAT3 phosphorylation than its isogenic partner PEA1. To address whether reduced basal levels of pSTAT3 might also contribute to the resistance of PEA2, or other resistant cell lines, western blotting was conducted to examine STAT3 activation. Y705 phosphorylated STAT3 did not differ by a large magnitude across cell lines examined. The lowest level was seen in PEA2 which contained roughly one third of the most activated, SKOV3. PEA2 possessed around half of the quantity of pSTAT3 as its sensitive isogenic pair PEA1 ($p=0.011$ unequal variance T-test). Whereas levels in PEO1 and PEO4 were very similar, being intermediate between PEA2 and SKOV3. Absolute expression of STAT3 was more consistent with no significant variation across the cell lines. Less than a twofold difference was observed between the highest expressor, PEA2 and the lowest PEO4.

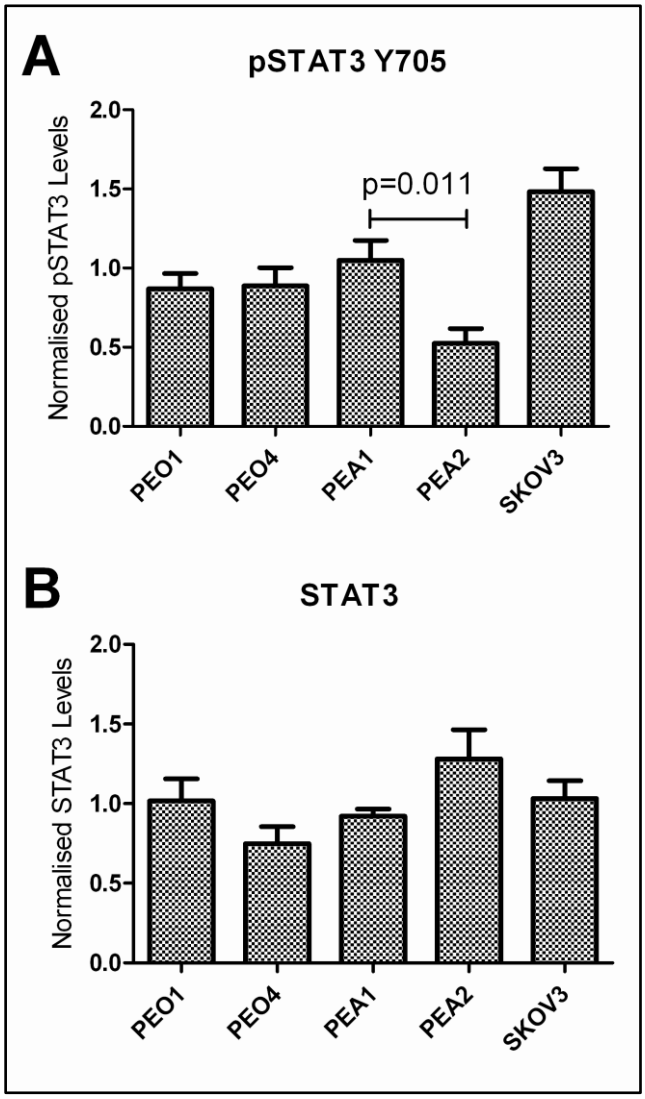

Figure 21. Western blot of **A,** pSTAT3, Y705, and **B,** STAT3 protein expression in the paired isogenic cell lines PEO1/PEO4 PEA1/PEA2 and SKOV3. Raw expression normalised to βTUB and then batch normalised. For **A**, pSTAT3 Y705 and **B** STAT3 values are the average of n=4 separate biological replicates. Error bars show the SEM of the replicates. P-value calculated from a T-test unequal variance.

4.2 siRNA Mediated Knockdown of STAT3 Inhibits Cell Growth, Increases Cisplatin IC_{50} and reduces expression of Cyclin D1

Perturbation of JAK2 by either siRNA or small molecule inhibition was able to reduce levels of both pSTAT3 and pERBB2, recapitulating some of the effects of exposure to high concentrations of cisplatin. In order to access the extent to which the phenotypic

consequences of JAK2 inhibition are mediated via STAT3, siRNA mediated knockdowns were carried out in conjunction with cell proliferation and cisplatin IC_{50} assays. If the growth promoting properties of JAK2 are mediated via its interaction with STAT3 then its ablation should also result in reduced in cell proliferation and an increased cisplatin IC_{50}.

4.21 siRNA Mediated Knockdown of STAT3 Inhibits Cell Growth

STAT3 RNAi was associated with a significant reduction in cell viability in the sensitive, resistant isogenic cell line pair PEA1, PEA2 as well as SKOV3, see Figure 34. RNAi was conducted in the same manner as for JAK2; the cells were transfected with one of three STAT3 siRNAs for 48 hours prior to the start of the proliferation assay. Three STAT3 siRNA species were used; siSTAT3 3, STAT3 4, and STAT3 5. Two previous siRNA were evaluated and not used due to poor efficacy in the case of one and off target effects, in the case of the other.

In PEA1 a significant reduction in cell viability after 72 hours was observed in response to each siRNA. On average PEA1 cells depleted for STAT3 had a doubling time increase of 16% from 33.6 to 39.1 hours, Figure 34D. A significant reduction in proliferation was associated with two of three STAT3 siRNAs in PEA2, siSTAT3 3 ($p=0.012$) and siSTAT3 4 ($p=0.015$), but not siSTAT3 5 ($p=0.15$). A failure to achieve significance in paired t-tests was due to the variation in the magnitude of effect (data noise) relative to mock transfected cells. A significant p value, at the 95% interval, is returned in an unequal variance T-test demonstrating this. Whereas in PEA1 each siRNA had a similar effect on inhibition of cell proliferation but in PEA2 siSTAT3 4 had a far greater inhibitory effect that the remaining siRNAs, which was presumably not specific. The two remaining siRNAs increased doubling time in PEA2 by an average of 20% whereas siSTAT3 4 increased it by 143% to 92.8 hours. In SKOV3 two of three STAT3 siRNAs significantly reduced proliferation, increasing doubling times by an average of 21% from 35.5 hours to 43.2 hours.

Why one siRNA would not increase doubling time is unclear, however it was capable of reducing both STAT3 and cyclin D1 protein levels. The greatest increase in doubling time occurred in SKOV3 in response to STAT3 knockdown.

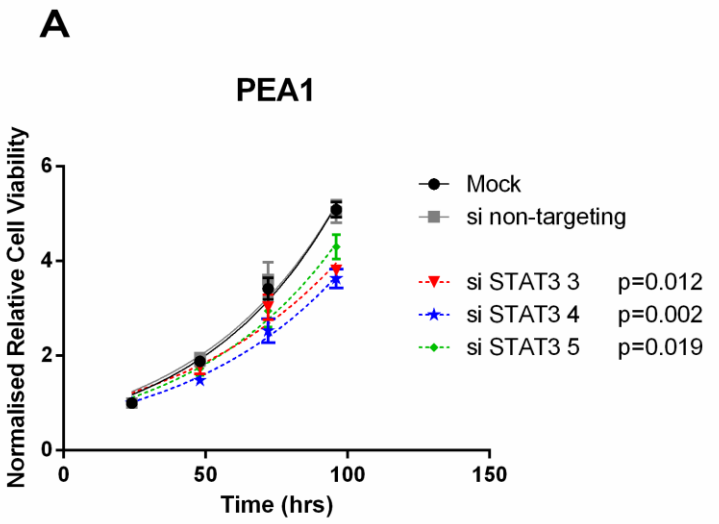

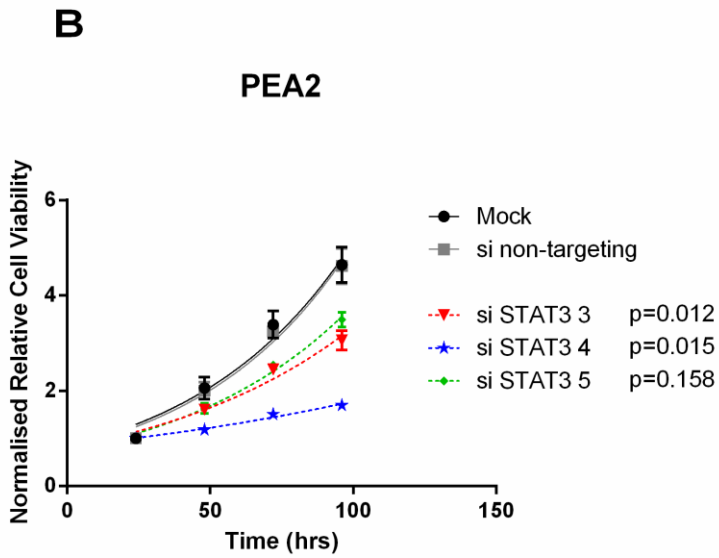

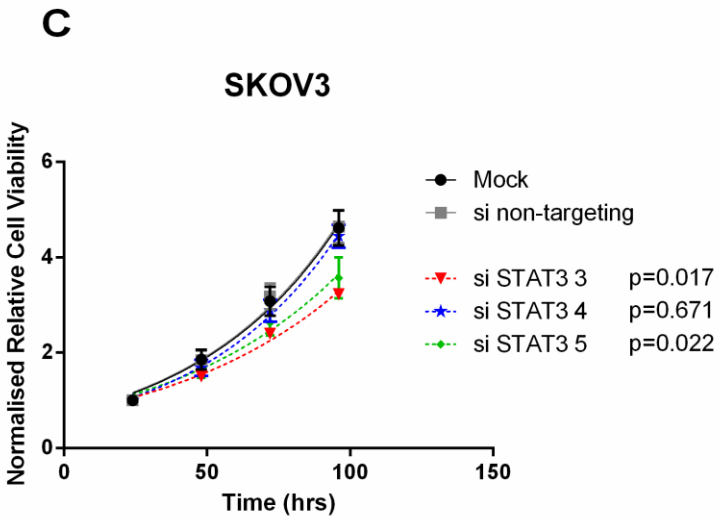

D

Doubling Time (hrs)

Cell Line / siRNA	PEA1	PEA2	SKOV3
Mock	33.6	38.2	35.5
Non targeting	34.9	37.4	35.6
STAT3 3	42.4	49.0	44.1
STAT3 4	38.9	92.8	34.6
STAT3 5	36.5	42.6	42.2

Figure 34. Proliferation assay showing effects of STAT3 siRNA in **A,** PEA1 **B**,PEA2 and **C** SKOV3. Cells treated with a final concentration of, 50nM single species siRNA, except for mock transfected controls which contained no siRNA, for 48 hours. Cell viability for each treatment normalised to 24hr time point. Each point is the average of 3 independent biological replicates and error bars show the SEM between these replicates. Lines are plotted using a least squares exponential regression model, which was also used to estimate doubling times. P values are calculated from a paired T-test against mock transfected at the 72 hours. Table **D** shows the estimated doubling times for each treatment, calculated in PRISM data analysis software.

4.22 siRNA Mediated Knockdown of STAT3 Induces Apoptosis But Does Not Sensitise To Cisplatin

Data presented here suggests that STAT3 knockdown would provide a protective effect against cisplatin induced cell death. To address this issue STAT3 knockdown was combined with an assessment of apoptotic induction and IC_{50} shift (shown in the subsequent section) in combination with cisplatin. To maximise the probability of observing an effect SKOV3 cells were chosen as they are both chemo-naive and expressed the highest levels of pSTAT3.

Cells were transfected for 48 hours before reseeding into 96 well culture plates for cell viability and caspase activation quantitation for each siRNA, either alone on in the presence of 25μM cisplatin, results are shown in Figure 35. Each siRNA induced caspase activation alone, this was significant for siSTAT3 3 (P=0.003) borderline significant for siSTAT3 4 (P=0.056) and not significant for siSTAT3 5 although the magnitude induction was very similar for each ranging from 1.8 to 1.9 fold background levels, this was marginally in excess of caspase activation caused by exposure to 25μM cisplatin. To further examine the possibility of a cisplatin sensitisation effect associated with STAT3 siRNA the ratio of cisplatin induced caspase activation for each siRNA treatment was calculated, shown in B. Each siRNA caused a reduction in the ratio of apoptosis induced by the addition of cisplatin, although none were statistically significant, suggesting STAT3 siRNA might confer a degree of protection to cisplatin induced apoptosis, despite increasing background levels.

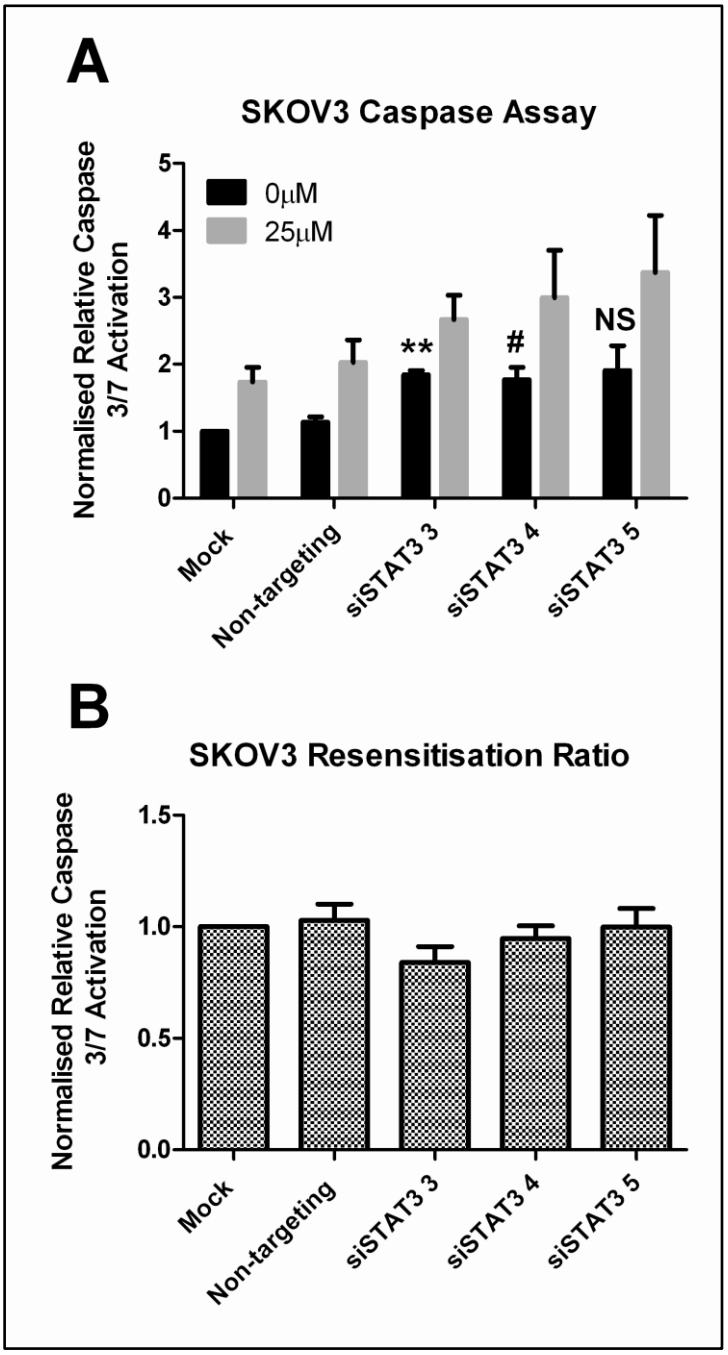

Figure 35. Cisplatin caspase apoptosis assay in SKOV3 cells after knockdown of STAT3. Cells were transfected with either no siRNA (mock) non-targeting siRNA or 1 of 3 STAT3 siRNAs for 48 hours. Cells were then reseeded for cell viability and caspase activation quantitation, using MTT and caspase 3/7 glo assays respectively, either alone or in combination with 25μM cisplatin. **A,** shows the cell viability normalised caspase activation for each siRNA transfection. Values are the average of 3 separate biological replicates, error bars show their SEM. All values relative to mock transfected 0μM cddp = 1. ****** - p <0.01. **#** - p =0.056, **NS** = not significant. All p-values T-tests unequal variance calculated against non-targeting 0μM cddp. **B,** The cisplatin resensitisation ratio shows the fold caspase activation induced for each siRNA associated with the addition of cisplatin. Calculated by dividing the 25μM cddp treated activated caspase levels by the 0μM cddp treatment for each siRNA.

4.23 siRNA Mediated Knockdown of STAT3 Increases Cisplatin IC_{50}

As JAK2 knockdown was associated with both reduced tyrosine 705 phosphorylated STAT3 as well as an increased cisplatin IC_{50} while rIL6(RA) treatment was associated with a decrease in cisplatin IC_{50}, the effect of STAT3 knockdown on cisplatin IC_{50} was also investigated. Experiments were conducted in parallel with STAT3 siRNA proliferation assays shown in Figure 34. Consistent with the results of JAK2 knockdown, siRNA to STAT3 was also associated with a significant increase in the cisplatin IC_{50} of PEA1, PEA2 and SKOV3. In cisplatin sensitive PEA1 cells it was not possible to accurately quantify the magnitude of this effect as the interpolated IC_{50} for each siRNA was above 5μM, maximum concentration used for this cell line in the assay. Despite this each siRNA had an at least 79% increase in cisplatin IC_{50} and each was significantly increased, compared to mock transfected, based on non-overlapping 95% confidence intervals.

Similarly in PEA2 each siRNA caused an increase in cisplatin IC_{50} however only 2 of the 3 oligos were significant. On average of the two oligos that were significant STAT3 knockdown caused a 102% increase in IC_{50}. In SKOV3 like PEA2 only 2 of 3 oligos used was associated with a significant increase in IC_{50} which was increased on average by 94%. In PEA2 and SKOV3 it was the same oligo that failed to significantly increase cisplatin IC_{50}. This siRNA was able to both efficiently reduce STAT3 expression (see Figure 37) and reduce proliferation rates in all cell lines, therefore a lack of on target efficacy can't account for this discrepancy. Given that this behaviour is at odds with the other two siRNAs it is assumed to be an off target effect.

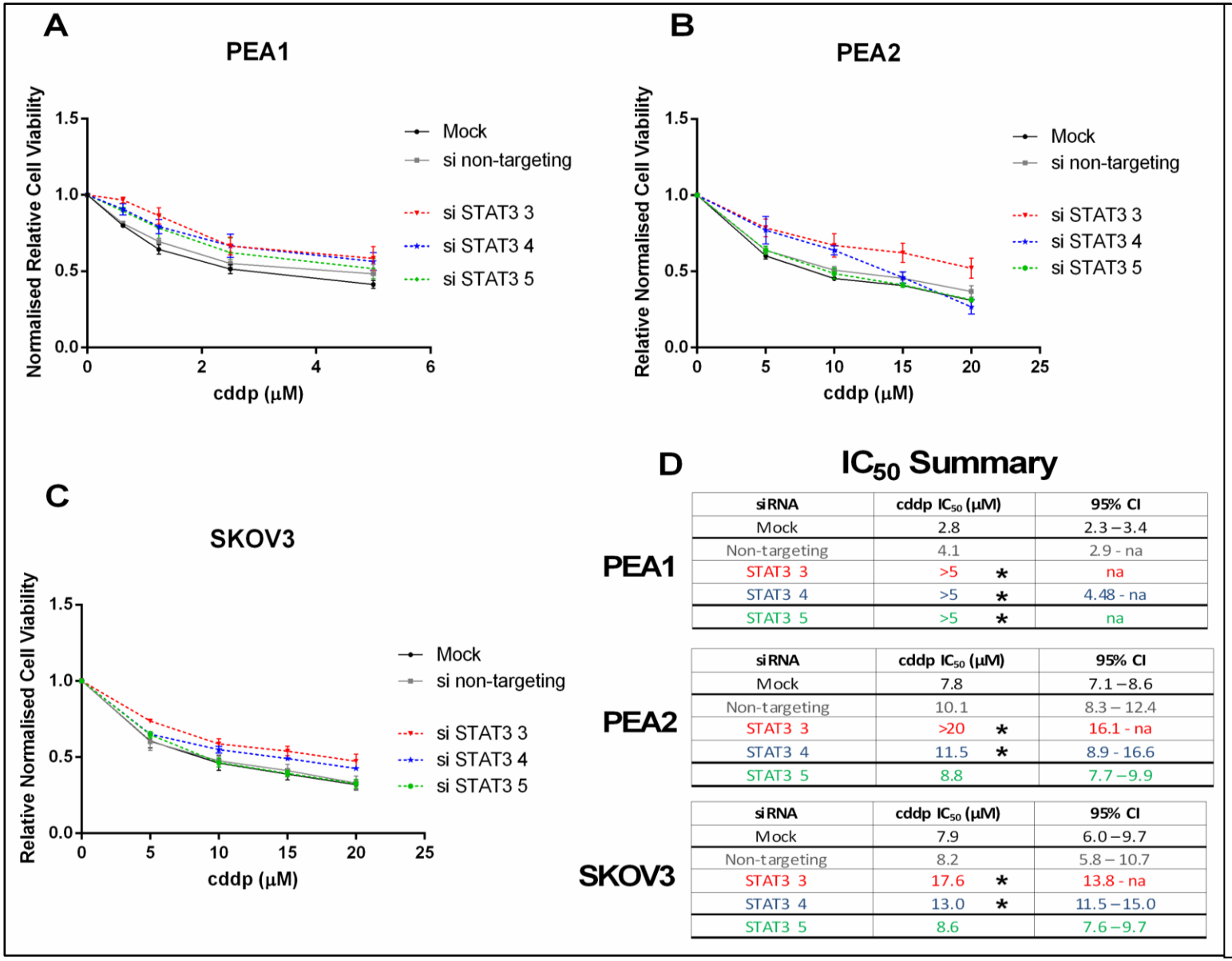

D

IC_{50} Summary

PEA1

siRNA	cddp IC_{50} (µM)		95% CI
Mock	2.8		2.3 – 3.4
Non-targeting	4.1		2.9 - na
STAT3 3	>5	*	na
STAT3 4	>5	*	4.48 - na
STAT3 5	>5	*	na

PEA2

siRNA	cddp IC_{50} (µM)		95% CI
Mock	7.8		7.1 – 8.6
Non-targeting	10.1		8.3 – 12.4
STAT3 3	>20	*	16.1 - na
STAT3 4	11.5	*	8.9 - 16.6
STAT3 5	8.8		7.7 – 9.9

SKOV3

siRNA	cddp IC_{50} (µM)		95% CI
Mock	7.9		6.0 – 9.7
Non-targeting	8.2		5.8 – 10.7
STAT3 3	17.6	*	13.8 - na
STAT3 4	13.0	*	11.5 – 15.0
STAT3 5	8.6		7.6 – 9.7

Figure 36. Cisplatin IC50 of PEA1, A, PEA2, B and SKOV3 C, in response to STAT3 knockdown. Cells were transfected with either, one of three STAT3 siRNAs, a non-coding siRNA or no siRNA (mock) for 48 hours. After which they were treated with the indicated concentrations of cisplatin for 72 hours before viability assay was conducted. Viability shown is relative to 0µM treated cells and averaged over three or four independent biological replicates. IC50 estimations were interpolated from this average. 95% CI boundaries were calculated using a least squares model in the software package Prism.

*** no overlap at p = 0.05**

D shows a summary of interpolated IC50 values.

4.24 siRNA Mediated Knockdown of STAT3 Reduces Expression of Cyclin D1

Simultaneous to the collection of data presented in Figure 34 and Figure 36 protein lysates were collected to allow for a validation of knockdown and an assessment of any effects on canonical STAT3 transcriptional targets. Due to the reduction in proliferation associated with STAT3 knockdown cyclin D1 expression was examined, as a reduction of this key regulator of G1 to S phase transition could account of this effect. Four siRNAs targeting STAT3 were used, only three of these have been presented prior to this section, largely as siSTAT3 1 induced a large amount of apoptosis in contrast to the other 3 siRNAs. This may have also contributed to it exhibiting unique effects in the IC_{50} shift experiment, in Figure 36. Each siRNA was capable of reducing levels of STAT3. While siSTAT3 3 behaved consistently with the two remaining siRNA in growth and IC_{50} assays due to the apparent off target nature of its effects on cyclin D1 expression STAT3 1 has been included in the western blots presented in Figure 37, as its behaviour is consistent with the other siRNAs.

STAT3 knockout reduced expression of cyclin D1. In each cell line tested 3 of 4 siRNAs used caused a reduction in the levels of cyclin D1, siSTAT3 1, 4 and 5, however siSTAT3 3 did not despite having the highest efficiency of knockdown. In order to further examine the extent of cyclin D1 downregulation associated with STAT3 knockdown, protein quantitation of 3 replicates in PEA1 was carried out. The average normalised cyclin D1 expression associated with each siRNA is shown in Figure 37D. The mean reduction in cyclin D1 expression excluding siSTAT3 3, was 50% ranging from 41% in siSTAT3 4 to 58% in siSTAT3 1 transfected cells. Reductions in cyclin D1 expression were only significant in response to siSTAT3 4 transfection ($p=0.042$), significance was borderline in response to siSTAT3 5 transfection ($p=0.055$) and non-significant for siSTAT3 1.

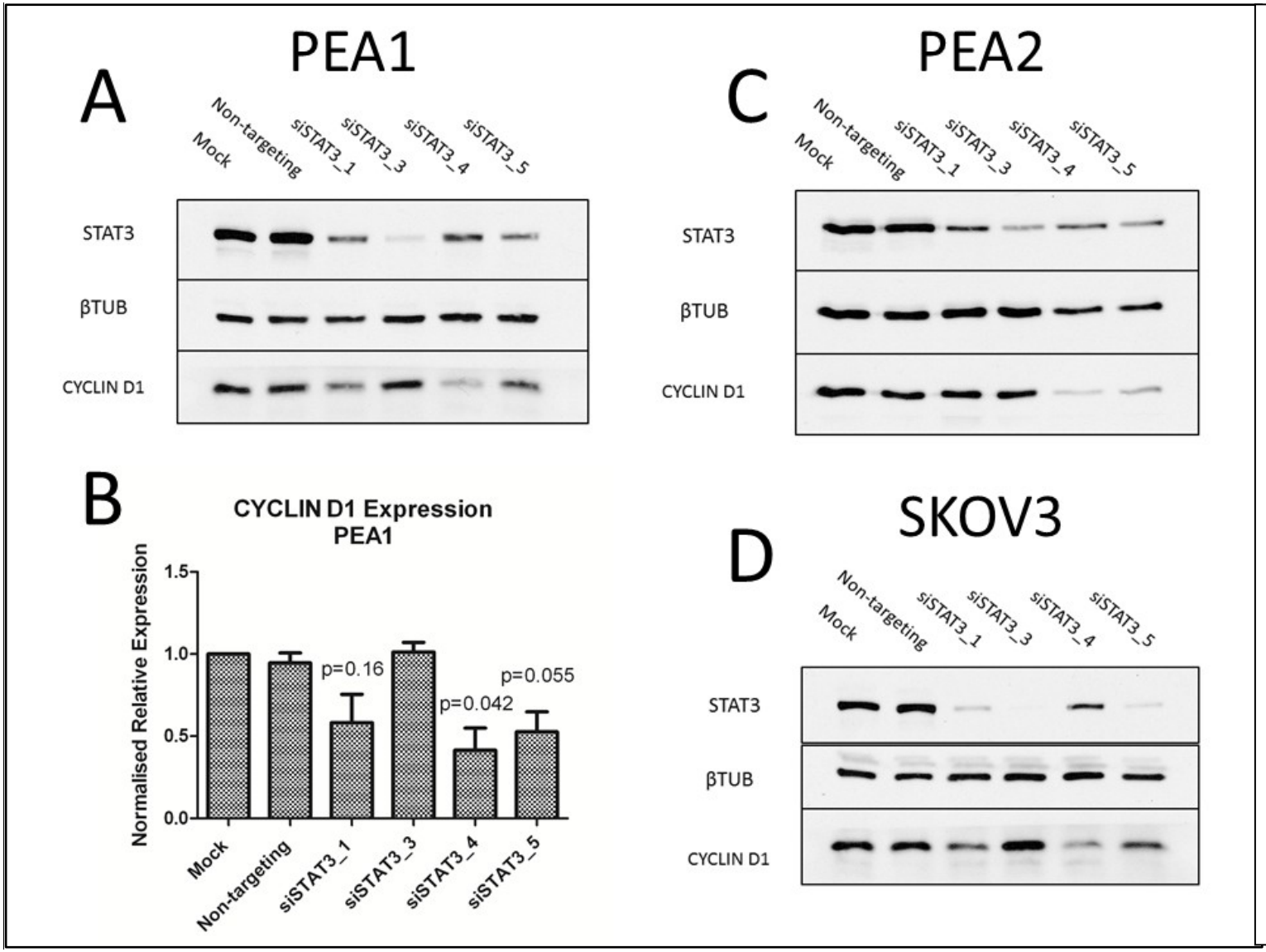

Figure 37. Western blot of STAT3 siRNA transfected cells. **A** **C** and **D** individual westerns for PEA1 PEA2 and SKOV3 respectively. Cells were transfected with either no siRNA (mock), non-targeting siRNA or one of 4 STAT3 siRNAs for 48 hours prior to reseeding and an additional 24 hours for attachment prior to lysis. siSTAT3 1 was included for comparison, despite having been excluded from previous analysis. **B** quantitation of 3 biological replicates from PEA1. Cyclin D1 expression normalised to βTUB. Band quantitation carried out in Image J software. Error bars show the standard error of replicates from 3 separate biological replicates. P-values show the significance of unequal variance T-test between the replicates.

4.3 STAT3 Overexpression Increases Cell Proliferation, Cisplatin Induced Apoptosis and Decreases IC_{50}.

Data for STAT3 RNAi has shown that decreased STAT3 expression was associated with a significant decrease in proliferation rates and commensurate increases in cisplatin IC_{50} in PEA1, PEA2 and SKOV3. STAT3 depletion was also associated with decreased cyclin D1expression, an important promoter of G1 – S phase transition. In order to both validate and further understand the mechanism of by which STAT3 elicits these effects transient overexpression of STAT3 was conducted. Overexpression of mutant forms of STAT3, generated by site directed mutagenesis, allowed for an inspection of the importance of phosphorylative activation in comparison to absolute expression when overexpressing STAT3. Site directed mutagenesis was used to generate a tyrosine 705 to phenylalanine substitution. Tyrosine 705 is the target of JAK2 phosphorylation and is required for DNA binding activity of STAT3. As such overexpression of STAT3 Y705F should not lead to an increase in the expression of STAT3 transcriptional targets.

4.31 Overexpression of STAT3 Was Not Possible in PEA1 or PEA2 but Was Possible in SKOV3

For methodological results relating to the preparation of different overexpression vectors see the supplementary methods section S1, at the end of this document.

Due predominantly to differential changes in the levels of pSTAT3 between PEA1 and PEA2, when exposed to cisplatin, this model has been the focus of examination thus far. For unknown reasons it was not possible to successfully transfect either PEA1 or PEA2 with a STAT3 expressing vector. The ability of STAT3 pcDNA 3.1 overexpression vectors to acts as a viable template for STAT3 expression was validated in alternative cell lines. As was the ability of the effectene (Qiagen) transfection protocol to successfully express an alternative exogenous protein, in this case green fluorescent protein (GFP), shown Figure 38A.

In order to optimise STAT3 overexpression in PEA1 and PEA2 a number of different ratios of DNA to effectene (Qiagen) transfection reagent were tested. These ranged from 0.4µg of plasmid DNA to 4µl (1:10) of transfection reagent to 0.4µg of DNA to 1µl (1:2.5) of transfection reagent, all volumes relate to a single well of a 6 well plate. The results of this optimisation are shown in Figure 38A and B. Each ratio of DNA to transfection reagent used

was capable of expressing the exogenous GFP. However none of these conditions resulted in a discernable increase in STAT3 expression, the reason for this remains unclear. Despite this the ability of this vector to produce protein was validated in SKOV3, see Figure 38C. Using a ratio of DNA to transfection reagent of 1:10, STAT3 overexpression was clearly detectable. HDAC4 and GFP were used as additional technical controls as these vectors were previously validated as functional.

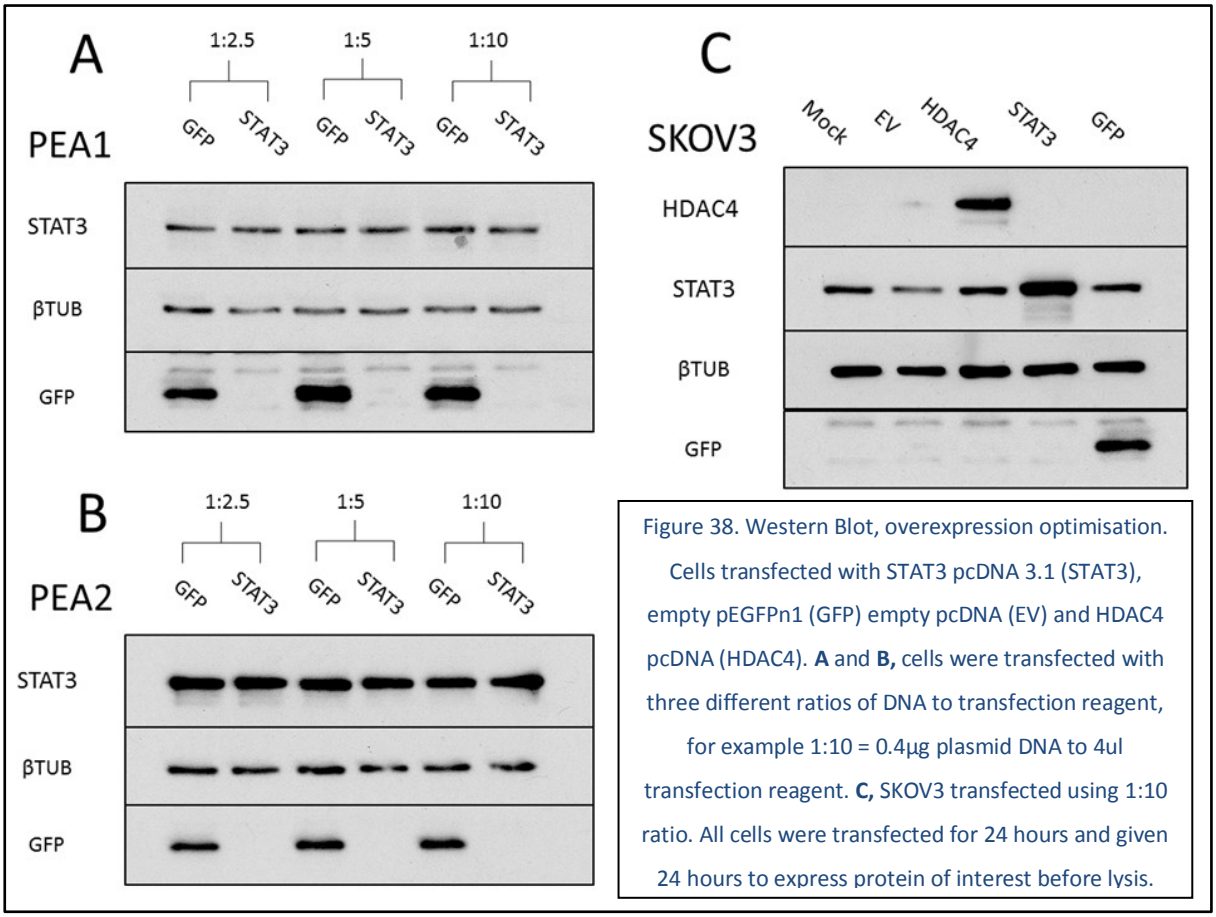

Figure 38. Western Blot, overexpression optimisation. Cells transfected with STAT3 pcDNA 3.1 (STAT3), empty pEGFPn1 (GFP) empty pcDNA (EV) and HDAC4 pcDNA (HDAC4). **A** and **B,** cells were transfected with three different ratios of DNA to transfection reagent, for example 1:10 = 0.4µg plasmid DNA to 4ul transfection reagent. **C,** SKOV3 transfected using 1:10 ratio. All cells were transfected for 24 hours and given 24 hours to express protein of interest before lysis.

4.32 Overexpression of STAT3 Increases Cell Proliferation

Over expression of STAT3 was carried out in the isogenic pair PEO1/PEO4 and SKOV3. Cells were transfected using an optimised concentration of effectene transfection reagent with either empty pcDNA (EV), wild type (WT) STAT3 pcDNA or Y705F STAT3 and then assessed for viability every 24 hours for 96 hours. In each cell line transfection with WT STAT3 was associated with an increase in proliferation. In PEA1 and SKOV3

transfection with WT STAT3 was associated a significant increase in cell viability after 96 hours incubation ($p=0.021$, $p=0.007$ in paired T-tests respectively). In both cell lines a small but insignificant increase in proliferation was detected in cells transfected with Y705F STAT3. A reproducible increase in proliferation in PEO4 also occurred when transfected with WT STAT3, this effect failed to reach significance ($p=0.11$), but was reversed by transfection with Y705F STAT3. A lack of significance in PEO4 upon WT STAT3 transfection was likely due to the reduced magnitude of effects relative to PEO1 and SKOV3.

The magnitude of effect in each cell line was modest. The smallest effect was experienced by PEO4 whose estimated doubling time fell by 7% from 45 hours to 42 hours. WT STAT3 overexpressing PEO1 saw a larger (11%) decrease in doubling time from 40.5 hours to 36.2 hours. The largest effect occurred in SKOV3 where a 15% reduction from 34.1 hours to 29.1 hours was observed. For SKOV3 the changes in doubling time resulting from RNAi and overexpression are broadly similar. The average of two efficacious siRNAs in SKOV3 reduced doubling time by 21%, taken together the range of doubling times between STAT3 over and under-expression was 29.1 hours to 43.2 hours.

The presence of a significant increase in viability associated with WT but not Y705F STAT3 overexpression suggests that the proliferative effects of STAT3 require its phosphorylation and are therefore mediated via its classical role as a transcription factor, upregulating the expression of proliferative factors.

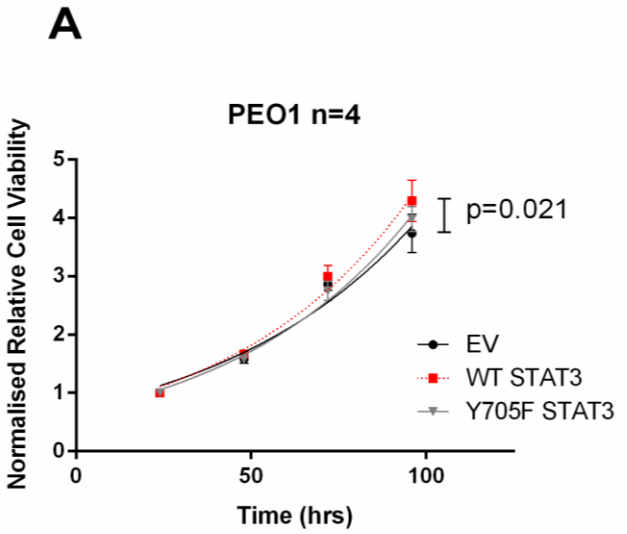

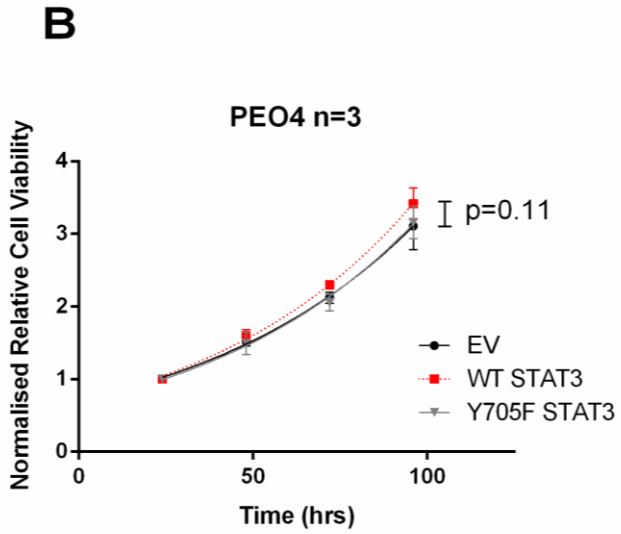

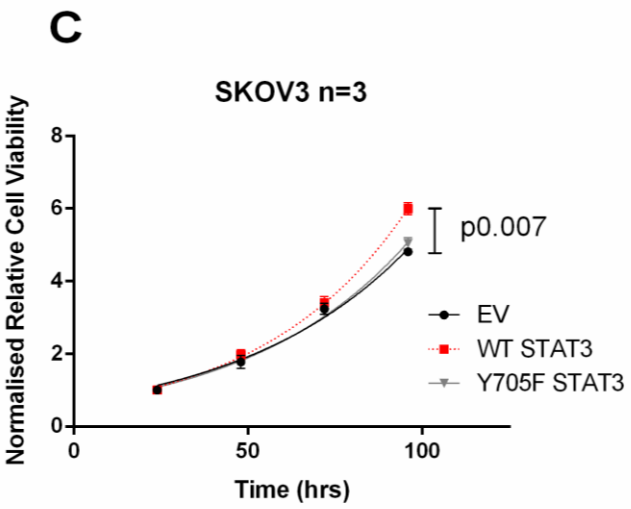

D

Doubling Time Summary

Cell Line \ Vector (hrs)	EV	WT	Y705F
PEO1	40.5	36.2	37.2
PEO4	45	42.0	43.5
SKOV3	34.1	29.1	32.3

Figure 39. Proliferation assay after overexpression of STAT3. **A – C** cells transfected with either empty vector (EV) pcDNA 3.1, wild type (WT) STAT3α pcDNA, or STAT3α Y705F pcDNA. In PEO1 **A**, PEO4 **B** or SKOV3 **C**. Relative changes in cell viability are shown normalised to 24 hours for each treatment. Values shown are the average of either 3 or 4 individual biological replicates. Error bars represent the SEM between the means of each biological replicate. Lines are plotted using a least squares exponential regression model, which was also used to estimate doubling times (analysis carried out in Prism). P values are calculated from a paired T-test between EV and WT. **D**, shows a summary of the doubling times for each treatment.

4.33 Overexpression of STAT3 Increases Cisplatin Induced Apoptosis

Simultaneous to the proliferation assay carried out in the section above caspase apoptosis assays were also conducted on STAT3 transfected cells to examine the effect of overexpression on cisplatin induced apoptosis. After transfection and a 24 hour recovery period cells were either treated with 10µM (PEO1) or 25µM (PEO4 and SKOV3) cisplatin for 24 hours prior to the measurement of activated caspase 3 and 7 levels using the caspase glo assay (Promega). The fold difference, in activated caspase 3/7, between each plasmid transfection alone and transfection in combination with cisplatin is shown in Figure 40.

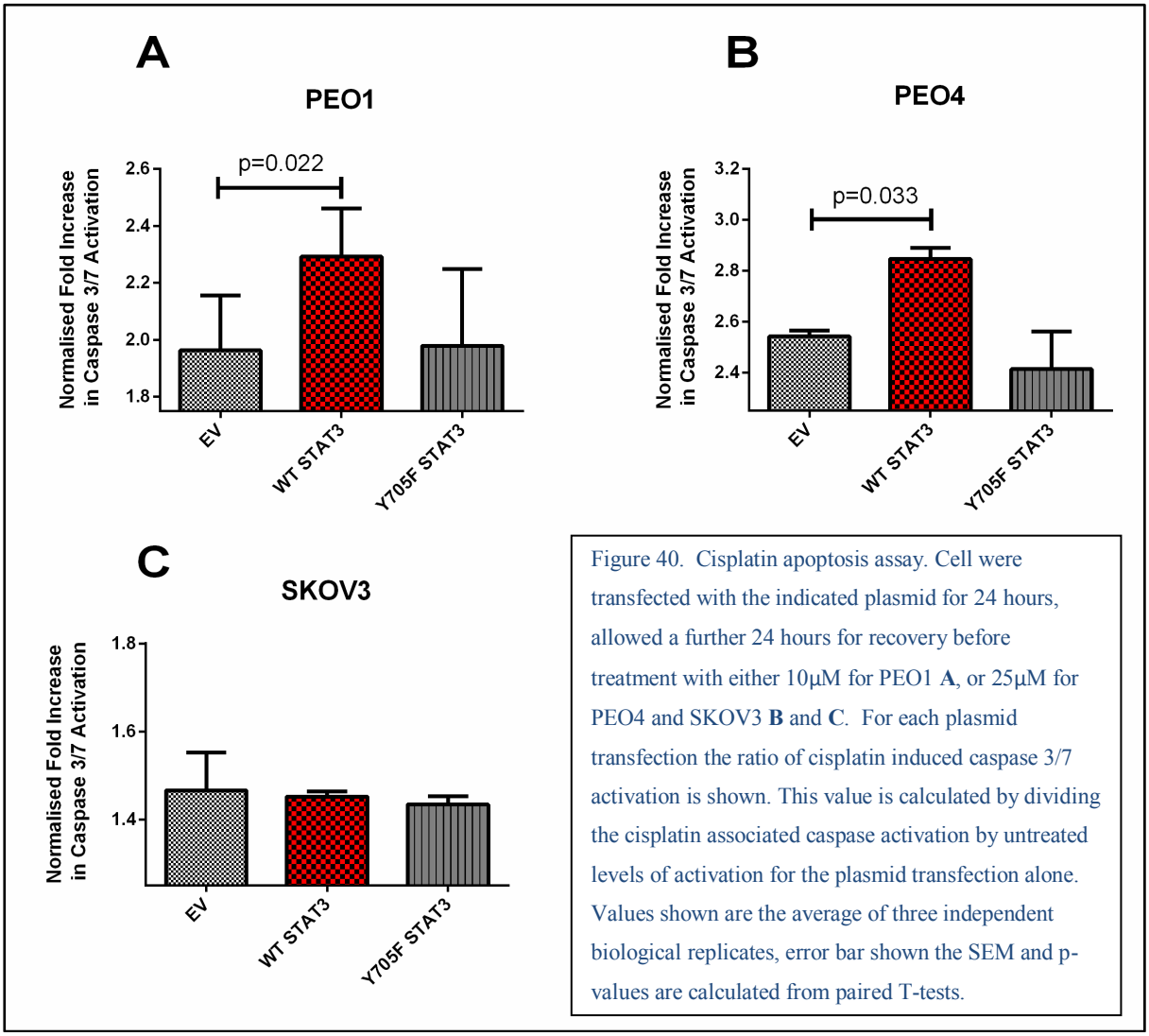

Figure 40. Cisplatin apoptosis assay. Cell were transfected with the indicated plasmid for 24 hours, allowed a further 24 hours for recovery before treatment with either 10µM for PEO1 **A**, or 25µM for PEO4 and SKOV3 **B** and **C**. For each plasmid transfection the ratio of cisplatin induced caspase 3/7 activation is shown. This value is calculated by dividing the cisplatin associated caspase activation by untreated levels of activation for the plasmid transfection alone. Values shown are the average of three independent biological replicates, error bar shown the SEM and p-values are calculated from paired T-tests.

In both PEO1 and PEO4 overexpression of WT STAT3 was associated with a significant increase in cisplatin induced caspase 3/7 levels (p=0.022 and p=0.033 respectively in paired T-tests). In PEO1, WT STAT3 overexpression caused a 21% increase in cisplatin induced apoptosis, this effect was smaller in PEO4 at 11%. Transfection with a phosphorylation refractory form of STAT3 Y705F was not associated with any change in cisplatin induced caspase 3/7 activation. Unlike PEO1 and PEO4 overexpression of STAT3 in SKOV3 (Figure 40C) was not associated with any changes in cisplatin induced apoptosis. The result obtained for PEO1 and PEO4 suggests that the increased cisplatin induced apoptosis is dependent on the phosphorylation of STAT3 and that this effect is mediated by the upregulation of downstream genes.

4.34 *Overexpression of STAT3 Reduces Cisplatin IC_{50} in PEO1 and PEO4 but not SKOV3*

After post-transfection recovery cells were also assayed for cisplatin IC_{50}. Cells were treated with a range of concentrations of cisplatin for 72 hours prior to assessment of cell viability. Each cell line experienced a vector only transfection effect, in which empty vector transfection reduced IC_{50} relative to mock transfected cells. For example, mock transfected PEO4s exhibited an IC_{50} of 10.4µM (data not shown), in line with expectations of this cell line, compared to an IC_{50} of 5.8µM for EV transfected cells. This transfection effect was also experienced by PEO1 but to a lesser extent. Mock transfected PEO1, assayed in parallel, had an IC_{50} of 2.1µM compared to 1.6µM for empty vector transfected cells, a fall of 24%. Because of vector only transfection effects in SKOV3 to facilitate accurate interpolation IC_{75} estimations were used as opposed to IC_{50}, see Figure 41C/D. For ease of comprehension mock transfected data has been omitted from Figure 41.

Transfection with WT STAT3 in PEO1 and PEO4 was associated with marginal decreases in cisplatin IC_{50} relative to empty vector transfection; this decrease was significant in PEO4 but not PEO1. A small and non-significant increase in SKOV3 was also seen. In PEO4 overexpression with WT STAT3 decreased cisplatin IC_{50} by 15% relative to EV transfection, from 5.8µM to 4.9µM (95% CI = 5.5 – 6.1 EV vs <5 – 5.1 WT). This decrease was reversed on overexpression of the phosphorylation refractory STAT3 Y705F variant, whose cisplatin IC_{50} was unchanged relative to EV.

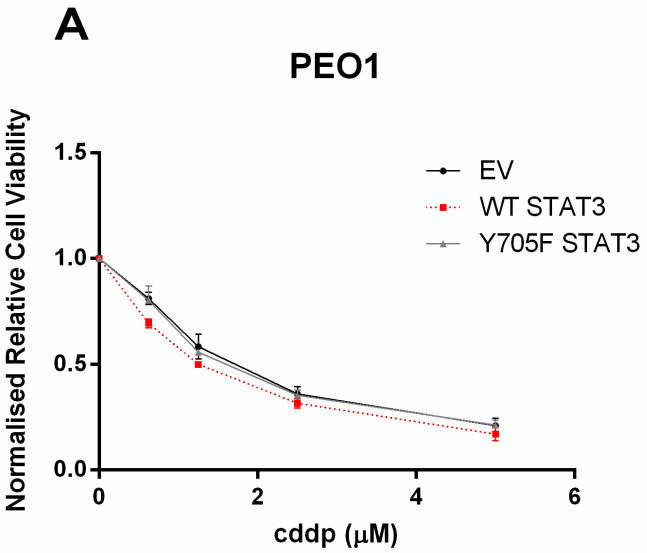

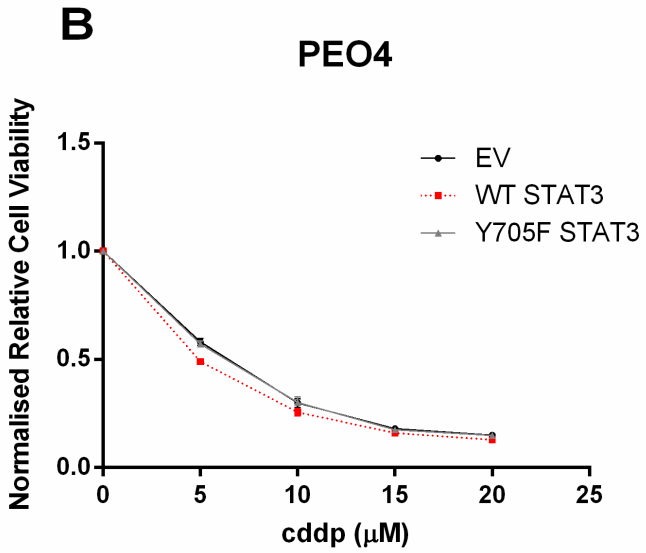

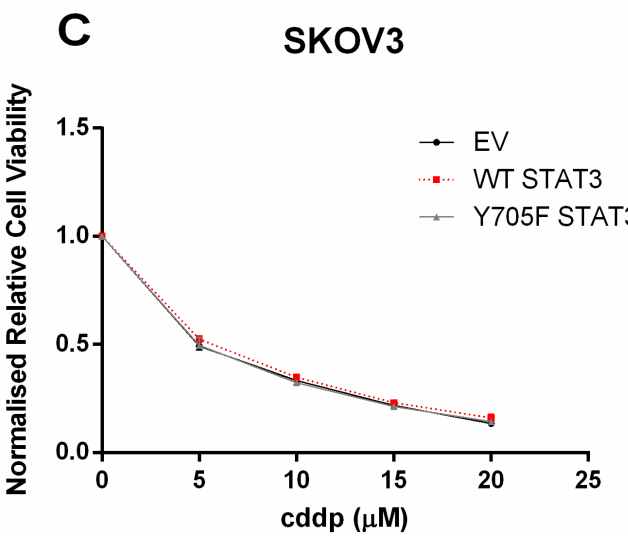

D

IC50 Summary

PEO1

Vector	cddp IC_{50}	95% CI
EV	1.6	1.2 – 2.1
WT	1.2	1.0 – 1.5
Y705F	1.5	1.1 – 1.9

PEO4

Vector	cddp IC_{50}	95% CI
EV	5.8	5.5 – 6.1
WT	4.9 *	<5 – 5.1
Y705F	5.7	5.4 – 6.0

SKOV3

Vector	cddp IC_{75}	95% CI
EV	13.6	12.5 – 15.0
WT	14.0	12.6 – 15.6
Y705F	13.1	11.4 – 15.5

Figure 41. Cisplatin IC_{50} shift assay with STAT3 overexpression. **A-C,** cells were transfected with either empty vector pcDNA 3.1 (EV), wild type (WT) STAT3 pcDNA or Y705F STAT3 pcDNA, for 24 hours. After 24 hours recovery cells were treated with the indicated concentration of cddp for 72 hours prior to assessment of cell viability by MTT assay. Each value is the average of three independent biological replicates , error bar shown the SEM. **D,** shows the IC_{50} values calculated from a least squares regression model in PRISM software with associated 95% confidence intervals.

* = no overlap at p=0.05

The same pattern was observed in PEO1. WT STAT3 overexpression resulted in a 25% reduction in IC_{50}, from 1.6μM to 1.2μM, although this reduction was not significant, as determined by non-overlapping 95% confidence intervals. In contrast to PEO1 and PEO4, SKOV3 did not experience a reduction in cisplatin IC_{75} on WT STAT3 overexpression, instead there was a small but insignificant increase. This increase on was reproducible but insufficient in magnitude to achieve significance.

While the magnitude of IC_{50} shift induced by WT STAT3 over expression was small for both PEO1 and PEO4 the negative result for SKOV3 does suggest that increased cisplatin induced apoptosis, seen for PEO1 and PEO4 but not SKOV3 in Figure 40, is a better predictor of an IC_{50} effect than increased proliferation, which occurred in each of the three lines.

4.35 Overexpression of STAT3 Causes Upregulation of Cyclin D1 and BCL2L1.

In order to confirm STAT3 over expression and examine expression of downstream transcriptional targets western blotting was conducted. Lysates were prepared in parallel to the carrying out of proliferation (Figure 39), caspase (Figure 40) and ic_{50} (Figure 41) shift assays. Cells were transfected for 24 hours with either EV, WT STAT or Y705F STAT3, then allowed 24 hours to recover and express the vector STAT3, after which cells were lysed for analysis.

Transfection with either WT or Y705F STAT3 was associated with an increase in STAT3 protein expression above EV levels. Due to the substitution of tyrosine 705 with phenylalanine in Y705F STAT3 this mutant protein should be resistant to phosphorylation at this residue. Levels of tyrosine 705 phosphorylation were assayed in SKOV3, Figure 42C, which was elevated in WT STAT3 transfected cells but not for Y705F, suggesting the protein transcribed from this template in not phosphorylated and therefore will not be able to form dimers and bind DNA. As such this vector should have no effect on the expression of STAT3 transcriptional targets.

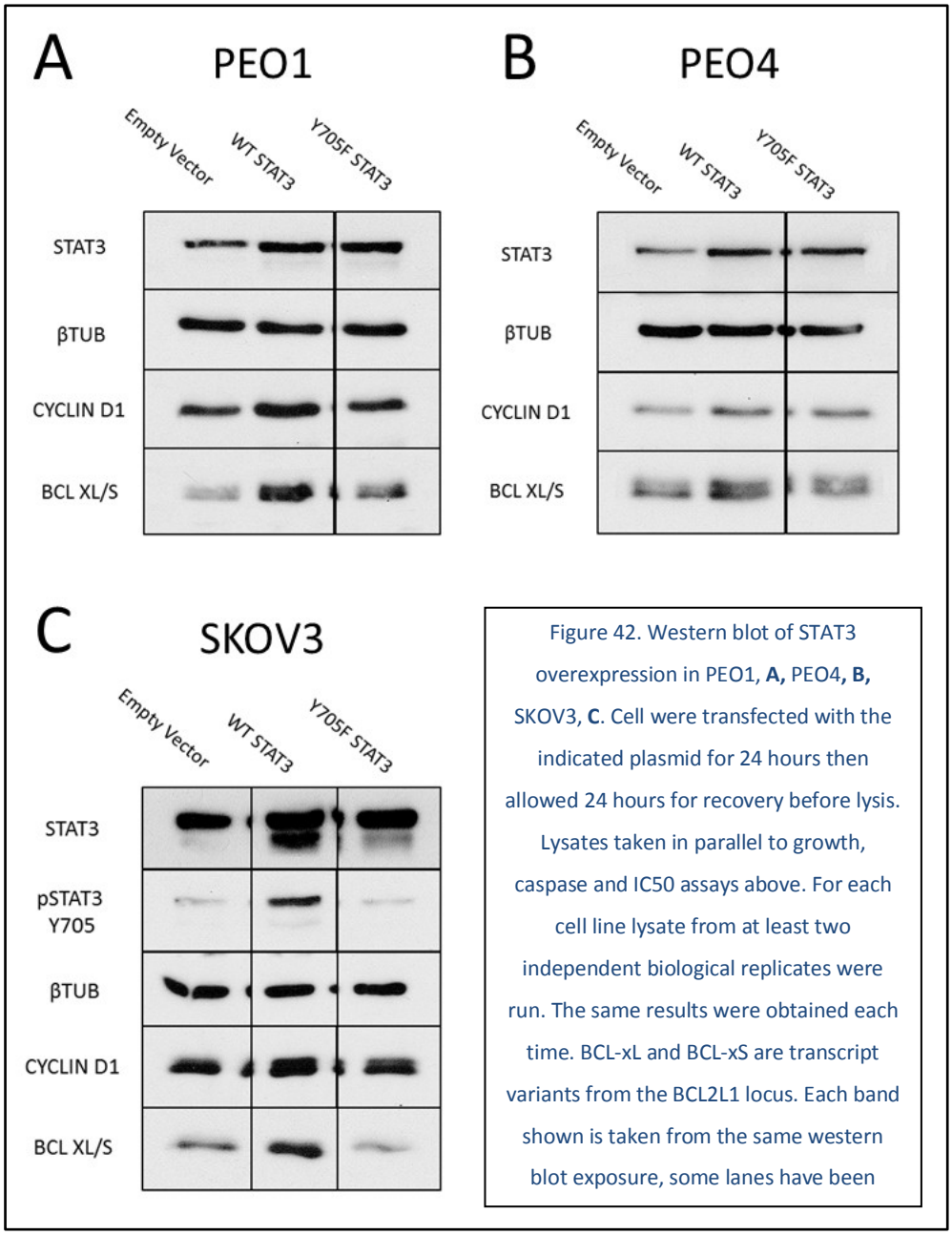

Figure 42. Western blot of STAT3 overexpression in PEO1, **A,** PEO4**, B,** SKOV3, **C**. Cell were transfected with the indicated plasmid for 24 hours then allowed 24 hours for recovery before lysis. Lysates taken in parallel to growth, caspase and IC50 assays above. For each cell line lysate from at least two independent biological replicates were run. The same results were obtained each time. BCL-xL and BCL-xS are transcript variants from the BCL2L1 locus. Each band shown is taken from the same western blot exposure, some lanes have been

Protein levels of STAT3 transcriptional targets were positively regulated by WT STAT3 expression. In PEO1, PEO4 and SKOV3 overexpression of WT STAT3 but not Y705F STAT3 was associated with an increase in both cyclin D1 and BCL2L1 (BCL-xL/S). The magnitude of increase of BCL2L1 was higher than cyclin D1. Interestingly in PEO1 and PEO4 both splice variants of BCL2L1 (BCL-xL and BCL-xS) were detected and upregulated by WT STAT3 transfection. However in SKOV3 only one splice variant was detected in either EV or STAT3 transfected cells. When both splice variants are present identification of each is possible, however when only one is present the resolution of western blotting is

insufficient to accurately quantify the molecular weight of the single band. Therefore without a control in an adjacent lane expressing both splice variants of BCL2L1 it is not possible to discern which variant is expressed and upregulated in SKOV3.

Discussion :-

Results Chapter 4

4.1 An Assessment of the Levels of pSTAT3 Y705 in the Paired Cell Lines PEO1/PEO4 and PEA1/PEA2

The isogenic cell line pair PEA1/PEA2 exhibit differential behaviour in terms of STAT3 activation in response to cisplatin exposure. PEA1 increased levels of pSTAT3 at low concentrations of cisplatin before decreasing them at higher concentrations, whereas PEA2 experienced no increase and reduced STAT3 activation more sensitively than PEA1, see Figure 16. This suggested that maintaining high levels of pSTAT3 in the presence of cisplatin placed PEA1 at a survival disadvantage relative to PEA2. Therefore it might be expected that PEA2 had been selected for reduced basal activation. This was found to be the case; PEA2 expressed significantly less pSTAT3 than PEA1.

The coincidence of decreased pSTAT3 and cisplatin resistance is somewhat at odds with the majority of published data on the role of STAT3 and drug resistance [424–426]. Each of which has suggested that targeting STAT3 is a mean of increasing sensitivity to various chemotherapeutic agents. Very few publications have specifically addressed the role of pSTAT3 in matched cell lines or tumour tissue, and only one examined cisplatin in ovarian tissue. In this study A2780 cells, selected for cisplatin resistance were reported to be hyper-activated for pSTAT3, a claim not overwhelming supported by data presented in this publication [427]. In addition A2780 is most likely not HGS in origin [428] and therefore not a good model especially as it contains very low levels of pSTAT3 relative to other HGS cell lines (data not shown). This study also doesn't show any functional mediation of cisplatin resistance by STAT3 in resistant clones.

Elevated pSTAT3 has also been reported in *in vitro* derived taxol resistant clones of SKOV3 and OVCAR8, which was shown to play a functional role in resistance [299]. The same study also suggests that there is a significant increase in pSTAT3 in relapsed tumour tissue relative to matched primaries, although the magnitude of this increase appears low.

Interestingly glioma cells selected for resistance to temozolomide, an alkylating agents that causes DNA damage in a similar fashion to cisplatin, were report to have reduced levels of pSTAT3 relative to their sensitive clones [429].

We are far from a consensus regarding the role of pSTAT3 in acquired resistance to cisplatin and many studies suggesting a role for STAT3 in drug resistance have used methodology insensitive to detect synergy between STAT3 ablation and chemotherapy. Therefore it would be relevant to examine additional isogenic cell lines to assess whether this reduction is a common feature.

4.2 siRNA Mediated Knockdown of STAT3 Inhibits Cell Growth, Increases Cisplatin IC_{50} and reduces expression of Cyclin D1

4.21 siRNA Mediated Knockdown of STAT3 Inhibits Cell Growth

A growth inhibitory phenotype associated with STAT3 knockdown is not unexpected and has been reported in ovarian and other cancers. The reductions in proliferation achieved with STAT3 abrogation were modest but in line with reports elsewhere showing similar degrees of growth inhibition in OVCAR3, A2870 and SKOV3, *in vitro*, after transfection with either STAT3 shRNA or siRNA respectively [293,304,430]. Interestingly each of these studies found enhanced growth inhibition in tumour xenografts, providing evidence that STAT3 has additional roles promoting tumour growth *in vivo*, that are dispensable in monolayer. Given that STAT3 is important for mediating communication between tumour cells and the micro environment [431] it is tempting to speculate that this might account for the difference. A suggestion supported by work conducted in non-ovarian models showing that STAT3 ablated B16 cells activate mature dendritic cells more efficiently that WT controls. Xenografts of these cells were associated with higher levels of adaptive immune cytokines, such as INF-γ, and tumour infiltrating T-cells [266]. Evidence exists to suggest STAT3 operates in a similar fashion in ovarian cancer, IGROV1 xenografts treated with the IL6 neutralising antibody stituziumab exhibited, in addition to reduced pSTAT3, reduced vascularisation and macrophage infiltration [289]. A similar reduction in vascularisation was observed in response to knockdown of STAT3 in ovarian xenografts quantified by a reduced detection of the vascular endothelial marker CD31, within tumour sections [304].

These studies suggest that tumour growth *in vivo* is more dependent on STAT3 than growth *in vitro* and this is dependent on STAT3 mediating communication between the tumour and the microenviroment to promote vascularisation and immune evasion. It will be interesting to tease apart the different functional downstream effects of STAT3 activation unique to the *in vivo* environment specifically to address the importance of immune evasion for tumour growth in ovarian models.

4.22 – 4.23 siRNA Mediated Knockdown of STAT3 Induces Apoptosis But Does Not Sensitise To Cisplatin. siRNA Mediated Knockdown of STAT3 Increases Cisplatin IC_{50}

Numerous studies have suggested that STAT3 contributes to resistance to a variety of cytotoxic compounds, in various cancer systems, including to paclitaxel [295,299], cisplatin [296,424–426] and doxorubicin [425], in ovarian [295,296,299], breast [432], colon [426] and nasopharyngeal carcinoma [424] as well as the leukemic cancers non-Hodgkin's lymphoma and multiple myeloma [425]. Each of these studies suggested that inhibition of STAT3 signalling combines favourably with chemotherapeutic intervention. The majority of these studies suffer from fundamental limitations in the methodology used to suggest or tacitly imply synergy between STAT3 ablation and a particular cytotoxic and few conduct a formal assessment. Some use non-specific inhibitors, such as AG490 at excessive concentrations, those using siRNA usually only one species and make no effort to assess whether the effects they observe are on-target. Often poor choices of cell line model are used including for example the use of A2780, which aside from being a poor model for HGS ovarian cancer [428] doesn't contain readily detectable levels of pSTAT3 Y705. However the predominant problem is probably the lack of a formal means of assessing the nature of interaction between STAT3 inhibition and a cytotoxic agent, using preferably an isobologram or at least an IC_{50} shift assay, which can allow an indication of synergy or antagonism. Of those papers listed above only two make a formal assessment of synergy or otherwise between STAT3 ablation and cytotoxic. One in non-Hodgkin's lymphoma and multiple myeloma demonstrating synergy between AG490 and cisplatin/doxorubicin [425].

The cisplatin induced levels of activated caspase 3/7 were no higher in a STAT3 depleted background than would be expected, based the activity of 3 different siRNAs as single agents. In fact data suggested a small, non-significant, protective effect associated with

knockdown. This would have been predicted on the basis of evidence presented in this thesis, primarily relating to the effects of JAK2 siRNA and IL6 treatment. IC_{50} shift experiments were carried out in PEA1, PEA2 and SKOV3 which allowed a more formal assessment of the interaction between STAT3 knockdown and cisplatin. Consistent with results presented elsewhere in this thesis STAT3 knockdown was associated with a significant increase in cisplatin IC_{50} for each siRNA in PEA1 and 2/3 for PEA2 and SKOV3. These results provide strong evidence of antagonism between cisplatin and STAT3 knockdown. Of most concern in PEA1 each siRNA was associated with a near doubling to cisplatin IC_{50} suggesting the combination of an anti-STAT3 therapy and cisplatin would not produce desirable clinical results. And this theme appears to apply to cell lines regardless of their inherent cisplatin resistance. This assertion is somewhat limited by the *in vitro* nature of the model used here as it cannot account for the possibility of synergistic interactions between STAT3 abrogation and cisplatin that may only exist *in vivo*.

4.24 siRNA Mediated Knockdown of STAT3 Reduces Expression of Cyclin D1

Although siSTAT3 1 was only shown in Figure 37 a total of four STAT3 siRNAs were used for each experiment in this chapter. The results for siSTAT3 1 had previously been excluded due to the presence of what was assumed to be off target toxicity which probably contributed to variable results in some experiments. siSTAT3 1 was included in Figure 37 partly as any off target effects were not apparent in this assay but also because it inclusion helped to address the problem that the siRNA with the greatest efficiency of STAT3 knockdown, no 3, did not affect the expression cyclin D1 as predicted. Cyclin D1 is widely used as a read out of the transcriptional activity of STAT3 [424,426] although interestingly recent high throughput analysis categorising the direct transcriptional targets of STAT3, using CHIP-chip and CHIP-seq, have apparently failed to identify direct binding to the cyclin D1 promoter [419,433], suggesting STAT3 regulates cyclin D1 via an intermediary. This idiosyncrasy of siSTAT3 3 does perhaps suggest that the growth inhibitory effects of STAT3 depletion are not governed by cyclin D1, as siSTAT3 3 which had a similar magnitude of effect in terms of growth inhibition had no effect of cyclin D1 expression. This data is somewhat co-incidental and would require, for example a recovery experiment to confirm. For example if cyclin D1 overexpression could rescue STAT3 knockdown associated growth inhibition, this would suggest cyclin D1 is responsible for mediated these effects.

4.3 Overexpression of STAT3 Increases, Cell Proliferation. In PEO1 and PEO4 but not SKOV3 STAT3 Overexpression, Increases Cisplatin Induced Apoptosis and Decreases IC_{50}.

4.31 Overexpression of STAT3 Was Not Possible in PEA1 or PEA2 but Was Possible in SKOV3

It is unclear why it was not possible to overexpress STAT3 in PEA1 or PEA2 despite the parallel transfection with GFP and clear demonstration of the functionality of the STAT3 vectors in other cell lines. However when viewed in light of an additional results it might suggest the existence of cellular mechanisms to prevent the perturbation of STAT3 signalling. Knockdowns of STAT3 were carried in PEO1 and PEO4, with little phenotypic effect despite efficient knock down of STAT3 protein. It wasn't until pSTAT3 and pJAK2 levels were examined in response to knockdown did a potential explanation become apparent. Despite significant reductions in total STAT3 after siRNA transfection levels of STAT3 phosphorylation were unchanged and this was associated with increases in pJAK2 and total JAK2 protein levels, shown in supplementary figure S7. While inherently interesting these possible feedback mechanisms fell outside of the main sphere of investigation and were not followed up.

4.32 – 4.34 Overexpression of STAT3 in PEO1, PEO4 and SKOV3

Results of STAT3 overexpression were highly consistent with data from both IL6 treatments, shown in chapter 2, and STAT3 knockdowns in this chapter. Comparing over expression of WT and Y705F STAT3 constructs supports a conventional view of STAT3 functioning here as a transcription factor. A reversal of the proliferative effects of transfection by mutation of the tyrosine residue targeted by JAKs, and required for DNA binding, suggest STAT3 dependent differential gene expression is crucial in eliciting the effects seen here.

Implying that sensitising effects of IL6 treatment in chapter 2 are mediated, at least in part by STAT3, overexpression was also able to increase apoptotic induction in response to cisplatin, in PEO1 and PEO4. While the magnitude of this effect was lower than in response to rIL6(RA), this could be explained by increased STAT3 activation associated with it. Again the effects of STAT3 overexpression on cisplatin induced apoptosis were reversed in the

Y705F mutant suggesting this phenotype is also a consequence of canonical STAT3 function. It is unclear why SKOV3 would experience the proliferative effects of STAT3 overexpression but not the cisplatin sensitisation effects. Although it might suggest that sensitisation is not simply a factor of increased proliferation and perhaps those genes upregulated by STAT3 overexpression and responsible for cisplatin sensitisation in PEO1 and PEO4 are not upregulated in SKOV3.

Changes in cisplatin IC_{50} mirrored apoptosis data, PEO1 and PEO4 experienced a reduction, whereas SKOV3 did not. Again these results are in line with expectations, based on results presented here, and provide support of the developing picture of reductions in STAT3 signalling in protecting the cell from cisplatin cytotoxicity.

Results of western blotting after STAT3 overexpression support findings in Figure 37 showing reductions in cyclin D1 expression. Expression of BCL2L1 was also assessed which altered in magnitude to a greater degree than cyclin D1. Interestingly overexpression of STAT3 in PEO1 and PEO4 resulted in upregulation of both variants transcribed from the BCL2L1 locus, both the pro-apoptotic BCLxS and the anti-apoptotic BCLxL. Whereas in SKOV3 upregulation of only one variant was apparent, unfortunately due to the similarity of their size and the resolution of western blotting it is not possible to discern which. QRT-PCR with transcript variant specific primers would be required to discriminate which was upregulated. However this discrepancy in BCL2L1 transcript variant expression might account for the difference in behaviour of PEO1/PEO4 and SKOV3 in response to STAT3 overexpression and cisplatin treatment.

Results Chapter 5:-
ERBB2 is Phosphorylated in a Range of Ovarian Cell Lines, where it Promotes Growth, Contributes to Cisplatin Resistance and Activation of JAK2 and STAT3

5. ERBB2 is Phosphorylated in a Range of Ovarian Cell Lines, where it Promotes Growth, Contributes to Cisplatin Resistance and Activation of JAK2 and STAT3

Results shown in Figure 17 demonstrate the presence of readily detectable levels of tyrosine 1248 phosphorylated ERBB2 in both of the isogenic pairs PEO1/PEO4 and PEA1/PEA2. As previously described ERBB2 genomic amplification is an important driver of growth and correlates with poor survival in breast cancer. While the incidence of ERBB2 over expression is lower in ovarian cancer the presence of ERBB2 protein overexpression is consistently reported to be higher than the incidence of gene amplification. Suggesting that ERBB2 hyperactivity can be selected for at different levels, not isolated to copy number. To investigate the functional consequences of detected levels of ERBB2 activation, the ERBB2 inhibitor CP-724714 was used. CP-724714 is a potent and selective ERBB2 ATP competitive kinase inhibitor, with an *in vitro* IC_{50} of 10nM and a 640 fold selectivity relative to EGFR [434].

5.1 ERBB2 is Phosphorylated in a Range of Ovarian Cell Lines Without Being Overexpressed.

To investigate whether ovarian cell lines, without a genomic amplification, might have elevated pERBB2 relative to non-cancerous controls and how this compared to a known ERBB2 amplified cell line western blotting was conducted, in conjunction with QRT-PCR, on a panel of ovarian cell lines. SKOV3 was used as a control for a known ERBB2 amplified line [435]. Other cell lines used, with the exception of OSE-C2, have been shown to not be amplified for ERBB2 [416,436].

ERBB2 phosphorylation is elevated in a range of HGS ovarian lines relative to the normal ovarian surface epithelial cell line OSE-C2, Figure 43A. Cell lines could be broadly divided into three groups; those with low levels of activation, including OSE-C2 and A2780, highly activated lines, including SKOV3, and moderately activated lines, including the remainder. Taking the moderate expressers as a group, on average they possessed 24 fold the normalised quantity of activated ERBB2 relative to OSE-C2. The difference between the moderately activated group and ERBB2 amplified SKOV3 was smaller, at only 3.4 fold less. The only cancerous cell line screened that contained a similar level of activated ERBB2 to OSE-C2 was A2780. The legitimacy of A2780 as a model for HGS ovarian cancer is

questioned by the observation that it is TP53 wild type, an event this is extremely rare in HGS tumours. As such the presence of elevated ERBB2 phosphorylation, was present in every model of HGS ovarian cancer examined here (7 of 7), suggesting it is a common event in carcinogenesis of this histotype. The authenticity of SKOV3 as a supposed HGS lines has also recently been challenged, these issues a discussed in more detail in the corresponding discussion section.

It was not possible to reliably detect absolute levels of ERBB2 protein in the majority of these cell lines, SKOV3 being a notable exception, suggesting that increased phosphorylation was not a result of increased protein expression, for the majority. To examine to what extent ERBB2 overexpression might be driving increased activation, QRT-PCR was carried out on the same panel of cell lines. The majority of lines expressed highly similar levels of *ERBB2* mRNA, see Figure 43B. Levels did not differ substantially between those cell lines with low or moderate ERBB2 activation. With the exception of PEA2 and SKOV3 all lines expressed *ERBB2* mRNA within 25% of OSE-C2. As expected SKOV3 expressed significantly more *ERBB2* than any other, approximately 45 fold the average of the non-amplified lines included in Figure 43B.

This data demonstrates that despite not containing elevated ERBB2 expression HGS cell lines possess elevated ERBB2 activation which is closer in magnitude to the ERBB2 amplified cell line SKOV3 than normal controls. Taken together it suggests that activation of ERBB2 is selected for in a range of ovarian cell lines and increased activation is not dependant on either genomic amplification or increased mRNA expression.

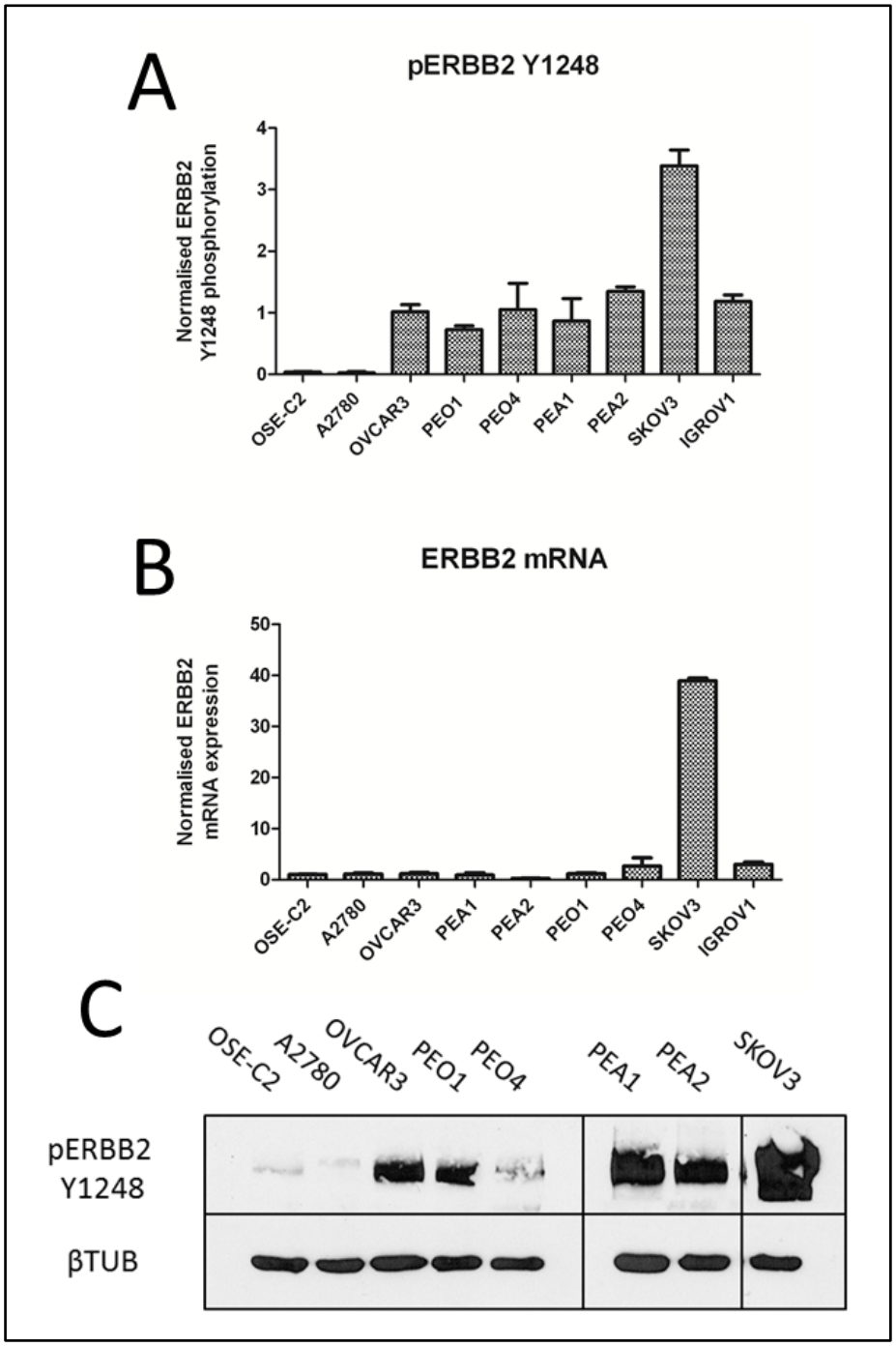

Figure 43**. A -** Western blot Y1248 phosphorylated ERBB2 in a panel of ovarian cell lines. Levels of pERBB2 were quantified and normalised to βtub. Results are averaged over 3 or 4 independent biological replicates. Error bars show the SEM of this average. **B –** QRT-PCR of ERBB2 mRNA levels in the same panel of ovarian cell lines. ERBB2 mRNA expression was normalised to PPIA. Results were average between 4 biological replicates and error bars show the SEM of this average. Results are shown relative to OSEC-2. **C –** Representative western blot used to calculate the values shown in **A**.

5.2 Sensitivity to the ERBB2 Inhibitor CP-724714 Correlates with Levels of Protein Activation

While elevated activation of ERBB2 was detected in a range of ovarian cell lines this was lower than that of ERBB2 amplified SKOV3 and any potential functional role of this activation was unknown. The potent and selective ERBB2 inhibitor, CP-724714 was used to assess the functionality of elevated pERBB2 in the cell line panel in Figure 43.

In order to access the sensitivity of the ovarian cell line panel used above to ERBB2 inhibition, $IC_{50/25}$ estimations were calculated by exposing cells to a range of concentration of drug over 72 hours, before assessing cell viability, the results are shown in Figure 44.

Based on sensitivity to CP-714714, with the exception of SKOV3, cells fell into groups, broadly corresponding to their level of ERBB2 activation. OSE-C2 and A2780 were the most resistant to ERBB2 inhibition, in both cells IC_{25} concentrations were in excess of 10μM. OSE-C2 and A2780 also had the lowest levels of pERBB2, see Figure 43A. Of the group of cells classified as moderately ERBB2 activated IC_{25} values differed by relatively small amount, from the lowest in PEA1 of 1μM to 2.1μM in PEO1. Surprisingly SKOV3 was not more sensitive to ERBB2 inhibition than the other non-amplified HGS lines, being only slightly more sensitive than PEO1, with an IC_{25} of 1.8μM. At the highest concentration of inhibitor used, 10μM, only two cell lines, PEA1 and OVCAR3 experienced a reduction in cell viability beyond 50%.

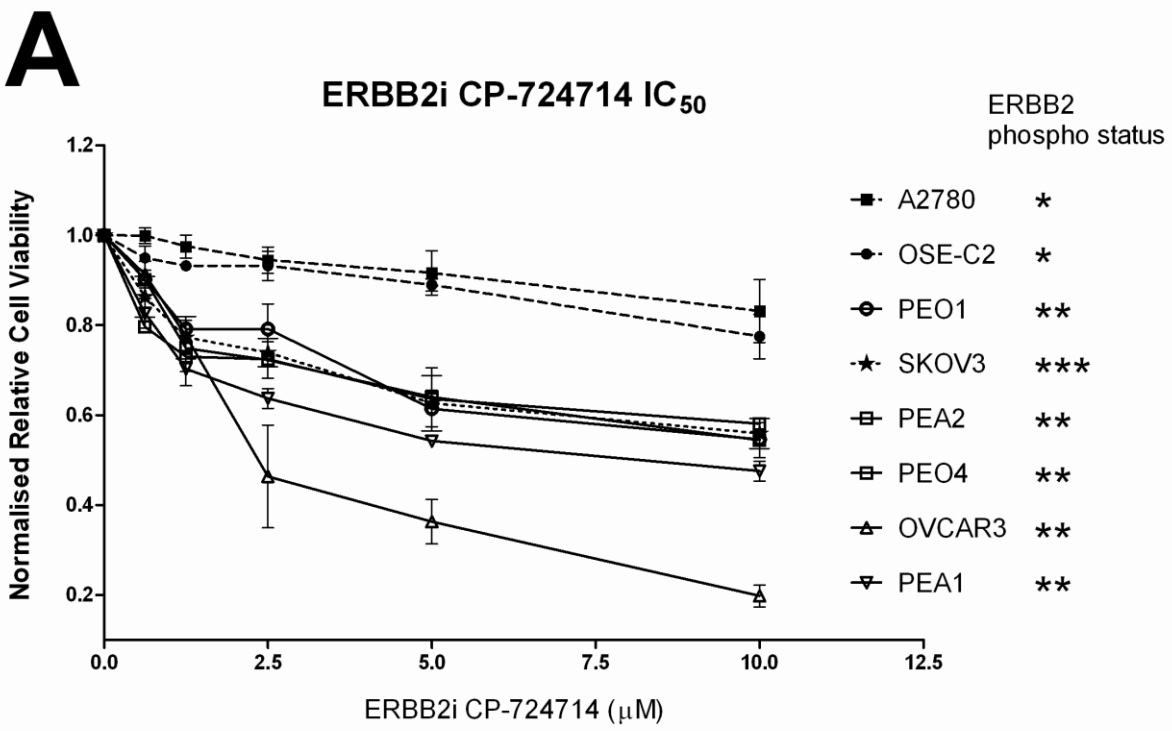

B

Cell Line	IC_{50} (μM)	IC_{25} (μM)
A2780	>10	>10
OSE-C2	>10	>10
PEO1	>10	2.1
SKOV3	>10	1.8
PEA2	>10	1.7
PEO4	>10	1.5
OVCAR3	2.9	1.2
PEA1	7.7	1.0

Figure 44. **A**. Cell viability associated with ERBB2 inhibition using CP-724714. Cells were treated with the indicated concentration of inhibitor or vehicle control for 72 hours prior to assessment of cell viability using the MTT assay. Each point is the average of 3 separate biological replicates (except PEO1 n=2). The error bars show the SEM of these replicates. Cells are assigned an ERBB2 phospho status based on Figure 43. * = low, ** = moderate, *** = high. **B**. Summary of IC_{50} and IC_{25} values for CP-724714. Cell lines are shown in descending IC_{25} order. Estimations were made using a least squares regression model.

5.3 ERBB2 Inhibition Sensitises Cells to Cisplatin

A number of previous studies have suggested that ERBB2 overexpression, *in vivo*, is associated with a poor response to platinum based chemotherapy [338,347] and overall poor prognosis [340–342]. *In vitro* data from ERBB2 overexpressing breast cancer cells has also suggested that ERBB2 inhibition can combine synergistically with both cisplatin and other

DNA damaging agents [346]. Considered alongside data presented here showing both elevated levels of activated ERBB2 in a range of ovarian cell lines and cisplatin dependant changes in the activation of ERBB2 creates the rational examining the ability of ERBB2 inhibition to sensitise ovarian cells to cisplatin. A number of cell line models were investigated including, OVCAR3, the isogenic pair PEA1/PEA2, which exhibit moderate ERBB2 activation, as well as ERBB2 amplified SKOV3, with high activation, and the normal OSE-C2, with low levels of activation.

Cells were treated with a range of doses of ERBB2 inhibitor, from 10μM to 0.156μM, for 16 – 18 hours before retreatment with the same concentration of inhibitor, either alone or in combination with cisplatin. After 24 hours of incubation with cisplatin measurements of cell viability and caspase 3 and 7 activation were made, the results are shown in Figure 45A and B.

ERBB2 inhibition caused a potentiation of cisplatin induced apoptosis in each cell line except for OSE-C2. This potentiation occurred in a dose dependant fashion, the greatest degree of sensitisation associated with the highest concentration of inhibitor used (10μM).

In PEA1 cells 10μM single agent cisplatin was associated with a 1.27 fold increase in activated caspase 3/7 this increased to 2 fold combination with 10μM ERBB2 inhibitor representing a 57% rise ($p=0.005$ paired T-test). A small but statistically insignificant increase in single agent inhibitor toxicity was observed at 10μM. Results were very similar for PEA2, 25μM cisplatin resulted in a fold activated caspase induction of 1.3 which increased to 2 fold in combination with 10μM of inhibitor representing a 54% rise ($p=0.055$ paired T-test). A small but statistically insignificant decrease in apoptosis was associated with single agent inhibitor at this concentration, in contrast to PEA1. OVCAR3's response was higher in magnitude, 25μM cisplatin alone caused a 3.6 fold increase in apoptosis which rose to 6.2 fold in combination with 10μM inhibitor an increase of 72% ($p< 0.001$ paired T-test). The largest effect was observed in SKOV3s, combination cisplatin (25μM) plus inhibitor (10μM) resulted in a 420% increase in apoptosis from 1.3 to 5.7 fold untreated levels ($p=0.11$ paired T-test). A failure to achieve significance at the 0.05 threshold due to variation in the magnitude of effect between replicates, despite an effect occurring in each. There was no effect on apoptosis levels for the inhibitor alone at this concentration. There was no effect on cisplatin induced apoptosis in OSE-C2 which do not contain elevated levels of ERBB2 phosphorylation (see Figure 46).

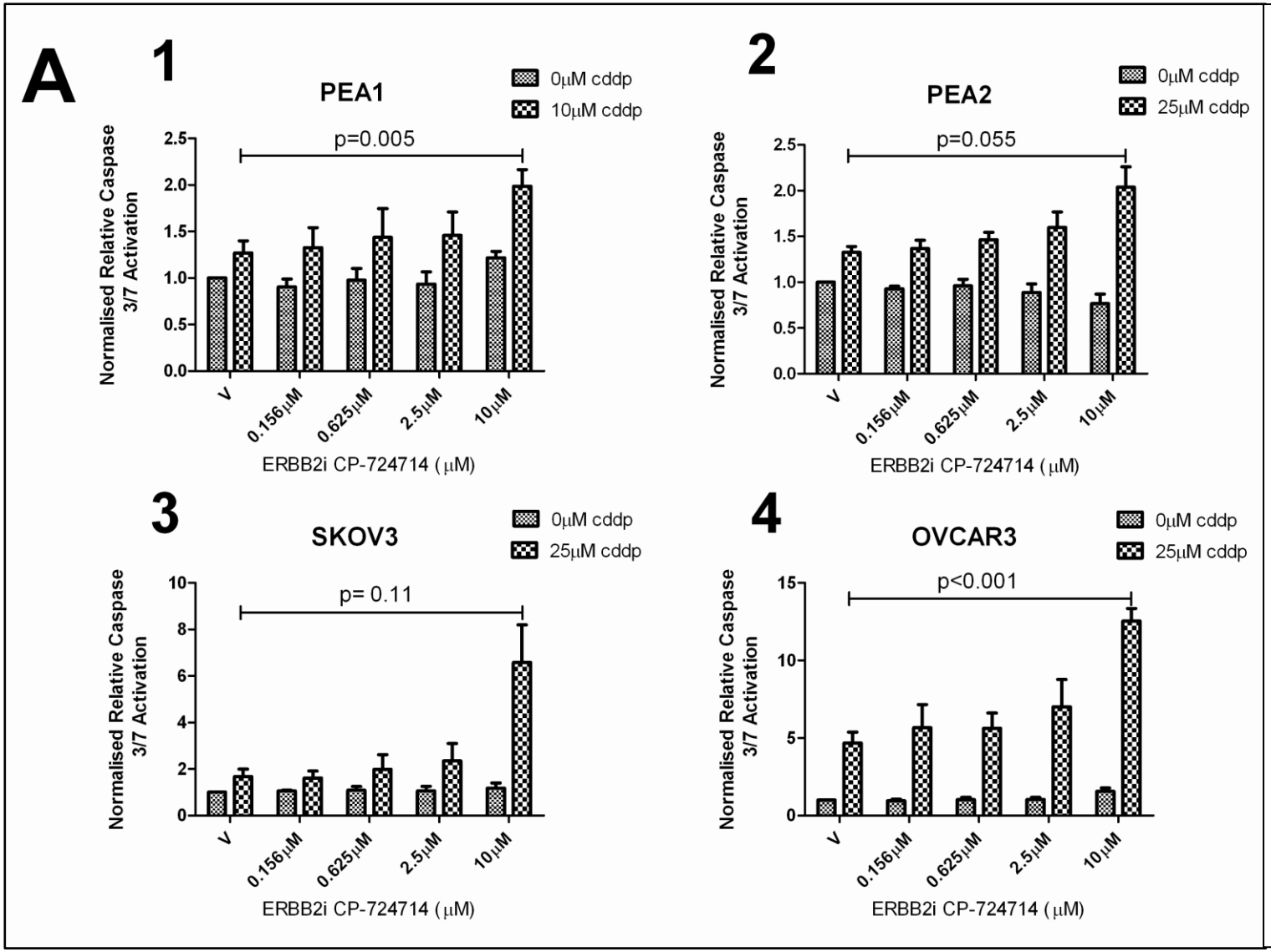

Figure 45A. Caspase 3/7 apoptosis assay of cisplatin in combination with ERBB2 inhibitor CP-724714. Cell were treated with the indicated concentration of ERBB2i O/N before being either retreated with the same concentration either alone or in combination with cddp at the indicated concentration. After 24 hours of incubation cell viability and apoptosis were estimated using the MTT and caspase glo (Promega) assays respectively. All values are normalised to untreated controls. Each point is the average of three separate biological replicates. Error bar represent the SEM between these error bars. P values are based on the paired T-test between cddp treated alone or in combination with 10μM inhibitor.

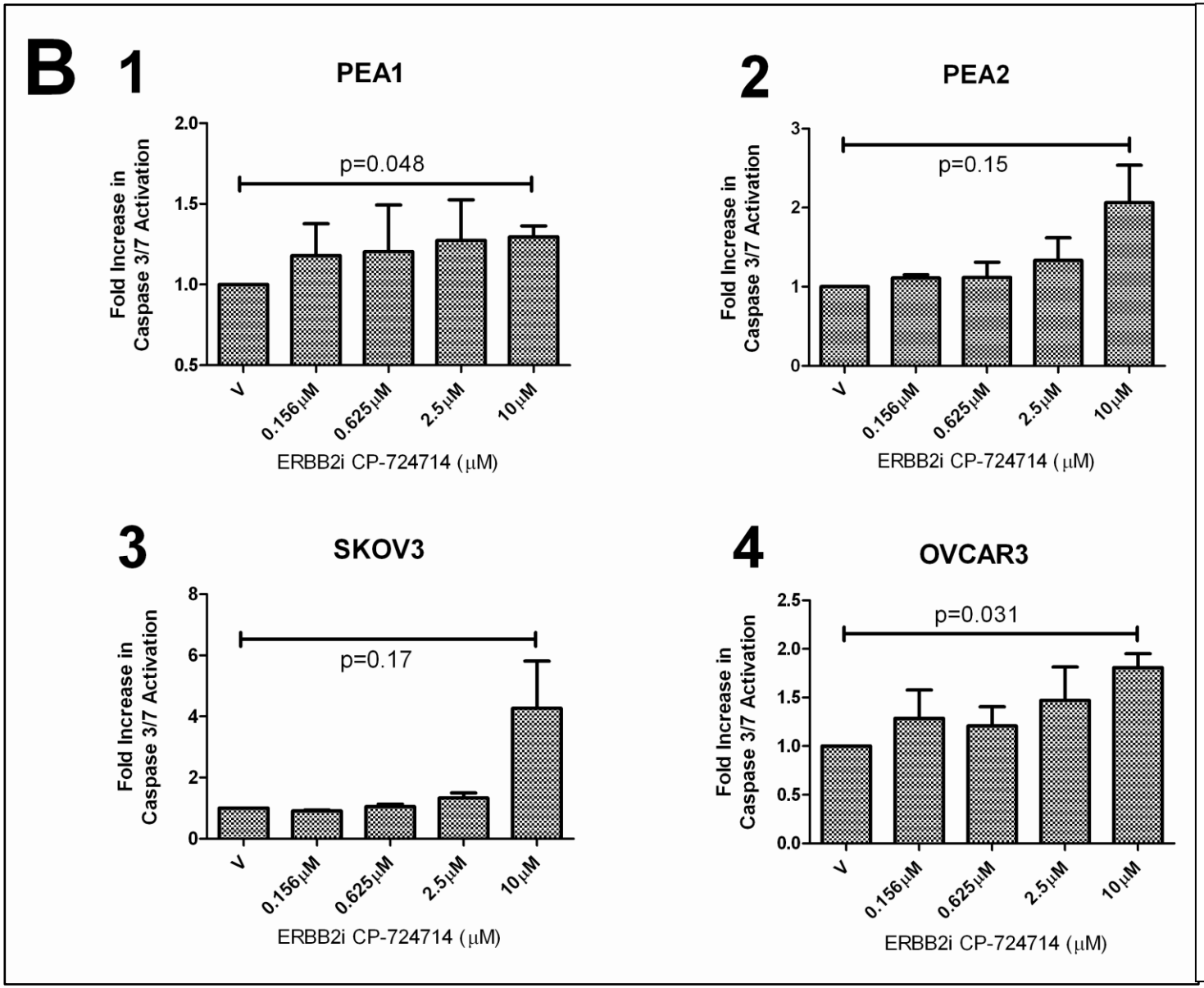

Figure 46B. Caspase 3/7 apoptosis assay of cisplatin in combination with ERBB2 inhibitor CP-724714. Graphs generated from plots in Figure 45A. Each value shows the ratio of activated caspase induced by cddp for each concentration of inhibitor used. This ratio is then normalised to the vehicle control cddp dependant apoptosis ratio. As such each values shows the fold increase in cddp induced caspase activation caused by each concentration of ERBB2i. The higher the fold increase in induced caspase activation the greater the sensitisation caused by exposure to the inhibitor.

P values are one samples T—tests.

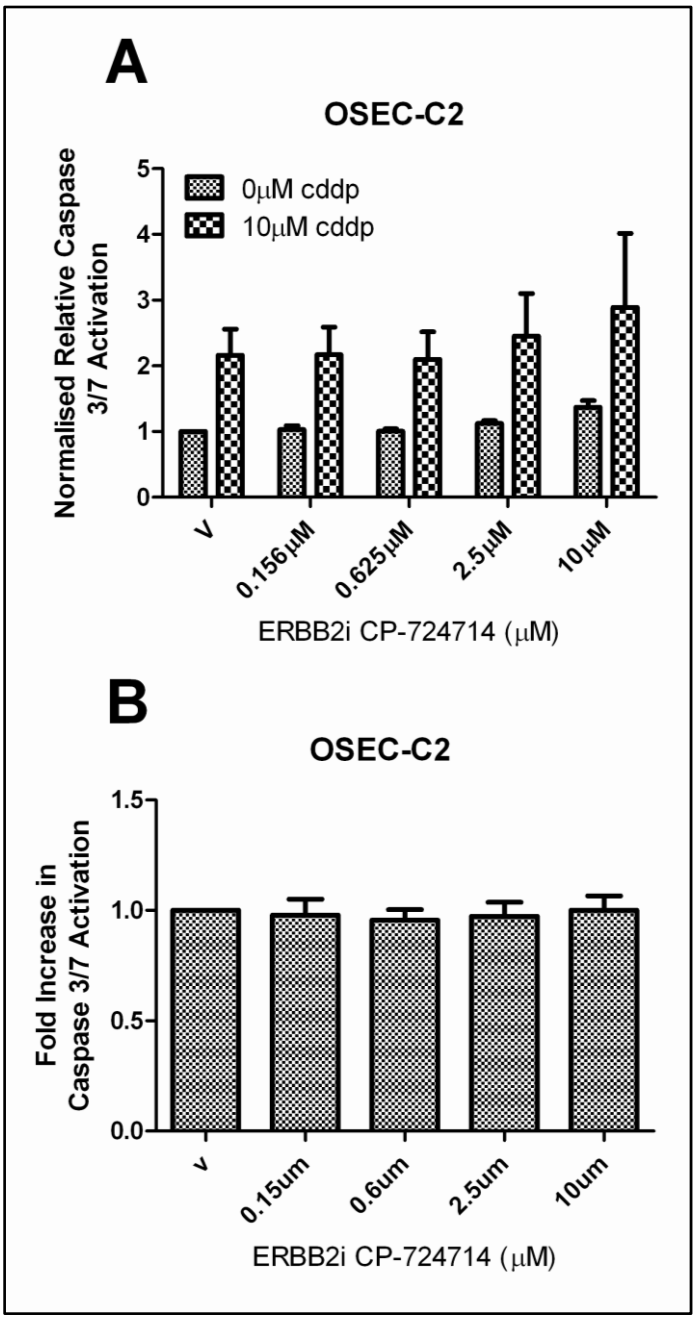

Figure 46. **A/B.** See legend for Figure 45A/B

In order to better quantify the magnitude of sensitisation to cisplatin caused by ERBB2 inhibition and represent any dose dependent effects figure 47B was compiled. It shows the fold increase in cisplatin induced apoptosis associated with each concentration of inhibitor, referred to as the sensitisation ratio. In each cell line there is correlation with dose and sensitisation, the highest degree of sensitisation achieved with the highest concentration of inhibitor used of 10μM.

The lowest degree of sensitisation achieved was for PEA1 where inhibitor treatment was associated with a sensitisation ratio of 1.3. That is the addition of inhibitor caused a 30% increase in the ratio of cisplatin induced apoptosis (p=0.048 one sample T-test). OVCAR3 and PEA2 experienced a similar degree of sensitisation with ratios of 1.8 and 2.1 respectively (p=0.031 and p=0.15 one sample T-test). The highest magnitude of sensitisation occurred in SKOV3s where the addition of ERBB2 inhibition resulted in a 4.3 fold increase the levels of apoptosis induced by cisplatin (p=0.17).

5.4 ERBB2 Inhibition Reduces Activation of ERBB1, AKT and ERK1/2 in Cells Lines Possessing Phosphorylated ERBB2 but Not in Those Without

Simultaneous to ERBB2 inhibitor treatments used to produce Figure 45, protein lysates were prepared to access the specificity, efficacy and the dependence on activated ERBB2, of ERBB2 inhibition by CP-724714. Cells were treated with the same range of concentrations of inhibitor for between 16 and 18 hours prior to lysis. The levels of activated phosphorylated AKT, ERK1/2 were examined as these are important downstream mediators of ERBB2 activation. EGFR phosphorylation at residue Y1068 was assayed to assess the importance of ERBB2 in activating other ERBB members. Although it seems unclear whether ERBB2 can directly phosphorylate this residue, it is known to be the docking site for GRB2 linking EGFR and the RAS/MEK/ERK pathway [437]. ERBB2 phosphorylation was also assessed to address the importance of mutualistic ERBB activation at this residue and therefore the extent to which ERBB2 activation is dependent on other ERBB proteins.

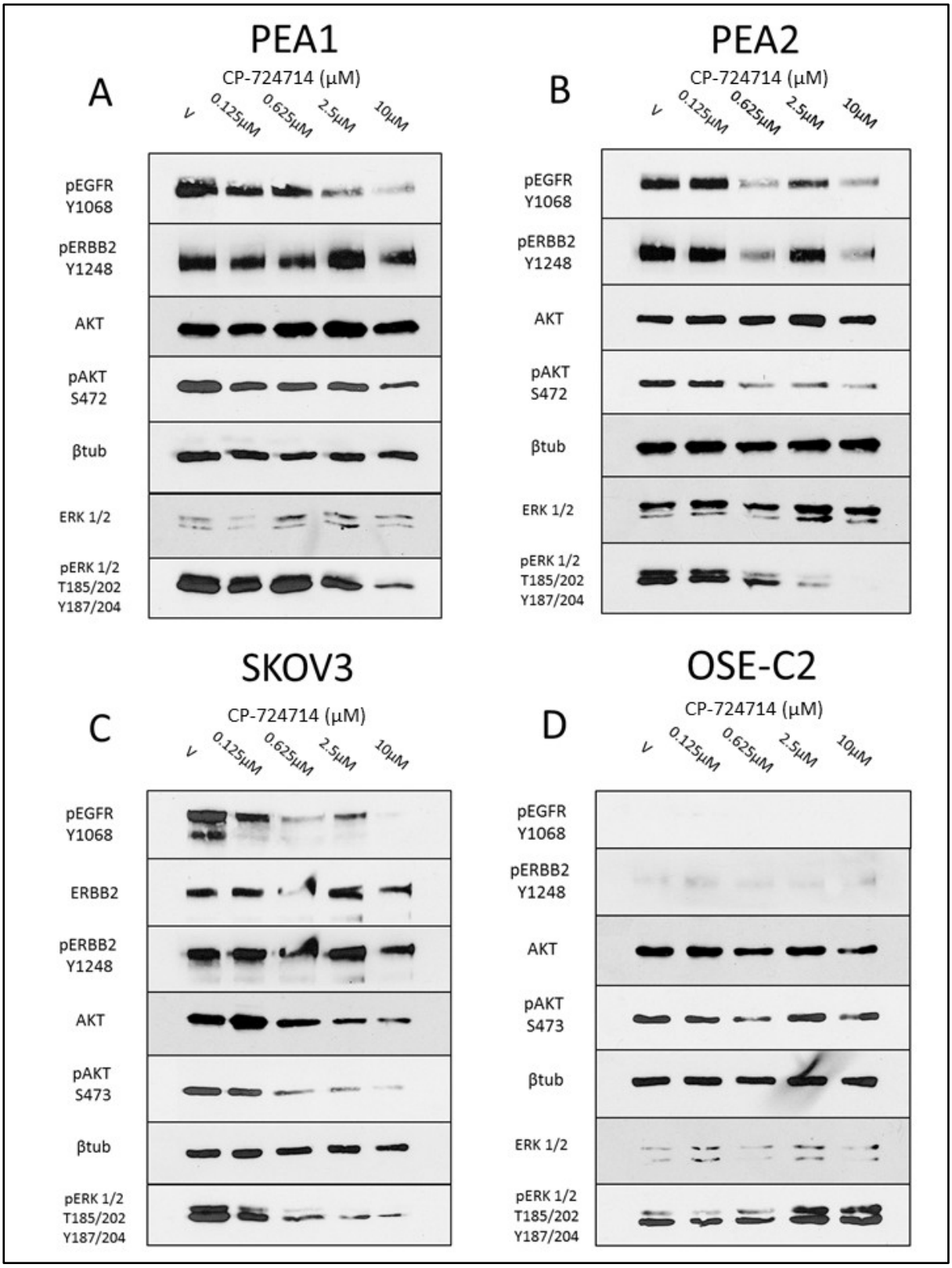

Figure 47. Western blot of ERBB2 inhibitor (CP-724714) treatment. Cells treated with either the indicated concentration of CP-724714, dissolved in DMSO, or DMSO only (V) for between 16-18 hours before lysis. Lysates from two separate biological replicates were run, the results shown here are representative. βTUB is included as a loading control. Membranes were first probed with phospho protein specific antibodies prior to stripping and reprobing with total antibodies.

Each cell line tested possessed readily detectable levels of S743 phosphorylated AKT (pAKT) and T185/202,Y187/204 dual phosphorylated ERK1/2 (pERK1/2) regardless of levels of ERBB2 phosphorylation. In contrast levels of Y1068 phosphorylated EGFR were only observed in cell lines with either moderate ERBB2 activation (PEA1 and PEA2) or ERBB2 amplification (SKOV3). In cells with activated ERBB2 (PEA1 PEA2 and SKOV3) treatment with the ERBB2 inhibitor resulted in a dose dependant decrease in the activation of both AKT and ERK1/2. Changes in levels of phosphorylation were not mirrored by changes in absolute levels of protein suggesting changes are genuine signalling modulations, as opposed to non-specific protein degradation. At the highest concentration of ERBB2 inhibitor used, 10μM, substantial decreases in the activation of these proteins suggest that ERBB2, potentially via other ERBB proteins, is the key driver for their activation. OSE-C2 cells with low levels of ERBB2 activation did not experience any change in the levels of pAKT whereas levels of pERK1/2 were increased at inhibitor concentrations of 2.5μM and above, Figure 47D. Suggesting that decreases in the activation of these proteins in PEA1 PEA2 and SKOV3 are specific on target effects of ERBB2 inhibition.

In PEA1, PEA2 and SKOV3, ERBB2 inhibition resulted in a dose dependant decrease in phosphorylation of Y1068 EGFR. As ERBB2 is unable to homodimerise, it instead heterodimerises and phosphorylates other ERBB family members, reduced EGFR activation implicates ERBB2 the maintenance of this activation. Like observed reductions in pAKT and pEGFR, pERK1/2 dropped by a large degree in all ERBB2 activated cells lines again suggesting ERBB2 is the key driver of phosphorylation at this residue.

Changes in phosphorylation of ERBB2 itself were generally smaller in magnitude that those seen of either AKT ERK1/2 or EGFR. Phosphorylation of Y1248 did not alter substantially in either PEA1 or SKOV3 at any concentration of inhibitor. Suggesting, at least for PEA1 and SKOV3, that ERBB2 is the key driver of activation of AKT, ERK1/2 and EGFR proteins and that its inherent activation is not simply secondary to the activation of other ERBB family members.

Discussion :-

Results Chapter 5

5.1 ERBB2 is Phosphorylated in a Range of Ovarian Cell Lines Without Being Overexpressed.

Data presented here suggests that elevated ERBB2 phosphorylation is a common feature of HGS cell lines. There was a high degree of consistency in normalised pERBB2 levels in all of the cancerous lines examined, with two exceptions, A2780, which was hypo-phosphorylated, and SKOV3, which was hyper-phosphorylated. Recently a large amount of molecular data has been collected relating to mutational status, expression profiles, and genome architecture of a large number of primary ovarian tumours. This has allowed for a comprehensive assessment of the similarities between well studied models of ovarian cancer and clinical tissue to infer their representativeness [428]. This study finds that the two most common models of HGS ovarian cancer, accounting of over 60% of publications in the field, were in fact the least likely, of the panel of 47 cell lines examined, to be HGS in origin, this perhaps speaks about the inherent difficultly of working with HGS cell lines. These two cells are A2780 and SKOV3. Both cell lines are genomically fairly uniform, not possessing large scale aberrations, unlike almost all HGS tumours. Additionally they both contain ARID1A mutations, which are very rare in HGS tumours, being much more common in endometrioid tumours. Neither do their expression profiles fit with either of the 4 reproducible HGS subtypes, expression based hierarchical clustering suggested A2780 was more similar to lung tissue than either ovarian or endometrial [438]. Two additional cell lines assayed for ERBB2 phosphorylation were included in this analysis, OVCAR3 and IGROV1, of which only OVCAR3 exhibits sufficient hallmarks for the authors to be confident it is HGS. Wider implications of this assessment aside, it does suggest that SKOV3 and A2870 are anomalous, suggesting therefore that ERBB2 activation across the remaining cells lines, is highly uniform. These findings therefore warrant further investigation of clinical material to examine whether this is a cell line artefact or a genuine property of HGS tumours.

An overabundance of ERBB2 in breast and ovarian cancer has been reported at a number of different levels, including copy number, mRNA, and protein, including a

proportion of breast cancers who have protein but not mRNA overexpression [439]. Given the mechanism by which ERBB2 contributes to hyperactivity of other ERBB family members, described in introduction section 2.7, it seems reasonable to suggest that any heritable process or event contributing to increased ERBB2 protein expression might be selected for. Put another way, the end point that is selected for is increased ERBB2 protein and any heritable changes leading to this end might exist in tumours. This perhaps explains why protein overexpression is observed in a higher proportion of cases of ovarian cancer than genomic amplification. Which appears to be partly caused by increased protein stability due to a selection for the deletion or epigenetic silencing of OPCML, which targets ERBB2 for degradation [440]. It might also explain why trastuzumab has therapeutic activity in patients without a genomic amplification [441]. Perhaps telling then that the frequency of mutations detected in ERBB2 in cases of breast and ovarian cancer are very low. A meta-analysis of next generation sequencing from a combined 1499 breast cancer patients found only 25 mutations in ERBB2, a rate of 1.7% [442]. The apparent frequency of mutations in ovarian cancer appears lower still. The TGCA data set of 316 cases found no mutations in ERBB2 at all [122]. So why is it that overexpression seems to be favoured more than constitutive activation?

The explanation may be that phosphorylation of ERBB2 and the direct consequences of downstream signalling are secondary to its ability to activate other ERBB family members. It would appear that a greater proportion of ERBB2 oncogenicity is attributable to its phosphorylation of other ERBB proteins, something that would be unaffected by increased Y1248 phosphorylation, or for example the presence of a constitutive phospho mimic mutation at this residue.

This question would not be difficult to address. Overexpression of mutants from of ERBB2 where, for example, one or more of the trans-phosphorylated, SH2 domain protein docking sites, including Y1248, have been substituted should still allow the protein to transactivate other ERBB members but not to recruit or directly activate downstream proteins. Conversely the reciprocal experiment in which a constitutively active ERBB2 (of which a number have been characterised [442]) also mutated in its ERBB dimerisation domain (the crystal structure of this region has been solved and mutational analysis of key residues conducted [324,443]) which constitutively activated signalling but did not dimerise and phosphorylate other family members would shed some light on the issue.

Despite the fact that a high proportion of ERBB2 mutations detected in breast cancer patients conferred greater ERBB2 activity their low frequency suggests that the elevated

levels of ERBB2 phosphorylation detected in ovarian cell lines (shown in Figure 43) are a consequence of other upstream changes. As such it appears that cell lines investigated here, neither amplified or overexpressing ERBB2, are not driven by ERBB2 in the same manner as either SKOV3 or other amplified cell lines or the rare cases of constitutively activated cells, where activation is 'hard wired' or even cases with protein overexpression without amplification, for example due to OPCML deletion.

Viewed in this way there appears to be four means by which elevated ERBB2 activity occurs, firstly 'hard wired' changes including common genetic amplification and rare constitutive activation. And secondly soft changes including increased protein expression without amplification, perhaps driven by OPCML deletion, and finally increased activation due to upstream signalling. Both PEO1/PEO4 and PEA1/PEA2 have been shown to not be deleted for OPCML [416] and therefore would appear to fall into the last category.

5.2 Sensitivity to the ERBB2 Inhibitor CP-724714 Correlates with Levels of Protein Activation

Regardless of whether ERBB2 phosphorylation is a primary 'hard wired' driver in the moderately activated ovarian cell lines identified here, it has functional role in promoting growth. This suggests that a high proportion of cases of HGS ovarian cancer possess elevated pERBB2 promoting growth and a higher proportion than has been shown to be either genetically amplified or overexpressing ERBB2 protein.

While ERBB2 amplified breast lines have been shown to exhibit increased sensitivity to CP-724714 relative those without. Interestingly this study also found that a number of breast lines, not possessing an amplification were also sensitive to the inhibitor [434]. Although ERBB2 phosphorylation was not assessed, when viewed in light of data from OSE-C2, demonstrating a requirement for phosphorylated ERBB2 for inhibitor function it suggests that these line possessed elevated pERBB2. This observation also supports the view, implied by the observation that patients without ERBB2 amplifications often benefit from trastuzumab, that relying on copy number dependent or even immunohisto chemical methods of screening patients for ERBB2 status, may underestimate the number of cases who would benefit from targeted therapy. Until clinical trials are conducted on non-amplified cases with a ERBB2 inhibitor this possibility will remain untested.

If it were found that a proportion of HGS tumours were in part driven by ERBB2 signalling the gene could represent an attractive target for therapy. The importance of ERBB2 amplification in breast cancer has resulted in the development of a number of humanised monoclonal antibodies and small molecule inhibitors not limited to CP-724714 at various stages of development, which would facilitate the testing of the efficacy of ERBB2 inhibition in ovarian cancer. Results presented here suggest that inhibiting ERBB2 in ovarian tumours would not only have activity but would also tumour specificity.

5.3 ERBB2 Inhibition Sensitises Cells To Cisplatin

Mainly due to clinical research investigating the efficacy of trastuzumab in breast cancer, ERBB2 has been implicated in *de novo* resistance to platinum agents. This has largely been possible due to the variety of different chemotherapy regimens available for comparison. Comparatively little research has been conducted into the role that ERBB2 plays in platinum resistance in ovarian cancer, for obvious reasons, and making inferences regarding its role is complicated as carboplatin is the standard treatment for all patients, preventing comparison against other chemotherapeutics. Results shown here suggest ERBB2 plays a role in resistance to cisplatin. When considered in relation to results shown in

Figure 15 and Figure 16 (demonstrating that not only does cisplatin exposure reduce phosphorylation of ERBB2 but that cisplatin resistant cell lines are more sensitive to this deactivation that their sensitive counterparts) the ability of ERBB2 inhibition to sensitise to cisplatin seems counterintuitive. A role for ERBB2 in cisplatin resistance would predict exactly the opposite, specifically that resistant cell lines would activate ERBB2 in response to cisplatin and this activation would be either with greater sensitivity and/or higher magnitude than their sensitive counterparts.

Given the demonstration of elevated pERBB2, promoting growth in cisplatin resistance in a number of ovarian cell lines it would be interesting to formally assess the interaction between ERBB2 inhibition and cisplatin by isobologram analysis. If synergy was detected this might warrant *in vivo* examination of the efficacy of combining these two compounds. Existing evidence is encouraging; trastuzumab has previously been shown to combine synergistically with cisplatin in an ERBB2 positive background [346]. In ovarian

cancer ERBB2 expression has been correlated with poor response to chemotherapy and reduced OS [338].

5.4 ERBB2 Inhibition Reduces Activation of ERBB1, AKT and ERK1/2 in Cells Lines Possessing Phosphorylated ERBB2 but Not in Those Without

Given the presence of phosphorylated Y1248, the docking site for SHC1, which in turn recruits GRB2 and PIK3R1, in the majority of ovarian cells assayed (see Figure 43A), the presence of activated AKT and ERK1/2 is not unexpected. It is perhaps less expected to find apparently high levels of basal activation of these proteins in the 'normal' cell line OSE-C2, which did not contain comparable levels of Y1248 phosphorylated ERBB2. This coupled with the observation that levels of pSTAT3 were similar to cancerous lines investigated questions the legitimacy of the utility of this cell line as a normal control. Despite this as OSE-C2 did not possess comparable ERBB2 or EGFR activation it provides an excellent control to test the specificity of ERBB2 inhibition to reduce pAKT and pERK1/2. For example, it might be possible for CP-724714 to reduce AKT and/or ERK1/2 activation via an off target mechanism or general toxicity and this would have been impossible to distinguish had OSE-C2 not contained readily detectable levels of these activated proteins. As it is, the lack of any effect in OSE-C2 associated with ERBB2i on pAKT and an increase in pERK1/2, when the opposite might have been expected, suggests the decreased activation of these proteins, seen in PEA1, PEA2 and SKOV3 is due to on target effects of ERBB2 inhibition.

In addition the magnitude of the reduction seen in AKT and ERK1/2 activation imply that ERBB2 is the predominant factor contributing to this, affirming the importance of the ERBB2 an important driver in cells in which it is phosphorylated.

Results Chapter 6:-

GP130 is Overexpressed in Cisplatin Resistant Cell Lines PEA2 and PEO23 and Contributes to Resistance and Proliferation. GP130 Knock Down Reveals Different Pathways to STAT3 Activation

6. GP130 is Overexpressed in Cisplatin Resistant Cells where it Promotes Growth, Platinum Resistance, Revealing Different Pathways to STAT3 Activation

A number of studies have shown a role of the ubiquitously expressed cytokine receptor GP130 in constitutive activation of STAT3 in both breast [444] and head and neck cancer [445]. One of these studies investigated GP130 signalling by transfecting with a dominant negative form of the gene lacking sequence relating to the cytoplasmic region of the protein containing the docking sites for STATs. Dominant negative GP130 transfection not only reduced basal STAT3 activation but also tyrosine phosphorylation of ERBB2. GP130 provided an interesting candidate to link both STAT3 activation to extra cellular signalling factors and elevated ERBB2 phosphorylation. As GP130 is the common low affinity receptor for not only IL6 but also IL10, OSM, LIF and CNTF, exposure to all of which are capable of activating STAT3, its inhibition allows the nature of STAT3 activation to be investigated, specifically whether STAT3 activation observed in these cell lines is maintained via IL6 type cytokine signalling. To investigate the role GP130 might play in both STAT3 and ERBB2 activation siRNA knockdowns were carried out in conjunction with cisplatin resistance, proliferation and protein assays.

6.1 GP130 is Overexpressed in Cisplatin Resistant Cell Lines PEA2 and PEO23 Relative to Their Sensitive Isogenic Counter Parts

To identify the best cell line model(s) to investigate any potential role for GP130 in promoting STAT3 or ERBB2 activation and/or promoting cisplatin resistance, QRT-PCR for *GP130* mRNA expression was carried out on the same panel of ovarian cell lines previously used.

GP130 mRNA expression did not vary to a large degree. Lowest expression was observed in cisplatin sensitive A2780. Resistant PEO23 had the highest expression, with 4.2 fold more. The majority of cell lines exhibited expression within a small range.

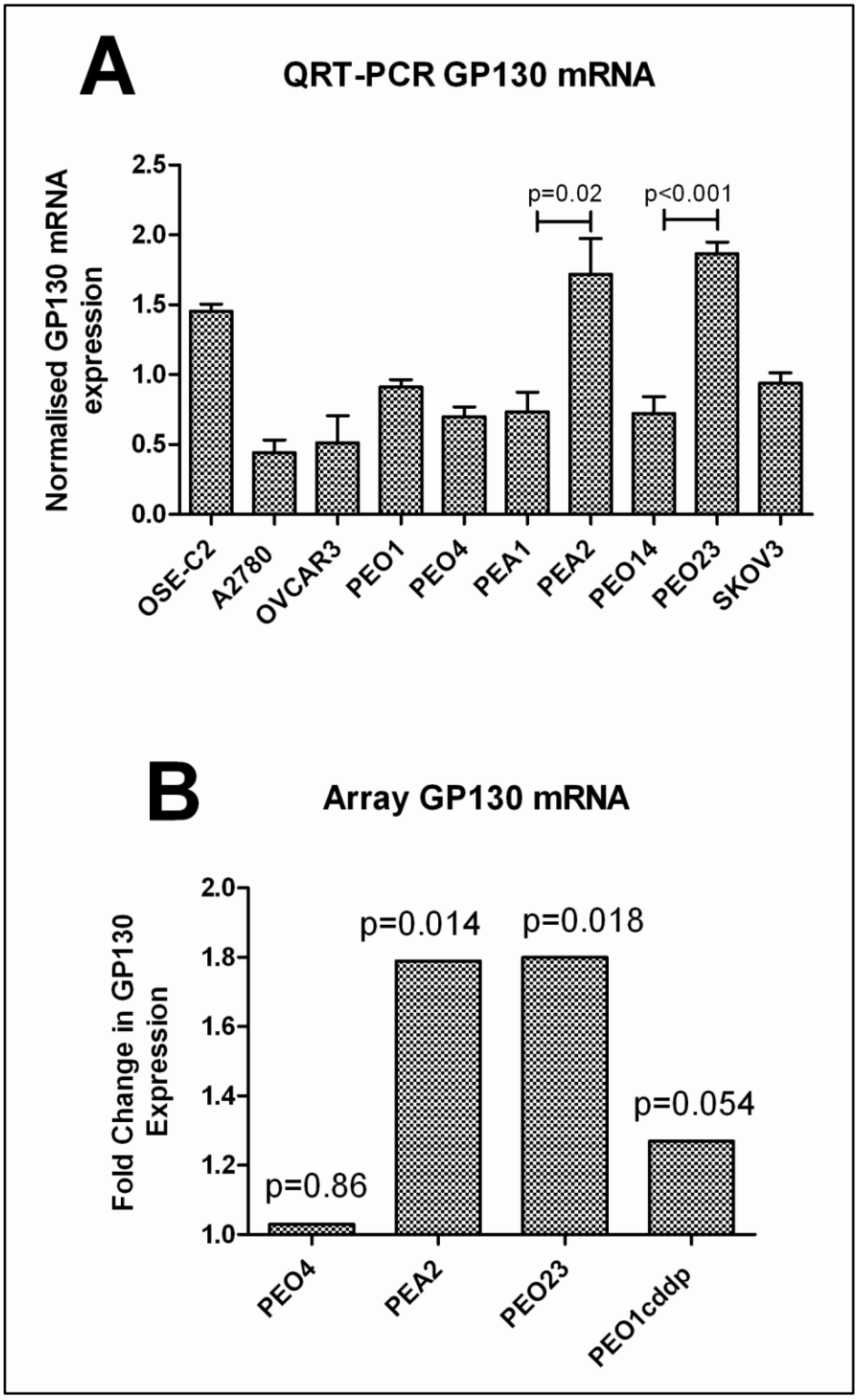

Figure 48. **A.** QRT-PCR of *GP130* mRNA expression in a panel of ovarian cell lines. Values are the average of 4 separate biological replicates. GP130 expression levels are normalised to the geometric mean of PPIA and TBP. Error bars represent the SEM of the replicates. P values calculated from heteroscedastic T-tests between replicates. **B**. Array based assessment of GP130 expression, showing the fold increase in normalised expression relative to sensitive isogenic partner. For simplicity only the resistant clone of each isogenic pair is shown. Values are the average of 4 replicates and p-values are T-tests including false discovery rate correction.

Most strikingly *GP130* expression was elevated in two of three isogenic cell line pairs assayed. PEA2 ($p=0.02$ unequal variance T-test) and PEO23 ($p<0.001$ unequal variance T-test) expressed 2.4 and 2.6 fold the levels of *GP130* than their sensitive isogenic pair respectively. Of those cancerous cells the next highest expression was found in cisplatin resistant SKOV3.

Having generated the results shown in Figure 48, the results of an earlier microarray experiment examining the expression profiles in the three isogenic pairs (PEO1/PEO4, PEA1/PEA2 and PEO14/PEO23) were reassessed. Array data confirmed existing QRT-PCR data in showing an over expression of GP130 in both PEA2 and PEO23 relative to their sensitive isogenic partner, see Figure 48B. The magnitude of overexpression was lower, both resistant clones exhibited a 1.8 fold overexpression, $p=0.014$ and $p=0.018$ for PEA2 and PEO23 respectively. Also included in this experiment was a cisplatin resistant clone of PEO1 (PEO1 cddp) which was *in vitro* selected for resistance through successive passages with cisplatin administration. Interestingly this resistant clone also exhibited an over expression of GP130 albeit of lower magnitude and borderline significance. In keeping with QRT-PCR results PEO4 showed no significant change in GP130 expression.

Based in the results obtained here it was decided to predominantly examine the role of GP130 in PEA2 and SKOV3. PEA2 as it has one of the highest expression levels in the panel and SKOV3 due to its high levels of ERBB2 expression and activation. Subsequently PEA1 and PEO4 were also included, PEA1 controlled for the possibility that any phenotype associated with GP130 ablation was not due to overexpression. For example if both PEA1 and PEA2 responded to GP130 knockdown in a similar manner it would suggest that GP130 overexpression was not related to this effect. PEO4 controlled for the possibility that all cisplatin resistant cells responded regardless of their expression of GP130.

6.2 siRNA Mediated Knock Down of GP130 Sensitises PEA2 and SKOV3 but not PEA1 to Cisplatin

PEA1, PEA2, SKOV3 and PEO4 were depleted for GP130 by means of siRNA transfection. 72 hours after siRNA transfection cells were exposed to cisplatin for an additional 24 hours prior to the measurement of activated caspase 3 and 7. In the platinum resistant cell lines PEA2 and SKOV3 each siRNA was associated with an increase in the ratio

of caspase activation, between the siRNA alone and siRNA plus cisplatin treatments. In contrast in platinum sensitive PEA1 and resistant PEO4, which have lower levels of relative GP130 expression, no increase in the ratio of induced caspase activation was observed, for data relating to PEO4 see supplementary figure S6.

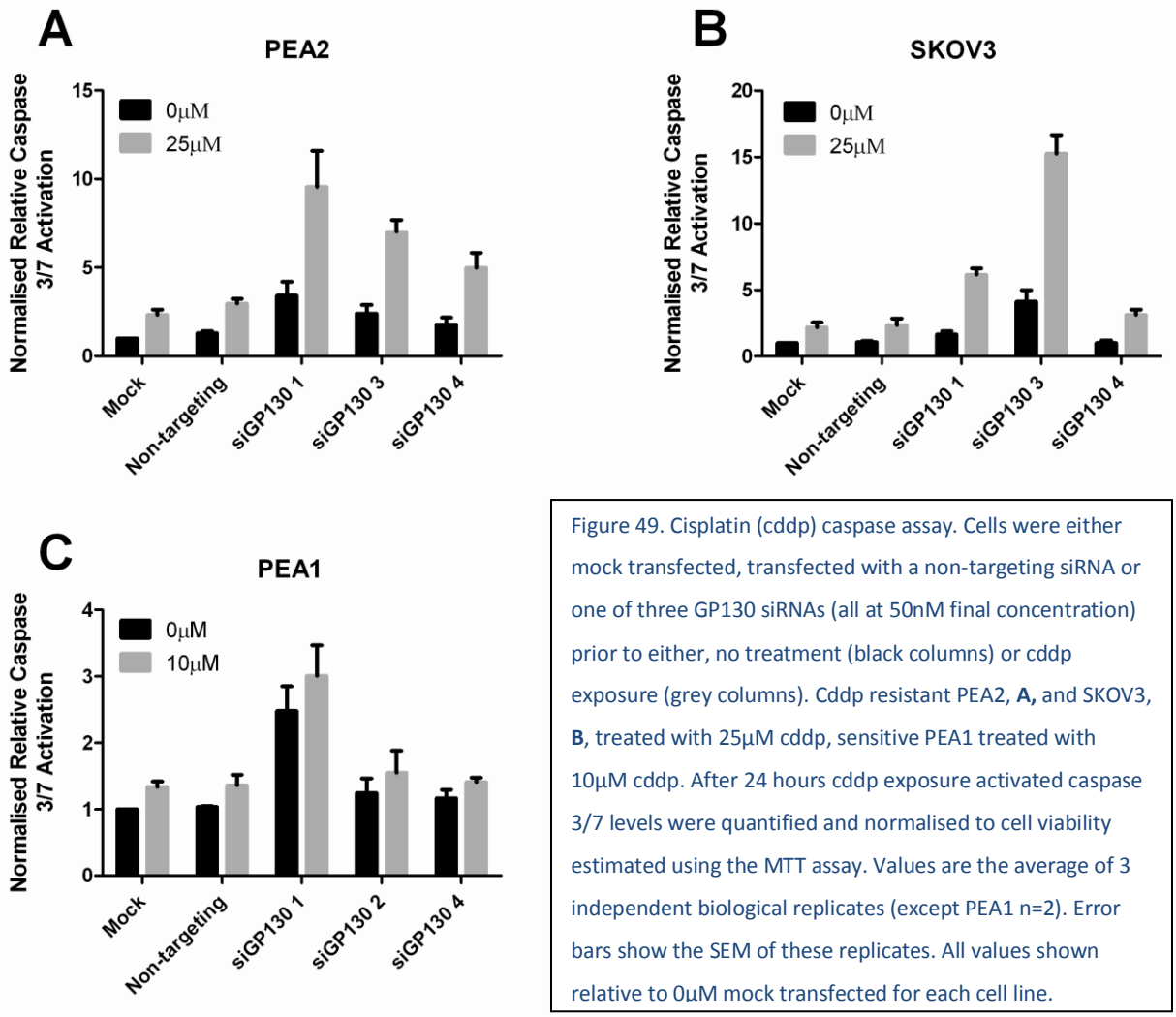

Figure 49. Cisplatin (cddp) caspase assay. Cells were either mock transfected, transfected with a non-targeting siRNA or one of three GP130 siRNAs (all at 50nM final concentration) prior to either, no treatment (black columns) or cddp exposure (grey columns). Cddp resistant PEA2, **A,** and SKOV3, **B**, treated with 25μM cddp, sensitive PEA1 treated with 10μM cddp. After 24 hours cddp exposure activated caspase 3/7 levels were quantified and normalised to cell viability estimated using the MTT assay. Values are the average of 3 independent biological replicates (except PEA1 n=2). Error bars show the SEM of these replicates. All values shown relative to 0μM mock transfected for each cell line.

Figure 49 shows the levels of activated caspase 3/7 induced by each GP130 siRNA either alone, in black columns, in in combination with cisplatin, in grey columns. In each cell line one siRNA has been excluded from analysis. In PEA2 and SKOV3 siGP130 2 was excluded due to low efficiency of knockdown. This siRNA was however effective in PEA1 and PEO4, whereas siGP130 2 was not, which was excluded from both. The reason for the differential siRNA efficacy between cell lines is unknown however it is tempting to speculate

this may be due to the differential expression of transcript variants responsible for exerting the effects the seen in PEA2 and SKOV3 but not PEA1 and PEO4.

Inferring whether GP130 knockdown induced apoptosis as a single agent was complicated by inconsistent behaviour of different siRNAs. The toxicity profiles of both siGP130 1 and 3 were mixed. For example siGP130 1, induced caspase activation, as a single agent in PEA1 and PEA2 but not SKOV3, whereas siGP130 3 was toxic as a single agent in SKOV3 and PEA1 but to a lesser extent in PEA2 and siGP130 4 was not toxic in any cell line.

The interaction with GP130 knockdown and cisplatin was however more consistent. Figure 50 was created by calculating the ratio of activated caspase 3/7 induced by cisplatin treatment for each GP130 siRNA. In each cell line, transfection with non-targeting siRNA had no effect on the ratio of caspase induced by cisplatin.

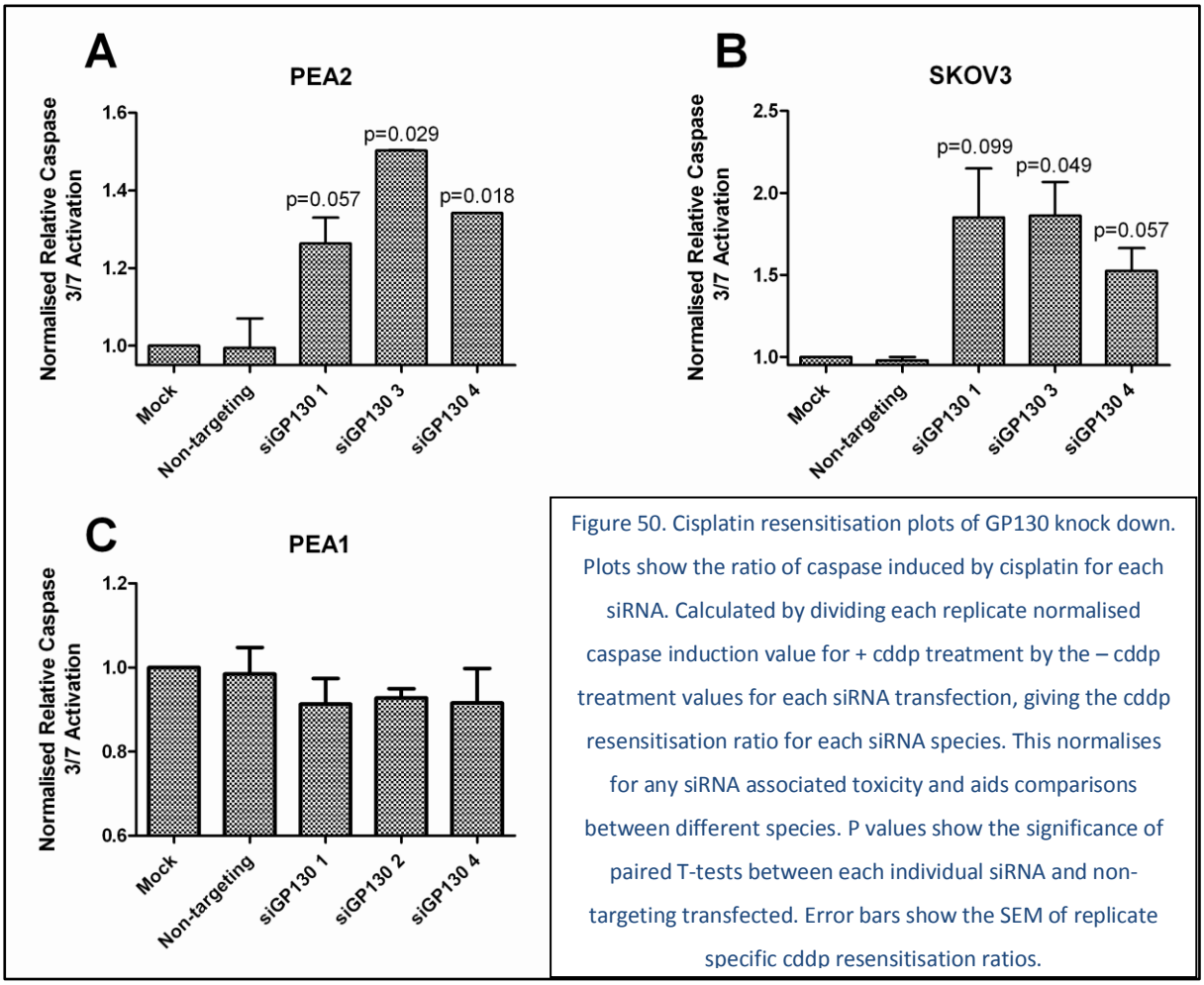

Figure 50. Cisplatin resensitisation plots of GP130 knock down. Plots show the ratio of caspase induced by cisplatin for each siRNA. Calculated by dividing each replicate normalised caspase induction value for + cddp treatment by the – cddp treatment values for each siRNA transfection, giving the cddp resensitisation ratio for each siRNA species. This normalises for any siRNA associated toxicity and aids comparisons between different species. P values show the significance of paired T-tests between each individual siRNA and non-targeting transfected. Error bars show the SEM of replicate specific cddp resensitisation ratios.

However for both PEA2 and SKOV3 transfection with each siRNA was associated with an increase in the ratio of caspase activated by cisplatin. The degree of cisplatin potentiation was greatest in SKOV3, on average knockdown of GP130 resulted in a 74% increase in the levels of induced caspase activation associated with cisplatin treatment. This ranged from 52% for siGP130 4 ($p=0.057$ paired T-test) to 86% for siGP130 3 ($p=0.049$ paired T-test). For PEA2 the average percentage increase in cisplatin induced apoptosis for each siRNA was 37% ranging from 26% ($p=0.057$ paired T-test) to 50% ($p=0.029$ paired T-test) in siGP130 1 and 3 respectively. Conversely in PEA1 and PEO4, which also express low levels of GP130 relative to PEA2, knockdown was not associated with any potentiation of cisplatin induced apoptosis.

6.3 siRNA Mediated Knockdown of GP130 Reduces Proliferation in Cisplatin Resistant PEA2 and SKOV3 but not in Sensitive PEA1.

GP130 is required for IL6 dependent STAT3 activation. Given the effects of STAT3 siRNA in PEA1 PEA2 and SKOV3, shown in Figure 34, if STAT3 activation were maintained via extra cellular signalling, utilising any of the IL6 type cytokines, GP130 knockdown would be predicted to also inhibit cell growth. For this reason simultaneous to the carrying out cisplatin caspase assays the effect of GP130 knockdown on proliferation was assessed. Knockdown of GP130 had a pronounced effect on proliferation rates in PEA2, doubling time increased on average by 73% from 35.5 hours to 61.6 hours. The magnitude of effect ranged from a 46% increase, siGP130 1 to 210% increase. Both siGP130 3 and siGP130 4 significantly reduced cell viability after 72 hours ($p=0.035$ and $p=0.034$ paired T-tests) relative to mock or negative control transfected cells. siGP130 1 had a borderline significant effect. Doubling times were also increased in SKOV3, but to a lesser extent, percentage increases in doubling time ranged from 7.5% to 20.8% with an average of 15%. Each siRNA significantly reduced cell viability after 72 hours relative to controls. PEA1 and PEO4 cells were also investigated which did not show any effect after GP130 depletion, doubling times were also unchanged by transfection with any siRNA, for PEO4 see supplementary figure S6.

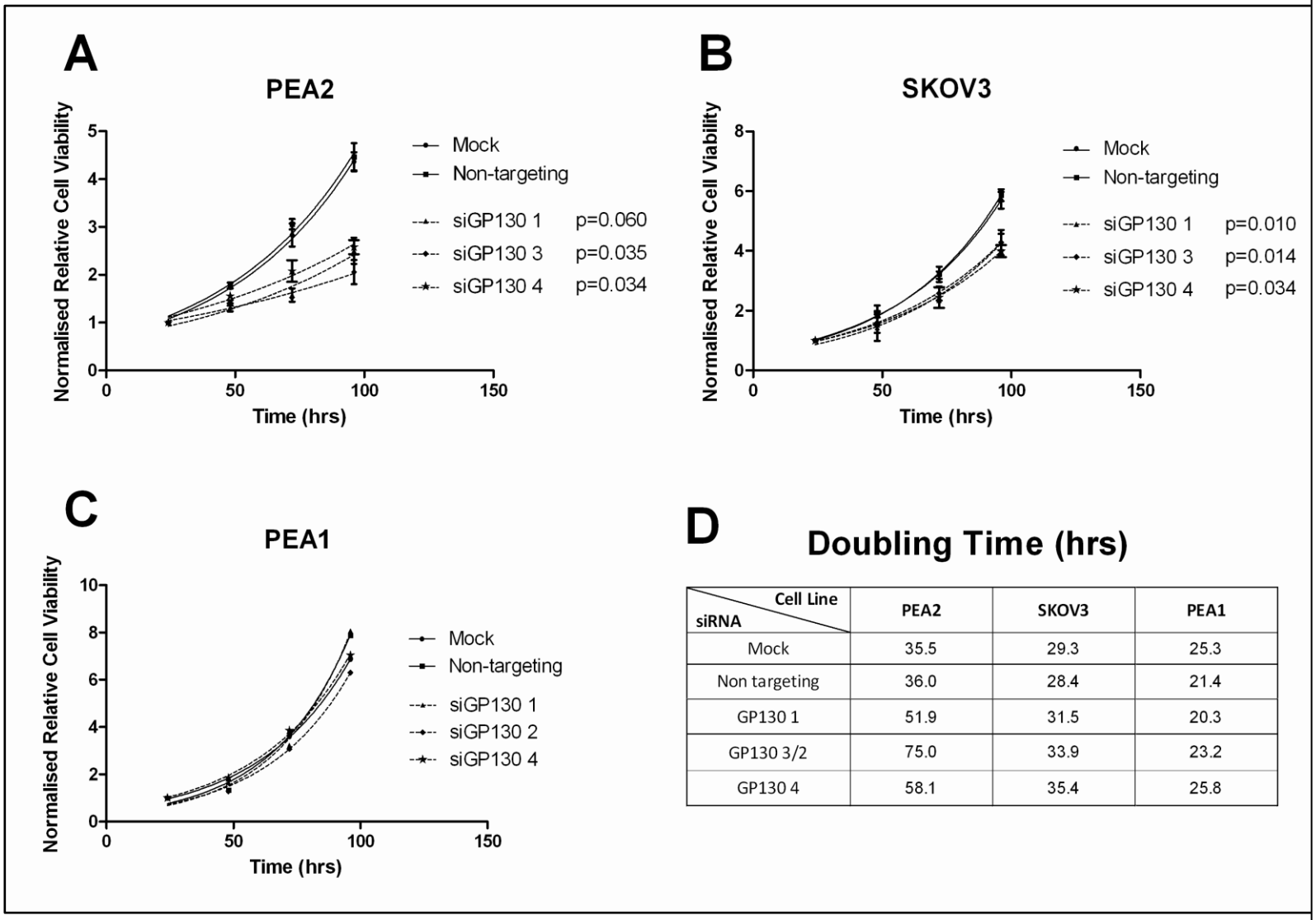

Cell Line / siRNA	PEA2	SKOV3	PEA1
Mock	35.5	29.3	25.3
Non targeting	36.0	28.4	21.4
GP130 1	51.9	31.5	20.3
GP130 3/2	75.0	33.9	23.2
GP130 4	58.1	35.4	25.8

Figure 51. Proliferation Assay after GP130 knockdown. Cells were either mock transfected, transfected with a non-targeting siRNA or one of three GP130 siRNAs for 48 hours before reseeding. Cell viability estimates made every 24 hours using the MTT assay. Values are the average of 3 independent biological replicates (except PEA1 n=1). All values normalised to 0 hours for each treatment. Error bars represent SEM between replicates. P values based on paired T-tests between 96hr time point for each siRNA and mock transfected cells.
D, shows doubling time estimates made from an exponential regression

6.4 siRNA Mediated knockdown of GP130 Decreases pSTAT3 in SKOV3 but not PEA2 and has no Effect on pERBB2.

GP130 was investigated as a candidate regulator of both STAT3 and ERBB2 activation. Western blotting revealed that GP130 knockdown had no effect of levels ERBB2 phosphorylation at Y1248 in either PEA2 or SKOV3. GP130 knockdown was similarly not associated with any reduction in levels of STAT3 activation in the isogenic pair of PEA1 and PEA2 or PEO4. Alternatively in SKOV3 GP130 knockdown reduced pSTAT3 to a large degree, but had no effect on total STAT3, see Figure 52. This suggests that STAT3 phosphorylation is maintained via an extracellular signalling pathway involving an IL6 type cytokine via GP130 in SKOV3 but not any of PEA1 PEO4 and PEA2.

ERK1/2 activation was used as a surrogate of ERBB2 activation, as there was no effect on ERBB2 phosphorylation it would be predicted that levels of ERK1/2 activation would also be unchanged. Surprisingly there was a correlation with those cell lines, exhibiting a phenotype of either cisplatin sensitisation or growth inhibition, PEA2 and SKOV3, in response to GP130 knock down and the incidence of increased ERK1/2 activation. In both PEA2 and SKOV3 each siRNA used resulted in an increase in detected levels of ERK1/2 dual T185/202 and Y187/204 phosphorylation that was matched by a reciprocal decrease in the amount of total ERK1/2 protein. Interestingly in PEA1, which displayed no phenotype in response to GP130 knockdown did not experience any change in ERK1/2 activation.

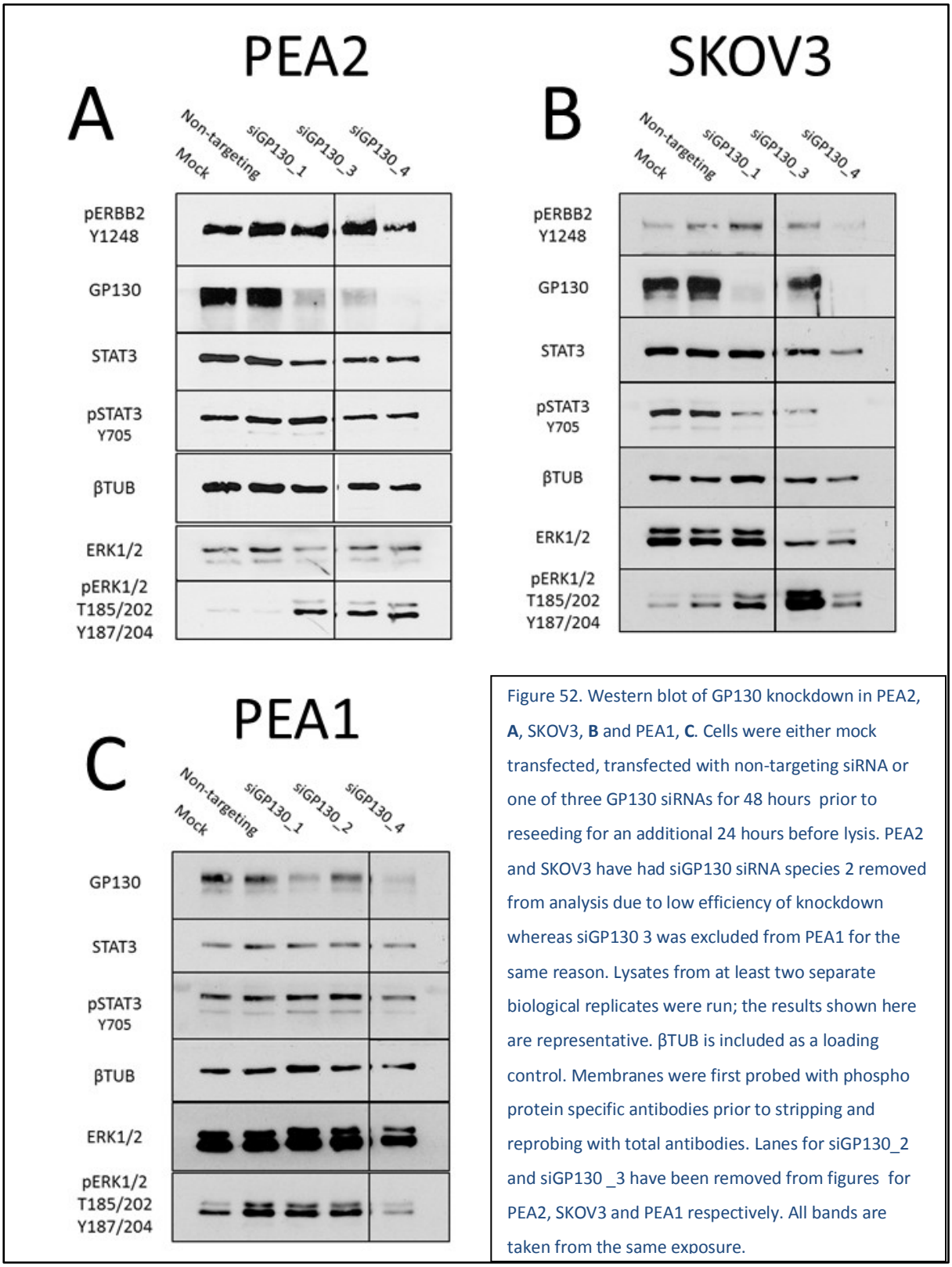

Figure 52. Western blot of GP130 knockdown in PEA2, **A**, SKOV3, **B** and PEA1, **C**. Cells were either mock transfected, transfected with non-targeting siRNA or one of three GP130 siRNAs for 48 hours prior to reseeding for an additional 24 hours before lysis. PEA2 and SKOV3 have had siGP130 siRNA species 2 removed from analysis due to low efficiency of knockdown whereas siGP130 3 was excluded from PEA1 for the same reason. Lysates from at least two separate biological replicates were run; the results shown here are representative. βTUB is included as a loading control. Membranes were first probed with phospho protein specific antibodies prior to stripping and reprobing with total antibodies. Lanes for siGP130_2 and siGP130 _3 have been removed from figures for PEA2, SKOV3 and PEA1 respectively. All bands are taken from the same exposure.

Discussion :-

Results Chapter 6

6.1 GP130 is Overexpressed in Cisplatin Resistant Cell Lines PEA2 and PEO23 Relative to Their Sensitive Isogenic Counter Parts

The incidence of GP130 overexpression in 2 of 3 ovarian isogenic cell lines pairs raises the possibility that this gene may play a role in cisplatin resistance. No reference to GP130 and acquired resistance either in ovarian, or any other cancer, to cisplatin, or any other cytotoxic drug, could be found in the literature. The validation of this QRT-PCR data with reference to a previously existing array data set also suggests that the over expression of *GP130* at the mRNA levels is a highly stable feature, as these experiments were conducted years apart. The apparently high level of expression of GP130 observed in OSE-C2 appears to challenge the suggestion this gene may play a functional role in cisplatin resistance. However recent evidence demonstrating the tissue of origin, for at least the majority, of ovarian HGS tumours is not the OSE but in fact the fallopian tube epithelium questions the relevance of OSE-C2 as a normal control. Unfortunately as no normal fallopian tube epithelial lines were accessible OSE-C2 was is current the 'best' control available.

Extension of these results into a clinical data set of matched pre and post platinum resistant relapse would be a priority for further research. This would address whether GP130 is a genuine clinical biomarker of resistance to cisplatin or just a cell line artefact, as well as quantify the proportion of cases where acquired resistance is associated with overexpression.

To examine the importance upfront GP130 expression may play in patient survival publically available expression data sets were queried, these include the TCGA plus additional combined data sets available at [446]. The results are shown in supplementary methods/results section S4. No link was found between upfront tumour *GP130* expression and either OS and PFS when controlling for age, grade, stage and residual disease.

6.2 – 6.3 siRNA Mediated Knock Down of GP130 Sensitises to Cisplatin and Reduces Proliferation in PEA2 and SKOV3 but not PEA1

Data presented here has demonstrated GP130 plays a functional role in cisplatin resistance and proliferation in PEA2 but not PEA1 cells. This has a number of important potential therapeutic implications, if these findings are borne out in wider data sets.

Firstly, it suggests that GP130 is not just a potential biomarker of platinum resistance but also a functional mediator of resistance and as such a potential therapeutic target.

Secondly, the apparent requirement on overexpression, for sensitisation upon knockdown, has the additional benefit that it could afford a convenient means screening patients for potential benefit from any anti-GP130 therapy. For example a comparison of biopsies taken at initial debulking and on relapse with platinum resistant disease, in which GP130 overexpression is detected in the second, relapsed, specimen could be used to inform treatment options.

Thirdly, the ability of GP130 knockdown to both decrease proliferation and sensitise to cisplatin increases potential utility of any anti-GP130 therapeutic. Suggesting targeting this protein would be effective both as a single agent and in combination with platinum.

Fourthly, as GP130 is a transmembrane receptor the development of novel therapeutic would be aided by the ease of access to the target by either humanised monoclonal antibody, blocking peptide or other therapeutic not easily passed through the cell membrane.

Finally, the anti-IL6 antibody siltuximab has been the subject of preclinical and clinical trials in ovarian, and other cancers, where it has shown some activity [289,447]. It remains to be seen whether this novel therapy will confer a survival advantage in large randomised trials, but IL6 remains an attractive therapeutic target. The rationale behind targeting IL6 is largely based on its ability to activate STAT3, a process mediated via GP130. Therefore targeting GP130 would be expected to recapitulate some of the effects of inhibiting IL6. However a comparison of the phenotypic consequences of STAT3 and GP130 knockdown presented here are somewhat different. Growth inhibition was a common feature of both but sensitisation to cisplatin, observed in PEA2 and SKOV3, was unique to GP130, suggesting this effect is not mediated via STAT3. Therefore it seems there are additional therapeutic benefits to targeting GP130, beyond those conferred by IL6/STAT3 inhibition alone that are mediated by a factor other than STAT3. Therefore it might be possible to combine the therapeutic benefits of targeting IL6 which those conferred by inhibiting an as yet unknown pathway regulated by GP130.

In conclusion GP130 has a number of attributes that make it an attractive target for therapy in a platinum resistant background. It might be possible to identify those patients likely to benefit from treatment. Any treatment targeting GP130 is likely to function as both a single agent and in combination with cisplatin. The protein is inherently drugable and targeting it should combine the apparent therapeutic effects, of an existing treatment, with additional benefits.

These extrapolations are however based on preliminary data. There are a number of future research objectives that would be required in order to validate GP130 as a genuine targetable mediator of chemoresistance.

Extending these findings to additional paired isogenic ovarian cell lines would be a simple and easily achievable means of validating initial findings. For example PEO23 has been shown to overexpress GP130 relative to its sensitive pair PEO14, however it is unknown whether PEO23 responds to knockdown. Other paired HGS isogenic cell line pairs exist, principally those created in the Peter MacCallum Centre in Melbourne Australia that could be also be investigated.

It would be relevant to investigate whether *GP130* mRNA overexpression translates to protein overexpression. In the absence of a constitutive activating mutations or other similar change, without clear protein overexpression it would be difficult to identify patients most likely to benefit from anti-GP130 therapy.

As previously described reproducing this data in a clinical data set would be crucial. Currently a tissue bank of ovarian specimens, collected during initial debulking and after relapse, is being compiled by the European consortium OCTIPS (Ovarian Cancer Therapy – Innovative Models Prolong Survival) which could provide the means to achieve this. Currently there are no publically available data sets expression profiling pre and post cisplatin resistant relapse tumours.

GP130 blocking antibodies, functioning as receptor agonists, are commercially available, which would be expected to recapitulate a knockdown phenotype in responder cell lines. Confirming the ability of a blocking antibody to function synonymously with knockdown would be an important step in demonstrating the plausibility of targeting GP130 in a clinical setting.If these criteria were met GP130 could represent an attractive prospect for both single agent and adjuvant therapy in a cisplatin resistant background.

Aside from issues pertaining to the GP130 as a therapeutic target, there are a number of mechanistic questions that have arisen from these results. For example the ability of GP130 knockdown to combine favourably with cisplatin warrants investigation of possible

synergy between a blocking antibody and cisplatin, and potentially, other DNA damaging agents. Isobologram analysis of drug interaction would allow the existence of synergy between cisplatin and GP130 blockade to be assessed.

Given the suggestion that GP130 is functioning via factors not limited to STAT3, in PEA2 and SKOV3, it would be mechanistically important to identify those proteins, immediately downstream, perturbed by knockdown and responsible for eliciting GP130 apparent proliferative and prosurvival effects. The most obvious candidates to screen would be other JAKs and STATs, particularly JAK1 and STAT5. Followed by ERBB family members, MAPK and PI3K pathways members GRB1/SHC1 and PIK3C which have been implicated in GP130 signalling [448,449].

Finally despite the initial cue for investigating GP130 being the elevated expression, (see Figure 48A), the effects of knockdown in PEA2 and SKOV3 cannot be explained by overexpression alone. Knockdown of GP130 in PEA1 and PEO4, which express only around 2.5 fold less *GP130* mRNA than PEA2, resulted in no growth inhibition or cisplatin sensitisation (see Figure 50C, Figure 51C and figure S6). PEA1 and PEO4 also expresses only slightly less *GP130* mRNA than SKOV3, and did not respond to knockdown. Levels of GP130 in PEA1 and PEO4 are readily detectable at both mRNA and protein level and sufficient of IL6 signal transduction, albeit with additional sIL6RA supplementation in PEA1.

It therefore seems likely than an unknown functional change has occurred between PEA1 and PEA2, and which may be inherent in SKOV3, which has contributed to selection for greater GP130 expression, presumably through successive cycles of platinum exposure during resistance acquisition. A model supported by two observations; first that, cisplatin naïve, SKOV3s respond to GP130 knockdown but do not have elevated expression. Second the *in vitro* selected cisplatin resistant cell line, PEO1 cddp, also has elevated *GP130* expression, relative to the parental cell line (see Figure 48B).

It would therefore be relevant to screen for expression of other IL6 type cytokines, functioning via GP130, whose expression may have increased in resistant cell lines. Interestingly reference to existing expression array data (used for Figure 48B), suggests OSM is also over expressed in PEA2 and PEO23 resistant cells relative to their sensitive counter parts. Other IL6 type cytokines that could be examined and not included on this array were LIF, IL11, IL27, CTF1 and CLCF1. It would also be relevant to sequence GP130 itself for the presence of any known or putative activating mutations which might account for the acquired behaviour of this gene, in PEA2 and SKOV3.

6.4 siRNA Mediated knockdown of GP130 decreases pSTAT3 in SKOV3 but not PEA2 and has no effect on pERBB2.

Results presented in Figure 52 suggest that ovarian cell lines possess different pathways activating STAT3. In SKOV3 appears to be via canonical signalling involving IL6. PEA1, PEA2 and PEO4 which did not experience any reduction in levels of pSTAT3 after GP130 knockdown, must according to current dogma, utilise an alternative pathway not involving any IL6 type cytokine.

Although GP130 has not previously been implicated in acquired chemoresistance, it has been shown to maintain constitutively activated STAT3 in breast cancer, via its function as the low affinity IL6 receptor [444]. In addition a reported 60% of inflammatory hepatocellular carcinomas, benign liver tumours, contain constitutively activating mutations in GP130 which activate STAT3 without the need for ligand [277]. While GP130 has some credentials as an oncogene, it is generally considered these characteristics are mediated via STAT3. As discussed in the previous section a disparity between the STAT3 and GP130 knockdown phenotypes in PEA1 PEA2 and SKOV3, suggest the effects of GP130 knockdown couldn't be explained exclusively through its interaction with STAT3, implying that GP130 must signal through an additional, as yet unknown, mediator.

Figure 52 provides evidence that GP130's promotion of cell growth and cisplatin resistance, in a cisplatin resistant background, is not mediated via STAT3. It was perhaps unsurprising that knockdown of GP130 did not reduce levels of pSTAT3 in PEA1 and PEA2 given that these cells were unresponsive, in terms of changes in pSTAT3, to rIL6 treatment. However PEO4 was responsive to rIL6 and also experienced no change to its levels of pSTAT3. This suggests that regardless of IL6 responsiveness in HGS cell lines, constitutive pSTAT3 is maintained without the requirement for GP130 and therefore any IL6 type cytokine. This therefore raises the question what are the upstream factors contributing to constitutive STAT3 activation? It would be relevant to screen JAKs for their phosphorylation levels after GP130 as this would offer an insight into the role they play in both STAT3 activation in SKOV3 and the activation of other theorised factors downstream of GP130, responsible for electing its effects.

On the other hand for SKOV3, it was perhaps surprising that GP130 seemed to be almost entirely responsible for maintaining levels of constitutive pSTAT3. Although SKOV3 is responsive to IL6, based on mRNA levels SKOV3 expressed the least *IL6* of any cell line with the exception of A2780, which did not express any, and over 300 fold less than PEA2

(see Figure 25). Whether or not IL6 is responsible for maintaining constitutive STAT3 activation in SKOV3 was not addressed, however data presented here would appear to suggest it is unlikely, this interpretation is with the caveat that this is based on *IL6* mRNA expression data and not protein levels.

ERK1/2 phosphorylation was probed in this experiment primarily as a read out of any effect on ERBB2. Given that there was no effect on ERBB2 Y1248 phosphorylation it was therefore surprising that ERK1/2 activation was increased in response to GP130 knockdown. Particularly when considered with reference to evidence that GP130 can directly activate the MAPK pathway via a direct interaction with GRB1 and SHC1 [450]. It was interesting to observe a correlation with increased ERK1/2 phosphorylation and a phenotype associated with GP130 knockdown for a number of reasons.

It supports the notion of an, as yet unidentified, pathway downstream of GP130 present in responding cell lines, of which an increase in ERK1/2 phosphorylation is apparently a consequence of perturbing. Although this is not the first suggestion of a functional link between the two proteins it appears to be the first evidence showing that knock down of GP130 can cause an increase in ERK1/2 activation, albeit only in cisplatin resistant cells.

It is unclear what the functional consequences of such an increase in phosphorylation are (this issue is addressed in greater detail in the subsequent chapter). Indeed viewed in isolation the coincidence growth inhibition and increased ERK1/2 activation is unusual given the conventional role of these proteins. Both transcription factor targets of GP130 signalling, STAT3, and MAPK signalling, FOS and JUN are capable of inducing the upregulation of CCND1 [451]. Therefore increased activation of ERK1/2 could represent a novel feedback mechanism maintaining cellular proliferation buy offsetting decreased CCND1 expression associated with reduced STAT3 activation.

Results Chapter 7:- ERK1/2 are Phosphorylated in Response to JAK2 Knockdown, JAK2 Inhibition, Cisplatin and IL6 Treatment. Inhibition of ERK1/2 Sensitises SKOV3 to Cisplatin and Reveals a Feedback Mechanism Involving ERBB2, JAK2 and STAT3

7. ERK1/2 are Phosphorylated in Response to JAK2 Knockdown, JAK2 Inhibition, Cisplatin and IL6 Treatment. Inhibition of ERK1/2 phosphorylation Sensitises SKOV3 to Cisplatin and Reveals a Feedback Mechanism Involving ERBB2, JAK2 and STAT3

The observation of increased ERK1/2 phosphorylation in response to GP130 knockdown raised a number of possibilities. First, that this effect occurs in response to perturbation of other proteins in the JAK/STAT pathway. If true, given that JAK2 and STAT3 exhibit differential expression and activation, respectively, in response to cisplatin exposure it would follow that ERK1/2 would also be activated by cisplatin. If levels of pERK1/2 were increased by cisplatin, the activation of a known prosurvival factor in response to platinum exposure would represents an attractive target for inhibition.

7.1 ERK1/2 are Phosphorylated in Response to JAK2 Knockdown, JAK2 Inhibition, Cisplatin and IL6 Treatment

To investigate the possibility that ERK1/2 activation is a common response to perturbation of other members of the JAK/STAT pathway lysates used to generate Figure 28 and Figure 31 relating to JAK2 inhibition and RNAi respectively were examined. As an additional control AKT phosphorylation was assessed to infer the specificity ERK activation. If any observed ERK1/2 activation was driven by one of the ERBB family, for example, it would be expected to also activate AKT.

The results of JAK2 inhibitor treated cells assayed for pERK1/2 and pAKT are shown in Figure 53A. In each cell line examined JAK2 inhibition caused a dose dependant increase in the activation of ERK1/2 (T185/202, Y187/204), with maximal activation occurring at the highest concentration of TG101348 used (1μM). Again, and as observed with cells knocked-down for GP130, ERK1/2 activation occurred concomitantly with a decrease in levels of total protein. The activation of ERK1/2 in this context is interesting as it occurs despite a simultaneous reduction pERBB2 y1248 (see Figure 28), an important driver of the RAS/RAF/MEK/ERK pathway. Despite both ERK1/2 and AKT being up activated by ERBB family members, JAK2 inhibitor dependent changes in AKT phosphorylation did not mirror those of ERK1/2. A modest decrease in pAKT occurred in PEA1 and PEA2 also in a dose dependant fashion while no change in pAKT was evident in hypo-ERBB2 phosphorylated

OSE-C2. Suggesting the decrease in PEA1 and PEA2 is consistent with commensurate decreases in pERBB2 associated with JAK inhibition.

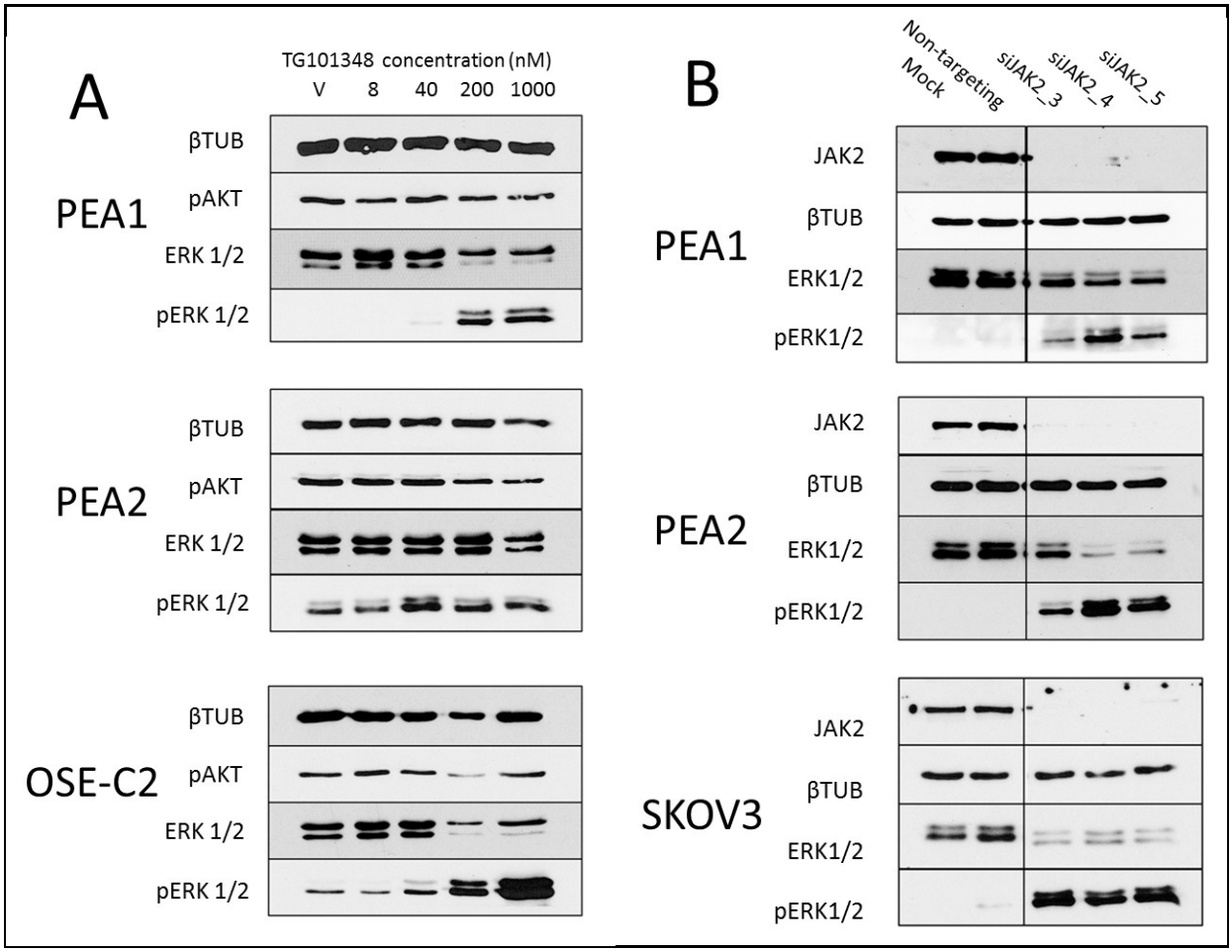

Figure 53. **A**,Western Blot of JAK2 Inhibitor (TG101348) treated cells. Cells were treated with the indicated concentration of inhibitor dissolved in DMSO or vehicle control (V) for between 16 and 18 hours before lysis. Western blots were run from at least two biological replicates for each cell line. The results obtained were consistent. βTUB is included as a loading control. Antibody for pAKT detects S473 phosphorylated AKT and pERK1/2 antibody detects duel phosphorylated T185/T202 and Y187/Y204 ERK1/2 . **B**, Western Blot of JAK2 siRNA treated cells. Cell transfected with either no siRNA (mock) a non-targeting siRNA or one of three JAK2 siRNAs for 48 hours, cells were then reseeded and given an additional 24 hours to reattach before lysis. pERK antibody detects duel phosphorylated S185/202 and Y187/204 ERK1/2. A lane relating to an additional JAK2 siRNA has been removed from each due to poor efficiency of knock down. In each case at least two separate biological replicates were analysed and results were consistent.

Lysates knocked down for JAK2 were also examined for their levels of activated ERK1/2. The results, shown in Figure 53B, recapitulate those generated from JAK2 inhibitor treated cells. Each siRNA was associated with an increase in pERK1/2 (S185/202 Y187/204)

relative to mock transfect and non-targeting transfected cells. Providing strong evidence that this effect is on target and a common feature of JAK2 perturbation, occurring in each cell line investigated. Again, in common with JAK2 inhibitor and siGP130 treated cells increases in pERK1/2 occurred simultaneous to a decrease in absolute levels of protein.

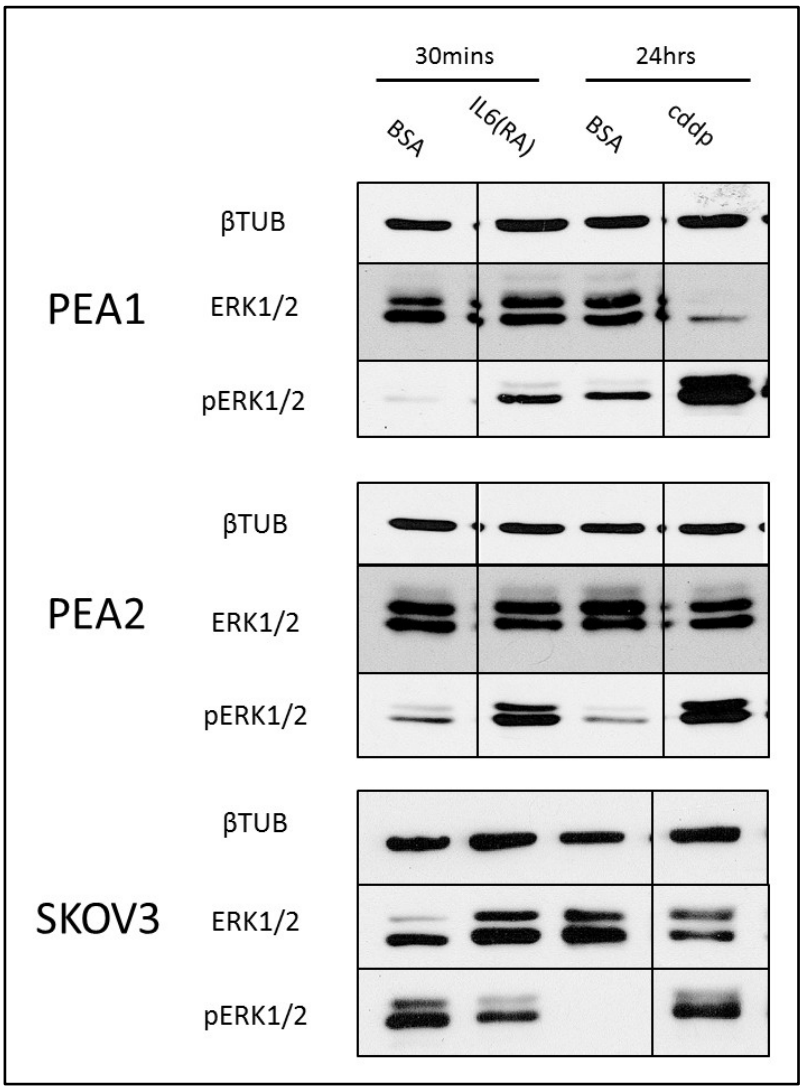

Figure 54. Western blot of cells stimulated with IL6 (RA) as previously described (see Figure 22) for 30 minutes or exposed to cddp for 24 hours. PEA1 and PEA2 were stimulated with both IL6 and sIL6RA while SKOV3 was treated with IL6 only. PEA1 sensitive cells were treated with 10μM cddp, resistant PEA2 and SKOV3 were treated with 25μM cddp. All cells exposed to cddp for 24 hours before lysis. pERK antibody detects duel phosphorylated T185/T202 and Y187/Y204 ERK1/2. βTUB is included as a loading control. For convenience some lanes have been removed but all bands are from the same exposure.

In results chapter 1 it was shown that cisplatin exposure decreases JAK2 expression. Therefore, based on results in Figure 53, cisplatin exposure would also be predicted to activate ERK. In addition as GP130 has been reported to interact with GRB1 and SHC1 and activated the MAPK pathway [450], therefore IL6 exposure should also active ERK1/2. Lysates generated when examining the effects of IL6 on cisplatin response were re-examined, probing levels of ERK1/2 activation in response to both stimuli. The results are shown in Figure 54.

IL6(RA) exposure was associated with an increase in ERK1/2 phosphorylation in PEA1 and PEA2 but not SKOV3. In fact the opposite occurred in SKOV3 where by IL6 treatment caused a decrease in ERK1/2 activation. Interestingly and hinting at the nature of potential feedback between levels of phospho and total ERK1/2 the IL6 induced reduction in pERK1/2, in SKOV3, was associated with an increase in total abundance of the protein. Cisplatin was associated with large fold increases in ERK1/2 phosphorylation which occurred in each cell line investigated.

As predicted cisplatin exposure also resulted in an increase in the phosphorylation of ERK1/2 and again this increase was at the expense of levels of total protein.

7.2 Signalling through ERBB2, JAK2, STAT3 and ERK1/2 are also affected by Other Cytotoxic Compounds.

Cisplatin's modulation of the signalling of a number of genes/pathways with important roles in tumourigenesis and tumour growth raised the question of how specific these responses are to either, cisplatin, DNA damaging agents, or cytotoxicity more generally. For this reason the ability of doxorubicin (an anthracycline, that causes DNA damage in a similar manner to cisplatin) and paclitaxel (a taxane that prevents microtubule disassembly and therefore chromosome segregation) to modulate signalling of the above proteins was investigated. The combination of both allows an assessment of whether the effects detected for cisplatin occur in response to exposure to additional DNA damaging agents or whether they are common to various cytotoxic drugs with differing mechanisms of action.

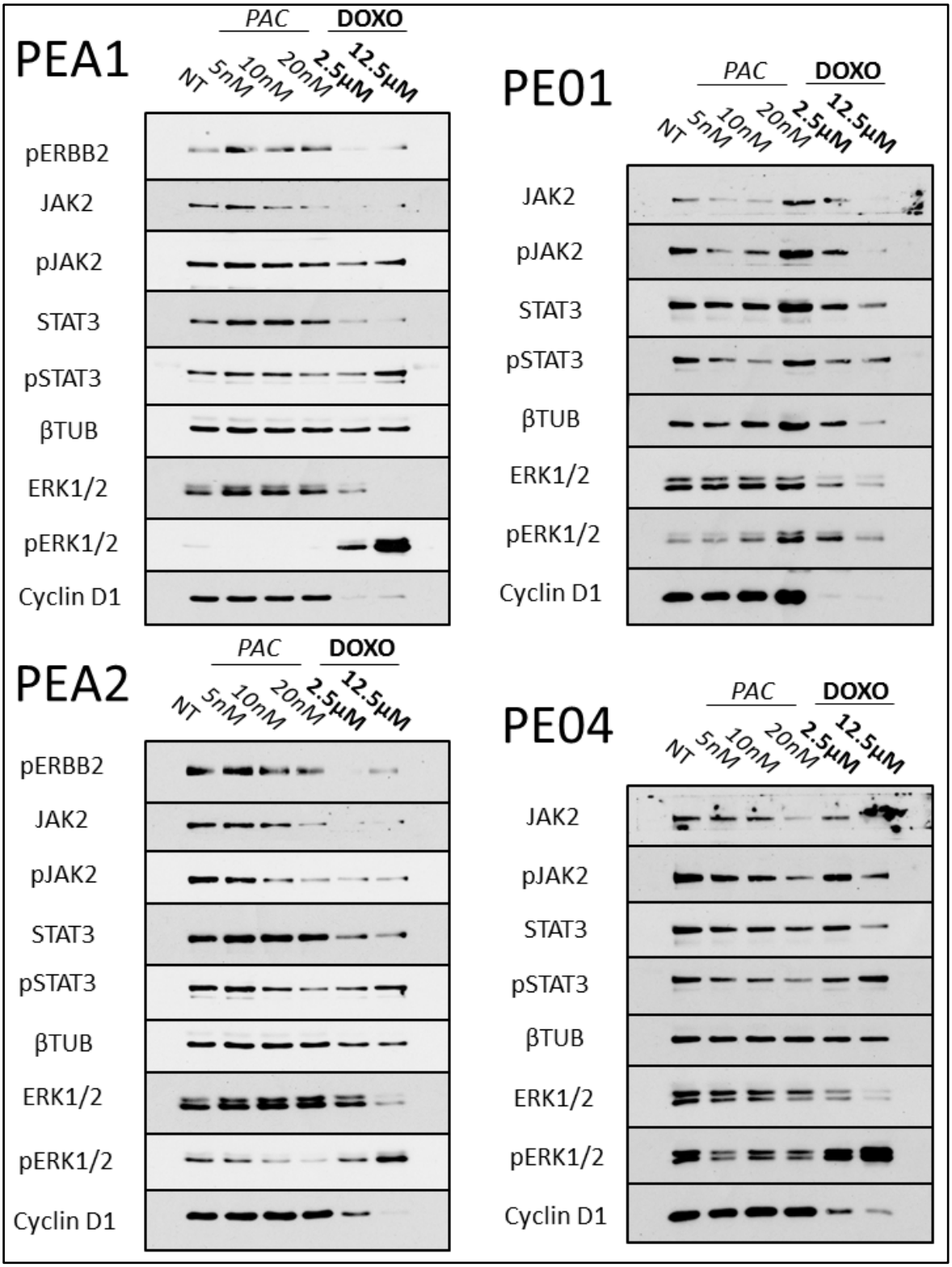

Figure 55. Western blot analysis of paclitaxel (PAC, in italics) and doxorubicin (DOX, in bold) treated cells. Cells were exposed to the indicted concentration of either drug for 24 hours prior to lysis. . βTUB is included as a loading control. Antibody for pAKT detects S473 phosphorylated AKT, pERK1/2 detects duel phosphorylated T185/T202 and Y187/Y204 ERK1/2, pJAK2 detects duel phosphorylated Y1007/1008 JAK2 and pSTAT3 detects Y705 phosphorylated STAT3. Membranes were probed with phospho specific antibodies before being stripped and reprobed with total antibodies.

The two isogenic pairs PEO1/PEO4 and PEA1/PEA2 were exposed to three different concentrations of paclitaxel (5nM, 10nM and 20nM) and two different concentrations of doxorubicin (2.5μM and 12.5μM) for 24 hours before lysis. Drug treated cells were examined for their levels signalling and absolute expression of ERBB2, JAK2, STAT3 and ERK1/2. Cyclin D1 was included as a read out of STAT3 signalling, the results are shown in Figure 55.

Each cell line responded similarly to both treatments and some clear parallels with cisplatin response emerged. Addressing paclitaxel treatment first, in sensitive PEA1, the lowest concentration used (5nM) was associated with an increase in JAK2, pJAK2, pERBB2, pSTAT3 and STAT3. Subsequent increases in paclitaxel concentration caused a progressive decrease in the activation of these proteins, in a highly analogous manner to those changes observed in response to cisplatin. Also like cisplatin exposure PEA2 did not experience any increase in the activity of these proteins instead, like cisplatin, paclitaxel caused a dose dependent decrease in JAK2, pJAK2, pERBB2 and pSTAT3. In this respect PEA1 and PEA2 respond to paclitaxel in a remarkably similar fashion to cisplatin. However unlike cisplatin, paclitaxel had no effect on the expression of cyclin D1 and had an opposite effect to cisplatin, on pERK1/2, which as opposed to increasing, fell, again accompanied by the reciprocal opposing change in levels of total ERK, which increased.

Response to doxorubicin treatment in PEA1 and PEA2 was more similar to cisplatin than paclitaxel dependant effects, with one exception. 2.5μM doxorubicin exposure caused a marked shut down of the ERBB2/JAK2/STAT3 axis. This was also associated with an increase in pERK and a decrease in cyclin D1, as seen for cisplatin. Interestingly 12.5μM doxorubicin resulted in an increase in pERBB2, pJAK2 and pSTAT3, relative to 2.5μM exposure, which occurred simultaneous to elevated pERK1/2 levels and decreased cyclin D1, implying this increase in ERBB2/JAK2/STAT3 was not due an error of dosing but a genuine feature of escalating exposure to doxorubicin.

Results obtained for PEO1 and PEO4 were very similar to PEA1/PEA2, paclitaxel caused a dose dependant decrease in JAK2, pJAK2 and pSTAT3, analogous to cisplatin, again like PEA1/PEA2 these decreases were not associated with any change in cyclin D1 and resulted in decreased pERK1/2. As with PEA1/PEA2 2.5μM doxorubicin was associated with a marked shutdown of JAK2/STAT3 signalling that was reversed when cells were exposed to

the higher concentration of 12.5μM. Again the higher (12.5μM) concentration of doxorubicin caused a step wise increase in pERK1/2 and decrease in cyclin D1.

7.3 Inhibition of ERK1/2 Phosphorylation Sensitises SKOV3 to Cisplatin and Doxorubicin. While Revealing Feedback Mechanism Involving ERBB2, JAK2 and STAT3 and that ERK1/2 Drives Cyclin D1 Expression

To investigate the mechanism and function of cisplatin/doxorubicin induced ERK1/2 phosphorylation the MEK1/2 inhibitor PD0325901 was used. In canonical MAPK signalling phosphorylation of ERK1/2 is carried out of MEK1/2 in a redundant fashion, of example MEK1 can phosphorylate ERK1 and ERK2 as can MEK2 [452]. Therefore were ERK1/2 activated via the MAPK pathway in response to cisplatin induced phosphorylation should be reversed by inhibiting MEK1/2. SKOV3 was used as a model due to its high level of pERK, pERBB2 and absolute ERBB2 expression. In order to focus on the consequences of inhibiting induced ERK activation as opposed to baseline activity cells were first exposed to cytotoxic for 6 hours before removal and treatment with 200nM of MEK inhibitor for an additional 18 hours. For caspase apoptosis assays SKOV3 was treated with two concentrations of cisplatin (15μM and 30μM) and doxorubicin (10μM and 20μM). A cisplatin IC_{50} assay was also conducted in which cells were exposed to a range of concentrations either alone or in combination with 200nM MEK inhibitor.

Treatment with PD0325901 had no effect on levels of apoptosis alone. However when combined with a cytotoxic agent either cisplatin (Figure 56A), or doxorubicin (Figure 56B), a potentiation of apoptotic induction was observed. This was perhaps most striking for 15μM cisplatin treated cells which experienced no increase in their levels of apoptosis alone however when combined with MEK1/2 inhibition levels of apoptosis increased 40%, ($p=0.12$ paired T-test). A failure to achieve significance was due to variation in the ratio of caspase induction between replicates however an increase occurred in each. Cells treated with 30μM cisplatin exhibited 1.8 fold levels of caspase induction and also experienced a 40% increase in apoptosis when treated in combination with PD0325901 ($p=0.0006$ paired T-test).

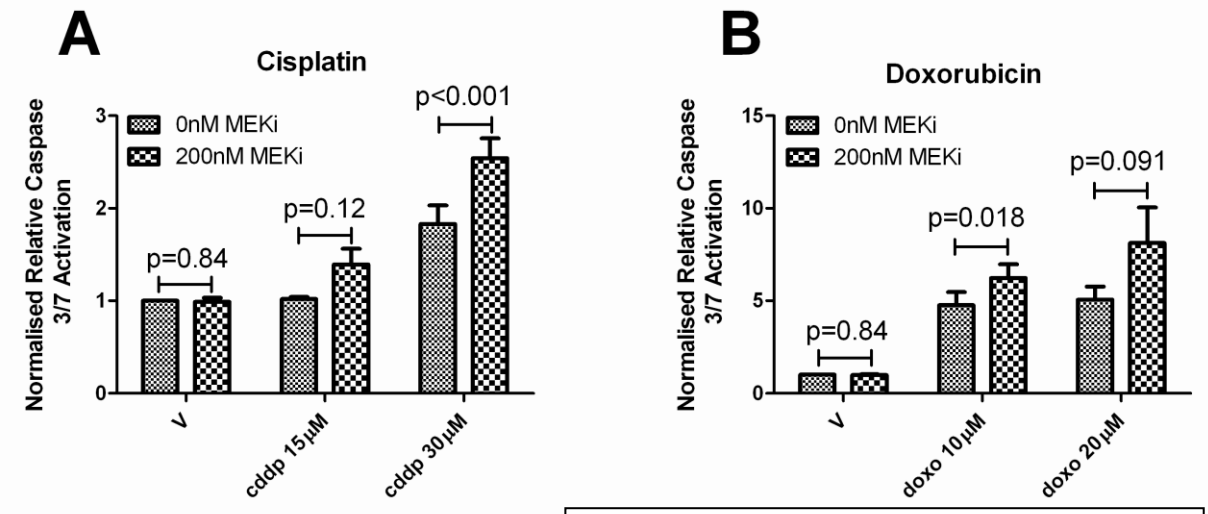

Figure 56. **A** and **B** caspase apoptosis assay in response to cddp and doxo treatment. Cells treated with either vehicle (V) or indicted concentration of cddp **A** or doxo **B** for 6 hours before addition of 200nM MEK inhibitor PD0325901 for 18 hours. Apoptosis/viability quantified using caspase glo/ MTT assays respectively. All values normalised to cell viability and V, 0nM MEKi. **C** – cisplatin IC_{50} shift. Cells treated to a range of concentrations of cddp either alone or in combination with 200nM MEKi for 72 hours prior to cell viability estimation using MTT assay. A + B n=4 C n=3. Errors bars represent SEM, p values calculated from paired T-tests.

A similar effect was observed in MEK1/2 inhibited cells treated with doxorubicin. Doxorubicin was a more potent inducer of apoptosis per mole of drug, than cisplatin. 10μM doxorubicin induced a 4.8 fold increase in apoptosis which increased to 5.5, a 16% increase, with the addition of MEK1/2 inhibition (p=0.018 paired T-test). Cell pre-treated with 20μM of doxorubicin experienced a similar degree of sensitisation in combination with the inhibitor levels of activated caspase 3/7 increased from 5 fold with cytotoxic alone to 6.2 in combination, a 23% increase (p=0.091). Again significance was not reached due the variation in the magnitude of sensitisation in each replicate.

Figure 56C shows the results of an IC_{50} shift assay for cisplatin in combination with PD0325901. A modest decrease in cisplatin IC_{50} in combination was observed suggesting that these compounds would combine synergistically in a more formal analysis, such as an isobologram.

Simultaneous to the carrying out of experiments in Figure 56 lysates were collected to allow of an assessment of the efficacy of PD0325901 to inhibit ERK1/2 in response to either cisplatin or doxorubicin and what the signalling effects of inhibition were.

Consistent with the greater magnitude of apoptotic induction, doxorubicin also induced a greater amount of pERK1/2. One of the initial questions arising from the observation of ERK1/2 activation in response to the range of stimuli above was what is mediating the activation. The addition of 200nM of the MEK1/2 inhibitor PD0325901 was able to completely reverse increased ERK1/2 activation suggesting that ERK1/2 activation in response to either of these DNA damaging agents is MEK1/2 dependent. ERK1/2 are able to regulate the expression of CCND1 via the activation of FOS and JUN [451]. To prevent over saturation of the band relating to pERK it is not possible to see background levels of activity however inhibition of this base line activation of ERK1/2 had a marked effect on the expression of cyclin D1, shown in the first two lanes of vehicle -/+ inhibitor. Both DNA damaging cytotoxics behaved as previously demonstrated. Cisplatin reduced levels of pERBB2 JAK2/pJAK2/pSTAT3 and cyclin D1, while activating pERK1/2. The addition of MEK inhibition however reversed cisplatin dependent changes in each of these proteins. For both concentrations of cisplatin used reductions in these proteins, in some cases, were not only reversed but increased beyond background levels. This is perhaps most clear for 15μM cisplatin treatment where reductions in pERBB2, pJAK2, JAK2, and pSTAT3 with cytotoxic alone are associated with a greater than control rebound on the addition of MEK1/2 inhibition. Crucially this inhibitor dependent rebound appears to be mediated by changes in JAK2 expression, the only protein which appeared to experience a change its absolute abundance.

The MEK inhibitor dependent rebound is broadly recapitulated in combination with doxorubicin, with the caveat that as seen in PEO1/PEO4 and PEA1/PEA2 the concentrations of doxorubicin used here induce pERBB2 as a single agent. Interestingly this increase in pERBB2 occurs despite a substantial reduction in JAK2, suggesting a factor other than JAK2 is responsible for inducing pERBB2 at these high concentrations of cytotoxic. Paclitaxel treated lysates were also included to control for the effects of inhibition of background activity of ERK1/2. While 30nM paclitaxel behaved in the same manner as for PEO1/PEO4 and PEA1/PEA2 reducing JAK2, pJAK2, pERBB2 and pSTAT3 there was no rebound of the activity of these proteins with the addition of MEK inhibition.

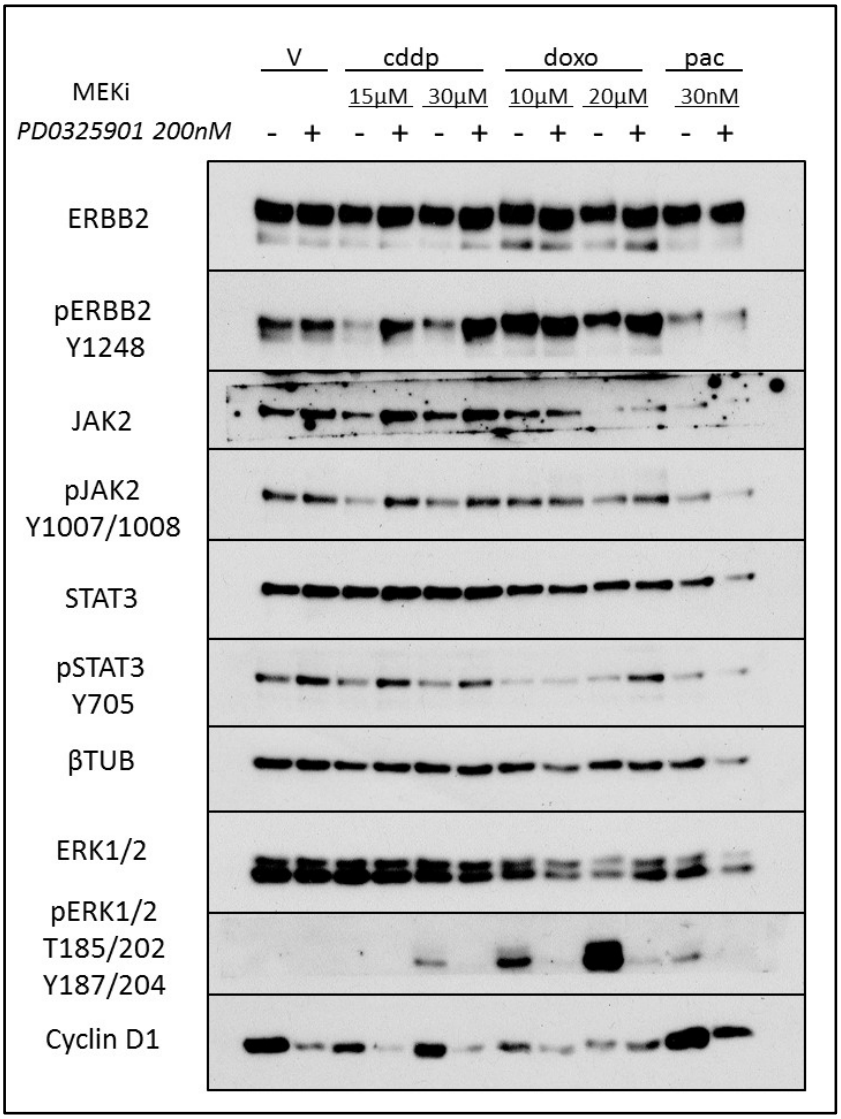

Figure 57. Western blot analysis of the effect of MEK1/2 inhibition in combination with either cisplatin (cddp), doxorubicin (doxo), or paclitaxel (pac). Cells were treated with the indicated concentration of cytotoxic for 6 hours before treatment with 200nM PD0325901. Lysates from two biological replicates were examined and the results were consistent.

Discussion :- Results Chapter 7

7.1 ERK1/2 are Phosphorylated in Response to JAK2 Knockdown, JAK2 Inhibition, Cisplatin and IL6 Treatment

ERK1/2 phosphorylation in response to cisplatin exposure has been observed in other systems including neuronal tissue [453] and hepatocellular carcinoma cells [454] suggesting it is a ubiquitous effect and not unique to ovarian cancer. The incidence of ERK1/2 activation in response to a range of stimuli, JAK2 inhibition and siRNA, GP130 siRNA and cisplatin, raises a number of possibilities. It suggests a feedback mechanism operates which detects reductions in the activity of one of more proteins down-stream of GP130, capable of resulting in the activation of ERK1/2. It is tempting to speculate that this increase in ERK1/2 phosphorylation might act to compensate for the growth inhibitory effects of JAK2/GP130 down regulation. This theory is given some credence by the fact that both pathways regulate the expression of CCND1.

Given STAT3's transcriptional regulation of CCND1 it would be interesting to examine ERK1/2 activation in response to STAT3 knockdown to see whether this was able to recapitulate the effects of JAK2 and GP130 knockdown. However as GP130 knockdown activated ERK1/2 in PEA2, when no change in pSTAT3 levels occurred, it suggests against STAT3 being capable of activating ERK1/2.

Given that both JAK2 perturbation and cisplatin treatment were associated with reductions in levels of Y1248 phosphorylated ERBB2, a SHC1 docking site [455], simultaneous to increased ERK1/2 phosphorylation suggests that activation in these circumstances is independent of ERBB2 and probably all ERBB family members. It would be interesting to combine cisplatin or doxorubicin treatment with the ERBB2 inhibitor CP-724714 or other ERBB family inhibitor, to examine whether this would have prevented the ERK1/2 activation associated with either of these cytotoxics.

A common feature of ERK1/2 signalling, and another apparent feedback loop, was the reciprocal relationship between phosphorylated and absolute levels of protein. Increases in activated ERK1/2 occurred at the expense of levels of absolute expression of the protein. This difference cannot, apparently, be accounted for by the most parsimonious explanation, that

the total ERK1/2 antibody does not detect the phosphorylated from of the protein, as the immunogen is located by the C-terminal region of either protein and does not overlap with either phosphorylation site (Cell Signalling personal communication). Unlike PEA1 and PEA2, ERK1/2 phosphorylation was reduced in SKOV3 treated with IL6. The reasons for this are not clear but it does further highlight the reciprocal relationship between levels of the phospho and total protein. As the reduction in pERK1/2 caused by IL6 was also associated with the corresponding opposite effect on total ERK, suggesting this reciprocal change in levels of phospho and total protein is not a nuance of either cisplatin exposure, or JAK2 knockdown but mediated directly by a sensing for the levels of ERK activation itself.

7.2 Signalling through ERBB2, JAK2, STAT3 and ERK1/2 are also affected by Other Cytotoxic Compounds.

The factors contributing to transcriptional downregulation of JAK2, in response to cisplatin, which appears to be one of the initiating steps in eliciting the other pathway changes described in chapter 2, are unknown. Signalling changes in the ERBB2/JAK2/STAT3 axis could have been unique to cisplatin. Results presented in Figure 55 provide evidence that changes in this signalling axis are common to cisplatin, doxorubicin and paclitaxel. Despite the number of similarities that emerged from this experiment there were some interesting differences.

For example it suggested that the role STAT3 plays in maintaining the expression of cyclin D1 is small. The highest concentration of paclitaxel used (20nM) resulted in marked reductions in pERBB2, JAK2, pJAK2 and pSTAT3 in all lines tested, but there was no effect on cyclin D1 expression. At first appearances it may seem odd that the expression of cyclin D1, a protein whose expression would be expected to change significantly through the cell cycle and is required for G1/S transition, would remain unchanged in paclitaxel treated cells, paclitaxel a drug which causes profound G2 arrest by inhibiting cytokinesis. However cyclin D1 levels have been shown to peak in both G1 and G2 phase [456].

It is also difficult to reconcile the results obtained in relation to JAK2 inhibition and knockdown activating ERK1/2 and the fact that paclitaxel, while mimicking these stimuli, not only failed to activate ERK1/2 but in fact caused a reduction in phosphorylation. This result

implies that the cue for ERK1/2 activation is not JAK2 but something downstream of it that is apparently unaffected by paclitaxel treatment.

Response to doxorubicin was perhaps more similar to cisplatin, at the lower dose of 2.5μM, predicted changes in signalling of ERBB2, JAK2 and STAT3 were observed. However at the higher dose of 12.5μM doxorubicin a reversal of those changes was observed, in each cell line this higher dose was associated with increased pSTAT3 relative to 2.5μM treated cells and in some cases more than untreated controls. It is relevant to point out here that this higher dose probably confers and far higher cytotoxicity than an eqimolar dose of cisplatin, based on the levels of caspase 3/7 activation seen in SKOV3 in Figure 56. As such an equivalent dose of cisplatin would probably be in excess of any used in this thesis. The implications of which being two fold. First it raises the possibility that this effect could be mimicked by cisplatin at sufficiently high dose. Second it questions the results in terms of their pharmacological relevance, if those concentrations could never be achieved clinically. Purely mechanistically it remains interesting, and is discussed in more detail in the next section in relation to SKOV3 response to doxorubicin.

7.3 Inhibition of ERK1/2 Phosphorylation Sensitises SKOV3 to Cisplatin and Doxorubicin. While Revealing Both That, ERK1/2 Drives Cyclin D1 Expression, and a Feedback Mechanism Involving ERBB2, JAK2 and STAT3

Despite the rather narrow substrate specificity of MEK1/2, ERK1/2 have hundreds of target substrates [457]. Effects of ERK1/2 activation are pleiotropic and variable. Generally these effects are considered proliferative, anti-apoptotic and migratory. They achieve this, in part, by phosphorylating a family of transcription factors known as the ternary complex factors or TCFs which includes FOS and JUN. Once phosphorylated by ERK1/2 these proteins dimerise forming a complex known as activating protein 1 (AP1) and up regulate the expression of genes associated with cell cycle progression including CCND1. ERK1/2 also activates the ternary complex factor MYC whose mutation, and in the case of ovarian cancer, amplification is frequent. Transcriptional targets of MYC include POLD2 (Polymerase (DNA directed), delta 2, regulatory subunit) HK2 (Hexokinase 2) genes involved in DNA synthesis and metabolism respectively [458]. ERK1/2 activation can also directly result in the inhibition of apoptosis by activating BCL-xL and MCL-1, by inhibiting caspase 8/9, BIM and BAD while enhancing DNA repair by activating ERRC1 and ATM [459]. It is therefore perhaps only

surprising that the magnitude of sensitisation to either cisplatin or doxorubicin achieved by inhibiting ERK1/2 activation in Figure 56A and B wasn't higher.

It is not unknown for signalling pathways to exert negative feedback on related or partially redundant pathways. The consequence of inhibiting such pathways is to relieve such negative feedback leading to compensatory increases in activation that can act to undermine the effectiveness of single agent inhibitor therapies.

For example AKT and PI3K inhibitors have been shown to reduce inherent negative feedback on ERBB receptors leading to partial reactivation of the pathway and activation of RAS/RAS/MEK/ERK signalling [460,461].

Similarly the ability of MEK inhibition to cause an increase in activity of the PI3K pathway was found to be an important determinant of resistance to these inhibitors as single agents in breast cancer models [462]. More recently it was discovered that the mechanism of negative feedback from the RAS/RAF/MEK pathway to PI3K is in part mediated by an inhibitory threonine phosphorylation of ERBB3. Under conditions of MEK inhibition this inhibitory marker is reduced contributing to ERBB3's hyper-activation and the subsequent activation of AKT [463].

However the ability of MEK1/2 inhibition to contribute to increased ERBB2,JAK2 and STAT3 activation is novel and has not been reported elsewhere. Also data presented here, in Figure 57, has suggested that this feedback is partly driven by an increase in JAK2 expression. MEK1/2 inhibition was associated with an increase in JAK2 protein expression that based on data presented in this thesis would be predicted to drive increased activation of both ERBB2 and STAT3, again highlighting the importance of this protein in maintaining active signalling to these two important oncogenes. This data is only preliminary and further investigation would be required to establish whether JAK2 expression is a functional driver of this phenomena.

For example the addition of either JAK2 siRNA or a JAK2 inhibitor to MEK1/2 inhibition would allow an assessment of the importance of JAK2 in driving the observed increases in STAT3 and ERBB2 activation. It would also be interesting to address the mechanism of apparent JAK2 overexpression using QRT-PCR and proteasomal inhibitors. Especially as Turke et al have demonstrated MEK inhibition dependant increases in ERBB3 activity that could account of the increase in ERBB2 phosphorylation described here.

Interestingly our group has also investigated the signalling consequences of AKT inhibition using the compound GSK-795 by reverse phase protein array in SKOV3. SKOV3 tumour xenografts experienced a modest but significant up regulation of pERK1/2,

pMEK1/2, pRAF1 but not SHC1 (unpublished data). Suggesting this feedback mechanism operates in ovarian cell lines and could act to reduce the efficacy of AKT inhibitors.

It would be relevant to attempt to reproduce MEK1/2 inhibitor dependent PI3K feedback in other cell lines not driven by either ERBB2 over expression or ERBB1 mutation, as thus far this feedback mechanism has only been shown in this background. Especially as the targeting of these pathways is a potential therapeutic strategy for a number of cancers, particularly those harbouring activating RAS/RAF or PI3K mutations, and the existence of feedback between these pathways in such situations could have important implications of the efficacy of such treatment. Some of the ovarian HGS cell lines used here would represent a potential intermediate model being not ERBB2 amplified but moderately activated for ERBB1/2.

A future experiment highlighted by this data would be the combination of, for example a GP130 blocking antibody with MEK1/2 inhibitor plus a cytotoxic agent. This assumes that a GP130 blocking antibody was capable of recapitulating the effects of siRNA mediated knockdown. Given the reciprocal activation of these pathways in response to inhibition of the other, and the ability of inhibition of either GP130 or MEK1/2 to sensitise to cisplatin, implies that simultaneous targeting of both pathways is a good candidate for achieving synergy.

This notion is supported by the precedent that blockading mechanistic feedback between RAS/RAF/MEK and PI3K pathways using dual inhibition combines synergistically in response to a number of different compounds [464] and in a number of different systems [465] and both *in vitro* and *in vivo* [466].

The observation of ERK1/2 activation in response to GP130/JAK2 knockdown and JAK2 inhibition and now the reciprocal MEKi dependent feedback resulting in an increase in JAK2 expression and pSTAT3 highlights the importance of understanding not just the immediate downstream signalling effects of a particular inhibitor but the wider signalling changes. This is important as the more targeted therapies are brought into the clinic the more likely it seems that tumours will develop means to ameliorate or entirely circumvent the challenge they presented. Indeed the examples listed above suggest cancer cells are inherently poised to attenuate the potential impact of targeted therapies and therefore in order to have the best chance of delivering effective treatments it will probably become necessary to predict *in vitro* likely resistance mechanisms that develop *in vivo* to a particular therapeutic in order to maximise the efficacy or treatment using dual inhibition or at least to be ready with the next target when relapse occurs. Therefore based on the evidence present here it

would seem prudent to investigate the ability of ERBB2/JAK2/STAT3 activation to reduce the effectiveness of MEK1/2 inhibition and vice versa to better understand how tumours *in vivo* might respond to the inhibition of either pathway, and whether combination inhibition could be used to circumvent this potential problem.

Summary and Conclusions

1. The Identification of JAK2 as a Regulator of Response and Resistance to Cisplatin

A Summary of the Data

Cisplatin Upregulates *IL6*

Microarray analysis of the isogenic HGS ovarian cell line pair PEO1/PEO4 revealed that *IL6* mRNA expression was induced by cisplatin and to a greater degree in the sensitive line PEO1. This result was replicated and extended in the additional isogenic pair PEA1/PEA2 revealing cisplatin dependant *IL6* upregulation is concentration dependent and occurs on the same time scale. Maximal upregulation occurred at the same time point in each cell line and fold increases in expression were also higher in cisplatin sensitive lines.

Cisplatin Downregulates JAK2 Transcriptionally, Which is Associated with Reduced pSTAT3 and pERBB2

Given the link between IL6 and STAT3 activation, cisplatin treated cells were examined for their levels of pSTAT3 and pJAK2 at the times points exhibiting upregulation of IL6. IL6 expression did not correlate with either pSTAT3 or pJAK2 levels. In fact the opposite was observed. Sensitive cells treated with 2.5μM cisplatin were associated with increased pSTAT3 and pJAK2 however this was reversed at 5μM, despite this concentration being associated with increased *IL6* expression. Resistant cells were either unchanged or exhibited reduced pSTAT3 and pJAK2 at 5μM and increasing the concentration of cisplatin to 12.5μM resulted in clear reductions in both, again despite an associated increase in *IL6* expression.

The implications of these apparently contradictory results are twofold. Firstly it suggested a disconnect between IL6 and STAT3, in which IL6 expression was potentially

compensating for reductions in pSTAT3. Secondly it suggested that sensitive and resistant cell lines might respond differently, in their activation of these two proteins, to cisplatin.

Resistant Cells Downregulate JAK2, pSTAT3 and pERBB2 with Greater Sensitivity to Cisplatin

To investigate this possibility further a cisplatin titration was carried out. It revealed that resistant cells exhibit significantly different dose responses for JAK2, pERBB2 and pSTAT3 than their sensitive counterpart. Cisplatin resistant cells responded more sensitively in reducing the activation of ERBB2, JAK2 and STAT3 (pSTAT3 profile did not significant differ between PEO1 and PEO4). Additionally a high correlation was observed between pJAK2 and pERBB2 suggesting that these two proteins were in tight co-regulation possibly with one phosphorylating the other.

The cisplatin titration had suggested that unlike STAT3 and ERBB2, changes in which were predominantly at the phospho level, cisplatin regulated absolute JAK2 protein expression. To examine the nature of this regulation further *JAK2* mRNA expression was assayed after cisplatin exposure. This showed that observed changes at the protein level were mirrored by those at the mRNA level. Suggesting that cisplatin dependant changes in JAK2 protein expression were initiated at the transcriptional level.

Subsequently establishing both whether JAK2 plays a functional role in regulating these proteins and whether cisplatin dependant changes in the activation/expression of these proteins had a phenotypic impact on drug response was the focus of a number of further experiments. The ability of JAK2 to both regulate the activity of STAT3 and ERBB2 as well as play a functional role in response to cisplatin was assessed. This was investigated using; JAK2 inhibition, with TG101348, JAK2 siRNA and transient JAK2 overexpression.

JAK2 inhibition Protects Cells from Cisplatin Induced Apoptosis and Reduces pSTAT3 and pERBB2

Whereas activation of STAT3 with IL6 resulted in sensitisation to cisplatin, JAK2 inhibition had the opposite effect. TG101348 both reduced background apoptosis as well as protecting cells from cisplatin induced apoptosis. The inhibitor had growth inhibitory effects, reducing proliferation in a dose dependent fashion. The extent that growth inhibition could

account for reductions in cisplatin induced apoptosis are not clear. However the ability of JAK2 inhibition to reduce background apoptosis suggests proliferation doesn't account for the entire effect and therefore implicates JAK2 in regulating the expression/activity of genes involved in apoptosis.

Providing the first evidence of a function role for JAK2 in regulating the activity of both ERBB2 and STAT3, JAK2 inhibition reduced the phosphorylation of both genes again in a dose dependent fashion. The ability of an ATP competitive kinase inhibitor to elicit this effect also implies that, despite cisplatin dependent changes in JAK2 protein expression, it is its kinase activity that is responsible for regulating STAT3 and ERBB2, notwithstanding that there may be additional effects, due to reducing total protein expression, that were not reproduced here.

JAK2 Knockdown and Overexpression Recapitulate Inhibitor Data

As the specificity of inhibitors is sometimes subject to speculation, siRNA mediated knockdowns using multiple different siRNAs were used to validate results generated with TG101348. JAK2 knockdowns were able to recapitulate the effects of inhibition. Each siRNA reduced proliferation rates and the activation of ERBB2 and STAT3. Reductions in STAT3 were unambiguously at the level of phosphorylation, despite a modest effect on total protein expression. Reductions in pSTAT3 observed in response to JAK2 inhibition were to a greater extent than RNAi, despite highly efficient knockdowns, suggesting an off target effect was responsible for the additional reduction. In comparison the nature of the interaction between JAK2 and ERRB2 was ambiguous. The use of SKOV3, an ERBB2 overexpressing cell line suggested that JAK2's regulation of ERBB2 was at the total protein level, in contradiction with results from the cisplatin titration showing no significant effects on ERBB2 protein expression. Although reductions in JAK2 expression with siRNA were higher in magnitude than the highest concentration of cisplatin used, which might account for this effect.

The ability of JAK2 inhibition to protect cells from cisplatin induced apoptosis suggested that perturbation of JAK2 would combine antagonistically with the drug. This was more formally assessed in response to JAK2 RNAi using IC_{50} shift assays. JAK2 knockdown increased cisplatin IC_{50}, providing strong evidence of an antagonistic effect. This should be addressed in the form of an isobologram to provide a definitive result.

The final technique used to investigate the role of JAK2 was over expression. The results of which were also broadly in accordance of those generated from inhibition and knockdown. JAK2 overexpression increased proliferation rates in PEA1 and SKOV3 and increased the activation of STAT3 and ERBB2. Again increases in STAT3 were unambiguously at the level of phosphorylation whereas cell line differences emerged in changes in ERBB2. However overexpression of wild type JAK2 consistently increased levels of phosphorylated ERBB2.

In Conclusion

This suggests a model of acquired resistance to cisplatin being, in part, mediated by JAK2, which in response to cisplatin exposure is down regulated at the transcriptional level. This transcriptional downregulation initiates a sequence of events which render the cell refractory to cisplatin cytotoxicity. The apparent importance of this pathway is underlined by the fact that it appears to have been selected for in both pairs of cisplatin resistant cell lines examined, PEO1/PEO4 and PEA1/PEA2. Cisplatin resistant cells downregulated JAK2 with greater sensitivity than their sensitive partner, and this was passed on to downstream proteins which were also more sensitively deactivated after cisplatin exposure in resistant cells. Downregulation of JAK2, in combination with cisplatin, conferred a survival advantage suggesting resistant cells receive a greater survival advantage due to their greater sensitivity to this downregulation.

Downregulation of JAK2 at both the mRNA and protein level causes reductions in STAT3, ERBB2 and possibly the signalling of an as yet unidentified factor(s). The consequence of which is to reduce proliferation rates possibly by reducing the expression of CCND1. Either via reduced proliferation or other changes in gene expression cells are better able to resist the genotoxic effects of cisplatin. While it seems unlikely that STAT3 is exclusively responsible for mediating these effects the presence of lower constitutive activation in PEA2, relative to PEA1, again suggests this pathway is selected for either, deactivation or greater sensitivity to deactivation in the acquisition of cisplatin resistance.

While knocking out STAT3 caused an increase in apoptosis, JAK2 inhibition was associated with reductions in both background and cisplatin induced apoptosis suggesting that these effects could not be mediated by STAT3.

Future Experiments

While STAT3 was responsible for mediating some effects of JAK2 downregulation it cannot account for them all. Specifically JAK2 inhibition reduced background apoptosis but STAT3 knockdown was associated with an increase. JAK2 dependent ERBB2 deactivation seems unlikely to account for this. In addition, JAK2 RNAi reduced pSTAT3 by a smaller degree than direct STAT3 knockdown despite this it was associated with greater reductions in doubling time in all cell lines. If JAK2 knockdown has a larger phenotypic effect while having a modest effect of pSTAT3, and greater reductions in pSTAT3 are associated a reduced phenotypic effect then it follows that there must be other factors mediating this reduction in proliferation. Screening the phosphorylation of JAK2 targets in a candidate fashion may reveal the factors responsible for mediating these additional effects of JAK2 ablation.

Data presented here has suggested antagonism between JAK2 perturbation and cisplatin. In order to validate whether this is true it would be necessary to carry out an isobologram analysis. This could easily be conducted with TG101348 and cisplatin. If confirmed this would have important implications for the use of any JAK2 inhibitor in a clinical setting and is relevant as inhibiting STAT3 has received some attention, not just ovarian cancer, as a potential for adjuvant therapy [467].

It would be interesting to investigate the nature of JAK2 downregulation post cisplatin treatment specifically what makes resistant cells more sensitive to it. This could take the form of screening known JAK2 transcription factors for cisplatin dependent expression changes. Failing this mRNA and miRNA expression arrays could help to identify unknown regulators of JAK2 expression.

2. Effects of JAK2 perturbation are in Part Mediated via STAT3

A summary of the Data

IL6 Sensitises To Cisplatin

IL6 activation of STAT3, interfering with cisplatin dependent deactivation, sensitised cells to chemotherapy, providing evidence that deactivation of STAT3 plays a functional role

in cisplatin response protecting the cell from cytotoxic induced cell death. Exposure of cells to either rIL6 alone or in combination with rsIL6RA referred to as IL6(RA), as both were required for STAT3 activation in PEA1 and PEA2, was associated with a significant increase in cisplatin induced apoptosis. Cells also experienced modest reductions in their cisplatin IC_{50}, providing the first functional data suggesting deactivation of STAT3 was protective to cisplatin, with the caveat the IL6 might not be functioning exclusively via STAT3.

STAT3 Knockdown and Overexpression Recapitulate the Effects of IL6

STAT3 knockdown and overexpression were able to inhibit and promote proliferation respectively. Increased proliferation associated with STAT3 overexpression was dependent on the ability of STAT3 to be phosphorylated at tyrosine 705. STAT3 knockdown and overexpression were able to decrease and increase respectively, the expression of the proliferative factor cyclin D1 as well as BCLxL/S.

Similarly to JAK2, STAT3 knockdowns were associated with an increase in cisplatin IC_{50} and overexpression caused an increase in the ratio of activated caspase 3/7 induced by cisplatin, again the presence of Y705 was required for this effect. However unlike JAK2 inhibition, STAT3 RNAi was not associated with protecting cell from cisplatin induced apoptosis. Instead STAT3 knockdowns increased background levels of apoptosis.

Background levels of STAT3 phosphorylation were also found to be lower in resistant PEA2s relative to its sensitive partner.

In Conclusion

Perturbation of STAT3 was able to recapitulate the majority of the effects observed for JAK2, suggesting that STAT3 directly mediates some of these effects. A number of studies have suggested a link between STAT3 activation and resistance to chemotherapy, including cisplatin. One effect of JAK2 knockdown that appears, at least in part, mediated by STAT3 is an increase in cisplatin IC_{50}. Suggesting STAT3 inhibition would combine antagonistically with cisplatin, therefore any therapy designed to target STAT3 would likely make a poor adjuvant for cisplatin in a clinical setting. However targeting STAT3 as a single agent strategy might have some efficacy as it seems would both inhibit growth and induce apoptosis in a tumour specific manner.

The apparent selection for greater sensitivity to downregulating JAK2 expression in response to cisplatin exposure is supported by the observation of significantly lower levels of background STAT3 activation in PEA2 relative to PEA1.

JAK2 does not exclusively maintain constitutive pSTAT3 in these cell lines. Cisplatin exposure was able to reduce STAT3 phosphorylation by around 90% in all cell lines when exposed to concentrations of cisplatin of 15μM or above. However knockdown of JAK2 which was associated with large reductions in JAK2 protein expression, greater than those observed in response to cisplatin exposure, did not reduce STAT3 phosphorylation to the same extent. This implies two things, firstly, that there are additional kinases phosphorylating STAT3 and second, that their activity is also modulated by cisplatin. The most obvious candidate would be JAK1 and indeed this seems to be the case for SKOV3. GP130 knockdown in SKOV3 was superior to JAK2 knockdown in reducing STAT3 activation. JAK1 has been shown to be constitutively bound to GP130 [231] therefore reducing GP130 expression would be predicted to reduce the activity of this STAT3 kinase. This however was not the case of all cell lines as GP130 knockdown in PEA2 or PEA1 did not reduce pSTAT3. This fact does not preclude JAK1 from maintaining phosphorylation of STAT3 in PEA1/PEA2 or any other cell line, but not via GP130. This also might explain why JAK2 inhibition was more efficient at reducing STAT3 phosphorylation than JAK2 RNAi, due to the off target effects on another STAT3 kinase, such as the paralogous JAK1 and the highly homologous JAK3.

Cyclin D1 expression was downregulated by STAT3 knockdown, however the extent to which this accounts for growth inhibitory effects of reductions in STAT3 were not investigated. Comparing the extent of cyclin D1 knockdown in response to different STAT3 siRNAs implies that differential expression of other transcription targets accounts for the majority of the effect. siSTAT3 3 which most efficiently reduced protein expression had no effect on cyclin D1 levels, suggesting STAT3 reduces the expression of addition factors driving proliferation.

Future Experiments

In common with JAK2, IC_{50} shift assays suggested STAT3 RNAi would combine antagonistically with cisplatin. An isobologram analysis using a STAT3 inhibitor would address the genuine existence of antagonism. The STAT3 SH2 domain inhibitor static has

been shown in vitro to reduce the activation dimerisation and nuclear translocation of STAT3 and would allow this question to be addressed [468].

As previously discussed the role cyclin D1 plays in STAT3 RNAi induced growth inhibition was not investigated. The ability of interference of STAT3 regulated genes to recapitulate the STAT3 RNAi phenotype, coupled with overexpression rescue experiments could help identify those downstream factors mediating these effects. MYC represents a potential transcriptional target that could account for the observed effects, that warrants investigation.

It would be relevant to investigate additional paired cell lines for background STAT3 activation to address whether a reduction in activation is a common feature of acquired resistance as this would likely have important implications for our understanding of the targets of selection for acquired resistance.

Data presented here suggests that kinases, additional to JAK2, contribute to the activation of STAT3. An siRNA screen, initially of other JAKs and then potentially SRC/ERBB family members, might allow the identification of such activators. Whatever the additional contributing kinase(s) might be, they also appear to be differentially regulated by cisplatin. Should the hypothesised additional STAT3 kinase be identified, an examination of its activation in response to cisplatin treatment, with reference to any differences between sensitive and resistant cell lines, would confer additional information regarding the nature of cisplatin response and whether like JAK2 such a kinases was subject to differential regulation associated with acquired resistance.

3. JAK2 Regulates ERBB2

A Summary of the Data

Levels of pJAK2 and pERBB2 correlate highly

Fluctuations in both the activation and expression of JAK2 and ERBB2 proteins correlated highly. This correlation was most strongly experienced between phosphorylated forms of both. The apparent tight co-regulation of these kinases raised the possibility that one

phosphorylates the other. An interaction between JAK2 and ERBB2 has previously been reported which was linked to activation of STAT3 [316].

JAK2 Inhibition, Knockdown and Overexpression modulate the activity of ERBB2

The JAK2 inhibitor TG101348 provided the first indication of a regulatory link between JAK2 and ERBB2. Treatment with the inhibitor was associated with a dose dependent decrease in levels of tyrosine 1248 phosphorylated ERBB2. Similarly JAK2 RNAi was also associated with reductions in pERBB2. Problems with antibody sensitivity had prevented the assaying for total ERBB2 protein levels in response to JAK2 inhibition. This problem was ameliorated with the acquisition of a higher sensitivity antibody; however it remained only possible to reliably detect expression in the ERBB2 amplified cell line SKOV3. Results from JAK2 knockdown in SKOV3 suggested that changes in phosphorylation of ERBB2 are driven at the total protein level. This was supported by overexpression of ERBB2 in PEA1 which also appeared to be driven by changes in protein expression. In PEA1 increased expression of ERBB2, caused by JAK2 overexpression, was reversed by mutation of the dual tyrosine residues in the activation loop of JAK2's kinase domain. The situation was somewhat different in SKOV3 in which JAK2 overexpression resulted in elevated pERBB2 but not absolute protein expression. In addition this effect was not reversed by overexpression of the kinase inactive form of JAK2 (Y1006/1007F).

No direct interaction between JAK2 and ERBB2 was detected despite multiple attempts using different methods to maximise the sensitivity of the assay.

In Conclusion

On balance it appears that JAK2 regulates ERBB2 expression and changes in phosphorylation are a surrogate of changes at the protein level. An insensitivity to detect small changes in ERBB2 protein expression, in SKOV3, as a consequences of modest changes in JAK2 in response to cisplatin treatment and overexpression may account for the contradictory results. Of example results of the cisplatin titration and overexpression in SKOV3 suggested total protein levels did not change markedly

Secondly on balance it appears that this regulation is dependent on the kinase activity of JAK2, as the inhibition had the same effects as knock down and the kinase dead mutant

revered effects of JAK2 over expression, in PEA1. This would suggest a scenario in which conventional JAK2 activity phosphorylating one of its substrates was responsible for the transcriptional upregulation of ERBB2.

Future Experiments

The nature of the interaction between JAK2 and ERBB2 is not clear. Protein assays with greater sensitivity than western blotting such as ELISA, could be used to establish whether JAK2 perturbation was associated with changes at the total of phospho protein level in cell lines other than SKOV3. Assuming that, as suggested above, regulation for ERBB2 is at the total protein level a combination of QRT-PCR and the use of MG132 could be used to examine whether changes in the protein levels were driven by transcriptional changes or protein degradation. Given that some data presented here has suggested different behaviour, in terms of the interaction between JAK2 and ERB2, between amplified SKOV3 and other non-amplified lines it would be relevant to investigate other ERBB2 positive cell lines such as SKBR3. This would also allow these effects to be generalised to non-ovarian models.

4. EBRR2 is Frequently Activated in HGS Cell Lines where it Promotes Cisplatin Resistance

A Summary of the Data

High Grade Serous Cell Lines Contain Elevated Phosphorylation of ERBB2 Y1248 without Overexpression

Examination of the activation of ERBB2 at Y1248 revealed that each HGS cell line, 6/6, possessed elevated levels relative to the normal control OSE-C2 and A2780, which most probably is endometrioid or clear cell line in origin. Phosphorylation in these lines was not as high as observed in the ERBB2 amplified line SKOV3, which contained around 3.5 times as much. To address whether elevated phosphorylation might be driven by an increase expression QRT-PCR was performed. mRNA levels between all cell lines examined was very similar with the exception of SKOV3 which expressed in the order of 40 times more *ERBB2*.

Reference to publicly available data has shown that none of the isogenic paired cell lines are amplified for ERBB2 [416].

Sensitivity of ERBB2 Inhibition depends on Phosphorylation and Inhibition Sensitises Cells to Cisplatin

The selective ERBB2 inhibitor CP-724714 was used to investigate the role phosphorylation of ERBB2 plays both promoting growth and cisplatin resistance. Levels of Y1248 phosphorylation inversely correlated with the IC_{25} of cell lines to inhibition. Cells with higher levels of phosphorylation were generally were more sensitive to inhibition. This was most clear in the difference between the two cell lines with little or no pERBB2, OSE-C2 and A2780, and the remainder of the cell lines with elevated levels. As ERBB2 amplification has been associated with resistance to chemotherapy the ability of CP-724714 to sensitise cells to cisplatin was investigated. CP-724714 potentiated cisplatin induced apoptosis in a dose dependent fashion, in cell lines with elevated ERBB2 but not the normal control OSE-C2.

In Conclusion

ERBB2 amplification has been observed in around 5% of ovarian tumours however the presence of elevated phosphorylation without overexpression appears novel. While ERBB2 phosphorylation was not as high as the amplified cell lines SKOV3 and SKBR3 (data not shown for SKBR3) is was significantly elevated above controls. Despite the lower levels of phosphorylation in HGS compared to SKOV3 it was functional driving proliferation.

Perhaps most strikingly this elevated phosphorylation was observed in 100% of the HGS cell lines investigated suggesting this might occur in a significant proportion of cases.

The use of the ERBB2 inhibitor CP-724714 suggested that targeting ERBB2 would be tumour specific and have efficacy as both a single agent and in combination with cisplatin. Results presented here certainly warrant further investigation with regard to combining these two compounds.

Future Experiments

The two most important experiments required to take these discoveries forward would be first, an *in vivo* validation of increased ERBB2 activation. Second a further examination of the interaction between ERBB2 inhibition and cisplatin treatment. Evidence from breast lines suggest the two will combine synergistically [346] however this was in an ERBB2 amplified background and the vast majority of HGS ovarian tumours are not. It would be relevant to show synergy in an isobologram in a HGS non amplified cell line.

However if these two criteria were satisfied then ERBB2 would make an attractive target for adjuvant cisplatin therapy.

5. GP130 Promotes Growth, Platinum and Resistance, Revealing Different Pathways to STAT3 Activation

A Summary of the Data

QRT-PCR analysis of isogenic cell line pairs revealed that GP130 is overexpressed in PEA2 and PEO23 but not PEO4 relative to their cisplatin sensitive partners. QRT-PCR validated previous microarray data which also showed a borderline significant overexpression of GP130 in the *in vitro* selected cisplatin resistant derivative PEO1cddp.

GP130 knockdown in SKOV3 and PEA2 but not PEA1 or PEO4 resulted in growth inhibition and the potentiation of cisplatin induced apoptosis. At the protein level GP130 knockdown caused a reduction in the phosphorylation of STAT3 in SKOV3 but not PEA2, PEA1 or PEO4.

Conclusion

GP130 has not been previously reported as playing a role in drug resistance and to the author's knowledge this is the first reference to either the presence of overexpression associated with cisplatin resistance or the ability of GP130 knockdown to sensitise to

cisplatin. GP130 has been shown to promote tumour growth in breast cancer cell lines, in which GP130 was shown to regulate STAT3 [444].

In support of GP130 overexpression, reference to publically available copy number data for the paired isogenic cell lines showed GP130 is also amplified in PEA2 relative to PEA1 [416], suggesting that various factors contributing to GP130 upregulation have been selected for in the acquisition of cisplatin resistance.

A number of different factors have been shown to contribute to STAT3 phosphorylation and accordingly it appears that pathways leading to constitutive STAT3 activation differ between SKOV3 and the other cells lines investigated. In SKOV3, STAT3 activation appears to be mediated by one of the IL6 type cytokines whereas in the isogenic pairs (PEO1/PEO4 and PEA1/PEA2) it does not.

Future Experiments

GP130 overexpression has only been demonstrated at the mRNA level it would be relevant to assess whether this was matched by protein overexpression.
A broadening of this observation to other isogenic paired cell lines would allow a better estimation of the frequency this event is associated with the acquisition of cisplatin resistance. For example the paired cell line PEO14 and PEO23, in which overexpression was detected but were not assessed for a phenotypic response.

Interestingly in the context of the isogenic cell line pairs investigated in this document there was a correlation with IL6 responsiveness and GP130 upregulation. It would be interesting to examine whether this was a coincidence or replicates in additional paired cell lines models.

Given that the effects of GP130 knockdown in PEA2 are not mediated by STAT3 it would be relevant to investigate what was responsible for transducing these effects. A screen for the activity of the remaining STATs would be a logical step followed by an expression array.

6. Mutual feedback between Inhibition of the GP130/JAK2 and ERK1/2 Pathways

A Summary of the Data

GP130 knockdown was associated with increased activation in ERK1/2. To examine whether ERK1/2 activation occurred in response to interference with JAK2 signalling, inhibitor and siRNA treated lysates were assayed, in both cases pERK levels were increased. Given that JAK2 is down regulated by high concentrations of cisplatin this raised the possibility that cisplatin would also activate ERK1/2, which was also found to be the case. Doxorubicin and paclitaxel were used to investigate whether ERK1/2 activation was unique to cisplatin. DNA damaging doxorubicin, but not paclitaxel, was found to induce ERK1/2 activation.

JAK2 RNAi was able to reproduce some of the effects of cisplatin exposure including ERK1/2 activation. This raised the possibility that JAK2 down regulation was the cue for DNA damage associated ERK1/2 activation. However exposure to high concentrations of doxorubicin reversed down regulation of the JAK2/STAT3/ERBB2 axis, observed at lower concentrations, while increasing the activation of ERK1/2.

The activation of a proliferative, prosurvival factor in response to cisplatin treatment suggested that ERK1/2 inhibition might combine favourably with drug treatment.
In SKOV3 MEK1/2 inhibition was found to reverse activation of ERK1/2 by both cisplatin and doxorubicin, which was also associated with a potentiation of apoptosis induced by either DNA damaging agents.

Interestingly MEK1/2 inhibition was associated with feedback contributing to the reversal of cytotoxic downregulation of JAK2, pSTAT3 and pERBB2. Cisplatin dependent down regulation of these genes could be completely reversed by the addition of a MEK1/2 inhibitor.

Conclusion

The activation of ERK1/2 in response to various DNA damaging agents including etoposide and UV damage has been previously reported [469]. While the consequences of ERK1/2 activation are generally considered to be prosurvival, it has been shown that under

certain conditions, particularly DNA damage it can adopt a predominantly proapoptotic role, reviewed in [459]. However here ERK1/2 appears to play a prosurvival role, all be it to a limited extent.

High concentration of doxorubicin activated JAK2 simultaneously with ERK1/2 suggesting JAK2 downregulation is dispensable for ERK activation. Therefore ERK1/2 appears to compute inputs from a range of sources, differentially regulated by DNA damage, of which JAK2 is one.

Activation of ERK1/2 in response to DNA damage is MEK1/2 dependant, as previously reported. A previously identified feedback mechanism that exists between MEK1/2 and ERBB3 appears to also result in the upregulation of JAK2 and pSTAT3 and pERBB2. Further based on data suggesting a functional role for JAK2 in promoting the activation of both ERBB2 and STAT3, this positive feedback appears to be partially driven by increased JAK2 protein expression.

This highlights the potential problem of inherent mechanisms of resistance to single agent target therapy that exist in cells which could act to attenuate the effective of novel therapeutics. This has led to interest in combining different inhibitors of pathways where feedback has been shown, and recently synergy between PI3K and MEK1/2 inhibition has been demonstrated [470].

Future Experiments

Given that JAK2 knockdown and inhibition were able to both reduce pSTAT3 and activate ERK1/2, it raises the possibility that STAT3 knockdown would also activate ERK1/2. If so this might suggest help to identify the crucial factor(s) contributing to ERK1/2 activation in this setting.

Data presented here suggested that ERK1/2 activation would offset STAT3 dependent reductions in cyclin D1 expression which could limit the extent of growth inhibition that knockdown could elicit. Therefore combining the MEK1/2 and JAK2 inhibition would be good candidates for synergy and warrants investigation.

Elucidating the nature of mutual feedback either from GP130/JAK2 to ERK1/2 and vice versa would be interesting mechanistically as well as identifying target for potential drug intervention to prevent feedback. This could be investigated in many ways, however one more obvious experiment would be to examine the role of JAK2 upregulation in response to

MEK inhibition, for example could siRNA to JAK2 reverse MEKi dependent STAT3, ERBB2 activation?

Similarly probing for the phosphorylation levels of proteins in the MAPK pathway upstream of MEK1/2 would facilitate an identification of the pathway node receiving the feedback signal.

Central Conclusion

Cisplatin resistant cells exhibit differential dose responses in the activation of JAK2, STAT3 and ERBB2 relative to their sensitive isogenic pairs. Cisplatin titration experiments demonstrated sensitive cells exposed to low concentrations experienced increased JAK2, STAT3 and ERBB2 activation. Conversely cisplatin resistant cells did not experience a corresponding increase; instead deactivating these proteins with greater sensitivity to cisplatin. Cisplatin dependant modulation of JAK2, STAT3 and ERBB2 activation, in addition to the differential behaviour observed between isogenic pairs reveals this pathway is involved in both cellular response to cisplatin and acquired resistance to chemotherapy.

Resistant cells have acquired increased sensitivity to cisplatin in regards deactivation of these proteins conferring protection from the cytotoxic effects of drug exposure. Knockdowns of STAT3 and its kinase JAK2 reduced proliferation and increased cisplatin IC_{50}, additional small molecule inhibition of JAK2 reduced cisplatin induced apoptosis. Cisplatin is most toxic to dividing cells suggesting resistant cells are able to avoid some of the genotoxic effects of cisplatin DNA adduct formation by reducing proliferation rates. This would have the dual effects of reducing the accumulation rate of highly genotoxic DNA double strand breaks and allowing more time for the repair of single stranded lesions before they transition to double stranded breaks through DNA replication. This hypothesis is supported by the ability of STAT3 over expression to both increase cisplatin induced apoptosis and decrease cisplatin IC_{50}.

Deactivation of STAT3 and ERBB2 in response to cisplatin exposure is transcriptionally regulated by JAK2. Knockdown of JAK2 was associated with reductions in STAT3 and ERBB2 activation, additionally cisplatin induced changes in JAK2 protein expression were mirrored by changes in JAK2 mRNA, implicating JAK2 as a key regulator of the differential response between sensitive and resistant isogenic cells.

Supplementary Methods/Results

Brief Description of Contents

S1/2 Preparation of STAT3/JAK2 pcDNA 3.1 +

Sections S1 and S2 contain methodical results relating to the preparation of pcDNA 3.1 mammalian expression vectors containing STAT3 and JAK2 as well as the generation of mutant forms of each. All steps in supplementary methods in section S1 and S2 were carried out as described in the methods and materials sections; cloning, site directed mutagenesis and sequencing.

S3 General Mutational Information

Section S3 provides a brief summary of available mutational and copy number changes conducted either by our research group and its collaborators or from publicly available data sources.

S4 Survival Data, Kaplan Meier plots According to GP130 Expression

Results section 6 addresses the role GP130 play in upfront resistance to chemotherapy. To investigate this potential role further and to attempt to extend the findings presented here into a clinical data set survival analysis was carried out on the publically available TCGA data set found at (http://kmplot.com/analysis/index.php?p=service&cancer=ovar).

S5 Western blot of JAK2 Inhibitor Treated PEO1 PEO4

The isogenic cell line pair PEO1 and PEO4 were also examined for the effects of JAK2 inhibitor exposure. The experiment was carried in an identical fashion to all other cell lines. Western blot shows JAK2 inhibition has the same effect of reducing pERBB2 and pSTAT3 as other cell lines.

S6 Knockdown of GP130 in PEO4

Data relating to GP130 knockdown in PEO4, showing cisplatin apoptosis assay, growth assay and western blot. GP130 knockdown has no effect of cisplatin sensitivity, growth of levels of pSTAT3.

S1 Preparation of STAT3 pcDNA 3.1 +

S2.1 PCR amplification of full length STAT3α from OSE-C2

The normal OSE-C2 ovarian surface epithelium cell line was used as the source of cDNA for PCR, to minimise the probability of amplifying a mutant sequence. Due to problems with obtaining sufficient high quality purified PCR product reaction volumes were increased fourfold. After band excision each band relating to STAT3 was combined onto the same Qiagen purification column for maximal recovery.

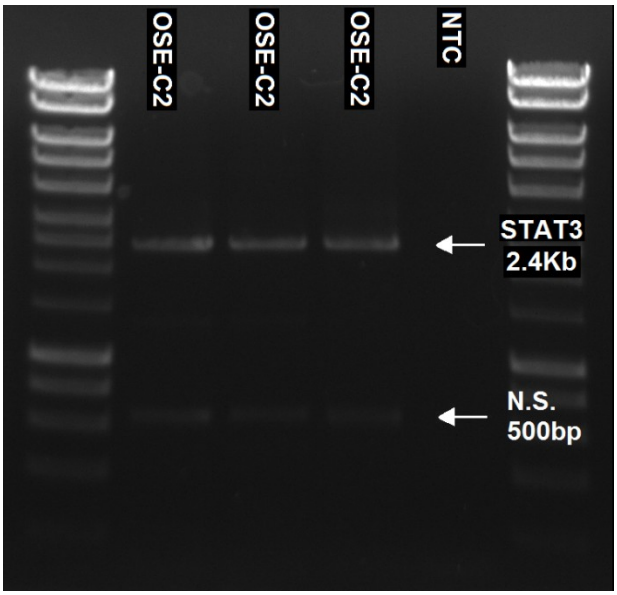

Supplementary figure S1.1. PCR of full length STAT3α from OSE-C2 cDNA. Entire 80µl PCR reaction run in 3 different lanes on a 1.75% agarose gel, in 1x TAE. Ladder used Bioline

hyperladder 1Kb. Gel stained with final concentration of ethidium bromide 0.3µg/ml. N.S = non-specific product

S2.2 Cloning of STAT3 into pcDNA

Both empty pcDNA 3.1+ and purified STAT3α PCR product were digested by NheI and HindIII. After Qiagen spin column purification, linearised vector and STAT3 with compatible sticky ends were mixed and ligated. Ligation reaction products were used to transform competent bacteria. Heat shocked bacteria were plated out onto ampicillin containing agar plates for selection of transformants. Colonies were picked, grown up, and screened by restriction digest.

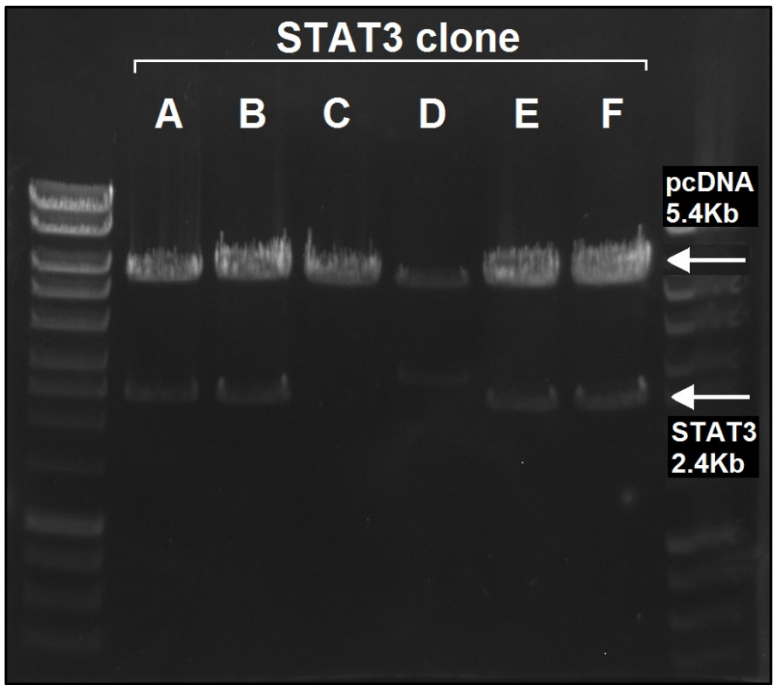

Figure S1.2 Restriction digest of ligated pcDNA 3.1 and STAT3. Ligated plasmid digested with NheI and HindIII. Six separate clones were picked for screening A-F. 4ul of digest run in each lane. 1.75% agarose gel, in 1x TAE. Ladder used Bioline hyperladder 1Kb. Gel stained with final concentration of ethidium bromide 0.3µg/ml.

Four of six clones picked contained an insert of the appropriate size. Other clones were discarded. Two of the four clones (E and F) were selected for sequencing and were verified to be mutation free (data not shown).

S2.3 Site directed mutagenesis of STAT3

Wild type STAT3 pcDNA 3.1+ was used as the template for the generation of mutant STAT3 Y705F, in which the tyrosine at codon 705 has been mutated to phenylalanine. Phenylalanine is structurally identical to tyrosine with the exception of the hydroxyl group which is the target moiety for the condensation reaction with ATP, leading to STAT3 phosphorylation. This renders the substituted residue immune to phosphorylation and therefor is useful as model for understanding the role that phosphorylative activation plays in the orchestration of downstream events.

After the site directed mutagenesis reaction had been carried out, competent bacteria were heat shock transformed and plated on selective agar. After overnight incubation colonies were picked and plasmid DNA purified. Initially only the region targeted for site directed mutagenesis was validated by sequencing. Those clones found to have been successfully mutated were selected for full length STAT3 sequencing to ensure no subsequent base substitutions had occurred. Finally before being used in transfections plasmids were purified using a maxi prep kit (Qiagen) to ensure sufficient purity and a lack of bacterial endotoxins.

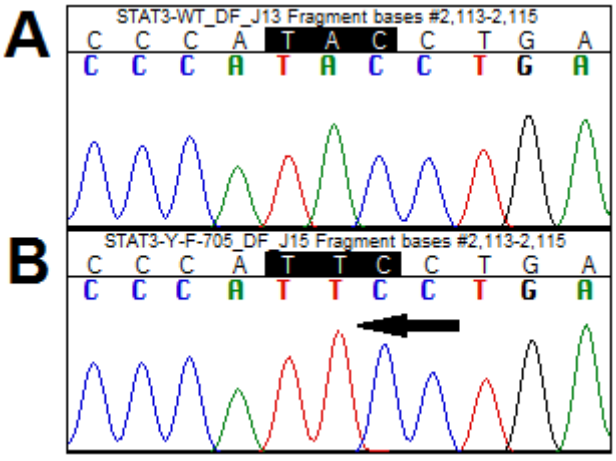

Figure S1.3. Sequencing of **A**, STAT3 WT, and **B** STAT3 Y705F mutant from pcDNA 3.1 + mammalian expression vector. Only the region surrounding tyrosine 705 is shown, this codon is highlighted in black. The arrow in **B** highlights the single base substitution required to change tyrosine to phenylalanine. Screen shot taken from Sequencher sequence analysis software (Genecodes)

S2 Preparation of JAK2 pcDNA 3.1 +

S2.1 PCR amplification of JAK2 from OSE-C2 and pDONNR223

Initially it was attempted to amplify full length JAK2 from OSE-C2 cDNA. This was not possible, for unknown reasons, see figure S2.1 B lane labelled 'full'. Consequently, utilising a naturally occurring unique restriction site within JAK2, it was attempted to amplify the gene in two fragments and ligate these together. JAK2 was divided into two halves a 2.5Kb 5' section, and a 2Kb 3' section. This strategy was also unsuccessful, again for unknown reasons. For this reason it was necessary to source an alternative form of JAK2. JAK2 pDONNR223, a gateway cloning vector was sourced from Addgene (http://www.addgene.org/23915/) courtesy of William Hahn and David Root.

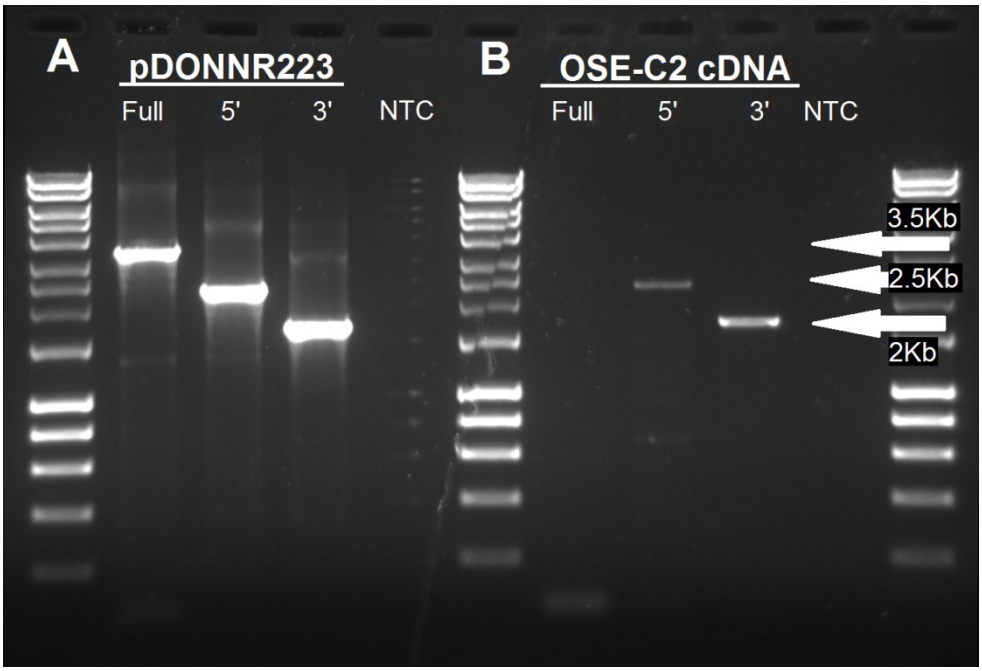

Supplementary figure S2.1. PCR of JAK2 from pDONNR223, **A**, OSE-C2 cDNA **B**. NTC = no template control. 5' and 3' two overlapping halves of JAK2. 1.75% agarose gel, in 1x TAE. Ladder used Bioline hyperladder 1Kb. Gel stained with final concentration of ethidium bromide 0.3µg/ml.

Before cloning the vector was sequenced and found to contain no non-synonymous mutations. Figure S2.1 shows the results of the PCR reaction carried out using Pfu DNA polymerase (Promega) amplifying from both JAK2 pDONNR223, A, and OSE-C2, B. Full

length JAK2 could only be amplified from pDONNR223. The PCR reaction containing full length JAK2 was then purified using minelute columns (Qiagen).

S2.2 Cloning of JAK2 into pcDNA3.1+

Both empty pcDNA 3.1+ and purified JAK2 PCR product were digested by NheI and ApaI. After Qiagen spin column purification, linearised vector and JAK2 with compatible sticky ends were mixed and ligated. Ligation reaction products were used to transform competent bacteria. Heat shocked bacteria were plated out onto ampicillin containing agar plates for selection of transformants. Colonies were picked, grown up, and screened by restriction digest.

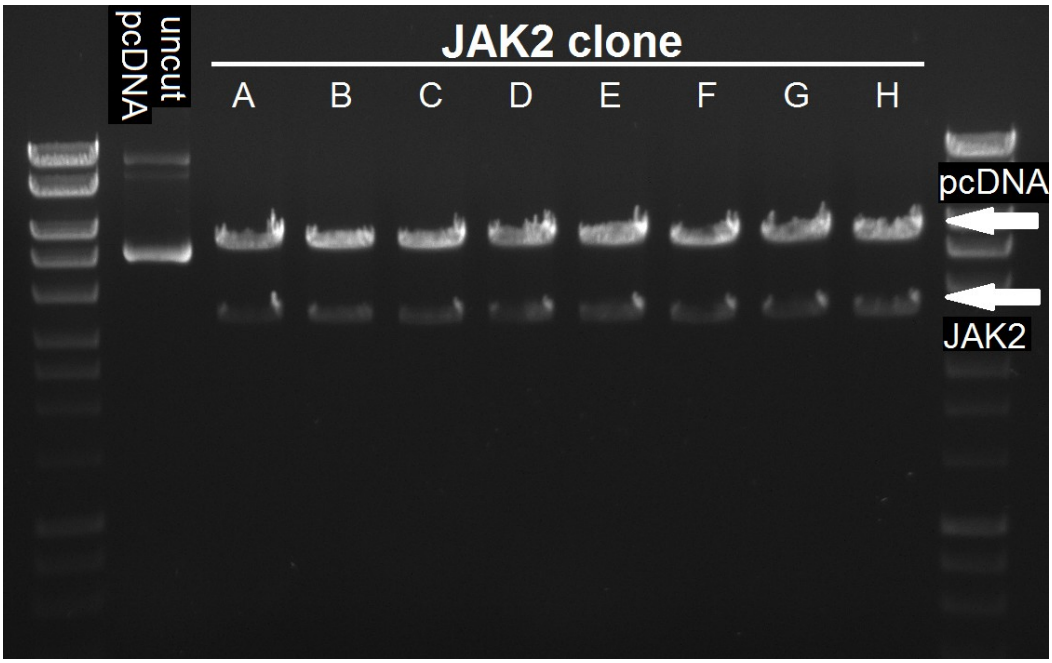

Figure S1.2 Restriction Digest of ligated pcDNA 3.1 and JAK2. Ligated plasmid digested with NheI and ApaI. Eight separate clones were picked for screening A-H. 4ul of digest run in each lane. 1.75% agarose gel, in 1x TAE. Ladder used Bioline hyperladder 1Kb. Gel stained with final concentration of ethidium bromide 0.3µg/ml.

Two clones A and D were sequenced and JAK2 verified to be unchanged from the vector (data not shown).

S2.3 Site Directed Mutagenesis of JAK2

Wild type JAK2 pcDNA 3.1+ was used as the template for the generation of a number of mutants, the duel tyrosine motif at residues 1007 and 1008 in the kinase loop are required for catalytic activity of the enzyme [471] were been mutated to mimic both constitutive activation, by substitution to glutamate (Y1007/1008E), and constitutive inactivation by substitution to phenylalanine (Y1007/1008F). As described in the introduction the V617F JAK2 mutant is the present in a number of haematological malignancies, including polycythemia vera [212]. Valine 617, found in the pseudo-kinase domain, of JAK2 plays a role in negatively regulating the catalytic activity of the enzyme and mutation of this residue has been shown to lead to hyper phosphorylation of JAK2 at Y1007/Y1008 [212]. Post site directed mutagenesis reaction step were carried out as described for STAT3 above. Sequencing results are shown in figure S2.3

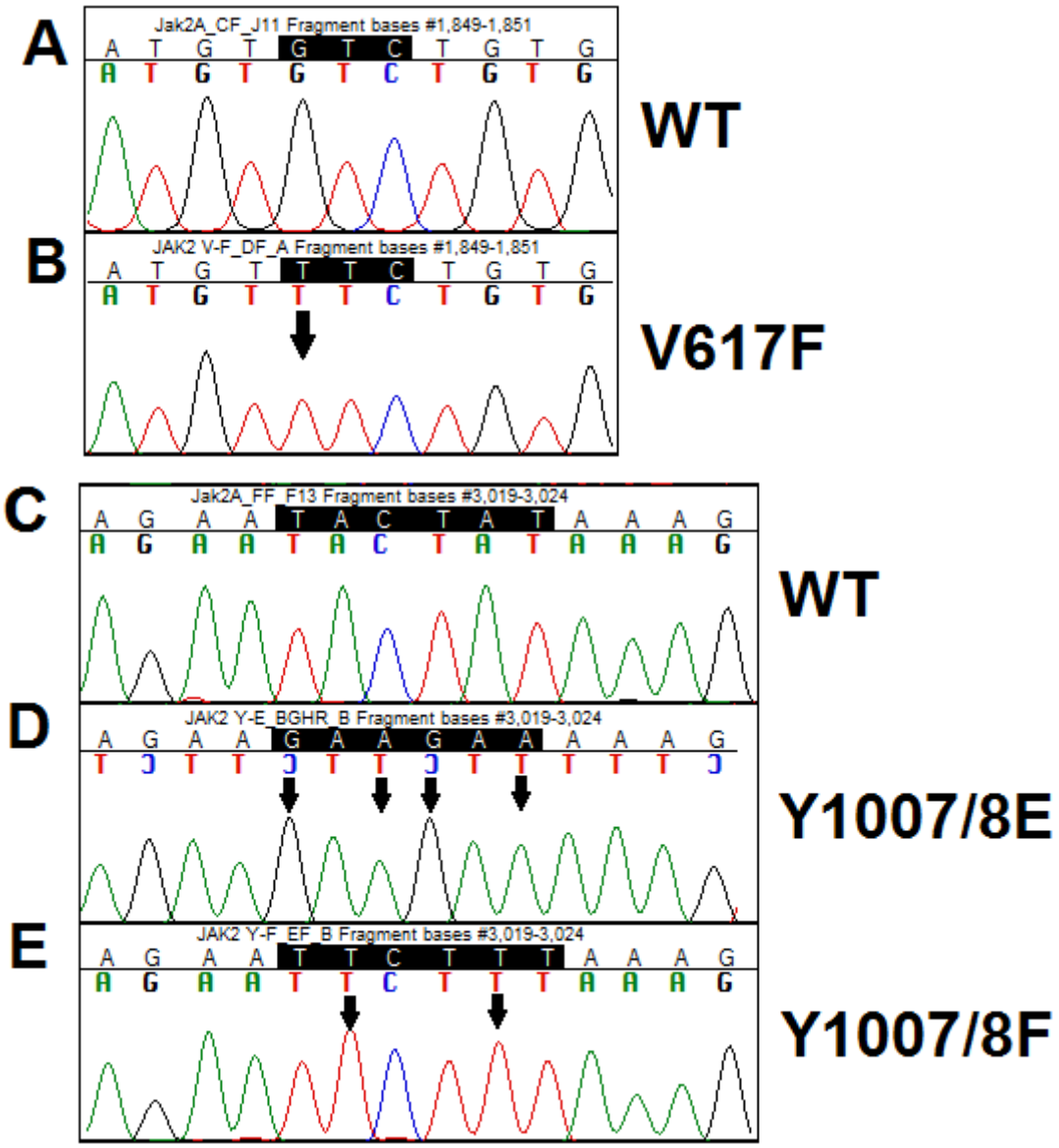

Figure S2.3 Sequencing of JAK2. **A + B** area surrounding V617, specific codon is highlighted in black. **A,** JAK2 WT. **B,** JAK2 V617F. Substituted base in designated by the arrow. **C + D + E** area surrounding Y1007/8, both codons are highlighted in black. **C**, JAK2 WT. **D** JAK2 Y1007/8E. **E**, JAK2 Y1007/8F. Arrows in **D + E** highlight the base substitutions. Screen shot taken from Sequencher sequence analysis software (Genecodes).

S3 Cell Line Mutational Information

The table below includes a summary of known mutations found in the cell lines included in this thesis.

Cell Line	P53 status	ERBB2 amplification	Other mutations
PEO1 *	mutant	No	ABCB1 VEGF
PEO4 *	mutant	No	ABCB1 VEGF
PEA1 *	mutant	No	VEGF
PEA2 *	mutant	No	ABCB1
A2780 #	wild type	No	PTEN
OVCAR3 #	mutant	No	CCNE1 amplified
IGROV3 #	mutant	No	MLH1 MSH6
SKOV3 #	mutant	Amplified	MLH1 PI3KCA CDKN2A

* Mutational analysis performed by Katherine Stemke-Hale at the 'Characterized Cell Line Core' at the MD Anderson Cancer Center, Texas USA, in collaboration with the group of Robert Bast. Analysis carried out using the OncoMap assay on the Sequenom iPLEX platform characterising 396 unique mutations in 33 common cancer genes as described in [472].
*Copy number analysis retrieved from [416].
mutation data retrieved from COSMIC [473]. Copy number data retrieved from the Cancer Genome Project [474]
#Copy number analysis retrieved from [428].

S4 GP130 Expression Predicts Poor Prognosis in Patients, However Multi-Variable Cox Proportional Hazard Analysis Suggest it is Not an Independent Prognostic Factor.

QRT-PCR and array expression profiling of GP130 in ovarian cell lines had suggested that overexpression of this gene might be a biomarker of cisplatin resistance. To address whether upfront GP130 expression might have any clinical relevance publicly available gene expression data sets were queried (http://kmplot.com/analysis/index.php?p=service&cancer=ovar)[164]. If GP130 expression, at time of patient presentation, plays a role in inherent platinum resistance it would be expected that high expression would predict poor survival. KM plotter contains survival data on 1171 cases of ovarian cancer, the vast majority of which are serous in histology. In all cases expression array profiling was carried out on material removed prior to administration of platinum or other chemotherapy. By plotting the average probe intensity for each high quality probe set available for GP130 figure S3 was generated.

To attempt to control for known prognostic factors the cohort was stratified in figure S3 B, C and D. In A the cohort was unstratified, in B composed of only grade 4 serous cases, C contained only cases with an optimal surgical debulk (less than 10mm residual disease after surgery) and D contains only cases categorised as stage 3.

Regardless of the type of stratification conducted the GP130 high expressing group was significantly associated with a reduced progression free survival, suggesting that GP130 is an independent prognostic marker for PFS in ovarian cancer. Hazard ratios ranged from 1.3 to 1.4 suggesting that GP130 is an important factor in determining survival.

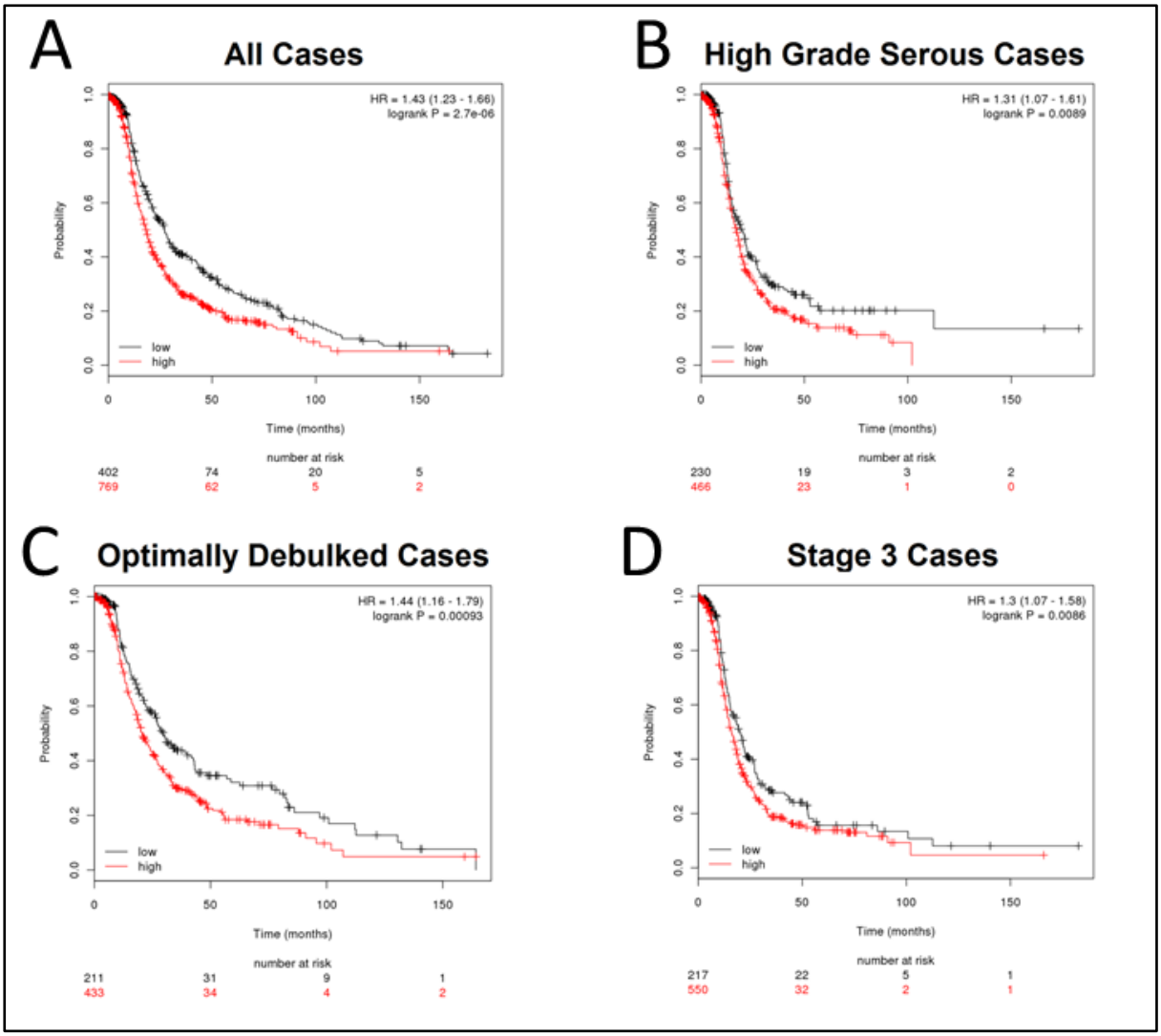

Figure S3. Keplan-Meier plots showing progression free survival in a combined cohort of 1171 patients according to GP130 expression, when grouped into either high (red) or low (black) expressers. The average intensity across every high quality control rated probe set using a variable cut-off between high and low groups is shown. In each case the results were consistent between probes. Plots show **A**, all cases. **B** only serous and grade 3. **C**, only optimally debulked cases. **D**, only stage 3 cases. For each graph the hazard ratio (HR) represents the increased risk of disease progression associated with falling into the high GP130 expressing group. Logrank p values of the significance of the difference in PFS between high (red) and low (black) is also shown with 95% CI in brackets. For each time point the number of cases in each group is shown. Affymetrix U133 probes used - 204863_s_at, 211000_s_at, 212195_at, 212196_at.

In order to further address whether GP130 is in fact a genuine independent prognostic factor Cox's proportional hazard modelling was carried out. This analysis was conducted on the TCGA component of this data set only, comprising 565 cases of HGS tumours only. The results are summarised below in table S3. The association between GP130 was controlled for in relation to; age of patient at diagnosis, surgery outcome (residual disease status after debulking), FIGO tumour stage, FIGO tumour grade and array batch.

Variable Probe set	PFS	Age	Surgery	Stage	Grade	Batch
204863_s_at	0.373	**0.006**	0.959	0.571	0.075	0.265
211000_s_at	0.490	**0.005**	0.885	0.576	0.083	0.240
212195_at	0.355	**0.005**	0.945	0.579	0.073	0.168
212196_at	**0.033**	**0.005**	0.759	0.500	0.067	0.131

Table S3. Summary of Multivariate analysis of GP130 expression. Columns show the Cox Proportional Hazards P value for each GPP130 probe set, shown the far left column, for each of the variables listed in the top row. PFS – progression free survival. Age – age of patient at diagnosis. Surgery – Residual disease status after debulking. Stage – FIGO tumour stage. Grad e FIGO tumour grade. Batch – array batch. Significant P values are shown in **bold**.

For three of the four probe sets investigated, previous significance differences in PFS (see figure S3) were reversed in multivariable modelling. GP130 expression was significantly associated with age at time of diagnosis for each probe set. Age is a commonly controlled for variable as it is known to correlate with survival. As such it appears that a significant association between GP130 expression and age at time of diagnosis is driving the previous significant associations. Further closer inspection of probe set 212196_at, which retained significance in multi variable analysis, revealed that it contains sequences only found within the 5' UTR, and not spanning the length of GP130, potentially questioning the validity of this anomalous result. In conclusion GP130 does not validate as an independent prognostic factor for PFS (or OS, data not shown) in upfront biopsies. However initial data suggesting GP130 plays a role in ovarian cancer suggested this was specifically in acquired resistance. Currently there are no clinical data sets of matched pre and post relapse, which platinum resistant disease, to allow an assessment of these findings.

S5 Western blot of JAK2 Inhibitor Treated PEO1 PEO4

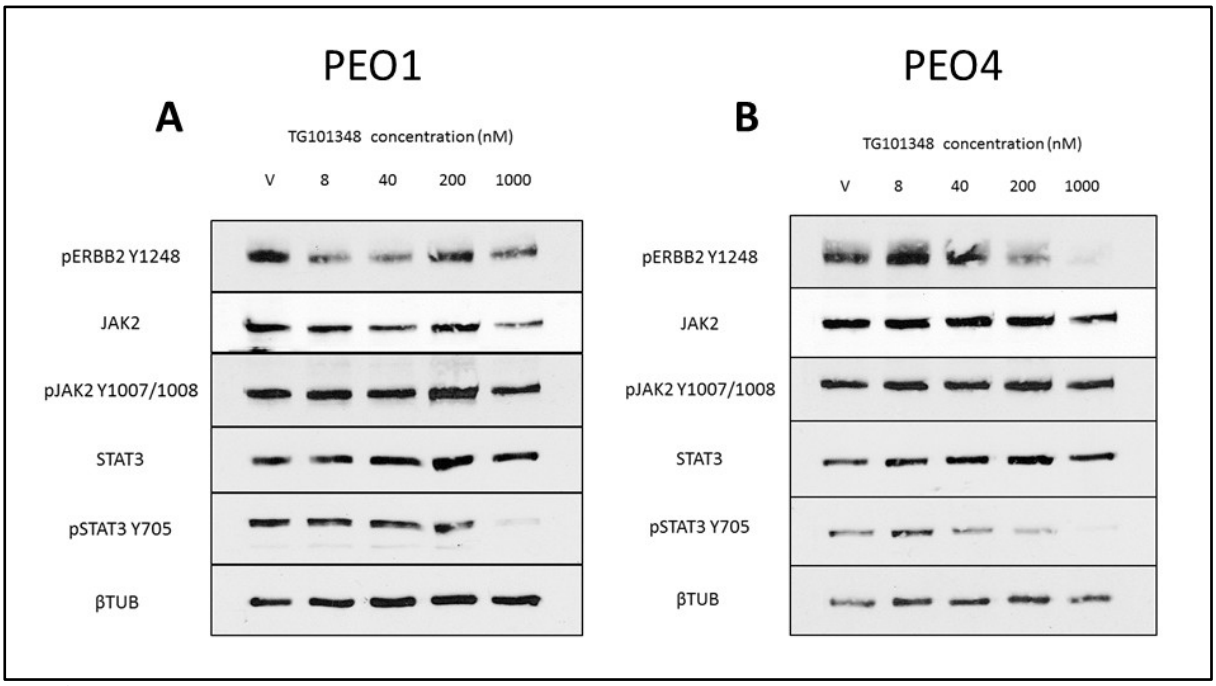

Figure S5.. Western Blot analysis of JAK2 inhibitor (TG101348) treated cells. Cells were treated with the indicated concentration of inhibitor dissolved in DMSO or vehicle control (V) for between 16 and 18 hours before lysis. Western blots were run from at least two biological replicates for each cell line. The results obtained were consistent. βTUB is included as a loading control.

S6 Knockdown of GP130 in PEO4

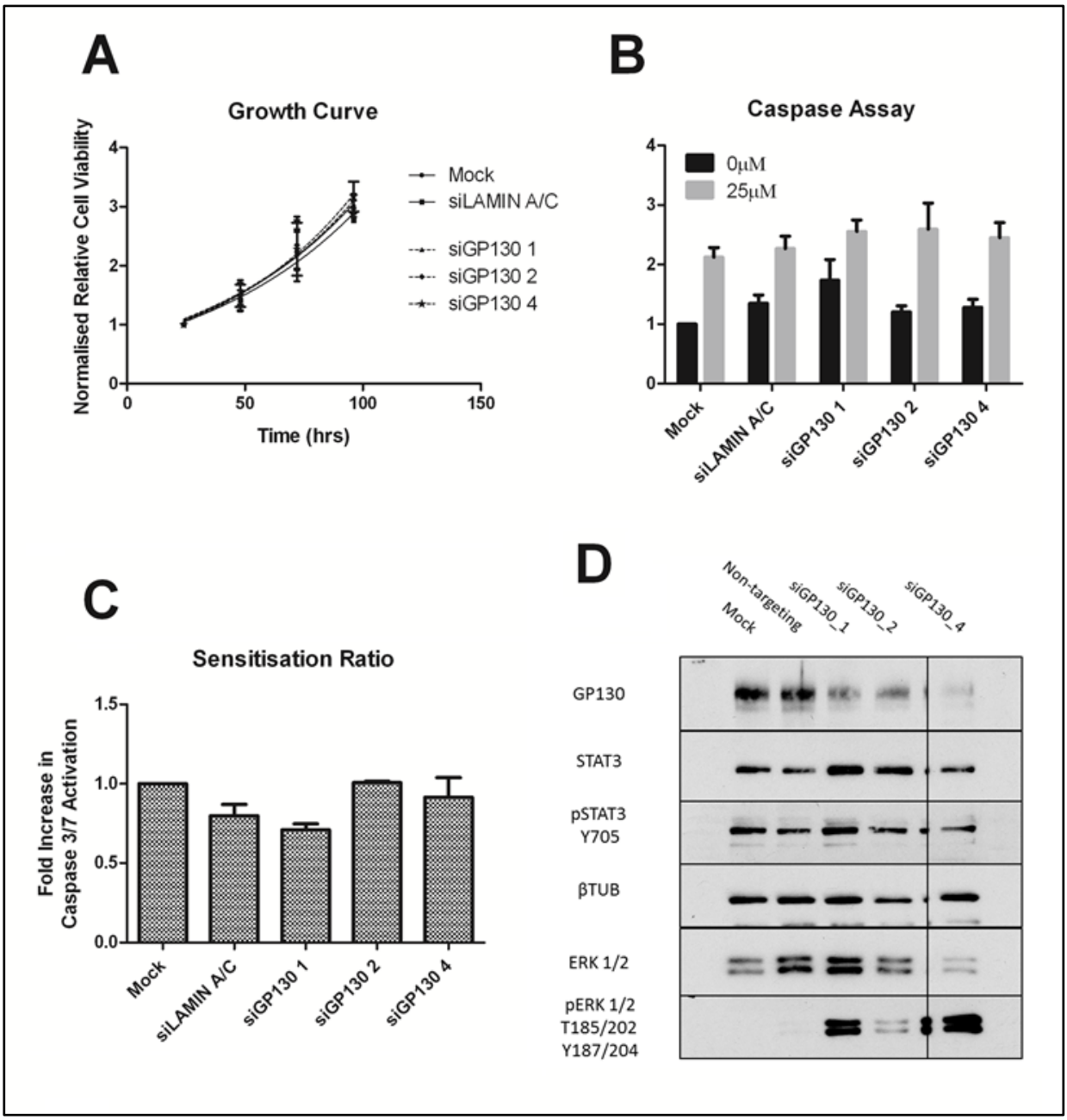

Figure S6. Effects of GP130 knockdown in PEO4. Cells were either mock transfected, transfected with siLAMIN A/C or one of three GP130 siRNAs, at 50nM final concentration, for 48 hours before reseeding for either proliferation or caspase assays or protein lysates. **A,** proliferation assay after GP130 knockdown. Cell viability estimates made every 24 hours using the MTT assay. For each siRNA values are normalised to 0 hours. **B,** cisplatin (cddp) caspase assay. Cells were transfected as described, prior to either, no treatment (black columns) or cddp exposure (grey columns) at 25μM. After 24 hours cddp exposure activated caspase 3/7 levels were quantified and normalised to cell viability estimated using the MTT assay. All values shown relative to 0μM mock transfected. **C,** cisplatin sensitisation plots of GP130 knockdown. Plots show the ratio of caspase induced by cisplatin for each siRNA. Calculated by dividing each replicate normalised caspase induction value for

+ cddp treatment by the – cddp treatment values for each siRNA transfection, giving the cddp resensitisation ratio for each siRNA species.

For **A**,**B** and **C** all values are the average of 2 independent biological replicates. Error bars show the SEM of these replicates. **D**, western blot of GP130 knockdown. Cells were transfected as previously described for 48 hours prior to reseeding and lysis after an additional 24 hours. siGP130 siRNA species 3 removed from analysis due to low efficiency of knockdown. Two separate biological replicates were run, the results shown here are representative. βTUB is included as a loading control. Membranes were first probed with phospho protein specific antibodies prior to stripping and reprobing with total antibodies.

S7 Knockdown of STAT3 in PEO1 Showing Reciprocal Increase in JAK2

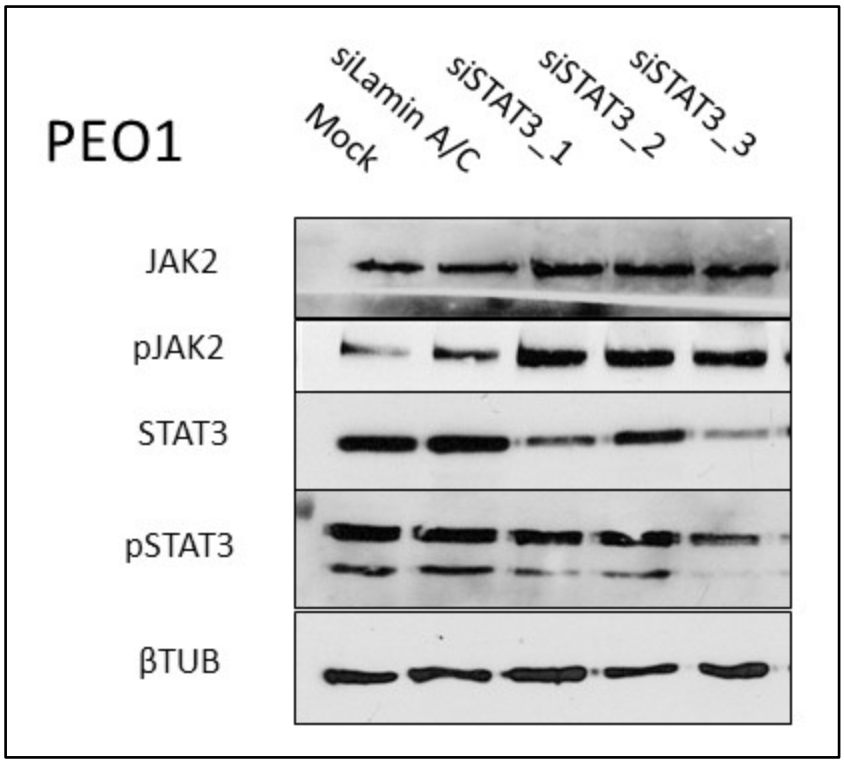

Figure S7. Western Blot analysis siSTAT3 transfected cells. Cells were treated with 50nM final concentration of the indicated siRNA for 48 hours before lysis. βTUB is included as a loading control.

References

1. Jemal, A. *et al.* Global cancer statistics. *CA a cancer J. Clin.* **61,** 69–90 (2011).

2. Howlader, N. *et al. SEER Cancer Statistics Review, 1975-2009 (Vintage 2009 Populations)*. *Natl. Cancer Inst. Bethesda MD* 1–107 (National Cancer Institute, 2012). at <http://seer.cancer.gov/csr/1975_2009_pops09/>

3. Ferlay J, Shin HR, Bray F, Forman D, M. C. and P. D. GLOBOCAN 2008 v2.0, Cancer Incidence and Mortality Worldwide. *IARC CancerBase No. 10 Int. Agency Res. Cancer; 2010.*

4. Hudson, C. Ind, T. Curling, O. in *Ovarian Cancer* 221–232 (2002).

5. Berek, J. & Hacker, N. in *Pract. Gynecol. Oncol.* 511–541 (Lippincot Williams and Wilkins, 2005).

6. Judson, P. L. & Boente, M. in *Ovarian Cancer* (Ozols) 231– 237 (Hamilton, 2003).

7. Kosary, C. L. Cancer of the Ovary SEER survival monograph. 133–144 (2001).

8. UK, C. R. Ovarian cancer survival statistics. *Cancer Res. UK* (2013). at <http://www.cancerresearchuk.org/cancer-info/cancerstats/types/ovary/survival/ovarian-cancer-survival-statistics#source5>

9. Silverberg, S. G. Histopathologic grading of ovarian carcinoma: a review and proposal. *Int. J. Gynecol. Pathol.* **19,** 7–15 (2000).

10. Seidman, J. D., Yemelyanova, A., Cosin, J. a, Smith, A. & Kurman, R. J. Survival rates for international federation of gynecology and obstetrics stage III ovarian carcinoma by cell type: a study of 262 unselected patients with uniform pathologic review. *Int. J. Gynecol. Cancer* **22,** 367–71 (2012).

11. Schmeler, K. M. *et al.* Neoadjuvant chemotherapy for low-grade serous carcinoma of the ovary or peritoneum. *Gynecol. Oncol.* **108,** 510–4 (2008).

12. Seidman, J. D. *et al.* Testing of two binary grading systems for FIGO stage III serous carcinoma of the ovary and peritoneum. *Gynecol. Oncol.* **103,** 703–8 (2006).

13. Heintz, A. P. *et al.* Carcinoma of the ovary. *Int. J. Gynaecol. Obstet. Off. organ Int. Fed. Gynaecol. Obstet.* **66,** 184–190 (2003).

14. Ovarian cancer incidence statistics. *Cancer Res. UK* (2013). at <http://www.cancerresearchuk.org/cancer-info/cancerstats/types/ovary/incidence/>

15. Herrinton, L. Ovarian cancer incidence among Asian migrants to the United States and their descendants. *J. Natl. Cancer Inst.* **86,** (1994).

16. Rubin, S., Sabbatini, P. & Viswanathan, A. *Cancer Management: 14th edition. Chaper - Ovarian Cancer*. (2011). at <http://www.cancernetwork.com/cancer-management/ovarian/article/10165/1802681>

17. Satagopan, J., Boyd, J. & Kauff, N. Ovarian cancer risk in Ashkenazi Jewish carriers of BRCA1 and BRCA2 mutations. *Clin. Cancer Res.* 3776–3781 (2002). at <http://clincancerres.aacrjournals.org/content/8/12/3776.short>

18. Stratton, J. F., Pharoah, P., Smith, S. K., Easton, D. & Ponder, B. a. A systematic review and meta-analysis of family history and risk of ovarian cancer. *Br. J. Obstet. Gynaecol.* **105,** 493–9 (1998).

19. Miki, Y. *et al.* A strong candidate for the breast and ovarian cancer susceptibility gene BRCA1. *Science (80-.).* **266,** 66–71 (1994).

20. Wooster, R., Bignell, G., Lancaster, J. & Swift, S. Identification of the breast cancer susceptibility gene BRCA2. *Nature* (1995). at <http://www.nature.com/nature/journal/v378/n6559/abs/378789a0.html>

21. Whittemore, A. S., Harris, R. & Itnyre, J. Characteristics Relating to Ovarian Cancer Risk: Collaborative Analysis of 12 US Case-Control Studies. *Amencan J. Epidemiol.* **136,** (1992).

22. Negri, E. *et al.* Pooled analysis of 3 European case-control studies: I. Reproductive factors and risk of epithelial ovarian cancer. *Int. J. Cancer* **49,** 50–6 (1991).

23. Franceschi, S. *et al.* Pooled analysis of 3 European case-control studies of epithelial ovarian cancer: III. Oral contraceptive use. *Int. J. Cancer* **49,** 61–5 (1991).

24. Rice, M. S., Murphy, M. a & Tworoger, S. S. Tubal ligation, hysterectomy and ovarian cancer: A meta-analysis. *J. Ovarian Res.* **5,** 13 (2012).

25. Ness, R. B. *et al.* Infertility, fertility drugs, and ovarian cancer: a pooled analysis of case-control studies. *Am. J. Epidemiol.* **155,** 217–24 (2002).

26. Zreik, T. G., Ayoub, C. M., Hannoun, A., Karam, C. J. & Munkarah, A. R. Fertility drugs and risk of ovarian cancer: dispelling the myth. *Curr. Opin. Obstet. Gynecol.* **20,** 313–9 (2008).

27. Shuster, L., Rhodes, D. & Gostout, B. Premature menopause or early menopause: long-term health consequences. *Maturitas* **65,** 1–11 (2010).

28. Stefanick, M. L. Estrogens and progestins: background and history, trends in use, and guidelines and regimens approved by the US Food and Drug Administration. *Am. J. Med.* **118 Suppl ,** 64–73 (2005).

29. Rossouw, J., Anderson, G. & Prentice, R. Risks and benefits of estrogen plus progestin in healthy postmenopausal women: principal results from the Women's Health Initiative randomized controlled trial. *JAMA* **288,** 321–333 (2002).

30. Beral, V., Bull, D., Green, J. & Reeves, G. Ovarian cancer and hormone replacement therapy in the Million Women Study. *Lancet* **369,** 1703–10 (2007).

31. Zhou, B. *et al.* Hormone replacement therapy and ovarian cancer risk: a meta-analysis. *Gynecol. Oncol.* **108,** 641–51 (2008).

32. McNeilly, A. S. Lactational control of reproduction. *Reprod. Fertil. Dev.* **13,** 583–590 (2001).

33. Tung, K.-H. Reproductive Factors and Epithelial Ovarian Cancer Risk by Histologic Type:A Multiethnic Case-Control Study. *Am. J. Epidemiol.* **158,** 629–638 (2003).

34. Danforth, K. N. *et al.* Breastfeeding and risk of ovarian cancer in two prospective cohorts. *Cancer Causes Control* **18,** 517–23 (2007).

35. Jordan, S. J., Cushing-Haugen, K. L., Wicklund, K. G., Doherty, J. a & Rossing, M. a. Breast-feeding and risk of epithelial ovarian cancer. *Cancer Causes Control* **23,** 919–27 (2012).

36. Bosetti, C. *et al.* Diet and ovarian cancer risk: a case-control study in Italy. *Int. J. Cancer* **93,** 911–5 (2001).

37. Kushi, L. & Mink, P. Prospective study of diet and ovarian cancer. *Am. J. Epidemiol.* **149,** 21–31 (1999).

38. Olsen, C. M. *et al.* Obesity and the risk of epithelial ovarian cancer: a systematic review and meta-analysis. *Eur. J. Cancer* **43,** 690–709 (2007).

39. Cleary, M. P. & Grossmann, M. E. Minireview: Obesity and breast cancer: the estrogen connection. *Endocrinology* **150,** 2537–2542 (2009).

40. Ramus, S. J. & Gayther, S. a. The contribution of BRCA1 and BRCA2 to ovarian cancer. *Mol. Oncol.* **3,** 138–50 (2009).

41. Breast Cancer Linkage Consortium, T. Cancer Risks in BRCA2 Mutation Carriers. *JNCI J. Natl. Cancer Inst.* **91,** 1310–1316 (1999).

42. Ford, D., Easton, D. F., Bishop, D. T., Narod, S. A. & Goldgar, D. E. Risks of cancer in BRCA1-mutation carriers. *Lancet* **343,** 692–695 (1994).

43. Antoniou, A. *et al.* Average risks of breast and ovarian cancer associated with BRCA1 or BRCA2 mutations detected in case Series unselected for family history: a combined analysis of 22 studies. *Am. J. Hum. Genet.* **72,** 1117–30 (2003).

44. Chen, S. & Parmigiani, G. Meta-analysis of BRCA1 and BRCA2 penetrance. *J. Clin. Oncol.* **25,** 1329–1333 (2007).

45. King, M.-C., Marks, J. H. & Mandell, J. B. Breast and ovarian cancer risks due to inherited mutations in BRCA1 and BRCA2. *Science (80-.).* **302,** 643–6 (2003).

46. Shen, S. X. *et al.* A targeted disruption of the murine Brca1 gene causes gamma-irradiation hypersensitivity and genetic instability. *Oncogene* **17,** 3115–24 (1998).

47. Patel, K. J. *et al.* Involvement of Brca2 in DNA repair. *Mol. Cell* **1,** 347–57 (1998).

48. Kraakman-van der Zwet, M. O. W. *et al.* Brca2 (XRCC11) deficiency results in radioresistant DNA synthesis and a higher frequency of spontaneous deletions. *Mol. Cell. Biol.* **2,** (2002).

49. Fong, P. C. *et al.* Poly(ADP)-ribose polymerase inhibition: frequent durable responses in BRCA carrier ovarian cancer correlating with platinum-free interval. *J. Clin. Oncol.* **28,** 2512–9 (2010).

50. Pal, T. *et al.* BRCA1 and BRCA2 mutations account for a large proportion of ovarian carcinoma cases. *Cancer* **104,** 2807–16 (2005).

51. Risch, H. a *et al.* Prevalence and penetrance of germline BRCA1 and BRCA2 mutations in a population series of 649 women with ovarian cancer. *Am. J. Hum. Genet.* **68,** 700–10 (2001).

52. Schrader, K. a *et al.* Germline BRCA1 and BRCA2 mutations in ovarian cancer: utility of a histology-based referral strategy. *Obstet. Gynecol.* **120,** 235–40 (2012).

53. Goodenberger, M. & Lindor, N. Lynch syndrome and MYH-associated polyposis: review and testing strategy. *J. Clin. Gastroenterol* **45,** 488–500 (2011).

54. Watson, P. *et al.* The risk of extra-colonic, extra-endometrial cancer in the Lynch syndrome. *Int. J. cancer* **123,** 444–449 (2008).

55. Malander, S. *et al.* The contribution of the hereditary nonpolyposis colorectal cancer syndrome to the development of ovarian cancer. *Gynecol. Oncol.* **101,** 238–43 (2006).

56. Pharoah, P. D. . & Ponder, B. a. . The genetics of ovarian cancer. *Best Pract. Res. Clin. Obstet. Gynaecol.* **16,** 449–468 (2002).

57. Ramus, S. & Harrington, P. Contribution of BRCA1 and BRCA2 mutations to inherited ovarian cancer. *Hum. Mutat.* **28,** 1207–1215 (2007).

58. Verhoog, L. C. *et al.* Large regional differences in the frequency of distinct BRCA1/BRCA2 mutations in 517 Dutch breast and/or ovarian cancer families. *Eur. J. Cancer* **37,** 2082–90 (2001).

59. Ford, D. *et al.* Genetic Heterogeneity and Penetrance Analysis of the BRCA1 and BRCA2 Genes in Breast Cancer Families. *Am. J. Hum. Genet.* **62,** 676–689 (1998).

60. Gayther, S. A. *et al.* The contribution of germline BRCA1 and BRCA2 mutations to familial ovarian cancer: no evidence for other ovarian cancer-susceptibility genes. *Am. J. Hum. Genet.* **65,** 1021–9 (1999).

61. Loveday, C. *et al.* Germline mutations in RAD51D confer susceptibility to ovarian cancer. *Nat. Genet.* **43,** 879–82 (2011).

62. Meindl, A. *et al.* Germline mutations in breast and ovarian cancer pedigrees establish RAD51C as a human cancer susceptibility gene. *Nat. Genet.* **42,** 410–4 (2010).

63. Rafnar, T. *et al.* Mutations in BRIP1 confer high risk of ovarian cancer. *Nat. Genet.* **43,** 1104–7 (2011).

64. Whittemore, S., Gong, G. & Itnyre, J. Prevalence and contribution of BRCA1 mutations in breast cancer and ovarian cancer: results from three U.S. population-based case-control studies of ovarian cancer. *Am. J. Hum. Genet.* **60,** 496–504 (1997).

65. Song, H. H. *et al.* A genome-wide association study identifies a new ovarian cancer susceptibility locus on 9p22.2. *Nat. Genet.* **42,** 768–771 (2009).

66. Goode, E. L. *et al.* A genome-wide association study identifies susceptibility loci for ovarian cancer at 2q31 and 8q24. *Nat. Genet.* **42,** 874–9 (2010).

67. Chan, J. K. *et al.* Patterns and progress in ovarian cancer over 14 years. *Obstet. Gynecol.* **108,** 521–528 (2006).

68. Trimbos, J. B. *et al.* International Collaborative Ovarian Neoplasm trial 1 and Adjuvant ChemoTherapy In Ovarian Neoplasm trial: two parallel randomized phase III trials of adjuvant chemotherapy in patients with early-stage ovarian carcinoma. *J. Natl. Cancer Inst.* **95,** 105–12 (2003).

69. Cancer, A. O. & Group., A. O. C. T. Chemotherapy in advanced ovarian cancer: an overview of randomised clinical trials. *Br. medial J.* **303,** 884–893 (1991).

70. Engel, J. *et al.* Moderate progress for ovarian cancer in the last 20 years: prolongation of survival, but no improvement in the cure rate. *Eur. J. Cancer* **38,** 2435–2445 (2002).

71. Chi, D. S. *et al.* Improved progression-free and overall survival in advanced ovarian cancer as a result of a change in surgical paradigm. *Gynecol. Oncol.* **114,** 26–31 (2009).

72. Bristow, R. E., Tomacruz, R. S., Armstrong, D. K., Trimble, E. L. & Montz, F. J. Survival effect of maximal cytoreductive surgery for advanced ovarian carcinoma during the platinum era: a meta-analysis. *J. Clin. Oncol.* **20,** 1248–59 (2002).

73. Yap, T. A., Carden, C. P. & Kaye, S. B. Beyond chemotherapy: targeted therapies in ovarian cancer. *Nat. Rev. Cancer* **9,** 167–181 (2009).

74. McGuire, W. P. *et al. Cyclophosphamide and cisplatin compared with paclitaxel and cisplatin in patients with stage III and stage IV ovarian cancer. N. Engl. J. Med.* **334,** 1–6 (1996).

75. Agarwal, R. & Kaye, S. B. Ovarian cancer: strategies for overcoming resistance to chemotherapy. *Nat. Rev. Cancer* **3,** 502–16 (2003).

76. Armstrong, D. K. *et al.* Intraperitoneal cisplatin and paclitaxel in ovarian cancer. *N. Engl. J. Med.* **354,** 34–43 (2006).

77. Burger, R. a *et al.* Incorporation of bevacizumab in the primary treatment of ovarian cancer. *N. Engl. J. Med.* **365,** 2473–83 (2011).

78. Aghajanian, C. *et al.* OCEANS: a randomized, double-blind, placebo-controlled phase III trial of chemotherapy with or without bevacizumab in patients with platinum-sensitive recurrent epithelial ovarian, primary peritoneal, or fallopian tube cancer. *J. Clin. Oncol.* **30,** 2039–45 (2012).

79. Ledermann, J. & Harter, P. Olaparib maintenance therapy in platinum-sensitive relapsed ovarian cancer. *N. Engl. J. Med.* **366,** 1382–92 (2012).

80. Bast, R. C. *et al.* Reactivity of a monoclonal antibody with human ovarian carcinoma. *J. Clin. Invest.* **68,** 1331–7 (1981).

81. Yin, B. W. & Lloyd, K. O. Molecular cloning of the CA125 ovarian cancer antigen: identification as a new mucin, MUC16. *J. Biol. Chem.* **276,** 27371–5 (2001).

82. Bast, R. C. *et al.* A radioimmunoassay using a monoclonal antibody to monitor the course of epithelial ovarian cancer. *N. Engl. J. Med.* **309,** 883–887 (1983).

83. Helzlsouer, K. J. *et al.* Prospective study of serum CA-125 levels as markers of ovarian cancer. *JAMA* **269,** 1123–1126 (1993).

84. Muyldermans, M., Cornillie, F. J. & Koninckx, P. R. CA125 and endometriosis. *Hum. Reprod. Update* **1,** 173–87 (1995).

85. Buys, S. S. *et al.* Effect of screening on ovarian cancer mortality: the Prostate, Lung, Colorectal and Ovarian (PLCO) Cancer Screening Randomized Controlled Trial. *JAMA* **305,** 2295–303 (2011).

86. Yurkovetsky, Z. *et al.* Development of a multimarker assay for early detection of ovarian cancer. *J. Clin. Oncol.* **28,** 2159–66 (2010).

87. Soslow, R. a. Histologic subtypes of ovarian carcinoma: an overview. *Int. J. Gynecol. Pathol.* **27,** 161–74 (2008).

88. Auersperg, N., Wong, A. S. T., Choi, K., Kang, S. K. & Leung, P. C. K. Ovarian Surface Epithelium : Biology , Endocrinology ,. *Endocr. Rev.* **22,** 255–288 (2001).

89. Fox, H. & Singh, N. *Ovarian Cancer*. 57–74 (Oxford University Press, 2002).

90. Naora, H. Developmental Patterning in the Wrong Context The Paradox of Epithelial Ovarian Cancers. *Cell cycle* **4:8,** 1033–1035 (2005).

91. Kabawat, S. E. *et al.* Tissue distribution of a coelomic-epithelium-related antigen recognized by the monoclonal antibody OC125. *Int. J. Gynecol. Pathol. Off. J. Int. Soc. Gynecol. Pathol.* **2,** 275–285 (1983).

92. Köbel, M. *et al.* Differences in tumor type in low-stage versus high-stage ovarian carcinomas. *Int. J. Gynecol. Pathol.* **29,** 203–11 (2010).

93. Pearce, C. L. *et al.* Association between endometriosis and risk of histological subtypes of ovarian cancer: a pooled analysis of case-control studies. *Lancet Oncol.* **13,** 385–94 (2012).

94. Gemignani, M. L. *et al.* Role of KRAS and BRAF gene mutations in mucinous ovarian carcinoma. *Gynecol. Oncol.* **90,** 378–381 (2003).

95. Singer, G. *et al.* Mutations in BRAF and KRAS characterize the development of low-grade ovarian serous carcinoma. *J. Natl. Cancer Inst.* **95,** 6–8 (2003).

96. Okuda, T. *et al.* P53 Mutations and Overexpression Affect Prognosis of Ovarian Endometrioid Cancer But Not Clear Cell Cancer. *Gynecol. Oncol.* **88,** 318–325 (2003).

97. Mangili, G. *et al.* Unraveling the two entities of endometrioid ovarian cancer: a single center clinical experience. *Gynecol. Oncol.* **126,** 403–7 (2012).

98. Wiegand, K. C. *et al.* ARID1A mutations in endometriosis-associated ovarian carcinomas. *N. Engl. J. Med.* **363,** 1532–43 (2010).

99. Lowery, W. *et al.* Loss of ARID1A-associated protein expression is a frequent event in clear cell and endometrioid ovarian cancers. *Int. J. Gynecol. Cancer* **22,** 9–14 (2012).

100. Tothill, R. W. *et al.* Novel molecular subtypes of serous and endometrioid ovarian cancer linked to clinical outcome. *Clin. Cancer Res.* **14,** 5198–208 (2008).

101. Gómez-Raposo, C., Mendiola, M., Barriuso, J., Hardisson, D. & Redondo, A. Molecular characterization of ovarian cancer by gene-expression profiling. *Gynecol. Oncol.* **118,** 88–92 (2010).

102. Anglesio, M. S. *et al.* Molecular characterization of mucinous ovarian tumours supports a stratified treatment approach with HER2 targeting in 19% of carcinomas. *J. Pathol.* **229,** 111–20 (2013).

103. Hofstetter, G. *et al.* The N-terminally truncated p53 isoform Δ40p53 influences prognosis in mucinous ovarian cancer. *Int. J. Gynecol. Cancer* **22,** 372–9 (2012).

104. Seidman, J. D., Kurman, R. J. & Ronnett, B. M. Primary and metastatic mucinous adenocarcinomas in the ovaries: incidence in routine practice with a new approach to improve intraoperative diagnosis. *Am. J. Surg. Pathol.* **27,** 985–93 (2003).

105. Khunamornpong, S. *et al.* Primary and metastatic mucinous adenocarcinomas of the ovary: Evaluation of the diagnostic approach using tumor size and laterality. *Gynecol. Oncol.* **101,** 152–7 (2006).

106. Chan, J. K. *et al.* Do clear cell ovarian carcinomas have poorer prognosis compared to other epithelial cell types? A study of 1411 clear cell ovarian cancers. *Gynecol. Oncol.* **109,** 370–6 (2008).

107. Sugiyama, T. *et al.* Clinical characteristics of clear cell carcinoma of the ovary: a distinct histologic type with poor prognosis and resistance to platinum-based chemotherapy. *Cancer* **88,** 2584–2589 (2000).

108. Jensen, K. C. *et al.* Microsatellite instability and mismatch repair protein defects in ovarian epithelial neoplasms in patients 50 years of age and younger. *Am. J. Surg. Pathol.* **32,** 1029–37 (2008).

109. Mayr, D., Hirschmann, A., Löhrs, U. & Diebold, J. KRAS and BRAF mutations in ovarian tumors: a comprehensive study of invasive carcinomas, borderline tumors and extraovarian implants. *Gynecol. Oncol.* **103,** 883–7 (2006).

110. Ho, E. S. *et al.* P53 Mutation Is Infrequent in Clear Cell Carcinoma of the Ovary. *Gynecol. Oncol.* **80,** 189–93 (2001).

111. Jones, S. *et al.* Frequent mutations of chromatin remodeling gene ARID1A in ovarian clear cell carcinoma. *Science (80-.).* **330,** 228–31 (2010).

112. Plaxe, S. C. Epidemiology of low-grade serous ovarian cancer. *Am. J. Obstet. Gynecol.* **198,** 459.e1–8; discussion 459.e8–9 (2008).

113. Bonome, T. *et al.* Expression profiling of serous low malignant potential, low-grade, and high-grade tumors of the ovary. *Cancer Res.* **65,** 10602–12 (2005).

114. Gershenson, D. M. *et al.* Clinical behavior of stage II-IV low-grade serous carcinoma of the ovary. *Obstet. Gynecol.* **108,** 361–8 (2006).

115. Malpica, A. *et al.* Grading ovarian serous carcinoma using a two-tier system. *Am. J. Surg. Pathol.* **28,** 496–504 (2004).

116. Sieben, N. L. G. *et al.* In ovarian neoplasms, BRAF, but not KRAS, mutations are restricted to low-grade serous tumours. *J. Pathol.* **202,** 336–40 (2004).

117. Burmer, G. C. & Loeb, L. a. Mutations in the KRAS2 oncogene during progressive stages of human colon carcinoma. *Proc. Natl. Acad. Sci.* **86,** 2403–7 (1989).

118. Li, W. Q. *et al.* BRAF mutations are associated with distinctive clinical, pathological and molecular features of colorectal cancer independently of microsatellite instability status. *Mol. Cancer* **5,** 2 (2006).

119. Tam, I. Y. S. *et al.* Distinct epidermal growth factor receptor and KRAS mutation patterns in non-small cell lung cancer patients with different tobacco exposure and clinicopathologic features. *Clin. Cancer Res.* **12,** 1647–53 (2006).

120. Velho, S. *et al.* BRAF, KRAS and PIK3CA mutations in colorectal serrated polyps and cancer: primary or secondary genetic events in colorectal carcinogenesis? *BMC Cancer* **8,** 255 (2008).

121. Anglesio, M. S. *et al.* Mutation of ERBB2 provides a novel alternative mechanism for the ubiquitous activation of RAS-MAPK in ovarian serous low malignant potential tumors. *Mol. cancer Res.* **6,** 1678–90 (2008).

122. The Cancer Genome Atlas Research Network. Integrated genomic analyses of ovarian carcinoma. *Nature* **474,** 609–15 (2011).

123. Singer, G. *et al.* Patterns of p53 mutations separate ovarian serous borderline tumors and low- and high-grade carcinomas and provide support for a new model of ovarian carcinogenesis: a mutational analysis with immunohistochemical correlation. *Am. J. Surg. Pathol.* **29,** 218–24 (2005).

124. Kuo, K.-T. *et al.* Analysis of DNA copy number alterations in ovarian serous tumors identifies new molecular genetic changes in low-grade and high-grade carcinomas. *Cancer Res.* **69,** 4036–42 (2009).

125. Etemadmoghadam, D. *et al.* Integrated genome-wide DNA copy number and expression analysis identifies distinct mechanisms of primary chemoresistance in ovarian carcinomas. *Clin. Cancer Res.* **15,** 1417–27 (2009).

126. Engler, D. a *et al.* Genome wide DNA copy number analysis of serous type ovarian carcinomas identifies genetic markers predictive of clinical outcome. *PLoS One* **7,** e30996 (2012).

127. Dang, C. V. MYC on the path to cancer. *Cell* **149,** 22–35 (2012).

128. Dang, C. c-Myc target genes involved in cell growth, apoptosis, and metabolism. *Mol. Cell. Biol.* **19,** (1999).

129. Baudis, M. progenetix.org - Genomic copy number aberrations in cancer. (2012). at <http://www.progenetix.org/cgi-bin/pgHome.cgi>

130. Mayr, D. *et al.* Analysis of Gene Amplification and Prognostic Markers in Ovarian Cancer Using Comparative Genomic Hybridization for Microarrays and Immunohistochemical Analysis for Tissue Microarrays. *Am. J. Clin. Pathol.* **126,** 101–109 (2006).

131. Snijders, A. M. *et al.* Genome-wide-array-based comparative genomic hybridization reveals genetic homogeneity and frequent copy number increases encompassing CCNE1 in fallopian tube carcinoma. *Oncogene* **22,** 4281–6 (2003).

132. Möröy, T. & Geisen, C. Cyclin E. *Int. J. Biochem. Cell Biol.* **36,** 1424–39 (2004).

133. Konstantinopoulos, P. a *et al.* Integrated analysis of multiple microarray datasets identifies a reproducible survival predictor in ovarian cancer. *PLoS One* **6,** e18202 (2011).

134. George, J. *et al.* Nonequivalent Gene Expression and Copy Number Alterations in High-Grade Serous Ovarian Cancers with BRCA1 and BRCA2 Mutations. *Clin. Cancer Res.* **19,** 3474–3484 (2013).

135. Santillan, A. *et al.* Differences of chemoresistance assay between invasive micropapillary/low-grade serous ovarian carcinoma and high-grade serous ovarian carcinoma. *Int. J. Gynecol. cancer Off. J. Int. Gynecol. Cancer Soc.* **17,** 601–606 (2007).

136. Fathalla, M. Incesent Ovulation - a factor in ovarian neoplasia? *Lancet* **17,** 163 (1971).

137. Feeley, K. M. & Wells, M. Precursor lesions of ovarian epithelial malignancy. *Histopathology* **38,** 87–95 (2001).

138. Fleming, J. S., Beaugié, C. R., Haviv, I., Chenevix-Trench, G. & Tan, O. L. Incessant ovulation, inflammation and epithelial ovarian carcinogenesis: revisiting old hypotheses. *Mol. Cell. Endocrinol.* **247,** 4–21 (2006).

139. Herbison, A. E. Rapid actions of oestrogen on gonadotropin-releasing hormone neurons; from fantasy to physiology? *J. Physiol.* **587,** 5025–30 (2009).

140. Biskind, G. R. & Biskind, M. S. Atrophy of Ovaries Transplanted to the Spleen in Unilaterally Castrated Rats ; Proliferative Changes Following Subsequent Removal of Intact Ovary Atrophy of O ^ raries Transplanted to the Spleen in Unilaterally Castrated Rats. *Science (80-.).* **108,** 137–138 (1948).

141. Rzepka-Górska, I., Chudecka-Głaz, a & Kosmowska, B. FSH and LH serum/tumor fluid ratios and malignant tumors of the ovary. *Endocr. Relat. Cancer* **11,** 315–21 (2004).

142. Lindholm, J., Korsgaard, O., Rasmussen, P. & Micic, S. Luteinizing hormone and follicle stimulating hormone and the response to luteinizing hormone releasing hormone in relation to sex and age. *Eur. J. Clin. Invest.* **6,** 249–254 (1976).

143. Wang, J. *et al.* Quantitative analysis of follicle-stimulating hormone receptor in ovarian epithelial tumors: a novel approach to explain the field effect of ovarian cancer development in secondary mullerian systems. *Int. J. Cancer* **103,** 328–34 (2003).

144. Lu, J. J. *et al.* Decreased luteinizing hormone receptor mRNA expression in human ovarian epithelial cancer. *Gynecol. Oncol.* **79,** 158–68 (2000).

145. Glasier, A., McNeilly, A. S. & Howie, P. W. Fertility after childbirth: changes in serum gonadotrophin levels in bottle and breast feeding women. *Clin. Endocrinol. (Oxf).* **19,** 493–501 (1983).

146. Syed, V., Ulinski, G., Mok, S., Yiu, G. & Ho, S. Expression of gonadotropin receptor and growth responses to key reproductive hormones in normal and malignant human ovarian surface epithelial cells. *Cancer Res.* 6768–6776 (2001). at <http://cancerres.aacrjournals.org/content/61/18/6768.short>

147. Choi, K., Kang, S. & Tai, C. Estradiol up-regulates antiapoptotic Bcl-2 messenger ribonucleic acid and protein in tumorigenic ovarian surface epithelium cells. *Endocrinology* **142,** (2001).

148. Galtier-Dereure, F., Capony, F., Maudelonde, T. & Rochefort, H. Estradiol stimulates cell growth and secretion of procathepsin D and a 120-kilodalton protein in the human ovarian cancer cell line BG-1. *J. Clin. Endocrinol. Metab.* **75,** 1497–1502 (1992).

149. Lindgren, P. R. *et al.* The pattern of estradiol and progesterone differs in serum and tissue of benign and malignant ovarian tumors. *Int. J. Oncol.* **21,** 583–589 (2002).

150. Yager, J. D. Chapter 3: Endogenous Estrogens as Carcinogens Through Metabolic Activation. *JNCI Monogr.* **2000,** 67–73 (2000).

151. Willcocks, D. *et al.* Estrogen and progesterone receptors in human ovarian tumors. *Gynecol. Oncol.* **16,** 246–253 (1983).

152. Williams, C. & Simera, I. Tamoxifen for relapse of ovarian cancer. *Cochrane Database Syst Rev* (2001). at <http://onlinelibrary.wiley.com/doi/10.1002/14651858.CD001034/pdf/standard>

153. Risch, H. A. Hormonal Etiology of Epithelial Ovarian Cancer , With a. *J. Natl. Cancer Inst.* **90,** (1998).

154. Batra, S., Sjöberg, N. O. & Aberg, A. Human placental lactogen, estradiol-17beta, and progesterone levels in the third trimester and their respective values for detecting twin pregnancy. *Am. J. Obstet. Gynecol.* **131,** 69–72 (1978).

155. Albrektsen, G., Heuch, I., Thoresen, S. & Kvåle, G. Twin births, sex of children and maternal risk of ovarian cancer: a cohort study in Norway. *Br. J. Cancer* **96,** 1433–5 (2007).

156. Whiteman, D. & Murphy, M. Multiple births and risk of epithelial ovarian cancer. *J. Natl. Cancer Inst.* **92,** (2000).

157. Ji, J., Försti, A., Sundquist, J. & Hemminki, K. Risks of breast, endometrial, and ovarian cancers after twin births. *Endocr. Relat. Cancer* **14,** 703–11 (2007).

158. Martin, N. G. *et al.* Elevation of follicular phase inhibin and luteinizing hormone levels in mothers of dizygotic twins suggests nonovarian control of human multiple ovulation. *Fertil. Steril.* **56,** 469–74 (1991).

159. Lambalk, C. B. *et al.* Increased levels and pulsatility of follicle-stimulating hormone in mothers of hereditary dizygotic twins. *J. Clin. Endocrinol. Metab.* **83,** 481–6 (1998).

160. Rosenberg, L. *et al.* A case-control study of oral contraceptive use and invasive epithelial ovarian cancer. *Am. J. Epidemiol.* **139,** 654–61 (1994).

161. Noguchi, T. *et al.* Relationship between aromatase activity and steroid receptor levels in ovarian tumors from postmenopausal women. *J. Steroid Biochem. Mol. Biol.* **44,** 657–660 (1993).

162. Akahira, J.-I. *et al.* Differential expression of progesterone receptor isoforms A and B in the normal ovary, and in benign, borderline, and malignant ovarian tumors. *Japanese J. Cancer Res.* **93,** 807–815 (2002).

163. Lau, K. K.-M., Mok, S. C. S. & Ho, S. S.-M. Expression of human estrogen receptor-Î± and-Î^2, progesterone receptor, and androgen receptor mRNA in normal and malignant ovarian epithelial cells. *Proc. Natl. Acad. Sci.* **96,** 5722–5727 (1999).

164. Gyorffy, B., Lánczky, A. & Szállási, Z. Implementing an online tool for genome-wide validation of survival-associated biomarkers in ovarian-cancer using microarray data from 1287 patients. *Endocr. Relat. Cancer* **19,** 197–208 (2012).

165. Coussens, L. L. M. & Werb, Z. Inflammation and cancer. *Nature* **420,** 860–867 (2002).

166. Huncharek, M., Geschwind, J. & Kupelnick, B. Perineal application of cosmetic talc and risk of invasive epithelial ovarian cancer: a meta-analysis of 11,933 subjects from sixteen observational studies. *Anticancer Res.* **23,** 1955–60 (2003).

167. Melin, A., Sparén, P. & Bergqvist, A. The risk of cancer and the role of parity among women with endometriosis. *Hum. Reprod.* **22,** 3021–6 (2007).

168. Modugno, F. *et al.* Oral contraceptive use, reproductive history, and risk of epithelial ovarian cancer in women with and without endometriosis. *Am. J. Obstet. Gynecol.* **191,** 733–40 (2004).

169. Risch, H. & Howe, G. Pelvic inflammatory disease and the risk of epithelial ovarian cancer. *Cancer Epidemiol. Biomarkers Prev.* 447–451 (1995). at <http://cebp.aacrjournals.org/content/4/5/447.short>

170. Lin, H.-W. *et al.* Risk of ovarian cancer in women with pelvic inflammatory disease: a population-based study. *Lancet Oncol.* **12,** 900–4 (2011).

171. Rothwell, P. M. *et al.* Short-term effects of daily aspirin on cancer incidence, mortality, and non-vascular death: analysis of the time course of risks and benefits in 51 randomised controlled trials. *Lancet* **379,** 1602–12 (2012).

172. Bosetti, C., Rosato, V., Gallus, S., Cuzick, J. & La Vecchia, C. Aspirin and cancer risk: a quantitative review to 2011. *Ann. Oncol.* **23,** 1403–15 (2012).

173. Vang, R., Shih, I. & Kurman, R. Ovarian low-grade and high-grade serous carcinoma: pathogenesis, clinicopathologic and molecular biologic features, and diagnostic problems. *Adv. Anat. Pathol.* **16,** 267–282 (2009).

174. Marquez, R. T. *et al.* Patterns of gene expression in different histotypes of epithelial ovarian cancer correlate with those in normal fallopian tube, endometrium, and colon. *Clin. Cancer Res.* **11,** 6116–26 (2005).

175. Cheng, W., Liu, J., Yoshida, H., Rosen, D. & Naora, H. Lineage infidelity of epithelial ovarian cancers is controlled by HOX genes that specify regional identity in the reproductive tract. *Nat. Med.* **11,** 531–7 (2005).

176. Genetic/Familial High-Risk Assessment: Breast and Ovarian NCCN Guidelines. at <https://subscriptions.nccn.org/gl_login.aspx?ReturnURL=http://www.nccn.org/professionals/physician_gls/pdf/genetics_screening.pdf>

177. Finch, A. *et al.* Salpingo-oophorectomy and the risk of ovarian, fallopian tube, and peritoneal cancers in women with a BRCA1 or BRCA2 mutation. *JAMA* **296,** 185–192 (2006).

178. Finch, A. *et al.* Clinical and pathologic findings of prophylactic salpingo-oophorectomies in 159 BRCA1 and BRCA2 carriers. *Gynecol. Oncol.* **100,** 58–64 (2006).

179. Lamb, J. D., Garcia, R. L., Goff, B. a, Paley, P. J. & Swisher, E. M. Predictors of occult neoplasia in women undergoing risk-reducing salpingo-oophorectomy. *Am. J. Obstet. Gynecol.* **194,** 1702–9 (2006).

180. Callahan, M. J. *et al.* Primary fallopian tube malignancies in BRCA-positive women undergoing surgery for ovarian cancer risk reduction. *J. Clin. Oncol.* **25,** 3985–90 (2007).

181. Bol, G. M. *et al.* Methylation profiles of hereditary and sporadic ovarian cancer. *Histopathology* **57,** 363–70 (2010).

182. Esteller, M. *et al.* DNA methylation patterns in hereditary human cancers mimic sporadic tumorigenesis. *Hum. Mol. Genet.* **10,** 3001–7 (2001).

183. Jazaeri, A. *et al.* Gene expression profiles of BRCA1-linked, BRCA2-linked, and sporadic ovarian cancers. *J. Natl. Cancer Inst.* **94,** 1506–7 (2002).

184. Zweemer, R. P. *et al.* Differences between hereditary and sporadic ovarian cancer. *Eur. J. Obstet. Gynecol. Reprod. Biol.* **82,** 151–3 (1999).

185. Pharoah, P. D. P., Easton, D. F. & Stockton, D. L. Survival in Familial , BRCA1 - associated , and BRCA2- associated Epithelial Ovarian Cancer. *Cancer Res.* 868–871 (1999).

186. Boyd, J. *et al.* Clinicopathologic features of BRCA-linked and sporadic ovarian cancer. *JAMA* **283,** 2260–5 (2000).

187. Wilks, A. & Harpur, A. Two novel protein-tyrosine kinases, each with a second phosphotransferase-related catalytic domain, define a new class of protein kinase. *Mol. Cell. Biol.* (1991). doi:10.1128/MCB.11.4.2057.Updated

188. Velazquez, L., Fellous, M., Stark, G. R. & Pellegrini, S. A protein tyrosine kinase in the interferon alpha/beta signaling pathway. *Cell* **70,** 313–22 (1992).

189. Kawata, T. *et al.* SH2 signaling in a lower eukaryote: a STAT protein that regulates stalk cell differentiation in dictyostelium. *Cell* **89,** 909–16 (1997).

190. Dale, T. C., Imam, a M., Kerr, I. M. & Stark, G. R. Rapid activation by interferon alpha of a latent DNA-binding protein present in the cytoplasm of untreated cells. *Proc. Natl. Acad. Sci.* **86,** 1203–7 (1989).

191. Fu, X. & Kessler, D. ISGF3, the transcriptional activator induced by interferon alpha, consists of multiple interacting polypeptide chains. *Proc. Natl. Acad. Sci.* **87,** 8555–9 (1990).

192. Zhang, J. J. *et al.* Two contact regions between Stat1 and CBP/p300 in interferon gamma signaling. *Proc. Natl. Acad. Sci.* **93,** 15092–6 (1996).

193. Schindler, C., Shuai, K., Prezioso, V. R. & Darnell, J. E. Interferon-dependent tyrosine phosphorylation of a latent cytoplasmic transcription factor. *Science (80-.).* **257,** 809–813 (1992).

194. Wegenka, U. & Buschmann, J. Acute-phase response factor, a nuclear factor binding to acute-phase response elements, is rapidly activated by interleukin-6 at the posttranslational level. *J. Mol. Cell. Biol.* **13,** 276–88 (1993).

195. Akira, S. *et al.* Molecular cloning of APRF, a novel IFN-stimulated gene factor 3 p91-related transcription factor involved in the gp130-mediated signaling pathway. *Cell* **77,** 63–71 (1994).

196. Chen, X. *et al.* Crystal structure of a tyrosine phosphorylated STAT-1 dimer bound to DNA. *Cell* **93,** 827–39 (1998).

197. Vinkemeier, U., Moarefi, I., Darnell, J. E. & Kuriyan, J. Structure of the Amino-Terminal Protein Interaction Domain of STAT-4. *Science (80-.).* **279,** 1048–1052 (1998).

198. Horvath, C. M., Stark, G. R., Kerr, I. M. & Darnell, J. E. Interactions between STAT and non-STAT proteins in the interferon-stimulated gene factor 3 transcription complex. *Mol. Cell. Biol.* **16,** 6957–6964 (1996).

199. Yang, E., Wen, Z., Haspel, R. L., Zhang, J. J. & Darnell, J. E. The linker domain of Stat1 is required for gamma interferon-driven transcription. *Mol. Cell. Biol.* **19,** 5106–5112 (1999).

200. Paulson, M. *et al.* Stat protein transactivation domains recruit p300/CBP through widely divergent sequences. *J. Biol. Chem.* **274,** 25343–25349 (1999).

201. Baran-Marszak, F. *et al.* Differential roles of STAT1alpha and STAT1beta in fludarabine-induced cell cycle arrest and apoptosis in human B cells. *Blood* **104,** 2475–2483 (2004).

202. Levy, D. E. & Darnell, J. E. Stats: transcriptional control and biological impact. *Nat. Rev. Mol. Cell Biol.* **3,** 651–62 (2002).

203. Decker, T. & Kovarik, P. Serine phosphorylation of STATs. *Oncogene* **19,** 2628–37 (2000).

204. Kovarik, P. *et al.* Stress-induced phosphorylation of STAT1 at Ser727 requires p38 mitogen-activated protein kinase whereas IFN-gamma uses a different signaling pathway. *Proc. Natl. Acad. Sci.* **96,** 13956–61 (1999).

205. Schuringa, J., Jonk, L. & Dokter, W. Interleukin-6-induced STAT3 transactivation and Ser727 phosphorylation involves Vav, Rac-1 and the kinase SEK-1/MKK-4 as signal transduction components. *Biochem. J.* **96,** 89–96 (2000).

206. Kim, H. & Baumann, H. The carboxyl-terminal region of STAT3 controls gene induction by the mouse haptoglobin promoter. *J. Biol. Chem.* **272,** 14571–9 (1997).

207. Tanner, J. W., Chen, W., Young, R. L., Longmore, G. D. & Shaw, a S. The conserved box 1 motif of cytokine receptors is required for association with JAK kinases. *J. Biol. Chem.* **270,** 6523–30 (1995).

208. Heinrich, P. C. *et al.* Principles of interleukin (IL)-6-type cytokine signalling and its regulation. *Biochem. J.* **374,** 1–20 (2003).

209. Haan, C. *et al.* Mapping of a region within the N terminus of Jak1 involved in cytokine receptor interaction. *J. Biol. Chem.* **276,** 37451–8 (2001).

210. Radtke, S. *et al.* The Jak1 SH2 domain does not fulfill a classical SH2 function in Jak/STAT signaling but plays a structural role for receptor interaction and up-regulation of receptor surface expression. *J. Biol. Chem.* **280,** 25760–8 (2005).

211. Saharinen, P. & Silvennoinen, O. The pseudokinase domain is required for suppression of basal activity of Jak2 and Jak3 tyrosine kinases and for cytokine-inducible activation of signal transduction. *J. Biol. Chem.* **277,** 47954–63 (2005).

212. Levine, R. L. *et al.* Activating mutation in the tyrosine kinase JAK2 in polycythemia vera, essential thrombocythemia, and myeloid metaplasia with myelofibrosis. *Cancer Cell* **7,** 387–97 (2005).

213. Ugo, V., James, C. & Vainchenker, W. A unique clonal JAK2 mutation leading to constitutive signalling causes polycythaemia vera. *Nature* **21,** 669–70 (2005).

214. Zhong, Z., Wen, Z. & Jr, J. D. Stat3: a STAT family member activated by tyrosine phosphorylation in response to epidermal growth factor and interleukin-6. *Science (80-.).* **264,** 95–98 (1994).

215. Hou, J. *et al.* An interleukin-4-induced transcription factor: IL-4 Stat. *Science (80-.).* **265,** 1701–1706 (1994).

216. Valdembri, D., Serini, G., Vacca, A., Ribatti, D. & Bussolino, F. In vivo activation of JAK2/STAT-3 pathway during angiogenesis induced by GM-CSF. *FASEB J.* 8–12 (2002). at <http://www.fasebj.org/content/16/2/225.short>

217. Shuai, K., Schindler, C., Prezioso, V. R. & Darnell, J. E. Activation of transcription by IFN-gamma: tyrosine phosphorylation of a 91-kD DNA binding protein. *Science (80-.).* **258,** 1808–12 (1992).

218. Raz, R., Lee, C. K., Cannizzaro, L. a, D'Eustachio, P. & Levy, D. E. Essential role of STAT3 for embryonic stem cell pluripotency. *Proc. Natl. Acad. Sci.* **96,** 2846–51 (1999).

219. Fornek, J. L. *et al.* Critical role for Stat3 in T-dependent terminal differentiation of IgG B cells. *Blood* **107,** 1085–91 (2006).

220. Darnell Jr., J. E. STATs and Gene Regulation. *Science (80-.).* **277,** 1630–1635 (1997).

221. Shuai, K. *et al.* Polypeptide signalling to the nucleus through tyrosine phosphorylation of Jak and Stat proteins. *Nature* **366,** 580–583 (1993).

222. Schindler, C. & Fu, X. Proteins of transcription factor ISGF-3: one gene encodes the 91-and 84-kDa ISGF-3 proteins that are activated by interferon alpha. *Proc. Natl. Acad. Sci.* **89,** 7836–9 (1992).

223. Bhinge, A. a, Kim, J., Euskirchen, G. M., Snyder, M. & Iyer, V. R. Mapping the chromosomal targets of STAT1 by Sequence Tag Analysis of Genomic Enrichment (STAGE). *Genome Res.* **17,** 910–6 (2007).

224. Robertson, G., Hirst, M. & Bainbridge, M. Genome-wide profiles of STAT1 DNA association using chromatin immunoprecipitation and massively parallel sequencing. *Nat. Methods* **4,** 651–657 (2007).

225. Jr, J. D., Kerr, I. & Stark, G. Jak-STAT pathways and transcriptional activation in response to IFNs and other extracellular signaling proteins. *Science (80-.).* **264,** 1415–1421 (1994).

226. Boulton, T. G. *et al.* STAT3 activation by cytokines utilizing gp130 and related transducers involves a secondary modification requiring an H7-sensitive kinase. *Proc. Natl. Acad. Sci.* **92,** 6915–9 (1995).

227. Weber-Nordt, R. M. *et al.* Stat3 recruitment by two distinct ligand-induced, tyrosine-phosphorylated docking sites in the interleukin-10 receptor intracellular domain. *J. Biol. Chem.* **271,** 27954–27961 (1996).

228. Hawthorne, V. S. *et al.* ErbB2-mediated Src and signal transducer and activator of transcription 3 activation leads to transcriptional up-regulation of p21Cip1 and chemoresistance in breast cancer cells. *Mol. cancer Res.* **7,** 592–600 (2009).

229. Schreiner, S. J., Schiavone, A. P. & Smithgall, T. E. Activation of STAT3 by the Src family kinase Hck requires a functional SH3 domain. *J. Biol. Chem.* **277,** 45680–7 (2002).

230. BioGPS: an extensible and customizable portal for querying and organizing gene annotation resources. at <http://biogps.org/#goto=welcome>

231. Giese, B. *et al.* Long term association of the cytokine receptor gp130 and the Janus kinase Jak1 revealed by FRAP analysis. *J. Biol. Chem.* **278,** 39205–13 (2003).

232. Murakami, M. & Narazaki, M. Critical cytoplasmic region of the interleukin 6 signal transducer gp130 is conserved in the cytokine receptor family. *Proc. Natl. Acad. Sci.* **88,** 11349–11353 (1991).

233. Narazaki, M. *et al.* Activation of JAK2 kinase mediated by the interleukin 6 signal transducer gp130. *Proc. Natl. Acad. Sci.* **91,** 2285–9 (1994).

234. Radtke, S. *et al.* Novel role of Janus kinase 1 in the regulation of oncostatin M receptor surface expression. *J. Biol. Chem.* **277,** 11297–305 (2002).

235. Guschin, D., Rogers, N. & Briscoe, J. A major role for the protein tyrosine kinase JAK1 in the JAK/STAT signal transduction pathway in response to interleukin-6. *EMBO J.* **14,** 1421–1429 (1995).

236. Gerhartz, C., Heesel, B. & Sasse, J. Differential activation of acute phase response factor/STAT3 and STAT1 via the cytoplasmic domain of the interleukin 6 signal transducer gp130 I. Definition of a novel. *J. Biol. Chem.* **271,** 12999–13007 (1996).

237. Schmitz, J. *et al.* The cytoplasmic tyrosine motifs in full-length glycoprotein 130 have different roles in IL-6 signal transduction. *J. Immunol.* **164,** 848–54 (2000).

238. Tomida, M., Heike, T. & Yokota, T. Cytoplasmic domains of the leukemia inhibitory factor receptor required for STAT3 activation, differentiation, and growth arrest of myeloid leukemic cells. *Blood* **93,** 1934–41 (1999).

239. Heim, M. H., Kerr, I. M., Stark, G. R. & Darnell, J. E. Contribution of STAT SH2 groups to specific interferon signaling by the Jak-STAT pathway. *Science (80-.).* **267,** 1347–9 (1995).

240. Shuai, K. *et al.* Interferon activation of the transcription factor Stat91 involves dimerization through SH2-phosphotyrosyl peptide interactions. *Cell* **76,** 821–8 (1994).

241. Mikita, T., Daniel, C., Wu, P. & Schindler, U. Mutational analysis of the STAT6 SH2 domain. *J. Biol. Chem.* **273,** 17634–42 (1998).

242. Vogt, M. *et al.* The role of the N-terminal domain in dimerization and nucleocytoplasmic shuttling of latent STAT3. *J. Cell Sci.* **124,** 900–9 (2011).

243. Ma, J. & Cao, X. Regulation of Stat3 nuclear import by importin alpha5 and importin alpha7 via two different functional sequence elements. *Cell. Signal.* **18,** 1117–26 (2006).

244. Cimica, V., Chen, H.-C., Iyer, J. K. & Reich, N. C. Dynamics of the STAT3 transcription factor: nuclear import dependent on Ran and importin-β1. *PLoS One* **6,** e20188 (2011).

245. Gauldie, J., Richards, C., Harnish, D., Lansdorp, P. & Baumann, H. Interferon beta 2/B-cell stimulatory factor type 2 shares identity with monocyte-derived hepatocyte-stimulating factor and regulates the major acute phase protein response in liver cells. *Proc. Natl. Acad. Sci.* **84,** 7251–5 (1987).

246. Alonzi, T., Maritano, D. & Gorgoni, B. Essential role of STAT3 in the control of the acute-phase response as revealed by inducible gene activation in the liver. *Mol. Cell. Biol.* (2001). doi:10.1128/MCB.21.5.1621

247. Durbin, J. E., Hackenmiller, R., Simon, M. C. & Levy, D. E. Targeted disruption of the mouse Stat1 gene results in compromised innate immunity to viral disease. *Cell* **84,** 443–50 (1996).

248. Liu, X. *et al.* Stat5a is mandatory for adult mammary gland development and lactogenesis. *Genes Dev.* **11,** 179–186 (1997).

249. Takeda, K. *et al.* Targeted disruption of the mouse Stat3 gene leads to early embryonic lethality. *Proc. Natl. Acad. Sci.* **94,** 3801–4 (1997).

250. Duncan, S., Zhong, Z., Wen, Z. & Darnell, J. STAT signaling is active during early mammalian development. *Dev. Dyn.* **198,** 190–198 (1997).

251. Yoshida, K. *et al.* Targeted disruption of gp130, a common signal transducer for the interleukin 6 family of cytokines, leads to myocardial and hematological disorders. *Proc. Natl. Acad. Sci.* **93,** 407–11 (1996).

252. Rodig, S. J. *et al.* Disruption of the Jak1 gene demonstrates obligatory and nonredundant roles of the Jaks in cytokine-induced biologic responses. *Cell* **93,** 373–83 (1998).

253. Soriano, P., Montgomery, C., Geske, R. & Bradley, a. Targeted disruption of the c-src proto-oncogene leads to osteopetrosis in mice. *Cell* **64,** 693–702 (1991).

254. Hansen, L. a *et al.* Genetically null mice reveal a central role for epidermal growth factor receptor in the differentiation of the hair follicle and normal hair development. *Am. J. Pathol.* **150,** 1959–75 (1997).

255. Takeda, K. *et al.* Enhanced Th1 activity and development of chronic enterocolitis in mice devoid of Stat3 in macrophages and neutrophils. *Immunity* **10,** 39–49 (1999).

256. Sano, S. *et al.* Keratinocyte-specific ablation of Stat3 exhibits impaired skin remodeling, but does not affect skin morphogenesis. *EMBO J.* **18,** 4657–68 (1999).

257. Boeuf, H., Hauss, C., Graeve, F. D., Baran, N. & Kedinger, C. Leukemia inhibitory factor-dependent transcriptional activation in embryonic stem cells. *J. Cell Biol.* **138,** 1207–17 (1997).

258. Matsuda, T. *et al.* STAT3 activation is sufficient to maintain an undifferentiated state of mouse embryonic stem cells. *EMBO J.* **18,** 4261–9 (1999).

259. Kortylewski, M. *et al.* Inhibiting Stat3 signaling in the hematopoietic system elicits multicomponent antitumor immunity. *Nat. Med.* **11,** 1314–21 (2005).

260. Sinibaldi, D., Wharton, W. & Turkson, J. Induction of p21WAF1/CIP1 and cyclin D1 expression by the Src oncoprotein in mouse fibroblasts: role of activated STAT3 signaling. *Oncogene* **2,** (2000).

261. Catlett-Falcone, R. *et al.* Constitutive activation of Stat3 signaling confers resistance to apoptosis in human U266 myeloma cells. *Immunity* **10,** 105–15 (1999).

262. Gritsko, T. *et al.* Persistent activation of stat3 signaling induces survivin gene expression and confers resistance to apoptosis in human breast cancer cells. *Clin. Cancer Res.* **12,** 11–9 (2006).

263. Xu, Q. *et al.* Targeting Stat3 blocks both HIF-1 and VEGF expression induced by multiple oncogenic growth signaling pathways. *Oncogene* **24,** 5552–60 (2005).

264. Bowman, T. *et al.* Stat3-mediated Myc expression is required for Src transformation and PDGF-induced mitogenesis. *Proc. Natl. Acad. Sci.* **98,** 7319–7324 (2001).

265. Kinjyo, I. *et al.* Loss of SOCS3 in T helper cells resulted in reduced immune responses and hyperproduction of interleukin 10 and transforming growth factor-beta 1. *J. Exp. Med.* **203,** 1021–31 (2006).

266. Wang, T. *et al.* Regulation of the innate and adaptive immune responses by Stat-3 signaling in tumor cells. *Nat. Med.* **10,** 48–54 (2004).

267. Bromberg, J. F., Horvath, C. M., Besser, D., Lathem, W. W. & Darnell, J. E. Stat3 activation is required for cellular transformation by v-src. *Mol. Cell. Biol.* **18,** 2553–8 (1998).

268. Irby, R. B. *et al.* Activating SRC mutation in a subset of advanced human colon cancers. *Nat. Genet.* **21,** (1999).

269. Turkson, J. *et al.* Stat3 activation by Src induces specific gene regulation and is required for cell transformation. *Mol. Cell. Biol.* **18,** 2545–52 (1998).

270. Grivennikov, S. *et al.* IL-6 and Stat3 are required for survival of intestinal epithelial cells and development of colitis-associated cancer. *Cancer Cell* **15,** 103–13 (2009).

271. Garcia, R., Bowman, T. & GUILLIAN, N. Constitutive activation of Stat3 by the Src and JAK tyrosine kinases participates in growth regulation of human breast carcinoma cells. *Oncogene* **20,** 2499–2513 (2001).

272. Colomiere, M., Findlay, J., Ackland, L. & Ahmed, N. Epidermal growth factor-induced ovarian carcinoma cell migration is associated with JAK2/STAT3 signals and changes in the abundance and localization of alpha6beta1 integrin. *Int. J. Biochem. Cell Biol.* **41,** 1034–45 (2009).

273. Fossey, S. L., Bear, M. D., Kisseberth, W. C., Pennell, M. & London, C. a. Oncostatin M promotes STAT3 activation, VEGF production, and invasion in osteosarcoma cell lines. *BMC Cancer* **11,** 125 (2011).

274. Kortylewski, M. *et al.* Regulation of the IL-23 and IL-12 balance by Stat3 signaling in the tumor microenvironment. *Cancer Cell* **15,** 114–23 (2009).

275. Rosen, D. G. *et al.* The role of constitutively active signal transducer and activator of transcription 3 in ovarian tumorigenesis and prognosis. *Cancer* **107,** 2730–40 (2006).

276. Haura, E. B., Zheng, Z., Song, L., Cantor, A. & Bepler, G. Activated epidermal growth factor receptor-Stat-3 signaling promotes tumor survival in vivo in non-small cell lung cancer. *Clin. Cancer Res.* **11,** 8288–94 (2005).

277. Rebouissou, S. *et al.* Frequent in-frame somatic deletions activate gp130 in inflammatory hepatocellular tumours. *Nature* **457,** 200–204 (2009).

278. Gao, S., Mark, K. & Leslie, K. Mutations in the EGFR kinase domain mediate STAT3 activation via IL-6 production in human lung adenocarcinomas. *J. Clin. Invest.* **117,** (2007).

279. Veeriah, S. & Brennan, C. The tyrosine phosphatase PTPRD is a tumor suppressor that is frequently inactivated and mutated in glioblastoma and other human cancers. *Proc. Natl. Acad. Sci.* (2009). at <http://www.pnas.org/content/106/23/9435.short>

280. He, B., You, L., Uematsu, K. & Zang, K. SOCS-3 is frequently silenced by hypermethylation and suppresses cell growth in human lung cancer. *Proc. Natl. Acad. Sci.* **100,** 14133–14138 (2003).

281. Schmitz, J., Weissenbach, M., Haan, S., Heinrich, P. C. & Schaper, F. SOCS3 exerts its inhibitory function on interleukin-6 signal transduction through the SHP2 recruitment site of gp130. *J. Biol. Chem.* **275,** 12848–56 (2000).

282. Feener, E. & Rosario, F. Tyrosine phosphorylation of Jak2 in the JH2 domain inhibits cytokine signaling. *J. Mol. Cell. Biol.* **24,** 4968–4978 (2004).

283. Min, H. & Wei-hong, Z. Constitutive activation of signal transducer and activator of transcription 3 in epithelial ovarian carcinoma. *J. Obstet. Gynaecol. Res.* **35,** 918–25 (2009).

284. Silver, D. L., Naora, H., Liu, J., Cheng, W. & Montell, D. J. Activated signal transducer and activator of transcription (STAT) 3: localization in focal adhesions and function in ovarian cancer cell motility. *Cancer Res.* **64,** 3550–8 (2004).

285. Lane, D., Matte, I., Rancourt, C. & Piché, A. Prognostic significance of IL-6 and IL-8 ascites levels in ovarian cancer patients. *BMC Cancer* **11,** 210 (2011).

286. Lutgendorf, S. & Weinrib, A. Interleukin-6, cortisol, and depressive symptoms in ovarian cancer patients. *J. Clin. Oncol.* **26,** (2008).

287. Scambia, G., Testa, U. & Panici, P. Prognostic significance of interleukin 6 serum levels in patients with ovarian cancer. *Br. J. Cancer* 354–356 (1995). at <http://www.ncbi.nlm.nih.gov/pmc/articles/PMC2033591/>

288. Tempfer, C., Zeisler, H. & Sliutz, G. Serum evaluation of interleukin 6 in ovarian cancer patients. *Gynecol. Oncol.* **30,** 27–30 (1997).

289. Coward, J. *et al.* Interleukin-6 as a therapeutic target in human ovarian cancer. *Clin. Cancer Res.* **17,** 6083–96 (2011).

290. Rath, K. S., Funk, H. M., Bowling, M. C., Richards, W. E. & Drew, A. F. Expression of soluble interleukin-6 receptor in malignant ovarian tissue. *Am. J. Obstet. Gynecol.* **203,** 230.e1–230.e8 (2010).

291. Coffelt, S. & Marini, F. The pro-inflammatory peptide LL-37 promotes ovarian tumor progression through recruitment of multipotent mesenchymal stromal cells. *Proc. Natl. Acad. Sci.* **106,** (2009).

292. Nilsson, M. B., Langley, R. R. & Fidler, I. J. Interleukin-6, secreted by human ovarian carcinoma cells, is a potent proangiogenic cytokine. *Cancer Res.* **65,** 10794–800 (2005).

293. Cai, L. *et al.* Growth inhibition of human ovarian cancer cells by blocking STAT3 activation with small interfering RNA. *Eur. J. Obstet. Gynecol. Reprod. Biol.* **148,** 73–80 (2010).

294. Burke, W. M. *et al.* Inhibition of constitutively active Stat3 suppresses growth of human ovarian and breast cancer cells. *Oncogene* **20,** 7925–34 (2001).

295. Zhang, X., Liu, P., Zhang, B., Wang, A. & Yang, M. Role of STAT3 decoy oligodeoxynucleotides on cell invasion and chemosensitivity in human epithelial ovarian cancer cells. *Cancer Genet. Cytogenet.* **197,** 46–53 (2010).

296. Han, Z. *et al.* Silencing of the STAT3 signaling pathway reverses the inherent and induced chemoresistance of human ovarian cancer cells. *Biochem. Biophys. Res. Commun.* **435,** 188–194 (2013).

297. Helleman, J. *et al.* Molecular profiling of platinum resistant ovarian cancer. *Int. J. Cancer* **118,** 1963–71 (2006).

298. Roberts, D. *et al.* Identification of genes associated with platinum drug sensitivity and resistance in human ovarian cancer cells. *Br. J. Cancer* **92,** 1149–58 (2005).

299. Duan, Z. *et al.* Signal transducers and activators of transcription 3 pathway activation in drug-resistant ovarian cancer. *Clin. Cancer Res.* **12,** 5055–63 (2006).

300. Zajchowski, D., Bartholdi, M. & Gong, Y. Identification of gene expression profiles that predict the aggressive behavior of breast cancer cells. *Cancer Res.* 5168–5178 (2001). at <http://cancerres.aacrjournals.org/content/61/13/5168.short>

301. Lo, H.-W. *et al.* Epidermal growth factor receptor cooperates with signal transducer and activator of transcription 3 to induce epithelial-mesenchymal transition in cancer cells via up-regulation of TWIST gene expression. *Cancer Res.* **67,** 9066–76 (2007).

302. Colomiere, M. *et al.* Cross talk of signals between EGFR and IL-6R through JAK2/STAT3 mediate epithelial-mesenchymal transition in ovarian carcinomas. *Br. J. Cancer* **100,** 134–44 (2009).

303. Thabard, W. *et al.* Myeloma cells release soluble interleukin-6Ralpha in relation to disease progression by two distinct mechanisms: alternative splicing and proteolytic cleavage. *Clin. Cancer Res.* **5,** 2693–2697 (1999).

304. Jiang, Q. *et al.* Efficient inhibition of intraperitoneal ovarian cancer growth in nude mice by liposomal delivery of short hairpin RNA against STAT3. *J. Obstet. Gynaecol. Res.* 1–9 (2012). doi:10.1111/j.1447-0756.2012.02007.x

305. Yu, H., Pardoll, D. & Jove, R. STATs in cancer inflammation and immunity: a leading role for STAT3. *Nat. Rev. Cancer* **9,** 798–809 (2009).

306. Park, S.-J. *et al.* IL-6 regulates in vivo dendritic cell differentiation through STAT3 activation. *J. Immunol.* **173,** 3844–54 (2004).

307. Langrish, C. L. *et al.* IL-12 and IL-23: master regulators of innate and adaptive immunity. *Immunol. Rev.* **202,** 96–105 (2004).

308. Langowski, J. L. *et al.* IL-23 promotes tumour incidence and growth. *Nature* **442,** 461–5 (2006).

309. Braumüller, H. *et al.* T-helper-1-cell cytokines drive cancer into senescence. *Nature* (2013). doi:10.1038/nature11824

310. Bettelli, E. *et al.* Reciprocal developmental pathways for the generation of pathogenic effector TH17 and regulatory T cells. *Nature* **441,** 235–8 (2006).

311. Yang, X. O. *et al.* STAT3 regulates cytokine-mediated generation of inflammatory helper T cells. *J. Biol. Chem.* **282,** 9358–63 (2007).

312. Chen, Z. *et al.* Selective regulatory function of Socs3 in the formation of IL-17-secreting T cells. *Proc. Natl. Acad. Sci.* **103,** 8137–42 (2006).

313. Korn, T., Bettelli, E., Oukka, M. & Kuchroo, V. K. IL-17 and Th17 Cells. *Annu. Rev. Immunol.* **27,** 485–517 (2009).

314. Hanahan, D. & Weinberg, R. A. Hallmarks of cancer: the next generation. *Cell* **144,** 646–674 (2011).

315. Zhang, Y. *et al.* Activation of Stat3 in v-Src-transformed fibroblasts requires cooperation of Jak1 kinase activity. *J. Biol. Chem.* **275,** 24935–44 (2000).

316. Ren, Z. & Schaefer, T. S. ErbB-2 activates Stat3 alpha in a Src- and JAK2-dependent manner. *J. Biol. Chem.* **277,** 38486–93 (2002).

317. Wernig, G. *et al.* Efficacy of TG101348, a selective JAK2 inhibitor, in treatment of a murine model of JAK2V617F-induced polycythemia vera. *Cancer Cell* **13,** 311–20 (2008).

318. Looyenga, B. D. *et al.* STAT3 is activated by JAK2 independent of key oncogenic driver mutations in non-small cell lung carcinoma. *PLoS One* **7,** e30820 (2012).

319. Burgess, A., Cho, H. & Eigenbrot, C. An open-and-shut case? Recent insights into the activation of EGF/ErbB receptors. *Mol. Cell* **12,** 541–552 (2003).

320. Ferguson, K. M. *et al.* EGF Activates Its Receptor by Removing Interactions that Autoinhibit Ectodomain Dimerization. *Mol. Cell* **11,** 507–517 (2003).

321. Fukazawa, T., Miyake, S., Band, V. & Band, H. Tyrosine phosphorylation of Cbl upon epidermal growth factor (EGF) stimulation and its association with EGF receptor and downstream signaling proteins. *J. Biol. Chem.* **271,** 14554–9 (1996).

322. Peles, E., Lamprecht, R., Ben-Levy, R., Tzahar, E. & Yarden, Y. Regulated coupling of the Neu receptor to phosphatidylinositol 3'-kinase and its release by oncogenic activation. *J. Biol. Chem.* **267,** 12266–74 (1992).

323. Yarden, Y. & Sliwkowski, M. X. Untangling the ErbB signalling network. *Nat. Rev. Mol. Cell Biol.* **2,** 127–37 (2001).

324. Garrett, T., McKern, N. & Lou, M. The crystal structure of a truncated ErbB2 ectodomain reveals an active conformation, poised to interact with other ErbB receptors. *Mol. Cell* **11,** 495–505 (2003).

325. Ferguson, K. M., Darling, P. J., Mohan, M. J., Macatee, T. L. & Lemmon, M. a. Extracellular domains drive homo- but not hetero-dimerization of erbB receptors. *EMBO J.* **19,** 4632–43 (2000).

326. Yarden, Y. Biology of HER2 and its importance in breast cancer. *Oncology* **61,** 1–13 (2001).

327. Sliwkowski, M. & Schaefer, G. Coexpression of erbB2 and erbB3 proteins reconstitutes a high affinity receptor for heregulin. *J. Biol. Chem.* **269,** 14661–14665 (1994).

328. Akiyama, T. *et al.* The transforming potential of the c-erbB-2 protein is regulated by its autophosphorylation at the carboxyl-terminal domain. *Mol. Cell. Biol.* **11,** 833–842 (1991).

329. Mikami, Y. *et al.* Carboxyl-terminal deletion and point mutations decrease the transforming potential of the activated rat neu oncogene product. *Proc. Natl. Acad. Sci.* **89,** 7335–7339 (1992).

330. Shih, C., Shilo, B. Z., Goldfarb, M. P., Dannenberg, A. & Weinberg, R. a. Passage of phenotypes of chemically transformed cells via transfection of DNA and chromatin. *Proc. Natl. Acad. Sci.* **76,** 5714–8 (1979).

331. Padhy, L. C., Shih, C., Cowing, D., Finkelstein, R. & Weinberg, R. a. Identification of a phosphoprotein specifically induced by the transforming DNA of rat neuroblastomas. *Cell* **28,** 865–71 (1982).

332. Fiore, P. Di, Pierce, J., Kraus, M. & Segatto, O. erbB-2 is a potent oncogene when overexpressed in NIH/3T3 cells. *Science (80-.).* **237,** 178–182 (1987).

333. Slamon, D. J. *et al.* Human breast cancer: correlation of relapse and survival with amplification of the HER-2/neu oncogene. *Science (80-.).* **235,** 177–182 (1987).

334. Rody, a *et al.* The erbB2+ cluster of the intrinsic gene set predicts tumor response of breast cancer patients receiving neoadjuvant chemotherapy with docetaxel, doxorubicin and cyclophosphamide within the GEPARTRIO trial. *Breast* **16,** 235–40 (2007).

335. Pritchard, K. I. K. *et al.* HER2 and responsiveness of breast cancer to adjuvant chemotherapy. *N. Engl. J. Med.* **354,** 2103–2111 (2006).

336. Seshadri, R. *et al.* Clinical significance of HER-2/neu oncogene amplification in primary breast cancer. The South Australian Breast Cancer Study Group. *J. Clin. Oncol.* **11,** 1936–1942 (1993).

337. Andrulis, I. L. *et al.* neu/erbB-2 amplification identifies a poor-prognosis group of women with node-negative breast cancer. Toronto Breast Cancer Study Group. *J. Clin. Oncol.* **16,** 1340–1349 (1998).

338. Lassus, H. *et al.* ERBB2 amplification is superior to protein expression status in predicting patient outcome in serous ovarian carcinoma. *Gynecol. Oncol.* **92,** 31–39 (2004).

339. Cloven, N. G., Kyshtoobayeva, A., Burger, R. A., Yu, I. R. & Fruehauf, J. P. In vitro chemoresistance and biomarker profiles are unique for histologic subtypes of epithelial ovarian cancer. *Gynecol. Oncol.* **92,** 160–166 (2004).

340. Høgdall, E. V. S. *et al.* Distribution of HER-2 overexpression in ovarian carcinoma tissue and its prognostic value in patients with ovarian carcinoma: from the Danish MALOVA Ovarian Cancer Study. *Cancer* **98,** 66–73 (2003).

341. Camilleri-Broët, S. *et al.* HER-2 overexpression is an independent marker of poor prognosis of advanced primary ovarian carcinoma: a multicenter study of the GINECO group. *Ann. Oncol.* **15,** 104–112 (2004).

342. Meden, H. *et al.* Overexpression of the oncogene c-erb B2 in primary ovarian cancer: evaluation of the prognostic value in a Cox proportional hazards multiple regression. *Int. J. Gynecol. Pathol. Off. J. Int. Soc. Gynecol. Pathol.* **13,** 45–53 (1994).

343. Slamon, D. J. *et al. Use of chemotherapy plus a monoclonal antibody against HER2 for metastatic breast cancer that overexpresses HER2. N. Engl. J. Med.* **344,** 783–792 (Massachusetts Medical Society, 2001).

344. Rouzier, R. *et al.* Breast cancer molecular subtypes respond differently to preoperative chemotherapy. *Clin. Cancer Res.* **11,** 5678–85 (2005).

345. Hayes, D. F. *et al.* HER2 and response to paclitaxel in node-positive breast cancer. *N. Engl. J. Med.* **358,** 198; author reply 198–9 (2008).

346. Pegram, M. *et al.* Inhibitory effects of combinations of HER-2/neu antibody and chemotherapeutic agents used for treatment of human breast cancers. *Oncogene* **18,** 2241–2251 (1999).

347. Meden H, Marx D, Roegglen T, Schauer A, K. W. Overexpression of the oncogene c-erbB-2 (HER2/neu) and response to chemotherapy in patients with ovarian cancer. *Int. J. Gynecol. Pathol. Off. J. Int. Soc. Gynecol. Pathol.* **22,** 182–185 (1998).

348. Kartalou, M. & Essigmann, J. M. Mechanisms of resistance to cisplatin. *Mutat. Res.* **57,** 23–43 (2001).

349. Bahar, I., Erman, B., Haliloglu, T. & Jernigan, R. L. Characterization of the adducts produced in DNA by cis-diamminedichloroplatinum(II) and cis-dichloro(ethylenediamine)platinum(II). *Biochemistry* **22,** 13512–13523 (1983).

350. Ciccarelli, R. B., Solomon, M. J., Varshavsky, A. & Lippard, S. J. In vivo effects of cis- and trans-diamminedichloroplatinum(II) on SV40 chromosomes: differential repair, DNA-protein cross-linking, and inhibition of replication. *Biochemistry* **24,** 7533–7540 (1985).

351. Mello, J. A., Lippard, S. J. & Essigmann, J. M. DNA adducts of cis-diamminedichloroplatinum(II) and its trans isomer inhibit RNA polymerase II differentially in vivo. *Biochemistry* **34,** 14783–14791 (1995).

352. Sorenson, C. M., Barry, M. A. & Eastman, A. Analysis of events associated with cell cycle arrest at G2 phase and cell death induced by cisplatin. *J. Natl. Cancer Inst.* **82,** 749–755 (1990).

353. Eastman, A. & Barry, M. A. Interaction of trans-diamminedichloroplatinum(II) with DNA: formation of monofunctional adducts and their reaction with glutathione. *Biochemistry* **26,** 3303–3307 (1987).

354. Anson, R. M. *et al.* Differential human nucleotide excision repair of paired and mispaired cisplatin-DNA adducts. *Nucleic Acids Res.* **25,** 480–491 (1998).

355. Dabholkar, M., Vionnet, J., Bostick-Bruton, F., Yu, J. J. & Reed, E. Messenger RNA levels of XPAC and ERCC1 in ovarian cancer tissue correlate with response to platinum-based chemotherapy. *J. Clin. Invest.* **94,** 703–8 (1994).

356. Dijt, F. & Fichtinger-Schepman, A. Formation and repair of cisplatin-induced adducts to DNA in cultured normal and repair-deficient human fibroblasts. *Cancer Res.* 6058–6062 (1988). at <http://cancerres.aacrjournals.org/content/48/21/6058.short>

357. Schmoll, H. J. *et al.* European consensus on diagnosis and treatment of germ cell cancer: a report of the European Germ Cell Cancer Consensus Group (EGCCCG). *Ann. Oncol.* **35,** 1377–1399 (2004).

358. Mayer, F., Honecker, F., Looijenga, L. H. J. & Bokemeyer, C. Towards an understanding of the biological basis of response to cisplatin-based chemotherapy in germ-cell tumors. *Ann. Oncol. Off. J. Eur. Soc. Med. Oncol. ESMO* **14,** 825–832 (2003).

359. Koberle, B. *et al.* DNA repair capacity and cisplatin sensitivity of human testis tumour cells. *Int. J. cancer J. Int. du cancer* **70,** 551–555 (1997).

360. Welsh, C. *et al.* Reduced levels of XPA, ERCC1 and XPF DNA repair proteins in testis tumor cell lines. *Int. J. cancer J. Int. du cancer* **110,** 352–361 (2004).

361. Köberle, B., Masters, J. R., Hartley, J. A. & Wood, R. D. Defective repair of cisplatin-induced DNA damage caused by reduced XPA protein in testicular germ cell tumours. *Curr. Biol.* **9,** 273–276 (1999).

362. Fuertes, M. a, Alonso, C. & Pérez, J. M. Biochemical modulation of Cisplatin mechanisms of action: enhancement of antitumor activity and circumvention of drug resistance. *Chem. Rev.* **103,** 645–62 (2003).

363. Pil, P. & Lippard, S. Specific binding of chromosomal protein HMG1 to DNA damaged by the anticancer drug cisplatin. *Science (80-.).* **10,** 234–7 (1992).

364. Huang, J. C., Zamble, D. B., Reardon, J. T., Lippard, S. J. & Sancar, A. HMG-domain proteins specifically inhibit the repair of the major DNA adduct of the anticancer drug cisplatin by human excision nuclease. *Proc. Natl. Acad. Sci.* **91,** 10394–10398 (1994).

365. Durant, S. T. & Nickoloff, J. A. Good timing in the cell cycle for precise DNA repair by BRCA1. *Cell cycle* **4,** 1216–1222 (2005).

366. Russell, P. A. *et al.* Frequent loss of BRCA1 mRNA and protein expression in sporadic ovarian cancers. *Int. J. cancer J. Int. du cancer* **87,** 317–321 (2000).

367. Wang, C. *et al.* Expression of BRCA1 protein in benign, borderline, and malignant epithelial ovarian neoplasms and its relationship to methylation and allelic loss of the BRCA1 gene. *J. Pathol.* **202,** 215–223 (2004).

368. Rubin, S. & Benjamin, I. Clinical and pathological features of ovarian cancer in women with germ-line mutations of BRCA1. *N. Engl. J. Med.* **335,** 1413–1416 (1996).

369. Ben David, Y. *et al.* Effect of BRCA mutations on the length of survival in epithelial ovarian tumors. *J. Clin. Oncol.* **20,** 463–6 (2002).

370. Cass, I. *et al.* Improved survival in women with BRCA-associated ovarian carcinoma. *Cancer* **97,** 2187–95 (2003).

371. Yang, D., Khan, S. & Sun, Y. Association of brca1 and brca2 mutations with survival, chemotherapy sensitivity, and gene mutator phenotype in patients with ovarian cancer. *JAMA* **306,** 1557–1565 (2011).

372. Tassone, P. *et al.* BRCA1 expression modulates chemosensitivity of BRCA1-defective HCC1937 human breast cancer cells. *Br. J. Cancer* **88,** 1285–1291 (2003).

373. Quinn, J. E. *et al.* BRCA1 functions as a differential modulator of chemotherapy-induced apoptosis. *Cancer Res.* **63,** 6221–6228 (2003).

374. Sgagias, M. K. *et al.* Brca1-deficient murine mammary epithelial cells have increased sensitivity to CDDP and MMS. *Cell cycle* **3,** 1451–1456 (2004).

375. Quinn, J. E. *et al.* BRCA1 mRNA expression levels predict for overall survival in ovarian cancer after chemotherapy. *Clin. Cancer Res.* **13,** 7413–7420 (2007).

376. McHugh, P., Sones, W. & Hartley, J. Repair of intermediate structures produced at DNA interstrand cross-links in Saccharomyces cerevisiae. *Mol. Cell. Biol.* **20,** 3425–3433 (2000).

377. Ward, J. DNA damage produced by ionizing radiation in mammalian cells: identities, mechanisms of formation, and reparability. *Prog. Nucleic Acid Res. Mol. Biol.* **35,** 95–125 (1988).

378. Li, X. & Heyer, W.-D. Homologous recombination in DNA repair and DNA damage tolerance. *Cell Res.* **18,** 99–113 (2008).

379. San Filippo, J. *et al.* Recombination mediator and Rad51 targeting activities of a human BRCA2 polypeptide. *J. Biol. Chem.* **281,** 11649–57 (2006).

380. Burma, S., Chen, B. P., Murphy, M., Kurimasa, a & Chen, D. J. ATM phosphorylates histone H2AX in response to DNA double-strand breaks. *J. Biol. Chem.* **276,** 42462–7 (2001).

381. Gatei, M. *et al.* Role for ATM in DNA damage-induced phosphorylation of BRCA1. *Cancer Res.* **60,** 3299–3304 (2000).

382. Yarden, R. I., Pardo-Reoyo, S., Sgagias, M., Cowan, K. H. & Brody, L. C. BRCA1 regulates the G2/M checkpoint by activating Chk1 kinase upon DNA damage. *Nat. Genet.* **30,** 285–9 (2002).

383. Huen, M. S. Y., Sy, S. M. H. & Chen, J. BRCA1 and its toolbox for the maintenance of genome integrity. *Nat. Rev. Mol. Cell Biol.* **11,** 138–48 (2010).

384. Hartman, A.-R. & Ford, J. M. BRCA1 induces DNA damage recognition factors and enhances nucleotide excision repair. *Nat. Genet.* **32,** 180–4 (2002).

385. Paull, T. T., Cortez, D., Bowers, B., Elledge, S. J. & Gellert, M. Direct DNA binding by Brca1. *Proc. Natl. Acad. Sci.* **98,** 6086–91 (2001).

386. Stojic, L., Brun, R. & Jiricny, J. Mismatch repair and DNA damage signalling. *DNA Repair (Amst).* **3,** 1091–1101 (2004).

387. Durant, S. T. *et al.* Dependence on RAD52 and RAD1 for anticancer drug resistance mediated by inactivation of mismatch repair genes. *Curr. Biol.* **9,** 51–54 (1999).

388. Duckett, D. R. *et al.* Human MutSalpha recognizes damaged DNA base pairs containing O6-methylguanine, O4-methylthymine, or the cisplatin-d(GpG) adduct. *Proc. Natl. Acad. Sci.* **93,** 6443–6447 (1996).

389. Crijnen, T. E. M. *et al.* Survival of patients with ovarian cancer due to a mismatch repair defect. *Fam. Cancer* **4,** 301–5 (2005).

390. Song, I.-S. *et al.* Role of human copper transporter Ctr1 in the transport of platinum-based antitumor agents in cisplatin-sensitive and cisplatin-resistant cells. *Mol. Cancer Ther.* **3,** 1543–1549 (2004).

391. Nakayama, K. *et al.* Copper transporting P-type adenosine triphosphatase (ATP7B) as a cisplatin based chemoresistance marker in ovarian carcinoma: comparative analysis with expression of MDR1, MRP1, MRP2, LRP and BCRP. *Int. J. Cancer* **101,** 488–95 (2002).

392. Kelland, L. R. New platinum antitumor complexes. *Crit. Rev. Oncol.* **15,** 191–219 (1993).

393. Sakamoto, M. *et al.* Analysis of gene expression profiles associated with cisplatin resistance in human ovarian cancer cell lines and tissues using cDNA microarray. *Hum. cell Off. J. Hum. Cell Res. Soc.* **14,** 305–315 (2001).

394. Ikeda, K. *et al.* Multivariate analysis for prognostic significance of histologic subtype, GST-pi, MDR-1, and p53 in stages II-IV ovarian cancer. *Int. J. Gynecol. cancer Off. J. Int. Gynecol. Cancer Soc.* **13,** 776–784 (2003).

395. Surowiak, P. *et al.* Augmented expression of metallothionein and glutathione S-transferase pi as unfavourable prognostic factors in cisplatin-treated ovarian cancer patients. *Virchows Arch. an Int. J. Pathol.* **447,** 626–633 (2005).

396. Selvakumaran, M., Pisarcik, D. & Bao, R. Enhanced cisplatin cytotoxicity by disturbing the nucleotide excision repair pathway in ovarian cancer cell lines. *Cancer Res.* 1311–1316 (2003). at <http://cancerres.aacrjournals.org/content/63/6/1311.short>

397. Vaisman, A. *et al.* The role of hMLH1, hMSH3, and hMSH6 defects in cisplatin and oxaliplatin resistance: correlation with replicative bypass of platinum-DNA adducts. *Cancer Res.* **58,** 3579–3585 (1998).

398. Brown, R. *et al.* hMLH1 expression and cellular responses of ovarian tumour cells to treatment with cytotoxic anticancer agents. *Oncogene* **15,** 45–52 (1997).

399. Edwards, S. L. *et al.* Resistance to therapy caused by intragenic deletion in BRCA2. *Nature* **451,** 1111–1115 (2008).

400. Sakai, W. *et al.* Secondary mutations as a mechanism of cisplatin resistance in BRCA2-mutated cancers. *Nature* **451,** 1116–1120 (2008).

401. Sakai, W. *et al.* Functional restoration of BRCA2 protein by secondary BRCA2 mutations in BRCA2-mutated ovarian carcinoma. *Cancer Res.* **69,** 6381–6386 (2009).

402. Swisher, E. M. *et al.* Secondary BRCA1 mutations in BRCA1-mutated ovarian carcinomas with platinum resistance. *Cancer Res.* **68,** 2581–2586 (2008).

403. Rottenberg, S. *et al.* Selective induction of chemotherapy resistance of mammary tumors in a conditional mouse model for hereditary breast cancer. *Proc. Natl. Acad. Sci.* **104,** 12117–12122 (2007).

404. Johannessen, C. M. *et al.* COT drives resistance to RAF inhibition through MAP kinase pathway reactivation. *Nature* **468,** 968–72 (2010).

405. Hutchins, A. P., Poulain, S. & Miranda-Saavedra, D. Genome-wide analysis of STAT3 binding in vivo predicts effectors of the anti-inflammatory response in macrophages. *Blood* **119,** e110–9 (2012).

406. Yun, U. J., Park, S. E., Jo, Y. S., Kim, J. & Shin, D. Y. DNA damage induces the IL-6/STAT3 signaling pathway, which has anti-senescence and growth-promoting functions in human tumors. *Cancer Lett.* **323,** 155–60 (2012).

407. Rodier, F. *et al.* Persistent DNA damage signalling triggers senescence-associated inflammatory cytokine secretion. *Nat. Cell Biol.* **11,** 973–9 (2009).

408. Petit-Frère, C. *et al.* Induction of interleukin-6 production by ultraviolet radiation in normal human epidermal keratinocytes and in a human keratinocyte cell line is mediated by DNA damage. *J. Invest. Dermatol.* **111,** 354–9 (1998).

409. Clarke, B. *et al.* Intraepithelial T cells and prognosis in ovarian carcinoma: novel associations with stage, tumor type, and BRCA1 loss. *Mod. Pathol.* **22,** 393–402 (2009).

410. Lee, J.-H. & Paull, T. T. Activation and regulation of ATM kinase activity in response to DNA double-strand breaks. *Oncogene* **26,** 7741–8 (2007).

411. Bolton, K. *et al.* Association between BRCA1 and BRCA2 mutations and survival in women with invasive epithelial ovarian cancer. *JAMA* **307,** 382–389 (2012).

412. Fong, P. P. C. *et al.* Inhibition of poly(ADP-ribose) polymerase in tumors from BRCA mutation carriers. *N. Engl. J. Med.* **361,** 123–134 (2009).

413. Drew, Y. *et al.* Therapeutic potential of poly(ADP-ribose) polymerase inhibitor AG014699 in human cancers with mutated or methylated BRCA1 or BRCA2. *J. Natl. Cancer Inst.* **103,** 334–46 (2011).

414. Stronach, E. a *et al.* HDAC4-regulated STAT1 activation mediates platinum resistance in ovarian cancer. *Cancer Res.* **71,** 4412–22 (2011).

415. Park, O. K., Schaefer, T. S. & Nathans, D. In vitro activation of Stat3 by epidermal growth factor receptor kinase. *Proc. Natl. Acad. Sci.* **93,** 13704–8 (1996).

416. Cooke, S. L. *et al.* Genomic analysis of genetic heterogeneity and evolution in high-grade serous ovarian carcinoma. *Oncogene* **29,** 4905–13 (2010).

417. Magnifico, A. *et al.* Tumor-initiating cells of HER2-positive carcinoma cell lines express the highest oncoprotein levels and are sensitive to trastuzumab. *Clin. Cancer Res.* **15,** 2010–21 (2009).

418. Pardanani, a *et al.* TG101209, a small molecule JAK2-selective kinase inhibitor potently inhibits myeloproliferative disorder-associated JAK2V617F and MPLW515L/K mutations. *Leukemia* **21,** 1658–68 (2007).

419. Vallania, F. *et al.* Genome-wide discovery of functional transcription factor binding sites by comparative genomics: the case of Stat3. *Proc. Natl. Acad. Sci.* **106,** 5117–5122 (2009).

420. Bast, R. C., Hennessy, B. & Mills, G. B. The biology of ovarian cancer: new opportunities for translation. *Nat. Rev. Cancer* **9,** 415–28 (2009).

421. Syed, V., Ulinski, G., Mok, S. C. & Ho, S.-M. Reproductive hormone-induced, STAT3-mediated interleukin 6 action in normal and malignant human ovarian surface epithelial cells. *J. Natl. Cancer Inst.* **01655,** 617–629 (2002).

422. Huang, M., Page, C., Reynolds, R. K. & Lin, J. Constitutive activation of stat 3 oncogene product in human ovarian carcinoma cells. *Gynecol. Oncol.* **79,** 67–73 (2000).

423. Pardanani, A. *et al.* Safety and efficacy of TG101348, a selective JAK2 inhibitor, in myelofibrosis. *J. Clin. Oncol.* **29,** 789–96 (2011).

424. Pan, Y., Zhou, F., Zhang, R. & Claret, F. X. Stat3 inhibitor stattic exhibits potent antitumor activity and induces chemo- and radio-sensitivity in nasopharyngeal carcinoma. *PLoS One* **8,** e54565 (2013).

425. Alas, S., Bonavida, B. & Apoptosis, C. D. Inhibition of constitutive STAT3 activity sensitizes resistant non-Hodgkin's lymphoma and multiple myeloma to chemotherapeutic drug-mediated apoptosis. *Clin. Cancer Res.* **9,** 316–326 (2003).

426. Huang, S. *et al.* Inhibition of activated Stat3 reverses drug resistance to chemotherapeutic agents in gastric cancer cells. *Cancer Lett.* **315,** 198–205 (2012).

427. Yue, P. *et al.* Hyperactive EGF receptor, Jaks and Stat3 signaling promote enhanced colony-forming ability, motility and migration of cisplatin-resistant ovarian cancer cells. *Oncogene* **31,** 2309–22 (2012).

428. Domcke, S., Sinha, R., Levine, D. a., Sander, C. & Schultz, N. Evaluating cell lines as tumour models by comparison of genomic profiles. *Nat. Commun.* **4,** 1–10 (2013).

429. Lee, E.-S., Ko, K.-K., Joe, Y. A., Kang, S.-G. & Hong, Y.-K. Inhibition of STAT3 reverses drug resistance acquired in temozolomide-resistant human glioma cells. *Oncol. Lett.* **2,** 115–121 (2011).

430. Zhao, S.-H. *et al.* Knockdown of stat3 expression by RNAi inhibits in vitro growth of human ovarian cancer. *Radiol. Oncol.* **45,** 196–203 (2011).

431. Yu, H., Kortylewski, M. & Pardoll, D. Crosstalk between cancer and immune cells: role of STAT3 in the tumour microenvironment. *Nat. Rev. Immunol.* **7,** 41–51 (2007).

432. Real, P. J. *et al.* Resistance to chemotherapy via Stat3-dependent overexpression of Bcl-2 in metastatic breast cancer cells. *Oncogene* **21,** 7611–8 (2002).

433. Snyder, M., Huang, X.-Y. & Zhang, J. J. Identification of novel direct Stat3 target genes for control of growth and differentiation. *J. Biol. Chem.* **283,** 3791–3798 (2008).

434. Jani, J. P. *et al.* Discovery and pharmacologic characterization of CP-724,714, a selective ErbB2 tyrosine kinase inhibitor. *Cancer Res.* **67,** 9887–93 (2007).

435. Rhodes, A. *et al.* A formalin-fixed, paraffin-processed cell line standard for quality control of immunohistochemical assay of HER-2/neu expression in breast cancer. *Am. J. Clin. Pathol.* **117,** 81–9 (2002).

436. Barretina, J. *et al.* The Cancer Cell Line Encyclopedia enables predictive modelling of anticancer drug sensitivity. *Nature* **483,** 603–307 (2012).

437. Yao, S., Rojas, M. & Lin, Y. Z. Controlling Epidermal Growth Factor (EGF)-stimulated Ras Activation in Intact Cells by a Cell-permeable Peptide Mimicking Phosphorylated EGF Receptor. *J. Biol. Chem.* **271,** 27456–27461 (1996).

438. Wang, H. *et al.* Comparative analysis and integrative classification of NCI60 cell lines and primary tumors using gene expression profiling data. *BMC Genomics* **7,** 166 (2006).

439. Noske, a *et al.* Comparison of different approaches for assessment of HER2 expression on protein and mRNA level: prediction of chemotherapy response in the neoadjuvant GeparTrio trial (NCT00544765). *Breast Cancer Res. Treat.* **126,** 109–17 (2011).

440. McKie, A. B. *et al.* The OPCML tumor suppressor functions as a cell surface repressor-adaptor, negatively regulating receptor tyrosine kinases in epithelial ovarian cancer. *Cancer Discov.* **2,** 156–71 (2012).

441. Paik, S., Kim, C. & Wolmark, N. HER2 status and benefit from adjuvant trastuzumab in breast cancer. *N. Engl. J. Med.* **358,** 1409–11 (2008).

442. Bose, R. *et al.* Activating HER2 mutations in HER2 gene amplification negative breast cancer. *Cancer Discov.* **3,** 224–37 (2013).

443. Penuel, E., Akita, R. W. & Sliwkowski, M. X. Identification of a region within the ErbB2/HER2 intracellular domain that is necessary for ligand-independent association. *J. Biol. Chem.* **277,** 28468–73 (2002).

444. Selander, K. S. *et al.* Inhibition of gp130 signaling in breast cancer blocks constitutive activation of Stat3 and inhibits in vivo malignancy. *Cancer Res.* **64,** 6924–33 (2004).

445. Sriuranpong, V. *et al.* Epidermal growth factor receptor-independent constitutive activation of STAT3 in head and neck squamous cell carcinoma is mediated by the autocrine/paracrine stimulation of the interleukin 6/gp130 cytokine system. *Cancer Res.* **63,** 2948–2956 (2003).

446. Kaplan Meier-plotter [Ovarian cancer]. at <http://kmplot.com/analysis/index.php?p=service&cancer=ovar>

447. Guo, Y., Nemeth, J., O'Brien, C. & Susa, M. Effects of Siltuximab on the IL-6–Induced Signaling Pathway in Ovarian Cancer. *Clin. Cancer Res.* (2010). doi:10.1158/1078-0432.CCR-10-1095

448. Giordano, V. *et al.* Shc mediates IL-6 signaling by interacting with gp130 and Jak2 kinase. *J. Immunol.* **158,** 4097–4103 (1997).

449. Chung, T. D., Yu, J. J., Kong, T. A., Spiotto, M. T. & Lin, J. M. Interleukin-6 activates phosphatidylinositol-3 kinase, which inhibits apoptosis in human prostate cancer cell lines. *Prostate* **42,** 1–7 (2000).

450. Lee, I.-S. S. *et al.* Vav is associated with signal transducing molecules gp130, Grb2 and Erk2, and is tyrosine phosphorylated in response to interleukin-6. *FEBS Lett.* **401,** 133–137 (1997).

451. Shen, Q. *et al.* The AP-1 transcription factor regulates breast cancer cell growth via cyclins and E2F factors. *Oncogene* **27,** 366–377 (2008).

452. Bardwell, a J., Flatauer, L. J., Matsukuma, K., Thorner, J. & Bardwell, L. A conserved docking site in MEKs mediates high-affinity binding to MAP kinases and cooperates with a scaffold protein to enhance signal transmission. *J. Biol. Chem.* **276,** 10374–86 (2001).

453. Gozdz, A. *et al.* Cisplatin-mediated activation of extracellular signal-regulated kinases 1/2 (ERK1/2) by inhibition of ERK1/2 phosphatases. *J. Neurochem.* **106,** 2056–67 (2008).

454. Guégan, J.-P., Ezan, F., Théret, N., Langouët, S. & Baffet, G. MAPK signaling in cisplatin-induced death: predominant role of ERK1 over ERK2 in human hepatocellular carcinoma cells. *Carcinogenesis* **34,** 38–47 (2013).

455. Schulze, W. X., Deng, L. & Mann, M. Phosphotyrosine interactome of the ErbB-receptor kinase family. *Mol. Syst. Biol.* **1,** 2005.0008 (2005).

456. Yang, K., Hitomi, M. & Stacey, D. W. Variations in cyclin D1 levels through the cell cycle determine the proliferative fate of a cell. *Cell Div.* **1,** 32 (2006).

457. Lee, T. *et al.* Docking motif interactions in MAP kinases revealed by hydrogen exchange mass spectrometry. *Mol. Cell* **14,** 43–55 (2004).

458. Marinkovic, D. *et al.* Identification of novel Myc target genes with a potential role in lymphomagenesis. *Nucleic Acids Res.* **32,** 5368–78 (2004).

459. Lu, Z. & Xu, S. ERK1/2 MAP kinases in cell survival and apoptosis. *IUBMB Life* **58,** 621–31 (2006).

460. Chakrabarty, A., Sánchez, V., Kuba, M. G., Rinehart, C. & Arteaga, C. L. Feedback upregulation of HER3 (ErbB3) expression and activity attenuates antitumor effect of PI3K inhibitors. *Proc. Natl. Acad. Sci.* **3,** 3–8 (2011).

461. Serra, V. *et al.* PI3K inhibition results in enhanced HER signaling and acquired ERK dependency in HER2-overexpressing breast cancer. *Oncogene* **30,** 2547–2557 (2011).

462. Mirzoeva, O. K. *et al.* Basal subtype and MAPK/ERK kinase (MEK)-phosphoinositide 3-kinase feedback signaling determine susceptibility of breast cancer cells to MEK inhibition. *Cancer Res.* **69,** 565–72 (2009).

463. Turke, A. B. *et al.* MEK inhibition leads to PI3K/AKT activation by relieving a negative feedback on ERBB receptors. *Cancer Res.* **72,** 3228–37 (2012).

464. Yu, K., Toral-Barza, L., Shi, C., Zhang, W.-G. & Zask, A. Response and determinants of cancer cell susceptibility to PI3K inhibitors: combined targeting of PI3K and Mek1 as an effective anticancer strategy. *Cancer Biol. Ther.* **7,** 307–315 (2008).

465. Liu, D. & Xing, M. Potent inhibition of thyroid cancer cells by the MEK inhibitor PD0325901 and its potentiation by suppression of the PI3K and NF-kappaB pathways. *Thyroid* **18,** 853–64 (2008).

466. Engelman, J. A. *et al.* Effective use of PI3K and MEK inhibitors to treat mutant Kras G12D and PIK3CA H1047R murine lung cancers. *Nat. Med.* **14,** 1351–6 (2008).

467. Sansone, P. & Bromberg, J. Targeting the interleukin-6/Jak/stat pathway in human malignancies. *J. Clin. Oncol.* **30,** 1005–14 (2012).

468. Schust, J., Sperl, B., Hollis, A., Mayer, T. U. & Berg, T. Stattic: a small-molecule inhibitor of STAT3 activation and dimerization. *Chem. Biol.* **13,** 1235–42 (2006).

469. Tang, D. *et al.* ERK activation mediates cell cycle arrest and apoptosis after DNA damage independently of p53. *J. Biol. Chem.* **277,** 12710–7 (2002).

470. Haagensen, E. J., Kyle, S., Beale, G. S., Maxwell, R. J. & Newell, D. R. The synergistic interaction of MEK and PI3K inhibitors is modulated by mTOR inhibition. *Br. J. Cancer* **106,** 1386–94 (2012).

471. Feng, J. *et al.* Activation of Jak2 catalytic activity requires phosphorylation of Y1007 in the kinase activation loop. *Mol. Cell. Biol.* **17,** 2282–2297 (1998).

472. Stemke-Hale, K. *et al.* An integrative genomic and proteomic analysis of PIK3CA, PTEN, and AKT mutations in breast cancer. *Cancer Res.* **68,** 6084–6091 (2008).

473. COSMIC: catalogue of somatic mutations in cancer. at <http://cancer.sanger.ac.uk/cancergenome/projects/cosmic/>

474. The Cancer Genome Project. *Sanger Inst.* at <http://www.sanger.ac.uk/genetics/CGP/>